Regulatory Mechanisms of the Plant G2/M Transition

PhD

Anne Lentz Grønlund

2007

ProQuest LLC
789 East Eisenhower Parkway
P.O. Box 1346
Ann Arbor, MI 48106-1346

DECLARATION

This work has not previously been accepted in substance for any degree and is not concurrently submitted in candidature for any degree.

Signed ..... Date 12/12/2007

STATEMENT 1

This thesis is being submitted in partial fulfillment of the requirements for the degree of PhD.

Signed ..... Date 12/12/2007

STATEMENT 2

This thesis is the result of my own independent work/investigation, except where otherwise stated.
Other sources are acknowledged by explicit references.

Signed ..... Date 12/12/2007

STATEMENT 3

I hereby give consent for my thesis, if accepted, to be available for photocopying and for inter-library loan, and for the title and summary to be made available to outside organisations.

Signed ..... Date 12/12/2007

Acknowledgements

The work presented in this thesis was performed at the School of Biosciences, Cardiff University, in the period December 2004 – December 2007. The PhD studentship was jointly funded by Cardiff University and University of Worcester.

I am grateful to my supervisors Drs. Hilary J. Rogers and Dennis Francis at Cardiff University and Dr. Rob Herbert at University of Worcester for funding, invaluable supervision, careful review of my thesis and for always keeping their doors open for me. Also to my advisors, Head of School Prof. John Harwood and Dr. Peter Kille, I am grateful for funding and all the helpful advice at various stages of the project. Finally, I would like to express my gratitude to Dr. Richard Dickinson for valuable advice and for passing on his excellent knowledge of working with *S. cerevisiae* and to Dr. John Doonan for the good collaboration.

My special thanks belong to all the current and former people in labs 1.57/1.58 and also I want to thank to Dr. David Sorrell for leaving his lab books behind.

My dearest and most sincere thanks belong to my family for their never ending support and encouragement in both good and bad times. I would also like to thank my parents-in-law for their great support.

Finally, I am sincerely indebted to Jesper, my husband and my closest friend. I would like to thank you, not only for reading the final draft of my thesis, but also for your million laughs, smiles and hugs in good times and bad times. Thanks for your never ending love, trust, integrity and for your belief in me. Thanks for your great support, encouragement, help and for passing on your excellent knowledge (human as well as scientific). And finally thanks for driving the many miles from Leamington to Cardiff two times a week to see me. I could not have managed with out you…

Abstract

The cell cycle is the life of a cell from one mitotic division to the next. In yeast and animals the transition from G2 to mitosis is regulated by the Wee1 kinases and Cdc25 phosphatases. Phosphoregulation of G2/M is also maintained by 14-3-3 proteins, which function in a wide range of additional processes including signal transduction and stress responses. The scope of this thesis was to investigate how the plant G2/M checkpoint functions and how features of the yeast and animal G2/M model apply to the plant model. A better knowledge of the mechanisms that regulate AtCDC25 and AtWEE1 activities was achieved by identifying interaction partners for the two proteins. Both proteins interact with proteins involved in protein biosynthesis, cell division and plant stress responses leading to many hypotheses about the localization, regulation and function of both AtCDC25 and AtWEE1. Moreover, AtWEE1 interacts with proteins involved in ubiquitin-mediated degradation, which might be the mechanism regulating WEE1 protein levels (Chapter 4). Additionally, AtWEE1 interacts with 14-3-3 proteins and its interaction with 14-3-3ω was confirmed *in vivo* in plant cells (Chapter 5). Furthermore, greater insights into the role of WEE1 in cell cycle regulation and plant development were obtained by investigation of the biochemistry of *N. tabacum* WEE1 during the cell cycle of synchronized *N. tabacum* BY-2 cells showing that both WEE1 protein level and kinase activity are sensitive indicators for the timing of mitosis (Chapter 6). Moreover, *A. thaliana wee1* T-DNA insertion lines were characterized. Under standard growth conditions the T-DNA insertions in the *WEE1* gene only mildly affect the plant root development. However, exposure to hydroxyurea results in a hypersensitivity response leading to a reduced primary root length and decreased rate of lateral root production linking *AtWEE1* with both stress responses and plant development (Chapter 7).

Contents

Abbreviations

3-AT	3-amino-1,2,4-triazole
aa	Amino acids
Ac	*Allium cepa, A. cepa*
ADH	Alcohol dehydrogenase
App.	Approximately
At	*Arabidopsis thaliana, A. thaliana*
ATM	Ataxia-telangiectasia mutated
ATP	Adenosine tri phosphate
ATR	ATM-related
A. tumefaciens	*Agrobacterium tumefaciens*
BiFC	Bimolecular fluorescence complementation
bp	Base pairs
BSA	Bovine serum albumin
BY-2	Bright yellow 2
CAK	CDK activating kinase
CBL	Calcineurin B-like
Cdc2	Cell division cycle 2
CDK	Cyclin dependent kinase
Ce	*Caenorhabditis elegans, C. elegans*
Cfu	Colony forming units
Chk1/2	Checkpoint kinase 1/2
Cip/Kip	CDK inhibitor protein/Kinase inhibitor protein
CiPK	Calcineurin B-like interacting protein
CKI	CDK inhibitor protein
CKS/Suc	CDK kinase subunit/Subunit of CDK
Cr	*Chlamydomonas reinhardii, C. reinhardii*
CTD	C-terminal domain
CYC	Cyclin
DBP	DNA binding protein
DEX	Dexamethasone
dH_2O	Distilled H_2O
Dm	*Drosophila melanogaster, D. melanogaster*
DMF	Dimethyl formamide
DMSO	Dimethyl sulfoxide
DO solution	Drop-out solution
DTT	Dithiothreitol
E2F	Adenovirus E2 promoter-binding factor
ECL	Enhanced chemiluminescence
E. coli	*Escherichia coli*
EDTA	Ethylenediamine tetraacetic acid
ER	Endoplasmatic reticulum
EtBr	Ethidium bromide
EtOH	Ethanol
G0/G1/G2	Gap phases 0/1/2 (cell cycle phases)
γ-TURC	γ -tubulin ring complex
Grf	General regulatory factor
HA	Hemagglutinin

HEPES	4-(2-hydroxyethyl)-1-piperazineethanesulfonic acid
Hs	*Homo sapiens, H. sapiens*
HU	Hydroxyurea
ICK	Inhibitors of CDK
IPTG	Isopropyl-β-D-thiogalactopyranoside
IR	Ionising radiation
kDa	Kilo Dalton
KAc	Potassium acetate
KRP	Kip-related protein
LiAc	Lithium acetate
Le	*Lycopersicon esculentum, L. esculentum*
MCS	Multiple cloning site
MetOH	Methanol
Mik1	Mitotic inhibitory kinase 1
Mm	*Mus musculus, M. musculus*
M-MLV RT	Moloney Murine Leukemia Virus Reverse Transcriptase
MMS	Methyl methanesulfonate
M	Mitosis (cell cycle phase)
MPF	M phase promoting factor
Ms	*Medicago sativa, M. sativa*
Myt1	Membrane-bound tyrosine threonine kinase 1
Nb	*Nicotiana benthamiana, N. benthamiana*
NOS	Nopaline synthetase
Nt	*Nicotiana tabacum, N. tabacum*
OD	Optical density
ONPG	*ortho*-Nitrophenyl-β-galactoside
Os	*Oryza sativa, O. sativa*
Ot	*Osterococcus tauri, O.tauri*
PAGE	Polyacrylamide gel electrophoresis
PCR	Polymerase chain reaction
PEG	Polyethylene glycol
PEI	Polyethylenimine
PI	Protease inhibitors
PPI	Protease and phosphatase inhibitors
PVDF	Polyvinylidene difluoride
Rb	Retinoblastoma
RNR	Ribonucleotide reductase
RT-PCR	Reverse transcriptase polymerase chain reaction
S	DNA synthesis (cell cycle phase)
SDS	Sodium dodecyl sulphate
SE	Standard error
SERK1	Somatic embryogenesis receptor-like kinase 1
Sc	*Saccharomyces cerevisiae, S. cerevisiae*
SCF	Skp1/Cullin/F-box complex
Sl	*Solanum lycopersicum, S. lycopersicum*
Sp	*Schizosaccharomyces pombe, S. pombe*
TBP	TATA-box binding protein
T-DNA	Transfer DNA
TF	Transcription factor
TEMED	N, N, N', N'-tetramethyl-ethylenediamine

TSA1	TONSOKU associating protein 1
TSK	TONSOKU
USS	Up-stream sequence
UTR	Un-translated region
UV	Ultra-violet
Wt	Wild type
Xl	*Xenopus laevis*, *X. laevis*
Y2H	Yeast two hybrid
YFP	Yellow fluorescent protein
Zm	*Zea mays*, *Z. mays*

1 General Introduction

In 1858 the German pathologist Rudolf Virchow proposed the principle that "Where a cell arises, there a cell must previously have existed" (Harris, 1999), which carried with it a profound message for the continuity of life. Cells are generated from cells, and the only way to make more cells is by division of those that already exist. All living organisms, from uni-cellular bacteria to multi-cellular mammals, are products of repeated rounds of cell growth and division extending back in time. This cycle of replication and division, known as the cell cycle, is the essential mechanism, by which all living things reproduce.

The following sections contain an overview of the eukaryotic cell cycle and how it is regulated by important key proteins that ensure a tight control and correct progression during the different stages of the cell cycle.

1.1 The Cell Cycle

Details of the cell cycle vary from organism to organism and variations may occur at different times in the life of an organism. Nevertheless, certain characteristics are universal. There is a minimum set of processes that a cell has to perform to allow it to accomplish its most fundamental task: the transfer of its genetic information to the next generation of cells. Therefore, the goal of the cell cycle is to produce two genetically identical daughter cells. Two major phases of the cell cycle are the DNA synthetic phase (S), where the DNA replication occurs, and the following mitotic phase (M), where chromosome segregation and cell division occurs (Figure 1). In somatic cells there are two additional phases and since these periods occur between M and S phases, they are designated gap phase 1 (G1) and gap phase 2 (G2), respectively (Mitchison, 1971).

If the conditions for continuous growth are not met in G1 phase the cell instead enters the quiescent state (G0). The G1 and G2 phases serve as more than simple time delays to allow cell growth. They provide time for the cell to 'check' the internal and external environment to ensure that an earlier event, such as S phase, has been properly executed before proceeding to a later event, such as M phase.

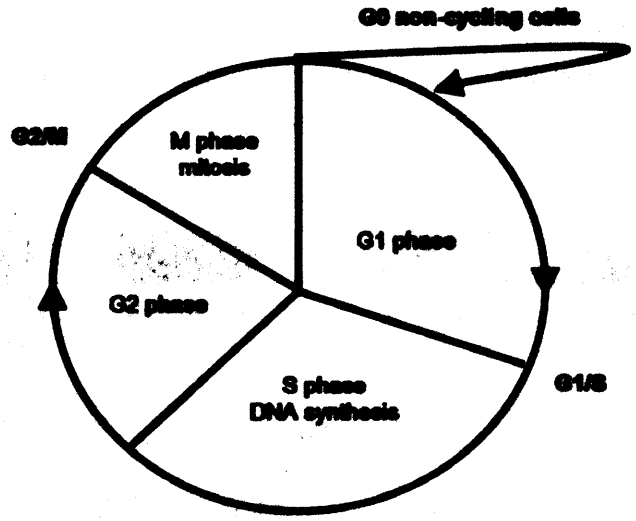

Figure 1 - Schematic diagram of the eukaryotic cell cycle displaying the different phases, mitosis (M), post-mitotic interphase (G1), DNA synthesis (S), the post-synthetic interphase (G2) and the quiescent state (G0) for non-cycling cells

This checkpoint concept also includes events such as blocking M-phase after DNA damage until damaged DNA has been repaired (Hartwell and Weinert, 1989; Nurse, 2000). The basic features of cell cycle regulation are remarkably conserved in all eukaryotes examined so far (Van't Hof, 1973; Huntley and Murray, 1999; Pines, 1999; Inze and De Veylder, 2006; Francis, 2007).

1.2 Regulation of the Cell Cycle

1.2.1 Cyclin Dependent Kinases (CDKs)

The progression through the eukaryotic cell cycle is regulated at multiple points, but all or most of these are regulated by the activation and deactivation of members of a conserved super-family of serine/threonine protein kinases known as the Cyclin dependent kinases (CDKs) (Nigg, 1995). Most CDKs are inactive as monomers and to be activated they have to heterodimerize with regulatory proteins called cyclins. All known eukaryotic CDKs share substantial structural similarity with a catalytic cleft containing ATP and substrate binding sites. Cyclin binding stabilizes the catalytic site within an otherwise rather flexible structure. However, access to the active site remains restricted by a section of the CDK known as the T-loop (Figure 2A and B).

In CDK monomers, the residues in the ATP binding site are misoriented and contribute to CDK inactivity. Upon cyclin binding, the relative orientation of the N- and C-terminal lobe and the conformation of the catalytic cleft of the CDK changes.

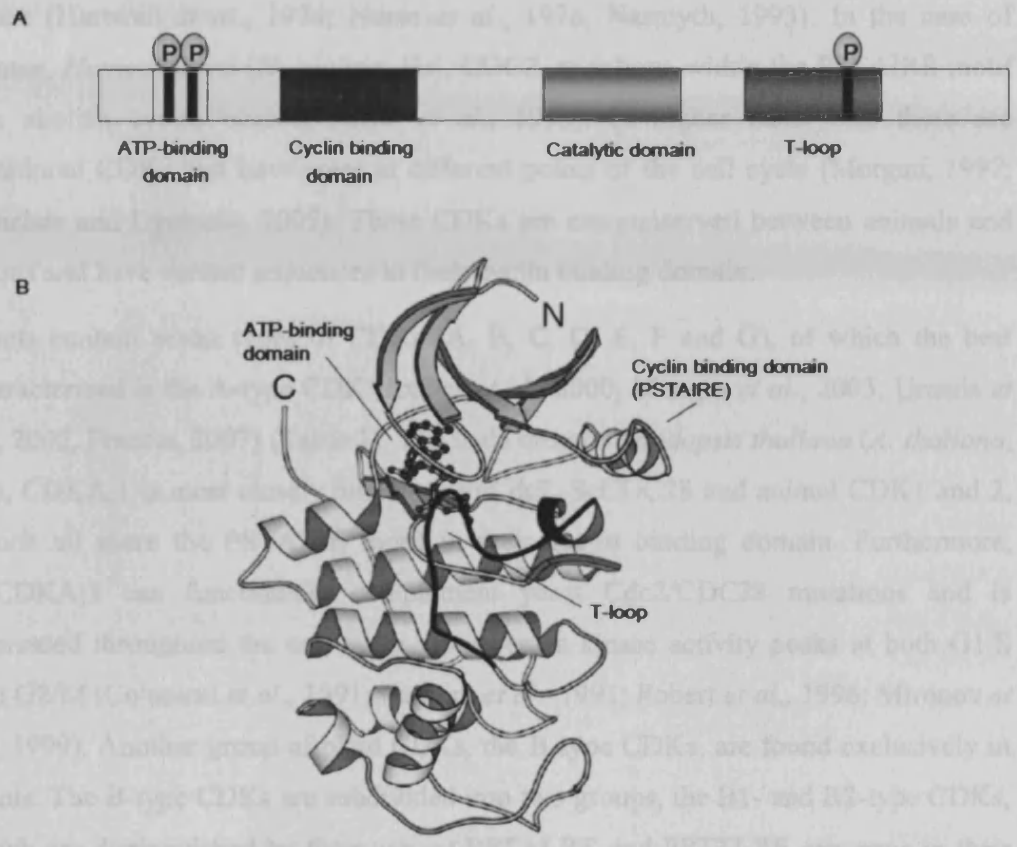

Figure 2 – A) A schematic diagram of CDK consisting of an ATP-binding domain, a cyclin binding domain, a catalytic domain and a T-loop (Adapted from Sorrell *et al.*, 2001) including the known phosphorylation sites of CDKs (T14, Y15 and T167). B) The structure of *H. sapiens* Cdk2 in complex with ATP showing the PSTAIRE cyclin binding motif, the ATP binding domain containing ATP (ball and stick representation), the N- and C-terminal lobes and the T-loop highlighted in black (Adapted from De Bondt *et al.*, 1993).

The most obvious change occurs in the T-loop leading to exposure of the substrate binding site and allowing activating phosphorylations at conserved threonine residues within the T-loop. In addition, the residues in the ATP binding site are reconfigured making it possible for the CDK to phosphorylate its substrate (De Bondt *et al.*, 1993; Jeffrey *et al.*, 1995; Morgan, 1997).

In the fission yeast, *Schizosaccharomyces pombe* (*S. pombe*, Sp), cell cycle only a single CDK has been identified, namely the Cell division cycle 2 (Cdc2), which has the canonical sequence PSTAIRE within its cyclin binding domain. It is required for

regulation of both G1/S and G2/M transitions. Homologues of CDKs are conserved in all eukaryotes. The budding yeast, *Saccharomyces cerevisiae* (*S. cerevisiae*, Sc), homologue CDC28 is expressed in G1 and is necessary for driving the cell into S phase (Hartwell *et al.*, 1974; Nurse *et al.*, 1976; Nasmyth, 1993). In the case of human, *Homo sapiens* (*H. sapiens*, Hs), CDC2, mutations within the PSTAIRE motif can abolish cyclin binding (Ohta *et al.*, 1998). In higher eukaryotes there are additional CDKs that have roles at different points of the cell cycle (Morgan, 1997; Sanchez and Dynlacht, 2005). These CDKs are not conserved between animals and plants and have variant sequences in their cyclin binding domain.

Plants contain seven types of CDKs (A, B, C, D, E, F and G), of which the best characterized is the A-type CDK (Joubes *et al.*, 2000; Menges *et al.*, 2005; Umeda *et al.*, 2005, Francis, 2007) (Table 1). The thale cress, *Arabidopsis thaliana* (*A. thaliana*, At), CDKA;1 is most closely related to SpCdc2, ScCDC28 and animal CDK1 and 2, which all share the PSTAIRE motif in their cyclin binding domain. Furthermore, AtCDKA;1 can functionally complement yeast Cdc2/CDC28 mutations and is expressed throughout the cell cycle, however its kinase activity peaks at both G1/S and G2/M (Colasanti *et al.*, 1991; Ferreira *et al.*, 1991; Fobert *et al.*, 1996; Mironov *et al.*, 1999). Another group of plant CDKs, the B-type CDKs, are found exclusively in plants. The B-type CDKs are subdivided into two groups, the B1- and B2-type CDKs, which are distinguished by their variant PPTALRE and PPTTLRE sequence in their cyclin binding domain (Van't Hof, 1973; Segers *et al.*, 1996; Mironov *et al.*, 1999). In animals only PSTAIRE CDKs are responsible for the G2/M transition, whereas in plants the kinase activity of B-type CDKs has been found to be predominantly linked to mitosis, suggesting that in plants the B-type CDKs are also important for the G2/M transition (Huntley and Murray, 1999; Sorrell *et al.*, 1999; Porceddu *et al.*, 2001). However, these B-type CDKs are unable to functionally complement temperature-sensitive Cdc2 yeast mutants (Fobert *et al.*, 1996). In *A. thaliana* additional CDKs have been identified, which display a high degree of homology to the yeast and animal CDKs (Vandepoele *et al.*, 2002), but these are less well characterized compared to the A- and B-type CDKs.

Table 1 – Classification of CDKs from higher plants and their peak of expression during the cell cycle (Joubes *et al.*, 2000; Menges *et al.*, 2005; Umeda *et al.*, 2005; Francis, 2007)

CDK type	Cyclin binding motif	Expression peak	Species	Gene name
CDKA	PSTAIRE	G1/S and G2/M	*Antirrhinum majus*	AmCDKA;1
				AmCDKA;2
			Arabidopsis thaliana	AtCDKA;1
			Lycopersicon esculentum	LeCDKA;1
				LeCDKA;2
			Medicago sativa	MsCDKA;1
				MsCDKA;2
			Nicotiana tabacum	NtCDKA;1
				NtCDKA;2
				NtCDKA;3
			Oryza sativa	OsCDKA;1
				OsCDKA;2
			Zea mays	ZmCDKA;1
				ZmCDKA;2
CDKB	PPTALRE and PPTTLRE	G2/M	*Antirrhinum majus*	AmCDKB;1
				AmCDKB2;1
			Arabidopsis thaliana	AtCDKB1;1
				AtCDKB1;2
				AtCDKB2;1
				AtCDKB2;2
			Medicago sativa	MsCDKB1;1
				MsCDKB2;1
			Oryza sativa	OsCDKB;1
CDKC	PITAIRE	G0/G1/S	*Arabidopsis thaliana*	AtCDKC;1
				AtCDKC;2
			Medicago sativa	MsCDKC;1
CDKD	N(I/F)TALRE	G1 and G2/M	*Arabidopsis thaliana*	AtCDKD;1
				AtCDKD;2
				AtCDKD;3
			Oryza sativa	OsCDKD;1
CDKE	SPTAIRE	G0 and G2/M	*Arabidopsis thaliana*	AtCDKE;1
			Medicago sativa	MsCDKE;1
CDKF	–	ND	*Arabidopsis thaliana*	AtCDKF;1
CDKG	PLTSLRE	G0/G1 and G2/M	*Arabidopsis thaliana*	AtCDKG;1
				AtCDKG;2

ND: No data

The C-type CDKs are characterized by a PITAIRE sequence in their cyclin binding domain. A function for the CDKCs may lie within the transcriptional machinery (Barrocco *et al.*, 2003; Fulop *et al.*, 2005). CDKCs have been shown to bind to T-type cyclins, which share homology with the T- and K-type cyclins that bind CDK9 in animals. The animal CDK9 has a divergent PITALRE sequence in the cyclin binding domain and functions in transcription elongation (de Falco and Giordano, 1998; Bregman *et al.*, 2000). The E-type CDKs have been identified in alfalfa, *Medicago sativa* (*M. sativa*, Ms), and *A. thaliana* and have a SPTAIRE motif in the cyclin binding domain (Joubes *et al.*, 2000; Vandepoele *et al.*, 2002). D- and F-type CDKs are also known as CDK-activating kinases (CAKs, section 1.2.3) (Vandepoele *et al.*, 2002; Umeda *et al.*, 2005). The D-type CDKs have a conserved N(I/F)TALRE motif closely related to the motif of the animal CDK7, which is involved in the phosphorylation and subsequent activation of other CDKs during the cell cycle (CAK activity). CDK7 regulates the activity of basal transcription by phosphorylation of the C-terminal domain (CTD) of RNA polymerase II (CTD activity) (Elledge and Harper, 1998). In *A. thaliana* both CDKD;2 and CDKD;3 have CAK and CTD activity, but only CDKD;3 is able to complement temperature-sensitive yeast *cak1* mutants (Shimotohno *et al.*, 2003). The *A. thaliana* F-type CDK has CAK activity, but no CTD activity and it is able to complement temperature-sensitive yeast *cak1* mutants (Shimotohno *et al.*, 2004). The *A. thaliana* CDKE is expressed at high levels in non-dividing cells (Menges *et al.*, 2005). Recently, G-type CDKs carrying a PLTSLRE motif in the cyclin binding domain have been described as a new class of CDKs that shares homology with the human cytokinesis-associated p58 galactosyltransferase protein (Menges *et al.*, 2005), but no activity data or functional homologies have so far been reported for this class.

1.2.2 Cyclins

Cyclins are a diverse group of proteins with low overall homology that share a large conserved region called the cyclin box, which is necessary for CDK binding and activation (Figure 3A). Besides being the key elements at the CDK/cyclin interaction interface, cyclin boxes also form the binding site for the cyclin binding domain and make contact to the T-loop of the CDK (Figure 3B). Many cyclins are synthesized and degraded in a highly coordinated process. The level of mitotic cyclins at specific points during mitosis is tightly controlled by ubiquitin-dependent proteolysis

conferred by an N-terminal destruction box (RXXLXX[L/I]XN motif) (Renaudin *et al.*, 1996; Genschik *et al.*, 1998). Some cyclins contain a C-terminal PEST sequence that is rich in proline, glutamate, serine and threonine residues and is thought to instabilize cyclin binding.

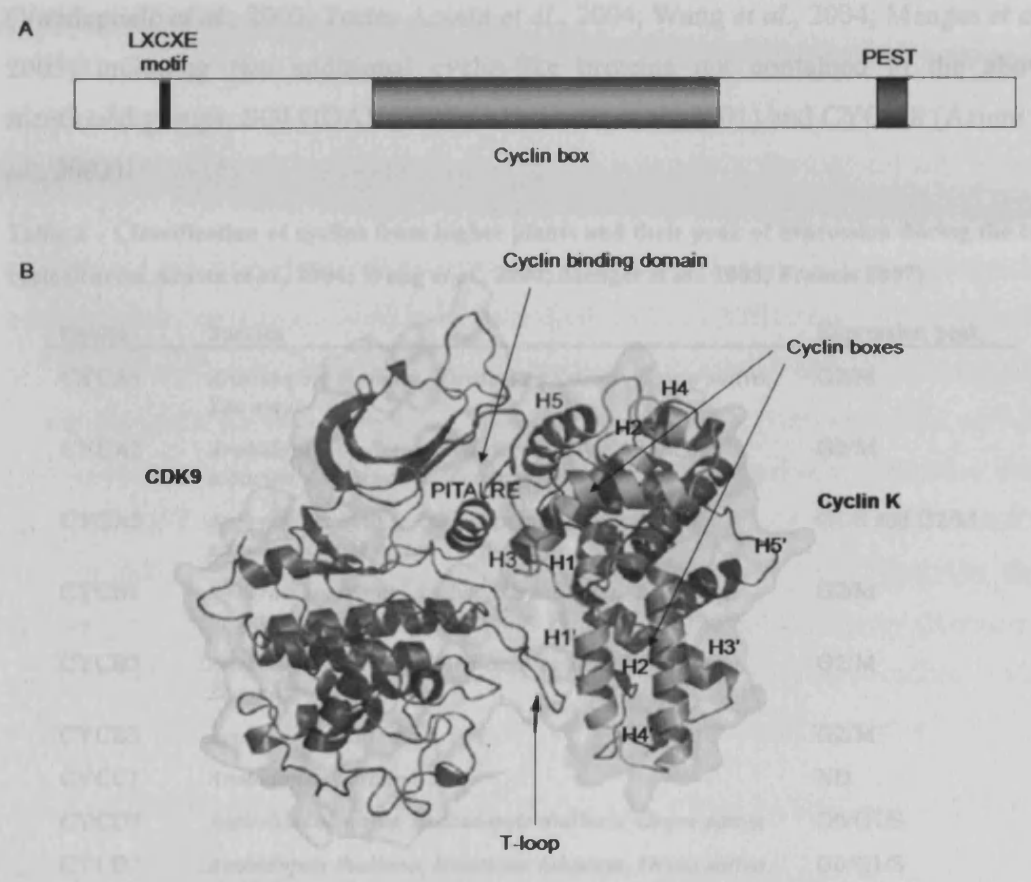

Figure 3 – A) A schematic diagram of the *N. tabacum* CYCD3;2 consisting of an cyclin box, an N-terminal LXCXE motif and a C-terminal PEST sequence (Adapted from Sorrell *et al.*, 1999). B) Model of the *H. sapiens* CDK9/cyclin K complex showing the CDK/cyclin interaction interface consisting of the cyclin binding domain of CDK9 and the N-terminal cyclin box (helices H1 – H5) and the C-terminal cyclin box (helices H1' – H5') of cyclin K. The cyclin boxes also form the binding site for the cyclin binding domain and make contact to the T-loop of the CDK (Adapted from Baek *et al.*, 2007).

Cyclins are divided into many subclasses that share structural and, to some extent, functional homology between animals and plants. At least 13 classes of cyclins (A – L and T) exist in animals (Pines, 1995), whereas only eight classes exist in plants (A – D, H, L, P and T) (Wang *et al.*, 2004; Menges *et al.*, 2005; Francis, 2007) (Table 2). Despite the lower number of classes, plants contain more cyclins than found in other groups of organisms examined. However, in relation to the plant cell cycle, most

is known about the A, B and D classes. Despite the small genome of *A. thaliana*, the number of cyclins was recently expanded from six classes containing 31 cyclins (Renaudin *et al.*, 1996) to 49 cyclins divided into eight classes with 23 subtypes (CYCA1-3, CYCB1-3, CYCC, CYCD1-7, CYCH, CYCL, CYCP1-4 and CYCT) (Vandepoele *et al.*, 2002; Torres Acosta *et al.*, 2004; Wang *et al.*, 2004; Menges *et al.*, 2005) including two additional cyclin-like proteins not contained in the above mentioned groups, SOLODANCERS (Abrahams *et al.*, 2001) and CYCJ18 (Azumi *et al.*, 2002).

Table 2 – Classification of cyclins from higher plants and their peak of expression during the cell cycle (Torres Acosta *et al.*, 2004; Wang *et al.*, 2004; Menges *et al.*, 2005; Francis 2007)

Cyclin	Species	Expression peak
CYCA1	*Arabidopsis thaliana, Nicotiana tabacum, Oryza sativa, Zea mays*	G2/M
CYCA2	*Arabidopsis thaliana, Medicago sativa, Nicotiana tabacum, Oryza sativa, Zea mays*	G2/M
CYCA3	*Antirrhinum majus, Arabidopsis thaliana, Nicotiana tabacum, Oryza sativa*	G1/S and G2/M
CYCB1	*Antirrhinum majus, Arabdopsis thaliana, Nicotiana tabacum, Oryza sativa, Zea mays*	G2/M
CYCB2	*Arabidopsis thaliana, Medicago sativa, Oryza sativa, Zea mays*	G2/M
CYCB3	*Arabidopsis thaliana*	G2/M
CYCC1	*Arabidopsis thaliana*	ND
CYCD1	*Antirrhinum majus, Arabidopsis thaliana, Oryza sativa*	G0/G1/S
CYCD2	*Arabidopsis thaliana, Nicotiana tabacum, Oryza sativa, Zea mays*	G0/G1/S
CYCD3	*Antirrhinum majus, Arabidopsis thaliana, Medicago sativa, Nicotiana tabacum,*	G0/G1/S
CYCD4	*Arabidopsis thaliana*	G2/M
CYCD5	*Arabidopsis thaliana, Oryza sativa, Zea mays*	G0/G1/S
CYCD6	*Arabidopsis thaliana, Oryza sativa*	G0/G1/S
CYCD7	*Arabidopsis thaliana, Oryza sativa*	G0/G1/S
CYCH1	*Arabidopsis thaliana, Oryza sativa*	G2
CYCL	*Arabidopsis thaliana, Oryza sativa*	G0/G1
CYCT1	*Arabidopsis thaliana, Oryza sativa*	ND
CYCP1	*Arabidopsis thaliana, Oryza sativa*	ND
CYCP2	*Arabidopsis thaliana, Oryza sativa*	ND
CYCP3	*Arabidopsis thaliana, Oryza sativa*	ND
CYCP4	*Arabidopsis thaliana, Oryza sativa*	ND

ND: No data

Cell cycle-related cyclins are broadly classified into G1 and mitotic cyclins based on their expression patterns during the cell cycle. A-type cyclins generally appear at the beginning of S-phase and are involved in the S-phase progression. B-type cyclins are present during G2, the G2/M transition and mitosis. In *H. sapiens* the G1 cyclins, CycC, CycD and CycE, were originally identified because of their ability to complement yeast mutants lacking the endogenous G1 cyclins CLN1 – 3 (Lew *et al.*, 1991). Based on similar experiments, the D-type cyclins from *A. thaliana* were described as G1-specific cyclins controlling the progression through G1 and into S-phase (Soni *et al.*, 1995). In plants, the genes encoding the D-type cyclins are induced at specific times during the cell cycle re-entry, but they generally remain expressed at an approximately constant level in actively dividing cells (Dahl *et al.*, 1995; Fuerst *et al.*, 1996; Sorrell *et al.*, 1999). H-type cyclins have been identified in *A. thaliana*, rice, *Oryza sativa* (*O. sativa*, Os), and poplar, *Populus tremulax* (*P. tremulax*). *In vitro* H-type cyclins can act as the regulatory subunit of CAKs positively controlling both CDK and CDT activities (Yamaguchi *et al.*, 2000; Vandepoele *et al.*, 2002). C- and T-type cyclins have not yet been experimentally characterized in plants. However, they are thought to be involved in the control of the transcriptional machinery (Barroco *et al.*, 2003; Fulop *et al.*, 2005). In contrast to the mitotic A- and B-type cyclins, which contain the highly conserved cyclin box, G1 cyclins are not highly conserved.

1.2.3 CDK Activating Kinases (CAKs) and CDK Inhibitors (CKIs)

The activity of CDK/cyclin complexes is not only controlled through the levels of CDK and cyclin due to regulated transcription, translation, protein turnover and intracellular localization, but also by activating and inhibitory phosphorylations. As mentioned, the association of CDKs and cyclins results in a partially activated kinase complex. Full activation of the complex requires phosphorylation of a threonine residue within the T-loop of the CDK. CAKs are responsible for this phosphorylation of threonine residues within the T-loop, as demonstrated for T160/T161 of HsCDK2 (Joubes *et al.*, 2000) and T167 of SpCdc2 (Nurse, 1990). The phosphorylation causes a conformational change that allows proper binding of the substrate and is therefore essential for full activation of the CDC2/cyclin complex (Ohta *et al.*, 1998). The vertebrate CAK is a complex consisting of CDK7/cyclinH/Mat1. CDK7 alone has a low CAK activity, whereas in the presence of cyclinH the CDK7 activity is stimulated. In addition to cyclinH, Mat1 also interacts with the CDK7/cyclinH

complex and functions to stabilize the complex (Tassan *et al.*, 1995). In plants, two classes of CAKs have been identified namely the D-type CDKs, which are functionally related to the vertebrate CAKs and the F-type CDKs, which are plant-specific CAKs (Umeda *et al.*, 2005). Conversely, the kinase activity of the CDKs can also be negatively regulated by the action of inhibitor proteins called CDK Inhibitors (CKIs), which repress the CDK/cyclin complex by masking the ATP binding domain of the CDK until the conditions are suitable and the cell can undergo mitosis (Morgan, 1997; Wang *et al.*, 1997). There is limited sequence conservation between the animal CKIs, known as Kip/Cip proteins, and plant CKIs. In *A. thaliana*, seven genes have so far been identified, which encode proteins with limited homology to the animal Kip/Cip family of CDK inhibitors (Wang *et al.*, 1997; De Veylder *et al.*, 1997; De Veylder *et al.*, 2001b). Since all known plant CKIs share a 31 amino acid domain with the mammalian Kip/Cip protein $p27^{Kip1}$, the plant CKIs have been designated as Kip-related proteins (KRPs). *A. thaliana* KRP1 and KRP2 are homologous to the previously discovered Inhibitors of CDKs, ICK1 and ICK2, which suppress CDK activity in G2 (Wang *et al.*, 1997). AtKRP1 and AtKRP2 are found to inhibit both CYCD2/CDKA and CYCD2/CDKB complexes (Nakai *et al.*, 2006).

1.2.4 The G1/S Transition

The mechanism that regulates cell cycle progression through G1 and into S phase appears to be conserved between mammals and plants and is controlled by the retinoblastoma/adenovirus E2 promoter-binding factor (Rb/E2F) pathway (Figure 4). In G1-phase the S phase transcription factor, E2F, is bound by the Rb protein and this binding represses transcription of E2F-dependent genes including several genes needed for DNA synthesis. In mammals, when the conditions are suitable for progression to S-phase, the Rb protein is phosphorylated by the cyclinD/Cdk4/6 complex. This releases the Rb protein from the E2F and thereby activates E2F (Ezhevsky *et al.*, 1997).

Plant homologues of the Rb protein have been identified in maize, *Zea mays* (*Z. mays*, Zm), tobacco, *Nicotiana tabacum* (*N. tabacum*, Nt), and in *A. thaliana* (Grafi *et al.*, 1996; Nakagami *et al.*, 1999; Kong *et al.*, 2000). In *A. thaliana* the Rb protein can be phosphorylated by the CDKA/CYCD complex, which thereby releases E2F (De Veylder *et al.*, 2002). *In vitro* both *Z. mays* and *H. sapiens* Rb proteins bind to all classes of plant D-type cyclins through the conserved N-terminal LXCXE motif.

Furthermore, *Z. mays* Rb protein can bind *H. sapiens* and fruit fly *Drosophila melanogaster* (*D. melanogaster*, Dm) E2F proteins and thereby inhibit the transcriptional activation of HsE2F (Huntley *et al.*, 1998).

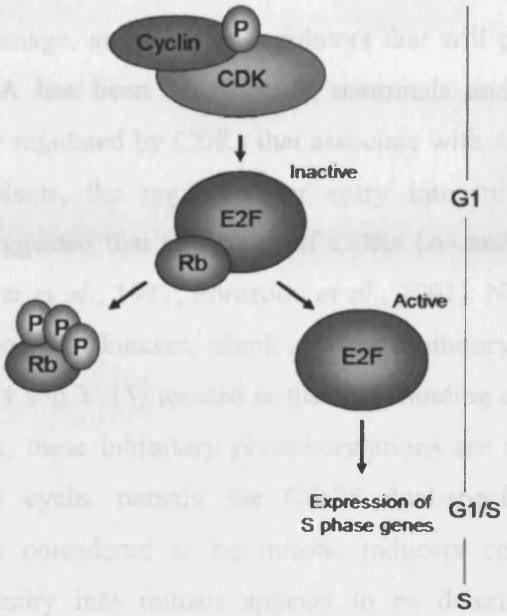

Figure 4 – Model of the regulation of the G1/S transition. In G1 phase, when the conditions are suitable for initiating S phase, the CDK/cyclin complex will phosphorylate the Rb protein, which is released from the E2F protein resulting in activation of E2F and expression of S phase genes (Adapted from Inze and De Veylder, 2006)

Overall, this indicates that the G1/S transition is remarkably similar in mammals and plants involving Rb/Rb-like proteins, E2F and D-type cyclins (Grafi *et al.*, 1996; Huntley *et al.*, 1998). Interestingly, functional homologues to the proteins involved in G1/S have not been found in yeast and other fungi, which could indicate that this G1 checkpoint is a defining event allowing the elaboration of complex multi-cellular organisms (Huntley *et al.*, 1998). However, an Rb protein homologue has been found in the unicellular green alga *Chlamydomonas reinhardii* (*C. reinhardii*, Cr). In contrast to mammalian Rb protein mutants, mutations in the *C. reinhardii* gene did not result in a shortened G1-phase or premature entry into S-phase. Furthermore, the cells differentiated normally (Umen and Goodenough, 2001). These findings indicate that the Rb protein-dependent pathway in unicellular organisms could have a different role than in mammals and plants.

1.2.5 The G2/M Transition

The G2/M phase is a major transition point of the cell cycle and, therefore, it requires negative regulators, which will arrest the cell and prevent it from undergoing mitosis in the case of DNA damage, and positive regulators that will promote the onset of mitosis when the DNA has been repaired. In mammals and insects, the G2/M transition is specifically regulated by CDKs that associate with A- and B-type cyclins (Morgan, 1997). In plants, the regulation or entry into mitosis is still poorly understood, but it is suggested that two types of CDKs (A- and B-type) control the G2/M transition (Magyar *et al.*, 1997; Porceddu *et al.*, 2001). Negative regulators of the cell cycle include the Wee1 kinases, which catalyse inhibitory phosphorylations of threonine residues (T-14 and Y-15) located in the ATP-binding cleft of the CDKs. In both animals and yeast, these inhibitory phosphorylations are removed by positive regulators of the cell cycle, namely the Cdc25 dual-specificity phosphatases. Therefore, Cdc25s are considered to be mitotic inducers controlling the G2/M transition. Moreover, entry into mitosis appears to be determined by a balance between the activities of Cdc25 and Wee1 (Kumagai and Dunphy, 1991; Lee *et al.*, 2001).

Models for cell cycle regulation upon DNA damage in *S. pombe* and higher eukaryotes have been proposed (reviewed in Francis 2003). Upstream of Cdc25 and Wee1 are the sensors of DNA damage, which in higher eukaryotes are the Ataxia-telangiectasia mutated/related (ATM/ATR) proteins and in *S. pombe* the RAD3 protein (Elledge, 1996; Weinert, 1998, Abraham, 2000). The protein kinases ATM and ATR are activated in response to DNA damage by ionising radiation (IR) and ultra-violet (UV) light or to DNA replication damage by hydroxyurea (HU) resulting in the phosphorylation and activation of checkpoint kinases Chk1 and/or Chk2 (Figure 5). These kinases phosphorylate and activate the Wee1 kinase, which then ensures that the phosphorylation of the CDK/cyclin complex is maintained and the cell is arrested in G2. At the same time Chk1/2 phosphorylates and inactivates the Cdc25 phosphatase in order to keep the CDK/cyclin complex in an inactive state. When the DNA damage is repaired and the conditions in the cell are suitable to undergo mitosis, Cdc25 is dephosphorylated and restores the activity of CDK/cyclin complex (Rhind and Russell, 2000; Boutros *et al.*, 2006)

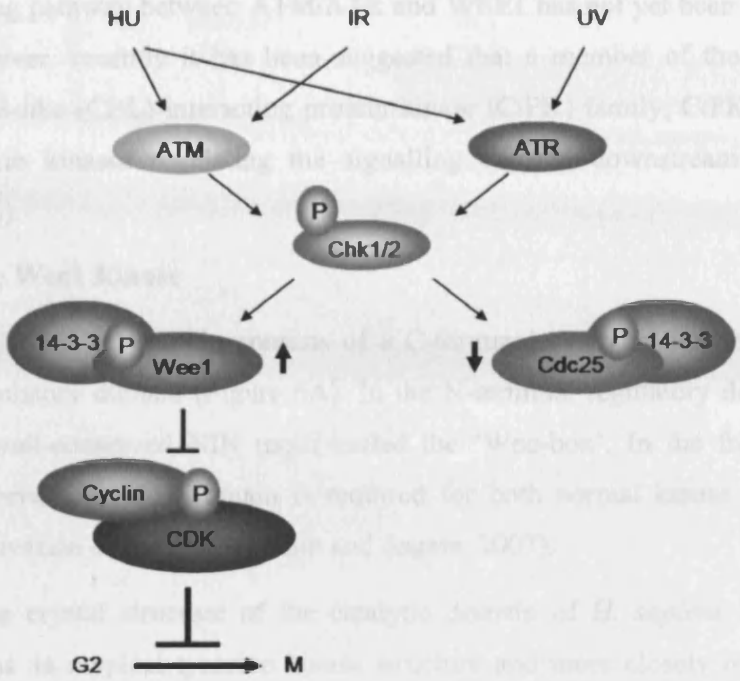

Figure 5 – Model for the eukaryotic G2 DNA damage checkpoint. DNA damage caused by ionising radiation (IR) and ultra-violet (UV) light or DNA replication damage caused by hydroxyurea (HU) is sensed by two kinases ATM and ATR, which then phosphorylates Chk1/2 kinases. This is followed by an activating phosphorylation of Wee1 and a deactivating phosphorylation of Cdc25. Wee1 then ensures that the phosphorylation of CDK/cyclin complex is maintained, whereas Cdc25 is inactive and unable to dephosphorylate and activate the CDK/cyclin complex. Bold arrows indicate change in protein activity following DNA damage.

This model for the G2/M transition has yet to be confirmed in plants, however many of the key proteins in this model have already been identified. Recently, homologues to the ATM and ATR proteins were identified in *A. thaliana* and *atm* mutant plants were found to be hypersensitive towards γ-radiation and the DNA damaging agent methyl methanesulfonate (MMS), but not to UV-B light. Additionally, the *atm* mutants failed to induce the transcription of genes involved in the repair and/or detection of DNA breaks upon irradiation (Garcia *et al.*, 2000; Garcia *et al.* 2003). *A. thaliana atr* mutants were hypersensitive to HU, aphidicolin, and UV-B light, but only mildly sensitive to γ-radiation (Culligan *et al.* 2004). All in all, this corresponds to the functions of the ATM/ATR proteins in other organisms (Wienert, 1988; Abraham, 2000). In addition, a Wee1 homologue and a putative Cdc25 homologue from *A. thaliana* (Sorrell *et al.*, 2002; Landrieu *et al.*, 2004; Sorrell *et al.*, 2005) have been identified and their credibility will be described in detail in the next two sections.

The signalling pathway between ATM/ATR and WEE1 has not yet been described in plants. However, recently it has been suggested that a member of the *A. thaliana* calcineurin B-like (CBL)-interacting protein kinase (CiPK) family, CiPK21, may act as the protein kinases regulating the signalling cascade downstream ATM/ATR (Appendix C).

1.2.5.1 The Wee1 Kinase

Structurally, the Wee1 protein consists of a C-terminal catalytic domain and an N-terminal regulatory domain (Figure 6A). In the N-terminal regulatory domain Wee1 includes a well-conserved NIN motif called the 'Wee-box'. In the frog, *Xenopus laevis* (*X. laevis*, Xl), this domain is required for both normal kinase activity and mitotic inactivation of Wee1 (Okamoto and Sagata, 2007).

Recently, the crystal structure of the catalytic domain of *H. sapiens* Wee1A was solved. It has an atypical tyrosine kinase structure and more closely resembles the structure of serine/threonine kinases. The catalytic domain contains the active site cleft, with the highly conserved motif HXD, which closely matches the protein kinase consensus sequence IV**HXD**LKPXNIX. The active site cleft is located between the N- and C-terminal lobes and provides the binding site for the Wee1A inhibitor PD0407824, which acts as an antagonist of the natural ATP substrate (Squire *et al.*, 2005) (Figure 6B)

Originally, the Wee1 protein was isolated as a negative regulator of cell division in *S. pombe*. Loss of Wee1 function resulted in a smaller cell size, due to premature entry into mitosis and conversely, an increased Wee1 expression resulted in an increased cell size, due to delayed entry into mitosis. These findings linked Wee1 activity with both timing of entry into mitosis and regulation of cell size (Russell and Nurse, 1987). Wee1 kinases have been reported in plants, such as *Z. mays*, *A. thaliana, O. sativa* and tomatoes, *Lycopersicon esculentum* (*L. esculentum*, Le) and *Solanum lycopersicum* (*S. lycopersicum*, Sl) (Sun *et al.*, 1999; Sorrell *et al.*, 2002; Vandepoele *et al.*, 2002; Gonzalez *et al.*, 2004; Gonzalez *et al.*, 2007; Guo *et al.*, 2007).

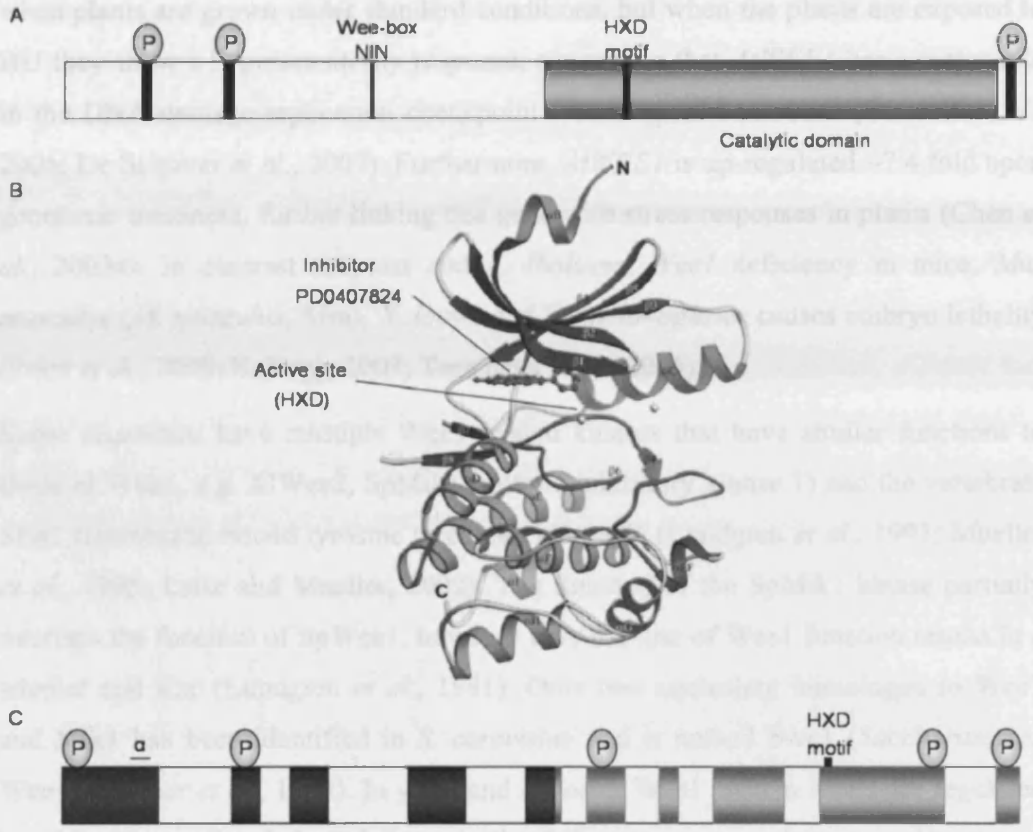

Figure 6 – A) Schematic diagram of a Wee1 kinase consisting of a C-terminal catalytic domain/kinase domain containing the active site (HXD) and an N-terminal regulatory domain. The known serine phosphorylation sites of *H. sapiens* Wee1A (S53, S121/S123 and S642) are shown. B) The structure of the catalytic domain of *H. sapiens* Wee1A The active site cleft is located between the N- and C-terminal lobes and provides the binding site for the Wee1A inhibitor PD0407824 (ball and stick representation) (Adapted from Squire *et al.*, 2005). C) Schematic diagram of *A. thaliana* WEE1 consisting of a C-terminal catalytic domain/kinase domain encoded by exons 5 – 10 (grey boxes) containing the active site (HXD) and an N-terminal regulatory domain encoded by exons 1 – 5 (black boxes). The phosphorylation sites in the putative 14-3-3 binding motifs (T15, S144, T247, S450 and S485) of AtWEE1 are shown including the AtWEE1 recognition site for the NtWEE1 antibody (α) (Chapter 6 and 7).

Over-expression of *A. thaliana* and *Z. mays* WEE1s in *S. pombe* inhibited cell division and caused the cells to enlarge significantly (Sun *et al.*, 1999; Sorrell *et al.*, 2002), which is consistent with the original findings in *S. pombe*. *AtWEE1* expression is confined to proliferative tissues (Sorrell *et al.*, 2002) and the AtWEE1 protein can phosphorylate CDKA and CDKD types *in vitro* (Shimotohno *et al.*, 2006) suggesting a similar function of the plant *WEE1* as its homologues in other organisms. However, *WEE1* deficiency in *A. thaliana* does not result in a distinctive mutant phenotype

when plants are grown under standard conditions, but when the plants are exposed to HU they show a hypersensitivity response, suggesting that *AtWEE1* has a major role in the DNA damage replication checkpoint when exposed to stress (Boudolf *et al.*, 2006; De Schutter *et al.*, 2007). Furthermore, *AtWEE1* is up-regulated ~7.4 fold upon genotoxic treatment, further linking this gene with stress responses in plants (Chen *et al.*, 2003a). In contrast to yeast and *A. thaliana*, *Wee1* deficiency in mice, *Mus musculus* (*M. musculus*, Mm), *X. laevis* and *D. melanogaster* causes embryo lethality (Price *et al.*, 2000; Kellogg, 2003; Tominaga *et al.*, 2006).

Some organisms have multiple Wee1-related kinases that have similar functions to those of Wee1, *e.g.* XlWee2, SpMik1 (mitotic inhibitory kinase 1) and the vertebrate Myt1 (membrane-bound tyrosine threonine kinase 1) (Lundgren *et al.*, 1991; Mueller *et al.*, 1995; Leise and Mueller, 2002). The function of the SpMik1 kinase partially overlaps the function of SpWee1, however only the loss of Wee1 function results in a smaller cell size (Lundgren *et al.*, 1991). Only one equivalent homologue to Wee1 and Mik1 has been identified in *S. cerevisiae* and is named Swe1 (*Saccharomyces* Wee1) (Booher *et al.*, 1993). In yeast and *X. laevis* Wee1 protein levels are regulated by ubiquitin-mediated degradation via the 26S proteasome, whereas in *H. sapiens* Wee1 is regulated both by phosphorylation and degradation (Michael and Newport, 1998; Goes and Martin, 2001; Watanabe *et al.*, 2004; Watanabe *et al.*, 2005). Furthermore, in *M. musculus* Wee1 levels are also controlled by components of the circadian clock, thereby linking the circadian clock, the cell cycle and cell proliferation (Matsuo *et al*,. 2003)

1.2.5.2 The Cdc25 Phosphatase

The positive regulation of the cell cycle is carried out by the dual-specificity phosphatase Cdc25. The generic Cdc25 protein consists of a variable N-terminal regulatory domain and a highly conserved C-terminal catalytic domain containing the CH2A, the active site between amino acids C-430 and R-436 (CXXXXXR) and the CH2B motifs (Figure 7A and B). The CH2A and CH2B motifs are important for maintaining the structural conformation of the Cdc25 protein (Fauman *et al.*, 1998). The Cdc25 phosphatases have a rhodanese-like topology, although they share only a limited sequence homology to this protein family (Fauman *et al.*, 1998; Bordo and Bork, 2002).

In *H. sapiens*, there are three Cdc25 genes encoding the proteins CDC25A, B and C, where the latter one is the closest homologue to SpCdc25 (Kumagai and Dunphy, 1991). During interphase, HsCDC25C is predominantly phosphorylated at S216 (Peng *et al.*, 1997). Conversely, this site is not phosphorylated during mitosis, suggesting that phosphorylation of S216 negatively regulates CDC25C function. Several kinases that phosphorylate specific serine residues of CDC25 have been described including Chk1 (Furnari *et al.*, 1997; Peng *et al.*, 1997; Sanchez *et al.*, 1997) and Cds1/Chk2 (Matsuoka *et al.*, 1998). In animals, most data indicate that phosphorylation of Cdc25 results in its sequesteration in the cytoplasm and thereby keeping it away from the Cdc2/CyclinB complex (Chan *et al.*, 1999). In contrast, this nuclear exclusion of Cdc25 is unnecessary in *S. pombe* (Lopez-Girona *et al.*, 2001).

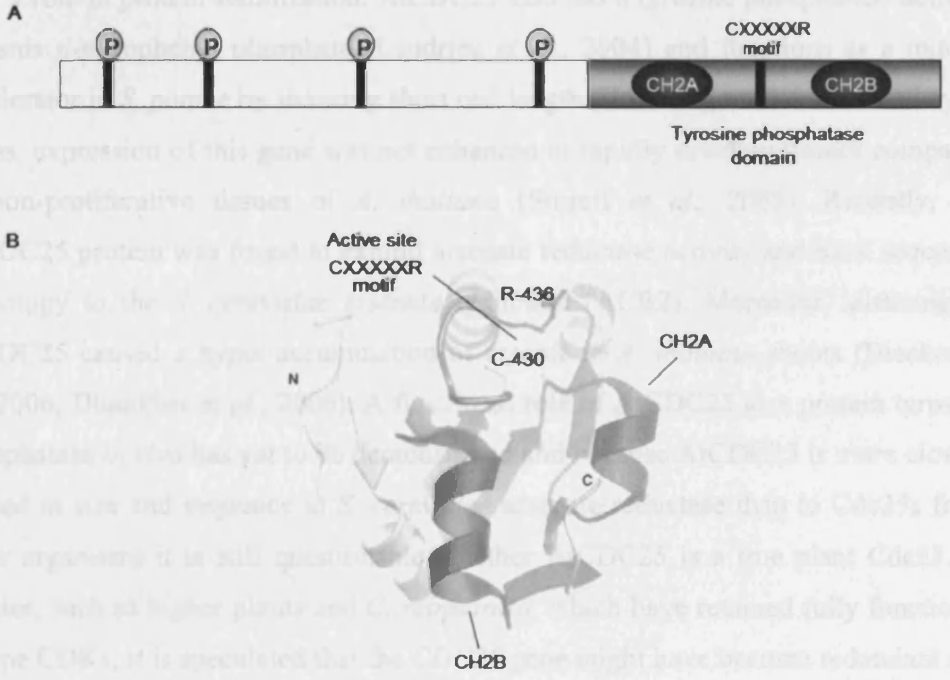

Figure 7 – A) Schematic diagram of a Cdc25 phosphatase consisting of an N-terminal regulatory domain and a C-terminal catalytic domain containing the CH2A, the active site (CXXXXXR) and CH2B motifs including known phosphorylation sites of *H. sapiens* CDC25 (S75, T130, S216 and S309/S323) (Adapted from Boutros *et al.*, 2006). B) The structure of the catalytic domain of *H. sapiens* CDC25A showing the CH2A and CH2B motifs, the active site between amino acids C430 and R436 (CXXXXXR) and finally the N- and C-terminal lobes (Adapted from Fauman *et al.*, 1998).

The first green lineage Cdc25 ortholog was discovered in the multicellular alga *Osterococcus tauri* (*O. tauri*, Ot). It encodes a protein, which is able to rescue the *S. pombe cdc25-22* conditional mutant (Khadaroo *et al.*, 2004). Furthermore, recombinant OtCdc25 was shown to dephosphorylate a CDK1/CyclinB complex *in vivo*. Recently, a small Cdc25 phosphatase isoform was discovered in *A. thaliana* consisting of only the catalytic domain with a similar fold to the catalytic domain of HsCDC25A and B. AtCDC25 contains the CXXXXXR phosphatase active site and the polypeptide shows 25 – 30% identity to the C-terminal domains of yeast and animal Cdc25 proteins. The 3D structure of AtCDC25 further confirms that the protein belongs to the CDC25 family by having a fold similar to the catalytic domain of HsCDC25A and HsCDC25B. In contrast to the CDC25 proteins from *H. sapiens*, the C-terminal domain of AtCDC25 contains a zinc-binding loop, which is thought to play a role in protein stabilization. AtCDC25 also has a tyrosine phosphatase activity towards *p*-nitrophenyl phosphate (Landrieu *et al.*, 2004) and functions as a mitotic accelerator in *S. pombe* by inducing short cell length. However, unlike other cell cycle genes, expression of this gene was not enhanced in rapidly dividing tissues compared to non-proliferative tissues of *A. thaliana* (Sorrell *et al.*, 2005). Recently, the AtCDC25 protein was found to exhibit arsenate reductase activity and have sequence homology to the *S. cerevisiae* arsenate reductase (ACR2). Moreover, silencing of AtCDC25 caused a hyper-accumulation of arsenic in *A. thaliana* shoots (Bleeker *et al.*, 2006; Dhankher *et al.*, 2006). A functional role of AtCDC25 as a protein tyrosine phosphatase *in vivo* has yet to be demonstrated and because AtCDC25 is more closely related in size and sequence to *S. cerevisiae* arsenate reductase than to Cdc25s from other organisms it is still questionable whether AtCDC25 is a true plant Cdc25. In species, such as higher plants and *C. reinhardtii*, which have retained fully functional B-type CDKs, it is speculated that the *CDC25* gene might have become redundant and consequently lost through evolution (Boudolf *et al.*, 2006). However, that AtCDC25 functions as an arsenate reductase should not exclude it from being a plant CDC25, since it was recently shown that the *H. sapiens* CDC25A can be suppressed by arsenite (Lehmann and McCabe, 2007).

In yeast and animals, the action of checkpoint phosphorylations of Wee1 and Cdc25 are, at least in part, mediated by the binding of 14-3-3 proteins (Forbes *et al.*, 1998; Kumagai and Dunphy, 1999; Yang *et al.*, 1999; Wang *et al.*, 2000; Lee *et al.*, 2001;

Rothblum-Oviatt *et al.*, 2001). These proteins have an important role in cell cycle checkpoints, where they function by binding and protecting the phosphorylations of both Wee1 and Cdc25 and thereby activating or inactivating them, respectively (Lee *et al.*, 2001).

1.2.6 14-3-3 Proteins

The 14-3-3 protein family was originally identified by Moore and Perez (1967) during a systematic classification of brain proteins. The name '14-3-3' denotes the elution fraction (14^{th}) containing these proteins after DEAE-cellulose chromatography and their migration position after subsequent starch gel electrophoresis (3.3). The 14-3-3 protein family is highly conserved in both plants and animals and they are expressed in a cell- and tissue-specific manner (Aitken, 2002; Alsterfjord *et al.*, 2004; Dougherty and Morrison, 2004). Two isoforms are present in yeasts, *X. laevis* and *Caenorhabditis elegans* (*C. elegans*, Ce), seven isoforms in *H. sapiens* and up to 15 isoforms in plants (Wang and Shakes, 1996; Rosenquist *et al.*, 2001; Aitken, 2002; Ferl *et al.*, 2002; Chen *et al.*, 2006) (Table 3). One possible reason for the 14-3-3 isoform diversity could be to assure fundamental 14-3-3 presence in all cell types and compartments where 14-3-3 function is required.

Table 3 - 14-3-3 isoforms in different organisms (Wang and Shakes, 1996; Rosenquist *et al.*, 2001; Aitken, 2002; Ferl *et al.*, 2002; Chen *et al.*, 2006).

Organism	14-3-3 isoforms
S. cerevisiae	Bmh1and Bmh2
S. pombe	Rad24 and Rad25
X. laevis	ε and ξ
C. elegans	PAR-5 (1 and 2)
H. sapiens	β, ε, η, γ, τ, ξ and σ
Z. mays	GF14-6 and 12
O. sativa	GF14 a, b, c, d, e and f
N. tabacum	A, B, C, D, E, F, G, H, I, J and K
A. thaliana	Grf1 – 13 (χ, ω, ψ, φ, υ, λ, ν, κ, μ, ε, ο, ι and π)

More than 200 proteins have been shown to interact with 14-3-3 proteins and the list is still expanding (Jin *et al*,. 2004; Meek *et al.*, 2004; Pozuelo Rubio *et al.*, 2004). Binding of 14-3-3 proteins can result in various effects largely depending on the

protein the 14-3-3 protein is bound to. In most cases 14-3-3 binding occurs after phosphorylation of the binding partner leading to activation or repression of enzymatic activity or function, prevention of degradation, cytoplasmic sequestration/nuclear retention or facilitation/prevention of protein modifications (reviewed in Tzivion *et al.*, 2001; Yaffe, 2002; Hermeking, 2003) (Figure 8A).

Two high affinity phosphorylation-dependent binding motifs are recognized by all 14-3-3 isoforms examined: RSXpSXP (mode I) and RXXXpSXP (mode II), where pS represents phosphoserine, which in some cases can be replaced by a phosphothreonine (Yaffe *et al.*, 1997; Rittinger *et al.*, 1999). However, phosphorylation-dependent sites, which diverge significantly from these motifs, have also been described (Aitken, 2002). In addition to the phospho-peptide binding ability of 14-3-3 proteins, they also bind to un-phosphorylated targets, such as WLDLE and RXSX(S/T)XP (Masters *et al.*, 1999; Wang *et al.*, 1999). Although target binding can occur in the same location as the phosphorylated targets the vast majority of 14-3-3 targets are bound in a phosphorylation-dependent manner (Pozuelo Rubio *et al.*, 2004). Additionally, a C-terminal mode III binding motif (pS/pTX_{1-2}) has a role in re-directing proteins to the cell surface (Coblitz *et al.*, 2005; Shikano *et al.*, 2005).

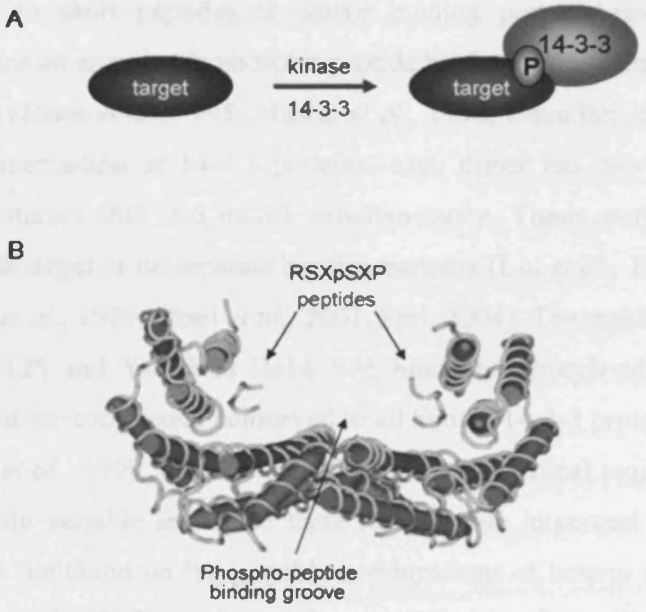

Figure 8 – A) Schematic diagram of a 14-3-3 protein binding to a phosphorylated target protein. B) The crystal structure of a 14-3-3 dimer complexed with mode I (RSXpSXP) target peptides showing the phospho-peptide binding groove composed of the two 14-3-3 monomers (Adapted from Ferl, 2004).

Animal 14-3-3s, and possibly also plant 14-3-3s, can be phosphorylated themselves and it has been suggested that phosphorylations of 14-3-3s can inhibit their interaction with the target proteins (Lu *et al.*, 1994; Dubois *et al.*, 1997; Olivari, 2000). Therefore, these phosphorylations could be a mechanism for isoform-specific regulation of 14-3-3 proteins since the phosphorylation sites are not conserved between the different 14-3-3 isoforms (Roberts, 2003). Because of the relatively simple 14-3-3 binding motif 14-3-3 proteins are in general thought to be 'sticky' and in a report by Sehnke *et al.* (2002a) it was estimated that if only the two general mode I and II 14-3-3 binding motifs were considered, the potential proteins containing these broadly defined binding motifs would be in excess of 30 – 40% of the *A. thaliana* proteome. Obviously, not all of these proteins would be affected by 14-3-3 binding either because the target protein is in another cellular compartment than the 14-3-3 protein or because many of the binding motifs might be found in interior regions of the protein and therefore be unavailable for phosphorylation or interaction with 14-3-3 proteins.

Structurally 14-3-3s are highly helical proteins that can form cup-shaped hetero- and/or homodimers (Figure 8B). Crystal structures and mutational studies of 14-3-3 dimers binding to short peptides or native binding partners revealed that each monomer contains an amphipatic phospho-peptide binding groove that acts as a ligand binding domain (Jones *et al.*, 1995; Muslin *et al.*, 1996; Chaudhri *et al.*, 2003). As a result of the dimerisation of 14-3-3 proteins, each dimer has two binding pockets allowing it to interact with two motifs simultaneously. These motifs can be found either on a single target or on separate binding partners (Liu *et al.*, 1995; Yaffe *et al.*, 1997; Rittinger *et al.*, 1999; Obsil *et al.*, 2001, Ferl, 2004). The residues equivalent to K-50, R-57, R-128 and Y-129 of Hs14-3-3ξ bind phosphorylated residues of the target protein and are completely conserved in all known 14-3-3 proteins (Yaffe *et al.*, 1997; Rittinger *et al.*, 1999; Obsil *et al.*, 2001). The N-terminal region of the 14-3-3 isoforms is highly variable and since these residues are important for dimerisation there could be a limitation on the possible combinations of hetero- and homodimers that could be formed, which may give a degree of functional specificity to the 14-3-3 proteins (Jones *et al.*, 1995; Chaudhri *et al.*, 2003).

To date many reasons have been proposed for the large 14-3-3 protein families. One reason could be that a very large amount of the protein is needed and therefore the

number of genes encoding the proteins is increased. Another reason could be that specific isoforms are localized to specific sub-cellular compartments or that the different isoforms are expressed during different developmental stages and/or in different cell types or tissues. Finally, it could be that each of the 14-3-3 isoforms are more or less specific for their target proteins.

1.2.6.1 14-3-3 Proteins in Cell Cycle Regulation

The connection between 14-3-3 proteins and cell cycle regulation was first discovered in *S. pombe*, where the two 14-3-3 genes, *rad24* and *rad25*, were found to be required for the G2/M checkpoint and have a function in determining the timing of mitosis (Ford *et al.*, 1994). As previously mentioned, 14-3-3 proteins can regulate cellular processes by modulating protein localization. A deletion of *rad24* in *S. pombe* causes nuclear accumulation of Cdc25 (Zeng and Piwnica-Worms, 1999) and in *H. sapiens* and *X. laevis* binding of 14-3-3 sequesters CDC25 in the cytoplasm preventing premature activation of the CDK (Graves *et al.*, 2001). Furthermore, for HsCDC25C to function during mitosis, 14-3-3 binding must be disrupted, exposing a nuclear localization motif that allows the translocation of CDC25C to the nucleus leading to activation of the CDK/cyclin complex (Kumagai and Dunphy, 1999; Yang *et al.*, 1999; Graves *et al.*, 2001). In *H. sapiens*, the *14-3-3σ* gene is strongly up-regulated in cells exposed to ionizing radiation and DNA damaging agents (Hermeking *et al.*, 1997) and appears to be essential for maintaining the G2/M checkpoint. However, in contrast to other *H. sapiens* 14-3-3 isoforms, 14-3-3σ does not bind CDC25C. Cells lacking 14-3-3σ are capable of initiating G2/M arrest, but are unable to remain in this state, leading to cell death (Chan *et al.*, 1999). This particular 14-3-3 protein contains a second phospho-independent ligand binding site, which is thought to be involved in selecting specific ligands (Wilker *et al.*, 2005). Binding of 14-3-3 proteins to HsCDC25A and HsCDC25B inhibits CDC25 activity by blocking the access of CDK/cyclin complex to its catalytic site (Conklin *et al.*, 1995; Forrest and Gabrielli, 2001; Chen *et al.*, 2003b). In *X. laevis*, 14-3-3 proteins together with Chk1 have been shown to function as positive regulators of Wee1. During mitosis the interaction between 14-3-3 and Wee1 proteins is reduced, leading to a loss in Wee1 kinase activity (Lee *et al.*, 2001). Similarly, *H. sapiens* 14-3-3β acts as a positive regulator for Wee1 during the cell cycle by binding to the C-terminal catalytic region of Wee1 and thereby increasing the stability of Wee1. Furthermore, a Wee1 S642A mutant was

found to be less active in phosphorylating CDK and therefore not efficient in inducing a G2 cell cycle delay (Wang *et al.*, 2000; Rothblum-Oviatt *et al.*, 2001). The importance of 14-3-3s is also evident by the lethal phenotype derived from the simultaneous knockout of *S. cerevisiae bmh1* and *bmh2* genes (Gelperin *et al.*, 1995) and the similar results that were obtained for the *S. pombe rad24/rad25* double mutant. However, knock-out of the *rad25* gene alone resulted only in a mild sensitivity to DNA damaging agents and a marginal reduction in the duration of mitotic delay following irradiation (Ford *et al.*, 1994).

If and how 14-3-3 proteins act in the plant cell cycle is yet largely unknown. So far only a few reports suggest that plant 14-3-3s are involved in cell cycle regulation. Three 14-3-3 proteins (ω, λ and κ) from *A. thaliana* were found to interact with *S. pombe* Cdc25, but only the 14-3-3ω isoform could complement a *S. pombe rad24*⁻ mutant (Sorrell *et al.*, 2003). In addition, other 14-3-3 isoforms (μ, υ, χ and φ) from *A. thaliana* were shown to complement the lethal *S. cerevisiae bmh* double mutant (van Heusden *et al.*, 1996; Kuromori and Yamamoto, 2000). Finally, the *A. thaliana* 14-3-3ω isoform accumulates differentially in the cell nucleus in a cell cycle-dependent manner suggesting a role in cell division (Cutler *et al.*, 2000).

1.2.6.2 *A. thaliana* 14-3-3 Proteins

The largest and best characterized 14-3-3 protein family in plants is found in *A. thaliana*. As mentioned, it consists of up to 15 isoforms, where 13 are translated isoforms and the remaining two are considered as pseudo-forms. The first isoforms discovered from the *A. thaliana* 14-3-3 protein family, the 14-3-3ω, ψ, χ, φ and υ isoforms, were found while studying the regulation of *Alcohol dehydrogenase* (*Adh*) genes in *A. thaliana* by detecting components of the G-box binding complex (Lu *et al.*, 1992; Lu *et al.*, 1994). Therefore, the *A. thaliana* 14-3-3 proteins are also referred to as General regulatory factors (Grf) 1 – 13. The 14-3-3 κ, λ and ε isoforms were identified subsequently by using the χ isoform as bait in a yeast two hybrid screen (Wu *et al.*, 1997b). The remaining isoforms μ, ν, ο, ι and π have been identified by database analyses as having sequence homology to the previously found 14-3-3 proteins (DeLille *et al.*, 2001; Rosenquist *et al.*, 2000; Wu *et al.*, 1997b).

The *A. thaliana* 14-3-3 isoforms range in length from 241 – 286 amino acids and share a conserved core, with the N-terminus and C-terminus being more divergent

suggesting that the different isoforms may perform different functions. Phylogenetically, the members of the *A. thaliana* 14-3-3 protein family break off into two major evolutionary branches, the Epsilon and the Non-Epsilon group (Figure 9A). Characteristic for the Non-Epsilon group is the presence of an EF hand-like divalent cation-binding motif (Lu *et al.,* 1994), which was recently shown by Manak and Ferl (2007) to be important for an enhanced binding of the 14-3-3 proteins to phospho-peptides.

The Epsilon group breaks into two sub-branches, with 14-3-3o and ι on one sub-branch and 14-3-3μ, ε and π in the second sub-branch. The Non-Epsilon group comprises three very distinct sub-branches. One sub-branch consists of 14-3-3κ and λ, the second of 14-3-3ψ, ν and υ and the third of 14-3-3φ, χ and ω. The grouping of the 14-3-3 isoforms into the Epsilon and Non-Epsilon groups is also well supported by exon-intron structure (Figure 9B). The members of the Non-Epsilon group contain four exons that are relatively conserved in size, while the members of the Epsilon group contain five and six exons (Wu *et al.,* 1997a; DeLille *et al.*, 2001).

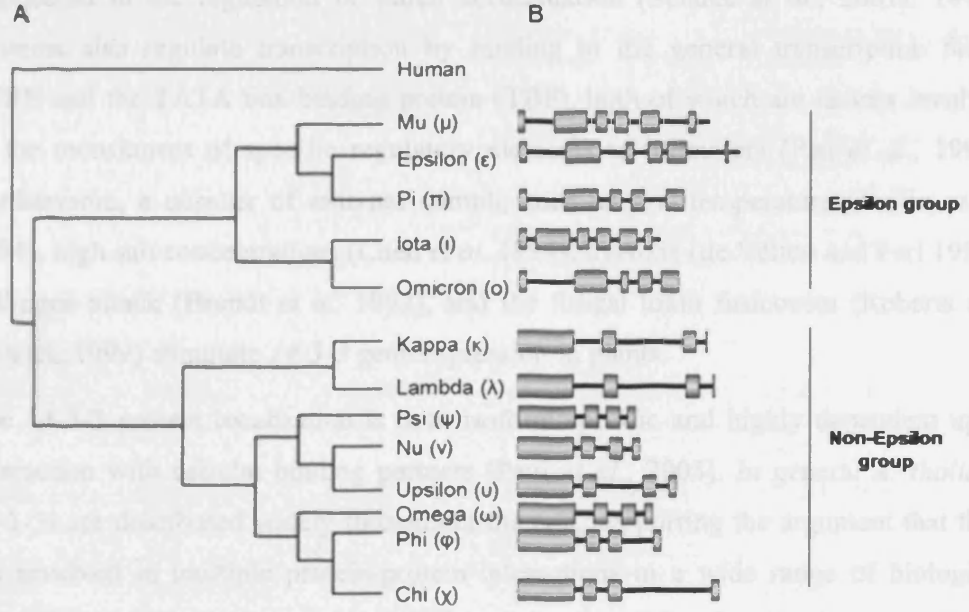

Figure 9 – A) A phylogenetic tree of the *A. thaliana* 14-3-3 family showing the two major evolutionary branches consisting of the Epsilon group and the Non-Epsilon group 14-3-3 proteins. *H. sapiens* 14-3-3 is used as an out group. The phylogenetic tree is based on phylogenetic analyses of sequence data and gene structure (Adapted from DeLille *et al.,* 2001). B) The structure of the *A. thaliana* 14-3-3 genes. Grey boxes represent exons and black lines represent introns (Adapted from http://www.hos.ufl.edu/ferllab/).

During the last decade the knowledge of the functional roles of the different *A. thaliana* 14-3-3 isoforms has increased considerably. They are found to play important roles in regulating enzyme reactions through functions in signal transduction and gene expression. One of the earliest defined functions for plant 14-3-3s was the inhibition of nitrate reductase, which is a key enzyme in nitrogen metabolism (Bachmann *et al.*, 1996; Moorhead *et al.*, 1996). In *A. thaliana* the 14-3-3 isoforms ω, χ and υ were found to have a lower affinity for nitrate reductase (binding motif R/KXXpSTP) *in vivo*, while the φ and ψ isoforms show very poor affinity compared to other isoforms (Bachmann *et al.*, 1996). Probably the best studied function of *A. thaliana* 14-3-3s is their involvement in the activation of the plasma membrane H^+ATPase (binding motif PSHYPTV) (Jahn *et al.*, 1997; Rosenquist *et al.*, 2000). The 14-3-3φ isoform has highest affinity for the H^+ATPase, followed by the χ and ν isoforms. The ψ, υ, and ε isoforms have intermediate binding affinity, whereas the ω isoform has below average binding affinity and the κ and λ isoforms have poor binding affinity (Rosenquist *et al.*, 2000). Additionally, At14-3-3μ and ε are implicated in the regulation of starch accumulation (Sehnke *et al.*, 2001). 14-3-3 proteins also regulate transcription by binding to the general transcription factor TFIIB and the TATA box-binding protein (TBP), both of which are factors involved in the recruitment of specific regulatory elements to promoters (Pan *et al.*, 1999). Furthermore, a number of external stimuli, such as low temperature (Jarillo *et al.* 1994), high salt concentrations (Chen *et al.* 1994), hypoxia (de Vetten and Ferl 1995), pathogen attack (Brandt *et al.* 1992), and the fungal toxin fusicoccin (Roberts and Bowles, 1999) stimulate *14-3-3* gene expression in plants.

The 14-3-3 protein localization is both isoform-specific and highly dependent upon interaction with cellular binding partners (Paul *et al.*, 2005). In general *A. thaliana* 14-3-3s are distributed widely throughout the cell, supporting the argument that they are involved in multiple protein-protein interactions in a wide range of biological roles. However, some degree of differential sub-cellular localization among the specific isoforms is found suggesting an element of specialization among the different isoforms (Ferl *et al.*, 2002; Sehnke *et al.*, 2002b) (Table 4). The 14-3-3 isoforms are distributed throughout the cell and all the 14-3-3 isoforms, except for the Epsilon group 14-3-3μ, are localized in the nucleus, plasma membrane/cell wall and in the cytoplasm (Bihn *et al.*, 1997; Sehnke *et al.*, 2002b). Interestingly, the Epsilon group

14-3-3 isoforms ε and μ are located in leaf starch grains, which could suggest that the Epsilon group 14-3-3s have functional properties different to those of the Non-Epsilon 14-3-3s (Sehnke *et al.*, 2001).

Table 4 – Overview of the *A. thaliana* 14-3-3 family displaying the gene and isoform name, locus, cellular localization and in which tissues and cellular compartments the different 14-3-3 proteins are expressed (Cutler *et al.*, 2000; Daugherty *et al.*, 1996; Ferl *et al.*, 2002; Sehnke *et al.*, 2002b; Sorrell *et al.*, 2003)

Gene	Isoform	Locus	Localization	Expression
Non-Epsilon group				
Grf1	Chi (χ)	At4g09000	Nucleus	Stigma, siliques, pollen, flowers, epidermal cells, roots
Grf2	Omega (ω)	At1g78300	Nucleus, cytoplasm	Suspension cells, roots, pollen, flowers, siliques
Grf3	Psi (ψ)	At5g38480	ND	Leaves, stems, flowers
Grf4	Phi (φ)	At1g35160	Nuclear and plasma membrane, cytoplasm	Cell suspension, seedlings, roots, shoot apex
Grf5	Upsilon (υ)	At5g16050	Nuclear and plasma membrane, cytoplasm	Cytosol, chloroplast stroma, roots, pollen
Grf6	Lambda (λ)	At5g10450	Nucleus, plasma membrane, cytoplasm	Seedlings, leaves, stems, flowers
Grf7	Nu (ν)	At3g02520	Nuclear and plasma membrane, cytoplasm	Cytosol, chloroplast stroma, shoot apex, flower, suspension cells
Grf8	Kappa (κ)	At5g65430	Nucleus, plasma membrane/cell wall, cytoplasm	Seeds, seedlings, root, root hairs, stem, leaves
Epsilon group				
Grf9	Mu (μ)	At2g42590	Leaf starch grains	Cytosol, chloroplast stroma, seedlings, flowers, stems, leaves
Grf10	Epsilon (ε)	At1g22300	Nuclear and plasma membrane, cytoplasm, leaf starch grains	Cytosol, chloroplast stroma, seedlings, roots, leaves
Grf11	Omicron (ο)	At1g34760	ND	Leaves, roots, flowers
Grf12	Iota (ι)	At1g26480	ND	Pollen, flowers, stamen
Grf13	Pi (π)	At1g78220	ND	Siliques, pollen, root, root hairs

ND: No data

2 Experimental Aims

The basic machinery that controls cell cycle progression in plants is similar to that of yeast and mammals, where the G2/M checkpoint acts as a size controller and also responds to DNA damage by delaying entry into mitosis. However, the general model for the G2/M transition in higher eukaryotes has still to be confirmed in plants, although many of the key proteins have already been identified, such as ATM/ATR, WEE1, a putative CDC25 and 14-3-3s (Garcia *et al.*, 2000; Ferl *et al.*, 2002; Sorrell *et al.*, 2002; Culligan *et al.*, 2004; Landrieu *et al.*, 2004; Sorrell *et al.*, 2005).

In the work presented in this thesis, I have investigated how the plant G2/M cell cycle checkpoint functions and how features of the yeast and animal G2/M model apply to the plant model. The main aims were:

The identification of interaction partners for *A. thaliana* WEE1 and CDC25

- Yeast two hybrid (Y2H) library screens were performed using WEE1 and CDC25 as bait against an *A. thaliana* root cDNA library
- Targeted Y2H screens were performed using WEE1 and CDC25 as bait against the eight members of the *A. thaliana* Non-Epsilon 14-3-3 protein family
- Confirmation of one selected protein-protein interaction *in vitro* using co-immunoprecipitation and *in vivo* in *N. tabacum* BY-2 cells using bi-molecular fluorescence complementation (BiFC)
- Identification and mutagenesis of a putative 14-3-3 protein binding site in the AtWEE1 protein

The analysis of *N. tabacum* WEE1 during the cell cycle

- WEE1 protein level and kinase activity were monitored in synchronised *N. tabacum* BY-2 cells using an antibody produced against *N. tabacum* WEE1.

The analysis of the *in vivo* function and stress response of *A. thaliana* WEE1

- Phenotype, transcript, protein and kinase activity levels of *wee1* T-DNA insertion lines were analyzed in the presence and absence of the DNA replication blocking agent, HU.

3 General Materials and Methods

This chapter comprises the material and methods used in two or more of the subsequent chapters of this thesis. Materials and methods specific to a subsequent chapter will be described therein.

3.1 Primers

Primers were all purchased from Sigma-Genosys, UK.

#	Application and primer name	Sequence	Bp
Genotyping of *wee1* T-DNA insertion lines			
1	P1	GGATTAAGGAGAGTTAATTCATGTTT	26
2	P2	CCATCTCAAATCTAAAGTCAGATCT	25
3	P3	GATGCCAATTGCGGAGAGAAGGA	23
4a	P4a	GACCAGGTAGAATTTGAATGATTTC	25
4b	P4b	GAAATCATTCAAATTCTACCTGGTC	25
5	SALK LB	GTTGCCCGTCTCACTGGTGA	20
6	GABI LB	ATATTGACCATCATACTCATTGC	23
Transcriptional analysis of *wee1* T-DNA insertion lines			
7	WEE1 5'UTR fw	GAGAGCGCGCAAATTTTGAA	20
8	WEE1 E1 fw	AGAAGAAGTCTTGGCTAAGAA	21
9	WEE1 E1 rv	TTGCTGATATCTAAGCCGCT	21
10	WEE1 E2 rv	ATTGGTGCTGGACATTTCAGT	20
11	WEE1 E6 fw	CTGATGCATAATCACCAAGAT	21
12	AtWEE1 fw	AGCTTGTCAGCTTTGCCT	18
13	AtWEE1 rv	TCAACCTCGAATCCTATCA	19
14	PUV2	TTCCATGCTAATGTATTCAGAG	22
15	PUV4	ATGGTGGTGACGGGTGAC	18
Cloning of pESC plasmids			
16	pESC-AtWEE1 fw *Bam*HI	ATCGGGATCCATGTTCGAGAAGAACGGAA	29
17	pESC-AtWEE1 rv *Sal*I	GCTAGTCGACACCTCGAATCCTATCAAAC	29
Cloning of BiFC plasmids			
18	BiFC-AtWEE1 fw *Spe*I	ATACTAGTATGTTCGAGAAGAACGGAAG	28
19	BiFC-AtWEE1 rv *Xho*I	TACTCGAGACCTCGAATCCTATCAAACA	28
20	BiFC-AtWEE1 rv *Kpn*I	TAGGTACCACCTCGAATCCTATCAAACA	28
21	BiFC-At14-3-3ω fw *Spe*I	ATACTAGTATGGCGTCTGGGCGTGAAGA	28
22	BiFC-At14-3-3ω rv *Xho*I	TACTCGAGCTGCTGTTCCTCGGTCG	27
23	BiFC-At14-3-3ω rv *Kpn*I	TAGGTACCCTGCTGTTCCTCGGTCG	25

Cloning of Y2H plasmids			
24	At14-3-3Psi fw *Bam*HI	AAGGATCCATGTCGACAAGGGAAGAGAATG	30
25	At14-3-3Psi rv *Nhe*I	AATTGCTAGCTTACTCGGCACCATCGGGCT	30
26	At14-3-3Nu fw *Bam*HI	AAGGATCCATGTCGTCTTCTCGGGAAGAG	29
27	At14-3-3Nu rv *Nhe*I	AATTGCTAGCTCACTGCCCTGTCTCAGCTG	30
28	At14-3-3Upsilon fw *Bam*HI	AAGGATCCATGTCCTCTGATTCGTCCCGG	29
29	At14-3-3Upsilon rv *Nhe*I	AATTGCTAGCTCACTGCGAAGGTGGTGGTT	30
30	At14-3-3Phi fw *Bam*HI	AAGGATCCATGGCGGCACCACCAGCAT	27
31	At14-3-3Phi rv *Nhe*I	AATTGCTAGCTTAGATCTCCTTCTGTTCTTCAG	33
32	At14-3-3Chi fw *Bam*HI	AAGGATCCATGGCGACACCAGGAGCTTC	28
33	At14-3-3Chi rv *Nhe*I	AATTGCTAGCCTAGGATTGTTGCTCGTCAGC	31
Sequencing			
34	At14-3-3ω seq fw	ACTTGGCTGAGTTTAAGACT	20
35	At14-3-3ω seq rv	ACCTGTGATAATCTCCCTTC	20
36	AtWEE1 (P38) seq fw	TGGTGATTATGCATCAGATAGC	22
37	AtWEE1 (P60) seq fw	TTGACACAGATGAGGTG	17
38	AtWEE1 (P61) seq rv	GTAATGCCTTTGCTATC	17
39	AtWEE1 (P62) seq rv	CACCTCACTTGTGTC	15
40	NtWEE1 (F2) seq fw	TCAAACTGTAGCAAGAAGAGG	21
41	NtWEE1 (F3) seq fw	AGGGGTAGCTCATTTAGA	18
42	NtWEE1 (R2) seq rv	GACCCTCTAATAAGTTCATA	20
43	NtWEE1 (R5) seq rv	TTATCCCCATCGGCAGCATCAG	22
Verification of Y2H transformants			
44	T7 terminator	AATACGACTCACTATAG	17
45	SpCdc25 fw	TTAGGTCCCCTTCTCCGATG	20
46	LaminC fw	TATAGTCGACATGGAAGAGGTGGTCAGCCG	30
47	At14-3-3ω fw	GCATCATATGGCGTCTGGGCGTGAAG	26
48	At14-3-3κ fw	GCGCCATATGGCGACGACCTTAAG	24
49	At14-3-3λ fw	TACGCATATGGCGGCGACATTAGGCAGAG	29
50	AtWEE1 fw	AGCTTGTCAGCTTTGCCT	18
51	AtCDC25 fw	GATGGAGAATTCATGGCGATGGCGAGAAGC	30
52	pAD Gal4 2.1 fw	AGGGATGTTTAATACCACTAC	21
53	pAD Gal4 2.1 rv	GCACAGTTGAAGTGAACTTGC	21
Cloning of pET15B plasmids			
54	At14-3-3ω fw *NdeI*	ATGGAAGCTTCATATGATGGCGTCTGGGCGTG	32
55	At14-3-3ω rv *BamHI*	ATGGATCCTCACTGCTGTTCCTCGGTCG	28
56	NtWEE1 fw *NdeI*	ATGGAAGCTTCATATGATGAAGAGGAAAACCC	32
57	NtWEE1 rv *BamHI*	ATGGATCCTTACTTGTTAGCATTTCTTTGACAT	31

AtWEE1 mutagenesis			
58	AtWEE1 (S483A) fw	GTCGGCCTGCTGCTAGAGAATTACTGGAC	29
59	AtWEE1 (S483A) rv	CTAGCAGCAGGCCGACGCTTCGGATC	26
60	AtWEE1 fw *Eco*RI	CATGGAGAATTCATGTTCGAGAAGAACG	28
61	AtWEE1 rv *SalI*	ACGTTCGACCTCAACCTCGAATCCTATC	28

3.2 Plasmids

#	Plasmid name	Description/use	Origin and reference
1	pBD-Gal4-Cam AtWEE1	Y2H bait plasmid used in Y2H library screening and targeted Y2Hs	Lab collection (I. Siciliano) (Chapter 4 and 5)
2	pBD-Gal4-Cam AtCDC25	Y2H bait plasmid used in Y2H library screening and targeted Y2Hs	Lab collection (A. Thompson) (Chapter 4 and 5)
3	pBD-Gal4-Cam SpCdc25	Y2H bait plasmid used in targeted Y2Hs (positive control in Y2H)	Sorrell *et al.* (2003) (Chapter 5)
4	pLaminC	Y2H control plasmid used in targeted Y2Hs (negative control in Y2H)	Stratagene, UK. (Chapter 5)
5	pAD-Gal4-2.1 At14-3-3ω	Y2H target plasmid used in targeted Y2H against AtWEE1 and AtCDC25	Sorrell *et al.* (2003) (Chapter 5)
6	pAD-Gal4-2.1 At14-3-3κ	Y2H target plasmid used in targeted Y2H against AtWEE1 and AtCDC25	Sorrell *et al.* (2003) (Chapter 5)
7	pAD-Gal4-2.1 At14-3-3λ	Y2H target plasmid used in targeted Y2H against AtWEE1 and AtCDC25	Sorrell *et al.* (2003) (Chapter 5)
8	pAD-Gal4-2.1 At14-3-3χ	Y2H target plasmid used in targeted Y2H against AtWEE1 and AtCDC25	**This work** (Chapter 5)
9	pAD-Gal4-2.1 At14-3-3ψ	Y2H target plasmid used in targeted Y2H against AtWEE1 and AtCDC25	**This work** (Chapter 5)
10	pAD-Gal4-2.1 At14-3-3φ	Y2H target plasmid used in targeted Y2H against AtWEE1 and AtCDC25	**This work** (Chapter 5)
11	pAD-Gal4-2.1 At14-3-3ν	Y2H target plasmid used in targeted Y2H against AtWEE1 and AtCDC25	**This work** (Chapter 5)
12	pAD-Gal4-2.1 At14-3-3υ	Y2H target plasmid used in targeted Y2H against AtWEE1 and AtCDC25	**This work** (Chapter 5)
13	pAD-Gal4-2.1	Used for cloning purposes	Lab collection (D. A. Sorrell) (Chapter 5)

14	pDestGADT AtCDKA1	Y2H target plasmid used in targeted Y2H against AtWEE1	Donated by J. Doonan (Appendix C)
15	pDestGADT AtCDKB2;1	Y2H target plasmid used in targeted Y2H against AtWEE1	Donated by J. Doonan (Appendix C)
16	pDestGADT AtCiPK21	Y2H target plasmid used in targeted Y2H against AtWEE1	Donated by J. Doonan (Appendix C)
17	pTA7002 AtWEE1	Used for cloning purposes	Lab collection (I. Siciliano) (Chapter 5)
18	pTA7002 NtWEE1	Used for cloning purposes	Lab collection (I. Siciliano) (Chapter 6)
19	pESC AtWEE1	Plasmid for expression of AtWEE1 in yeast	**This work** (Chapter 5)
20	pESC AtWEE1/At14-3-3ω	Plasmid for co-expression of AtWEE1 and At14-3-3 ω in yeast	**This work** (Chapter 5)
21	pESC At14-3-3ω	Plasmid for expression of At14-3-3ω in yeast	Sorrell *et al.* (2003) (Chapter 5)
22	pSPYNE 35S	Plasmid for expression of N-terminal part of YFP in plants (negative control)	Walter *et al.* (2004) (Chapter 5)
23	pSPYCE 35S	Plasmid for expression of C-terminal part of YFP in plants (negative control)	Walter *et al.* (2004) (Chapter 5)
24	pSPYNE 35S bZIP63	Plasmid for expression of bZIP63 fused to N-terminal part of YFP in plants (positive control)	Walter *et al.* (2004) (Chapter 5)
25	pSPYCE 35S bZIP63	Plasmid for expression of bZIP63 fused to C-terminal part of YFP in plants (positive control)	Walter *et al.* (2004) (Chapter 5)
26	pSPYNE 35S At14-3-3ω	Plasmid for expression of At14-3-3ω fused to N-terminal part of YFP in plants (test construct)	**This work** (Chapter 5)
27	pSPYCE 35S At14-3-3ω	Plasmid for expression of At14-3-3ω fused to C terminal part of YFP in plants (test construct)	**This work** (Chapter 5)
28	pSPYNE 35S AtWEE1	Plasmid for expression of AtWEE1 fused to N-terminal part of YFP in plants (test construct)	**This work** (Chapter 5)
29	pSPYCE 35S AtWEE1	Plasmid for expression of AtWEE1 fused to C-terminal part of YFP in plants (test construct)	**This work** (Chapter 5)

30	pET15B	Used for cloning purposes	Donated by P. Kille (Chapter 6)
31	pET15B At14-3-3ω	Plasmid for expression of At14-3-3ω fused to His-tag in bacteria (test construct)	Lab collection (J. Grønlund/ **this work**) (Chapter 6)
32	pET15B NtWEE1	Plasmid for expression of NtWEE1 fused to His-tag in bacteria (test construct)	Lab collection (J. Grønlund/ **this work**) (Chapter 6)
33	pBD-Gal4-Cam AtWEE1(S483A)	Y2H bait plasmid, used in targeted Y2Hs	**This work** (Chapter 5)
34	pSPYCE 35S AtWEE1(S483A)	Plasmid for expression of AtWEE1 (S483A) fused to C-terminal part of YFP in plants (test construct)	**This work** (Chapter 5)

3.3 Media and Antibiotics

Organism	Medium	Recipe
E. coli and *A. tumefaciens*		
	LB medium	10 g/L NaCl, 10 g/L bacto-peptone, 5 g/L yeast extract ± 10 g/L agar (pH 7)
	SOC medium	20 g/L tryptone, 5 g/L yeast extract, 0.5 g/L NaCl, 100 mL/L 1 M $MgCl_2$, 10 mL/L 2 M glucose (pH 7)
	2xYT	16 g/L tryptone, 10 g/L yeast extract, 5 g/L NaCl (pH 7)
	NZY broth	5 g/L NaCl, 2 g/L $MgSO_4 \cdot 7H_2O$, 5 g/L yeast extract, 10 g/L casein enzymatic hydrolysate (N-Z amine) (pH 7)
S. cerevisiae		
	YEPD medium	10 g/L Difco yeast extract, 20 g/L Difco bacto peptone, 20 g/L glucose, 0.1 g/L adenine (Sigma), 0.1 g/L uracil (Sigma) ± 20 g/L Difco bacto agar
	SD medium	1.67 g/L Difco Yeast Nitrogen Base (w/o amino acids), 5 g/L ammonium sulphate, 20 g/L glucose ± 20 g/L Difco bacto agar
	SG medium	1.67 g/L Difco Yeast Nitrogen Base (w/o amino acids), 5 g/L ammonium sulphate, 20 g/L galactose
	SGR medium	1.67 g/L Difco Yeast Nitrogen Base (w/o amino acids), 5 g/L ammonium sulphate, 20 g/L galactose, 10 g/L raffinose ± 20 g/L Difco bacto agar
A. thaliana		
	MS medium	4.708 g/L MS basic salts (Duchefa), 30 g/L sucrose, 10 g/L bacto agar (pH 5.8)
N. tabacum BY-2 cells		
	BY2 medium	4.3 g/L MS basic salts, 30 g/L sucrose, 10 mL of 1% myo-inositol, 10 mL of 2% KH_2PO_4, 1 mL of 0.1% thiamine HCl, 2 mL of 0.01% of 2.4-D ± 8 g/L bacto agar (pH 5.8)

Organism	Antibiotic and applied concentration
E. coli and *A. tumefaciens*	ampicillin (50 µg/mL), kanamycin (50 µg/mL), rifampicin (200 µg/mL), chloramphenicol (34 µg/mL), tetracycline (12.5 µg/mL) (all from Sigma)
A. thaliana	hygromycin (20 µg/mL) (Calbiochem)
N. tabacum BY2 cells	hygromycin (80 µg/mL), timentin (250 µg/mL) (Melford Laboratories)

3.4 Gel Electrophoresis

3.4.1 Agarose Gel Electrophosesis

For agarose gel electrophoresis (Sambrook and Russell, 2001) 1% gels were mainly used. For 1% gels, 0.5 g of agarose (Bioline) was added to 50 mL of 1x TAE buffer (50x: 242 g/L Tris, 100 mL/L 0.5M NaEDTA pH 8.0, 57.1 mL/L glacial acetic acid) and boiled. After cooling down to approximately 50°C, 5 µL of 10 mg/mL EtBr was added and the gel was cast in a tray. The gels were loaded with sample mixed with an appropriate amount of 10x loading buffer (50 mM Tris-HCl pH. 7.6, 60% glycerol, bromophenol blue) and run in 1x TAE buffer at 80 – 130 V. Afterwards, the DNA was detected by illuminating the gel with UV light using a Genius Bioimaging System (Syngene Ltd). The marker used for agarose gel electrophoresis was 250 – 500 ng 1 Kb DNA ladder (Invitrogen). Quantification of the intensities of the bands was done using the Gene Tool software package (Syngene Ltd).

3.4.2 SDS-PAGE

For SDS-PAGE (Schagger and von Jagow, 1987) 12% gels were mainly used. The separation gel was made by mixing 3.3 mL 40% acrylamide/*bis*-acrylamide (37.5:1) (Melford Laboratories), 4.4 mL 2.5x separation buffer (1.875 M Tris-HCl, pH 7.5, 0.25% SDS), 3.3 mL dH_2O, 100 µL 10% ammonium persulfate (APS), 10 µL N,N,N',N'-tetramethyl-ethylenediamine (TEMED) (Sigma) and cast between two glass plates. The stacking gel was made by mixing 0.56 mL 40% acrylamide/*bis*-acrylamide (37.5:1), 0.66 mL 5x stacking buffer (0.3 M Tris-HCl, pH 6.7, 0.5% SDS), 2 mL dH_2O, 30 µL 10% APS, 5 µL TEMED and cast on top of the separation gel. Samples were prepared by mixing with an appropriate amount of 5x loading buffer (250 mM Tris-HCl pH. 6.8, 10% SDS, 30% glycerol, 0.5 M DTT, 0.02% bromophenol blue) and boiled for 5 min. Samples were then loaded on the gel and run in 1x Laemmli buffer (10x: 10 g/L SDS, 30.3 g/L Tris base, 144.1 g/L glycine) at 100 – 200 V. Afterwards, the proteins were detected by staining the gel with Coomassie

Brilliant Blue stain (2.5 g Coomassie Brilliant Blue R-250 (Sigma), 450 mL EtOH, 100 mL acetic acid, 450 mL dH_2O). The marker used for SDS-PAGE was PageRuler™ pre-stained protein marker (Fermentas).

3.5 PCR

For PCR (Sambrook and Russell, 2001) either 10 ng of plasmid DNA, 1µL of genomic DNA or cDNA (RT-PCR) was used as template. For colony PCR either a bacterial or yeast colony was used as template.

For general PCR, either *Taq* DNA polymerase (Promega) or in house purified *Taq* polymerase was used. For PCR using the in house purified *Taq* polymerase the following was mixed: 2.5 µL 10x PCR buffer (100 mM Tris-HCl pH. 8.8, 200 mM KCl, 15 mM $MgCl_2$), 0.5 µL 10 mM dNTP, 1 µL of each 10 µM primers, 0.125 µL *Taq* polymerase. Template and distilled H_2O (dH_2O) were added to a final volume of 25 µL. For PCR using the Promega *Taq* DNA polymerase the following was mixed: 2.5 µL 10x PCR buffer (100 mM Tris-HCl pH. 9, 500 mM KCl, 1% Triton®X-100), 1.5 µL 25 mM $MgCl_2$, 0.5 µL 10 mM dNTP, 1 µL of each 10 µM primers, 0.125 µL *Taq* polymerase. Template and dH_2O were added to a final volume of 25 µL.

For cloning purposes polymerases with 3′→ 5′ exonuclease (proofreading) activity were used. For PCR using *Pfu* DNA polymerase (Promega) the following was mixed: 5 µL 10x PCR buffer (200 mM Tris-HCl pH 8.8, 100 mM KCl, 100 mM $(NH_4)_2SO_4$, 20 mM $MgSO_4$, 1.0% Triton® X-100, 1 mg/mL nuclease-free BSA), 1.6 µL 10 mM dNTP, 2 µL of each 10 µM primers, 0.4 µL *Pfu* DNA polymerase. Template and dH_2O were added to a final volume of 50 µL. For PCR using Platinium® *Pfx* DNA polymerase (Invitrogen) the following was mixed: 5 µL 10x *Pfx* amplification buffer, 1.5 µL 10 mM dNTP, 0.75 µL of each 10 µM primers, 0.4 µL Platinium® *Pfx* DNA polymerase. Template and dH_2O were added to a final volume of 50 µL.

PCR was performed on either a GeneAmp (Applied Biosystems) or a PTC-100™ (MJ Research Inc.) machine. The standard PCR program was as follows: 1 cycle of initial denaturation for 3 min at 95°C; 40 cycles of denaturation for 1 min at 95°C; annealing for 1 min at X°C; extension for Y min at 72°C; 1 cycle of final extension for 5 min at 72°C. Generally the annealing temperature (X) was set to app. 5°C lower than the calculated melting temperature of the primers and the extension time (Y) depended on the size of the fragment to be amplified and the polymerase used. The Promega *Taq*

DNA polymerase and the in house purified *Taq* polymerase extend app. 1000 base pairs (bp) per min and the Invitrogen *Pfx* and Promega *Pfu* polymerases extend app. 500 bp per min.

3.5.1 Production of *Taq* polymerase

A single colony of *Escherichia coli* (*E. coli*) DH5α transformed with the pTaq vector (Desai and Pfaffle, 1995) (kindly donated by Dr. P. Kille, Cardiff University) was inoculated into 10 mL LB with appropriate selection and incubated overnight at 200 rpm, 37°C.

BIOREX®70 resin (Biorad) for purification of the *Taq* polymerase was prepared by mixing it with buffer C (20 mM HEPES pH. 7.9, 1 mM EDTA, 0.5 mM PMSF, 0.5% Tween-20, 0.5% Igepal CA-630) and stirring for 1 – 2 h. The resin was allowed to settle and pH was recorded. The top liquid was discarded and replaced with fresh buffer C. This was repeated until the pH of the resin was 7.9 and then the resin was stirred overnight. The next day the resin was poured into a column (26 mm) until a bed volume of 17 mL (3.2 cm) was obtained. The column was stored at 4°C.

The overnight culture was harvested by centrifugation for 10 min at 2000 rpm, 4°C in a Beckman Coulter Avanti® J-E centrifuge fitted with a JA-20 rotor and the pellet was resuspended in 10 mL of fresh LB medium with appropriate selection. Then 2 x 500 mL LB with appropriate selection were inoculated with 1 mL of the overnight culture and incubated at 200 rpm, 37°C in a Gallenkamp orbital incubator until an optical density at 600 nm (OD_{600}) of 0.2 (app. 4 hours). At an OD_{600} of 0.2, cultures were added 0.5 mM isopropyl-1-thio-β-D-galactopyranoside (IPTG) and incubated overnight at 200 rpm, 37°C. The following day cultures were harvested by centrifugation for 20 min at 5000 rpm, 4°C in a Beckman Coulter Avanti® J-E centrifuge fitted with a JLA-10,5 rotor. Each pellet was resuspended in 50 mL cold Buffer A (50 mM Tris HCl pH 7.9, 50 mM glucose, 1 mM EDTA) and centrifuged at 5000 rpm, 20 min, 4°C in a Beckman Coulter Avanti® J-E centrifuge fitted with a JA-14 rotor. The pellets were resuspended in 10 mL Buffer A containing 0.4% lysozyme and incubated at room temperature for 30 min and then 10 mL Buffer B (10 mM Tris HCl pH 7.9, 50 mM KCl, 1 mM EDTA, 1 mM PMSF, 0.5% Tween-20, 0.5% Igepal CA-630) were added to the samples and incubated at 75°C for 20 min. Then the tubes were incubated on ice for 30 min and 0.15%. polyethylenimine (PEI) pH 7.0 added

drop-wise. The samples were incubated on ice for 10 min and then centrifuged for 20 min at 7000 rpm, 4°C in a Beckman Coulter Avanti® J-E centrifuge fitted with a JA-20 rotor. Pellets were resuspended in 10 mL Buffer C (20 mM HEPES pH 7.9, 1 mM EDTA, 0.5 mM PMSF, 0.5% Tween-20, 0.5% Igepal CA-630) + 25 mM KCl and centrifuged for 20 min at 8000 rpm, 4°C. Pellets were resuspended in 10 mL Buffer C + 0.15 M KCl and centrifuged for 20 min at 8000 rpm, 4°C and then the supernatants were transferred to fresh tubes and 20 mL Buffer C added.

Before loading the sample onto the prepared column, the column was drained of buffer C. Then the column was washed by adding 150 mL Buffer C + 50 mM KCl. The *Taq* polymerase was eluted from the column by adding 50 mL buffer C + 0.2 M KCl and collected in 5 mL fractions, which were stored at 4°C. 10 µL of each fraction were analyzed by SDS-PAGE and the protein containing fractions were pooled. The fractions were concentrated to 50% using a Centriprep Concentrator (YM10, Millipore) by centrifugation for 40 min at 3000xg, 4°C, in a Beckman Coulter Avanti® J-E centrifuge fitted with a JA-20 rotor. The concentrated sample was dialysed overnight at 4°C in 900 mL Buffer C + 50% glycerol.

The optimal working concentration for the *Taq* polymerase was determined by PCR and afterwards the concentrated *Taq* was diluted to the optimal concentration with buffer C + 50% glycerol and stored at -80°C.

3.6 Purification of DNA

Purification of DNA was either done directly using the QIAquick PCR Purification Kit (QIAGEN) or by extraction of DNA from an agarose gel using the QIAquick Gel Extraction Kit (QIAGEN). Purifications were performed according to the QIAquick® Spin Handbook (QIAGEN 06/02)

3.7 Plasmid Preparations

Small scale plasmid preparation (QIAGEN Plasmid Mini Prep) was performed according to the QIAprep® Miniprep Handbook (QIAGEN 11/05). Large scale plasmid preparations (QIAGEN Plasmid Midi Prep and QIAFilter Plasmid Maxi Prep) were performed according to the QIAGEN® Plasmid Purification handbook (QIAGEN 07/05).

3.8 Restriction Digestion

Restriction digests using various restriction enzymes were employed at different stages of the cloning work. The restriction enzymes were all purchased from Promega or New England Biolabs. Restriction digests were made by mixing plasmid DNA or PCR product, restriction enzyme, 1x restriction buffer and dH_2O. The amount of restriction enzyme used ranged from 5 – 10 U. Digests were performed for a minimum of 2 h and for plasmid DNA the digests were performed overnight. Digests were performed in appropriate buffers at temperatures recommended by the supplier. All restriction digests were either purified from an agarose gel using QIAquick Gel Extraction Kit (QIAGEN) or directly using QIAquick PCR Purification Kit (QIAGEN).

3.9 Ligation

For each ligation, plasmid DNA and insert DNA were mixed approximately in a molar ratio of 1:3. The DNA was mixed with 1x ligase buffer (300 mM Tris-HCl pH 7.8, 100 mM $MgCl_2$, 100 mM DTT, 10 mM ATP) and 1 U T4 DNA ligase (Promega) and sterile dH_2O to give a final volume of 10 – 25 µL. As controls, ligation reactions were performed without addition of insert DNA, in order to check for re-ligation of the plasmid DNA, and without addition of insert DNA and ligase, in order to check if the plasmid was completely digested. The ligation reactions were incubated overnight at 4°C.

3.10 Preparation of Competent Cells

Chemically competent *E. coli* DH5α cells (F′*phi80d lacZ*Δ (*lac*ZYA-*arg*F)U169 *deo*R *recA1 endA1 hsdR17* (rk-, m k+) *phoA supE44 lambda-thi-1 gyrA96 relA1*[F′ *proAB lacI*^{q}Z*ΔM15*]) were used for cloning purposes and for recombinant protein expression *E. coli* DE3 Rosetta pLysS cells (*F′ompT hsdS*$_B$(*R*$_B^-$ *m*$_B^-$) *gal dcm λ(DE3 [lacI lacUV5-T7 gene 1 ind1 sam7 nin5])* pLysSRARE (Cam^R)) were used. The competent cells were prepared (with minor modifications of the protocol) as previously described (Hanahan 1983) by inoculating 20 mL of SOC medium in a 250 mL flask with a freshly streaked single colony of *E. coli* DH5α and incubated overnight at 200 rpm, 37°C in a Gallenkamp orbital incubator. Next day two 500 mL flasks each containing 62.5 mL 2xYT medium were inoculated with 0.625 mL of the overnight culture.

Cultures were incubated at 200 rpm, 37°C until they reached an OD_{600} of 0.5 (approximately 1 – 3 h). The cells were harvested by centrifugation for 10 min at 5000 rpm, 1°C in a Beckman Coulter Avanti® J-E centrifuge fitted with a JA-14 rotor and each pellet was resuspended in 20.75 mL RF1 (100 mM rubidium chloride, 50 mM manganese chloride, 30 mM potassium acetate, 10 mM calcium chloride, 15% w/v glycerol pH 5.8) The cells were incubated in ice water for 1 h at 4°C and harvested by centrifugation for 10 min at 5000 rpm, 1°C. Each pellet was resuspended in 5 mL RF2 (10 mM MOPS, 10 mM rubidium chloride, 75 mM calcium chloride, 15% w/v glycerol) and incubated in ice water for 15 min at 4°C. Aliquots of 100 µL of cells were transferred to pre-chilled microcentrifuge tubes. The cells were frozen in liquid N_2 and stored at -80°C.

For plant and plant cell culture transformation, calcium competent *Agrobacterium tumefaciens* (*A. tumefaciens*) LBA4404 and EHA105 were used. The competent cells were prepared by inoculating 20 mL of LB-medium with appropriate selection with a freshly streaked single colony of *A. tumefaciens* LBA4404 and EHA105 and incubated overnight at 160 rpm, 30°C in a Gallenkamp orbital incubator. The overnight culture was used to inoculate 100 mL LB medium with appropriate selection in a 500 mL flask and the culture was incubated overnight at 160 rpm, 30°C until it reached an OD_{600} of 0.6. The culture was incubated on ice for 30 min and then harvested by centrifugation for 10 min, at 3000 rpm, 4 °C in a Beckman Coulter Avanti® J-E centrifuge fitted with a JA-20 rotor. The cells were then resuspended in 1 mL ice cold 20 mM $CaCl_2$. Aliquots of 100 µL of cells were added into pre-chilled microcentrifuge tubes. The cells were frozen in liquid N_2 and stored at -80°C.

3.11 Transformations

3.11.1 Transformation of *E. coli*

Competent cells were transformed with plasmid DNA by heat shock transformation. The cells were thawed on ice and 10 ng of plasmid DNA or 10 – 20 µL ligation mixture was added and the transformation was incubated on ice for 20 min. Then the cells were heat shocked for 45 s at 42°C and put on ice for 2 min. Afterwards, 900 µL of LB medium was added and the cells were incubated for 30 – 45 min at 37°C and 200 rpm in a Gallenkamp orbital incubator. For the plasmid DNA transformations aliquots of 50 µL were plated onto LB agar with appropriate selection and for the

ligation mixture transformations the cells were harvested by centrifugation for 30 s at full speed in an Eppendorf MiniSpin centrifuge, resuspended in 100 µl of LB medium and plated onto LB agar with appropriate selection. Plates were incubated overnight at 37°C.

3.11.2 Transformation of *S. cerevisiae*

Transformation of wild type *S. cerevisiae* YRG2 cells (*MAT***a** *ura3-52 his3-200 ade2-101 lys2-801 trp1-901 leu 2-3, 112 gal4-542, gal80-538, LYS2*::UAS_{GAL1}-$TATA_{GAL1}$-*HIS3 URA3*::$UAS_{GAL4\ 17mers(x3)}$-$TATA_{CYC1}$-*lacZ*, Stratagene) or YPH499 cells (*MAT***a** *ura3–52 lys2–801*$_{amber}$ *ade2–101*$_{ochre}$ *trp1–Δ63 his3–Δ200 leu2–Δ1*, Stratagene) was performed with minor modifications according to the Stratagene manual (Stratagene 07/06) Transformation was initiated by inoculating 100 mL YEPD medium in a 250 mL flask with a single yeast colony. The culture was incubated in a Gallenkamp orbital incubator at 160 rpm at 30°C. The OD_{600} of the culture was measured after 2 – 4 hours of incubation and then the culture was diluted, so that after an overnight incubation the cells would have a cell density of 1 – 5 x 10^7 mL^{-1} (OD_{600} 1 – 2). The next day the cells were harvested by centrifugation in a Beckman Coulter Avanti® J-E centrifuge fitted with a JA-14 rotor for 1 s at 8000 rpm and the pellet was washed three times in 20 mL sterile dH_2O. The cells were then resuspended in 10 mL of 0.1 M lithium acetate (LiAc), transferred to a 100 mL sterile flask and incubated for 1 h at 160 rpm, 30°C. Competent cells in aliqouts of 150 µL were transferred to microcentrifuge tubes and 1 µg of plasmid DNA was added to the cells. To serve as a negative control for the transformations, 5 µL of sterile dH_2O was added to a separate tube of competent cells. To each tube 350 µL of polyethylene glycol (PEG) 3350 (50% in dH_2O) was added and the tubes were inverted several times. The transformation mixtures were then incubated for 1 h at 30°C, heat-shocked for 5 min at 42°C and then cooled on ice for 2 – 3 min. The transformation mixtures in aliquots of 200 µL were plated onto SD agar plates containing 100 µL of appropriate supplement drop-out solution (DO solution) (Table 5) and incubated for 3 – 5 days at 30°C. The colonies obtained from the transformation were picked and patched onto a fresh SD agar plate with the appropriate DO solution and incubated for 3 – 5 days at 30°C.

The supplement DO solutions contain 4 mg/mL of each of the supplements listed in Table 5 except those that are omitted (*e.g.* a tryptophan (trp) DO solution contains all

supplements listed in Table 5 except for trp, hence a trp DO solution). 100 µL of appropriate DO solution was spread on top of the agar and allowed to dry before using the SD agar plate.

Table 5 – DO solutions consist of 4 mg/mL of each of the listed supplements except those that are omitted.

adenine (ade)	l-arginine (arg)
l-histidine (his)	l-leucine (leu)
l-lysine (lys)	l-methionine (met)
l-threonine (thr)	l-tryptophan (trp)
l-phenylalanine (phe)	l-isoleucine (ile)
l-tyrosine (tyr)	uracil (ura)
l-valine (val)	

3.12 Reporter Gene Screening

The *S. cerevisiae* YRG2 transformants were screened for their ability to activate the *HIS3* reporter gene by re-patching onto SD agar plates containing his DO. To circumvent basal expression of the yeast *HIS3* gene, the bait plasmid transformants were plated onto SD-agar plates containing his DO and 0 – 50 mM 3-AT (3-amino-1,2,4-triazole) (Sigma), which is a competitive inhibitor of the yeast HIS3 protein (Stratagene 07/06). The minimum concentration of 3-AT, which inhibited the growth of the transformants on SD agar plates containing his DO, was selected for the further experiments.

The transformants were also assayed for their ability to activate the *LacZ* reporter gene (*β-galactosidase* activity) in a filter lift assay (Stratagene 07/06). Prior to the filter lift assay the yeast was patched onto SGR agar plates containing the appropriate DO solution. The plates were incubated for 2 – 3 days at 30°C. To perform the filter lift a sterile filter paper (Whatman Grade 1) was placed in a Petri dish and completely wetted in 2 mL of Z-buffer (10.7 g/L $Na_2HPO_4 \cdot 2H_2O$, 6.2 g/L $NaH_2PO_4 \cdot 2H_2O$, 0.75 g/L KCl, 0.246 g/L $MgSO_4 \cdot 7H_2O$) containing 5.4 µL/mL β-mercaptoethanol and 33.4 µL/mL X-β-gal (20 mg/mL) (Fischer Scientific). A separate sterile filter paper was labelled and placed on the surface of the plate containing yeast patches. Air bubbles were carefully removed and the filter paper was pressed firmly onto the surface of an agar plate using a replica-plate block covered with a velvet cloth ensuring that the filter paper was in contact with all colonies on the plate for 1 – 2 min. The filter paper

was carefully lifted off the plate using sterile forceps. The filter was then placed colony side up in liquid N_2 for 5 – 10 s. and placed colony side up in a Petri dish to thaw. This process was repeated twice with each filter paper. The filter paper was then placed with the colony side up onto the filter paper wetted in Z-buffer and the air bubbles between the filter papers were carefully removed. The Petri dish containing the two pieces of filter paper was sealed with cling film and placed in an incubator at 30°C. The appearance of blue colour was monitored over the first three hours of incubation and then after an overnight incubation at 30°C.

An additional method for assaying the transformants ability to activate the *LacZ* reporter gene was the *ortho*-nitrophenyl-β-galactoside (ONPG) assay (Clontech 02/07). The assay was performed by inoculating transformed YRG2 cells into 5 mL SGR medium and cultures were incubated in a Gallenkamp orbital incubator at 160 rpm at 30°C until an OD_{600} 0.6 – 0.8. Cells were harvested by centrifugation in an MSE Centaur 2 centrifuge for 10 min at 4000 rpm and the pellet was resuspended in 5 mL of Z-buffer and placed on ice. OD_{600} was measured and each sample was added one drop of 0.1% SDS and two drops of chloroform. Tubes were vortexed for 15 sec and incubated at 30°C for 15 min and added 160 µL of 4 mg/mL ONPG (Sigma). Tubes were vortexed well for 10 s and incubated at 30°C for 20 min. After 20 min samples were removed and added 400 µL of 1 M sodium carbonate. Samples were spun down and OD_{420} and OD_{550} of the supernatant were measured. Miller units were calculated as follows: $U = 1000 \times [(OD_{420}) - (1.75 \times OD_{550})] / [(\text{time}) \times (\text{volume}) \times OD_{600}]$, where time is the incubation time with ONPG (min) and the volume is the volume of initial culture used (mL) (Miller, 1972).

3.13 RNA Extraction from Plant Tissue and Cell Culture

RNA from either plant tissue or cell culture was extracted by grinding the tissue in a sterile pre-cooled mortar with liquid N_2. Then 2 mL of Tri Reagent (Sigma) were added and the grinding was resumed to form a homogeneous phase. Equal amounts of liquid was transferred into two microcentrifuge tubes, vortexed and incubated at room temperature for 5 min. The samples were centrifuged in a Beckman Coulter Allegra™ 21R centrifuge fitted with a F2402H rotor for 10 min at 12000 rpm, 4°C. The clear supernatant was transferred to fresh microcentrifuge tubes and added 200 µL chloroform. Tubes were vortexed for 15 s and incubated at room temperature for 5

min. The samples were centrifuged for 15 min at 12000 rpm, 4°C. The top layer was transferred to fresh microcentrifuge tubes, 500 µL isopropanol added and then the extraction was incubated at room temperature for 10 min. Samples were centrifuged for 10 min at 12000 rpm, 4°C, the supernatant was removed, 1 mL of 75% EtOH was added to the pellet and vortexed for 15 s. Samples were centrifuged for 10 min at 12000 rpm, 4°C. The supernatant was removed and pellet was air dried for app. 20 – 30 min. The pellet was then resuspended in 50 µL sterile water and the contents of the two tubes were combined to give a volume of 100 µL total. Aliquots of 10 µL of the extracted RNA were mixed with 10x loading buffer and analyzed by agarose gel electrophoresis. The remaining RNA was stored at -80°C.

3.14 DNase Treatment and cDNA Synthesis

For DNase treatment app. 5 µg of RNA was mixed with 1x RQ1 DNase buffer (400 mM Tris-HCl pH 8, 100 mM $MgSO_4$, 10 mM $CaCl_2$) and 1 U RQ1 DNase (Promega) in a final volume of 20 µL. The samples were incubated at 37°C for 30 min, after which 2 µL of RQ1 DNase stop solution (20 mM EGTA pH 8.0) was added. The samples were then incubated at 65°C for 10 min.

For cDNA synthesis app. 1 µg of the DNase treated RNA was mixed with 500 ng of $Oligo(dt)_{15}$ primer (Promega) in a final volume of 20 µL. The samples were incubated for 10 min at 70°C and afterwards cooled on ice for 10 min. The samples were added 6 µL 5x M-MLV RT buffer (250 mM Tris-HCl pH 8.3, 375 mM KCl, 15 mM $MgCl_2$, 50 mM DTT), 2 µL 0.1 M DTT and 1 µL 10 mM dNTP mix and incubated at 42°C for 2 min. Then 200 U of M-MLV Reverse Transcriptase RNase H Minus, Point Mutant (Promega) was added and the samples were incubated at 42°C for 50 min. Samples were then incubated at 70°C for 15 min to stop the reaction. The synthesized cDNA was checked by using 1 – 5 µL as template in PCR (section 3.5) and the remaining cDNA was stored at -80°C.

3.15 Protein Extraction from Plant Tissue and Cell Culture

Protein extraction from either *A. thaliana* seedling material or from *N. tabacum* BY-2 cell culture was essentially performed as described in Cockcroft *et al.* (2000). Material for protein extraction was either harvested from seedling material and frozen in liquid N_2 or harvested from cell culture by centrifugation in an MSE Centaur 2

centrifuge for 5 min at 4000 rpm. After harvesting the supernatant was decanted and the pellet was frozen in liquid N_2. Proteins were extracted by grinding the material in a pre-cooled mortar with liquid N_2. Then 1 – 2 mL of ground material was transferred into a 14 mL culture tube and placed on ice and added 986 µL lysis buffer (50 mM Tris-HCl pH. 7.5, 75 mM NaCl, 15 mM EGTA, 15 mM $MgCl_2$, 60 mM β-glycerophosphate), 42 µL 25x PI (one complete protease inhibitors (Roche) dissolved in 2 mL sterile dH_2O and filter sterilized), 21 µL 50x PPI (50 mM NaF, 10 mM Na_3VO_4, 100 mM $Na_4P_2O_7$) and 1.05 µL 1M DTT. Samples were then homogenized by sonication (exponential tip, 10 µm amplitude) in a Soniprep 150 sonicator (MSE) for four times 30 s with 30 s on ice between each sonication. After sonication the samples were transferred to pre-chilled microcentrifuge tubes and centrifuged in a Beckman Coulter Allegra^{TM} 21R centrifuge fitted with a F2402H rotor for 30 min at 13000 rpm, 4°C. The supernatant was aliquotted into 100 µL aliquots and stored at -80°C.

3.16 Bradford Assay

The concentration of protein extracts was determined using a Bradford Assay (Bradford, 1976). The Bradford Reagent (Sigma) was gently mixed in the bottle and brought to room temperature. BSA protein standards were prepared in an appropriate lysis buffer ranging from 0.1 – 1.4 mg/mL. To a multi-well plate 5 µL of the protein standards were added to separate wells alongside 5 µL of each of the samples. To each well 250 µL of Bradford Reagent were added and mixed gently for app. 30 s. Samples were incubated at room temperature between 5 and 45 min and then the absorbance was measured at 590 nm. The absorbance (A_{590}(sample) – A_{590}(blank)) was then plotted against the protein concentration of each standard. The protein concentration of the unknown sample was determined from the standard curve.

3.17 Western Blotting

The samples were loaded in an SDS gel and run as described in section 3.4.2. For Western blotting (Burnette, 1981) a Hybond-P PVDF membrane (Amersham Pharmacia Biotech) was pre-wetted in 100% MetOH for 30 s and rinsed in dH_2O for 5 min. Then the PVDF membrane, sponges, filter paper and SDS gel were soaked in blotting buffer (20% MetOH, 0.01% SDS, 14 g/L glycine, 3g/L Tris base) for 10 to 15 min. A sandwich of sponge, filter paper, SDS gel, PVDF membrane, filter paper and

sponge was prepared and placed in the cassette of a Mini-Trans Blot® Western Blotting system (Bio-rad). The cassette was placed in the gel tank filled with blotting buffer and 0.35 mA was applied for 1 h. Afterwards, the transfer the cassette was disassembled and the PVDF membrane placed in 25 mL blocking solution (20mM Tris-HCl pH 7.5, 150mM NaCl, 0.05% Tween-20, 5% dry milk powder) and incubated on a shaking platform for 1 h. The primary antibody (FLAG (1:8000) (Sigma), c-myc (1:1250) (Sigma), NtWEE1 (1:1000) (Sigma)) was added to the membrane in the blocking buffer and incubated on the shaking platform for a further 1 h. Then the PVDF membrane was rinsed twice with wash buffer (20mM Tris-HCl pH 7.5, 150mM NaCl, 0.05% Tween-20, 1% Triton® X-100), washed once for 15 min and twice for 5 min. Another 25 mL of blocking buffer including the secondary antibody (For FLAG and c-myc primary antibodies: α-mouse IgG (1:10000) (Bio-rad) and for the NtWEE1 primary antibody: α-rabbit IgG (1:2500) (Sigma)) was added to the PVDF membrane and incubated on the shaking platform for 1 h. Then the PVDF membrane was rinsed twice with wash buffer, washed once for 15 min and twice for 5 min. The membrane was developed using the ECL Western blotting detection reagents (Amersham Pharmacia Biotech). First the PVDF membrane was placed on cling film and 0.125 mL/cm^2 ECL solution (reagent1:reagent2 (50:50)) was added, then the liquid was removed and the membrane wrapped in cling film and placed in an X-ray cassette (GRI Molecular Biology). Hyperfilm™ ECL (Amersham Biosciences) was placed on top of membrane and exposed for an appropriate amount of time ranging from 20 s to overnight. The film was developed using a Curix 60 developer (Agfa).

3.18 Immunoprecipitation and Kinase Assay

Immunoprecipitation and kinase assay were essentially performed as described in Cockcroft *et al.* (2000). The CDK substrate for the kinase assays was prepared using a p13^{SUC1} agarose conjugate (Upstate). 250 µg of protein extract extracted from either wild type *N. tabacum* BY2 cells or *A. thaliana* seedlings were mixed with 15 µL 50% (v/v) sepharose (Sigma) and incubated with rotation for 1 h at 4°C. Samples were centrifuged for 2 min at 5000g, 4°C and the supernatant was transferred to a fresh tube. To the supernatant 5 µL p13^{SUC1} (50% slurry) was added and the sample was incubated with rotation for 4 h at 4°C. The sample was centrifuged for 2 min at 5000g, 4°C and the pellet was washed twice with 1 mL SUC1 buffer (50 mM Tris-

HCl pH 7.5, 250 mM NaCl, 0.5 mM EDTA pH 8, 0.1 % Tween 20, 0.5 mM sodium fluoride) and once with 800 µL kinase buffer (50 mM Tris-HCl pH 7.5, 100 mM NaCl, 15 mM EGTA, 1 mM DTT).

WEE1 protein was immunoprecipitated from protein extract extracted from either *N. tabacum* BY2 cells or *A. thaliana* seedlings. 100 – 250 µg of protein extract was mixed with 15 µL 50% (v/v) protein A sepharose® 4B Fast Flow (Pharmacia Biotech) and incubated with rotation for 1 h at 4°C. Samples were centrifuged for 2 min at 5000g, 4°C and the supernatant was transferred to fresh tube. To the supernatant 5 µL of NtWEE1 antibody was added and the samples were incubated on ice for 2 h at 4°C. To each sample 15 µL 50% (v/v) protein A sepharose® 4B Fast Flow was added and the samples were incubated with rotation for 2 h at 4°C. Samples were centrifuged for 2 min at 5000g, 4°C and the pellet was washed twice with 1 mL SUC1 buffer (50 mM Tris-HCl pH 7.5, 250 mM NaCl, 0.5 mM EDTA pH 8, 0.1 % Tween 20, 0.5 mM sodium fluoride) and once with 800 µL kinase buffer (50 mM Tris-HCl pH 7.5, 100 mM NaCl, 15 mM EGTA, 1 mM DTT).

For the kinase assay, beads were combined (immunoprecipitated CDK and WEE1 proteins) and resuspended in kinase assay buffer (50 mM Tris HCl pH 7.5, 100 mM NaCl, 5 mM EGTA, 5 mM $MgCl_2$, 1 mM DTT, 1xPPI (1 mM NaF, 0.2 mM Na_3VO_4, 2 mM $Na_4P_2O_7$), 25 mM β-glycerophosphate, 0.5 µg/µL histone H1 (Roche), 74 kBq γ-^{32}P ATP (Amersham Pharmacia)) and reactions were incubated at room temperature for 30 min. Reactions were stopped by adding 3 µL 5x SDS loading buffer. Samples were subjected to SDS-PAGE and the gel was subsequently dried for 20 min at 80°C using a gel dryer model 583 (Bio-rad). Afterwards, the dried gel was placed in an X-ray cassette together with an intensifying screen. Hyperfilm™ ECL was placed on top of dried gel and exposed for an appropriate amount of time ranging from 3 to 6 days. The film was developed using a Curix 60 developer.

4 Identification of Interaction Partners for *A. thaliana* CDC25 and WEE1

4.1 Introduction

All biological processes in a cell depend on protein-protein interactions. The identification and mapping of these interactions provides valuable insights into the functionality of proteins. Both *in vitro* and *in vivo* techniques have been developed to detect and study protein–protein interactions starting from the molecular genetic approach, such as the Y2H technique, to biochemical approaches, such as protein complex purification using gel filtration/affinity chromatography and co-immunoprecipitation and fluorescent protein-based methods.

The Y2H technique is a relatively sensitive method for studying protein-protein interactions *in vivo*. Traditionally it is one of the preferred methods of finding interaction partners for a specific protein, because it is a relatively easy and fast method that allows large scale screening of cDNA libraries (Causier, 2002; Bhat *et al.*, 2006). For the experimental work in this thesis, the Y2H screens were performed using the Stratagene HybriZap® 2.1 Two-Hybrid System, a system based on the co-transformation of a bait plasmid (pBD-Gal4-cam) and a target plasmid (pAD-Gal4-2.1) into the *S. cerevisiae* YRG2 strain. For selection in *S. cerevisiae* the pAD-Gal4-2.1 contains the *LEU2* gene and the pBD-Gal4-cam contains the *TRP1* gene. Interaction between bait and target protein is identified by generating one hybrid of the yeast Gal4 binding domain (BD) fused to the bait protein (X) and another hybrid of the Gal4 activation domain (AD) fused to a specific protein or a library of proteins (Y) (Ma and Ptashne, 1987). The hybrids alone are not capable of initiating specific transcription of reporter genes in yeast, this only occurs when the bait and target protein interact specifically with each other (Figure 10A). This system takes advantage of two reporter genes, which are the *E. coli β-galactosidase* (*LacZ*) gene and the *S. cerevisiae HIS3* gene. Binding of the bait protein X to the upstream activating sequences (UAS) is not sufficient to initiate transcription of the reporter gene. Since protein Y alone is not localized to the reporter gene UAS this is not capable of initiating transcription of the reporter gene either. When a specific

interaction occurs between proteins X and Y both Gal4 BD and Gal4 AD are localized to the reporter gene UAS and transcriptional activation of the reporter gene occurs (Figure 10B).

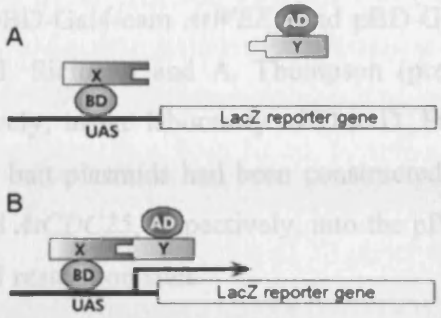

Figure 10 – A) The Gal4 BD hybrid protein binds to the Gal4 UAS that is present upstream of the *LacZ* reporter gene. The Gal4 AD hybrid protein binds transcription factors in the nucleus, but does not localize to the Gal4 UAS. B) If a specific interaction occurs between the two proteins, the Gal4 AD and Gal4 BD are brought in close proximity and act together with the bound transcription factors to initiate the transcription of the *LacZ* reporter gene (Stratagene 07/06).

The Y2H approach has been used widely to analyse interactions between plant proteins either in the analysis of known protein interactors or to find novel protein interaction partners. Protein-protein interactions occurring during a number of diverse processes, such as floral development (Davies *et al.*, 1996), self-incompatibility mechanisms (Mazzurco *et al.*, 2001), the circadian clock (Jarillo *et al.*, 2001), plant disease resistance (Ellis *et al.*, 2002) and phytohormone signalling (Ouellet *et al.*, 2001) have been investigated using the Y2H technique. In the work reported in this chapter the Y2H technique was used as a primary screen for identifying proteins interacting with *A. thaliana* CDC25 and WEE1. The Y2H library screen could reveal important interaction partners for both proteins, which could provide important information about the function and involvement of these two proteins in the plant cell cycle. Of particular interest would be to identify 14-3-3 proteins since they have been identified in both yeast and animals to interact with both Wee1 and Cdc25 in a cell cycle-dependent manner and thereby regulate their cellular localization and/or activity (Ford *et al.*, 1994; Conklin *et al.*, 1995; Peng *et al.*, 1997; Chan *et al.*, 1999; Rittinger *et al.*, 1999; Yang *et al.*, 1999; Zeng and Piwnica-Worms, 1999; Wang *et al.*, 2000; Graves *et al.*, 2001; Lee *et al.*, 2001; Rothblum-Oviatt *et al.*, 2001, Chen *et al.*, 2003b; Sorrell *et al.*, 2003).

4.2 Materials and Methods

4.2.1 Preparation of Bait and Target Plasmids

The two bait plasmids pBD-Gal4-cam *AtWEE1* and pBD-Gal4-cam *AtCDC25* were kindly donated by Dr. I. Siciliano and A. Thompson (previous PhD student and project student, respectively, in the laboratory of Drs. D. Francis and H. J. Rogers, Cardiff University). The bait plasmids had been constructed by inserting the coding sequence of *AtWEE1* and *AtCDC25*, respectively, into the pBD-Gal4-cam plasmid by the use of *Sal*I and *Eco*RI restriction sites.

For constructing the target plasmids to use for the Y2H screens, an *A. thaliana* seedling root primary cDNA library had previously been constructed in the HybriZAP-2.1 lambda vector (Stratagene) (Sorrell *et al.*, 2003). The primary library was amplified and converted by in vivo excision into a GAL4 transcriptional activation domain pAD-GAL4-2.1 library according to the manufacturer's protocol (Stratagene 07/06). *E. coli* XL1 Blue MRF' (Δ(*mcrA*)*183* Δ(*mcrCB-hsdSMR-mrr*)*173 endA supE44 thi-1 recA1 gyrA96 relA1 lac* [F′ *proAB lacI*^{q}ZΔ*M15* Tn*10* (Tetr)]) and *E. coli* XLOLR (Δ(*mcrA*)*183* Δ(*mcrCB-hsdSMR-mrr*)*173 endA1thi-1 recA1 gyrA96 relA1 lac* [F′ *proAB lacI*^{q}ZΔ *M15* Tn*10* (Tetr)]Su^{-}, λ^{R}) were streaked onto LB agar plates containing tetracycline and incubated overnight at 37°C. Single colonies of *E. coli* XL1 Blue MRF' and *E. coli* XLOLR were used to inoculate 10 mL of LB medium in 50 mL centrifuge tubes, which were incubated overnight in a Gallenkamp orbital incubator at 150 rpm, 37°C. Cultures were then spun down in an MSE Centaur 2 centrifuge for 10 min at 3500 rpm. Pellets were resuspended in 10 mM $MgSO_4$ to an OD_{600} of 1.0. A 250 µL aliquot of *E. coli* XL1 Blue MRF and *E. coli* XLOLR were added to each 50 mL of NZY broth containing 0.2% (w/v) maltose. Cultures were incubated at 150 rpm at 37°C until they reached an OD_{600} of 0.3 – 0.4 and then spun down for 10 min at 3500 rpm. The *E. coli* XL1 Blue MRF' culture was resuspended in 10 mM $MgSO_4$ to an OD_{600} of 5.0 (corresponding to a final cell concentration of $4x10^9$ cells) and the *E. coli* XLOLR culture was resuspended in 10 mM $MgSO_4$ to an OD_{600} of 1.0 (corresponding to a final cell concentration of ~$8x10^8$ cells). At this point the *E. coli* XLOLR cells were stored overnight at 4°C.

The phagemid library was excised by mixing 5.29 µL λ phage (~$1x10^8$ pfu), 230 µL *E. coli* XL1 Blue MRF' (~$1x10^9$ cells) and 24.21 µL helper phage (~$1x10^{10}$ pfu) in a 50 mL centrifuge tube following incubation for 15 min at 100 rpm, 37°C. Then 20 mL of LB medium was added to the mix and incubation was continued at 100 rpm at 37°C for 2 -3 h. The culture was then incubated for 20 min at 70°C and spun down for 10 min at 3500 rpm in an MSE Centaur 2 centrifuge. The supernatant containing the excised phagemid was transferred to a fresh 50 mL centrifuge tube and stored at 4°C until further use. To determine the titre of excised phagemids, $10^1 - 10^5$ dilutions of the excised phagemid were prepared. Aliquots of 10 µL of each dilution were mixed with 200 µL *E. coli* XLOLR cells (OD_{600} 1.0) in a microcentrifuge tube and incubated for 15 min at 37°C. The cells were plated onto LB agar containing ampicillin and incubated overnight at 37°C. The number of colony forming units (cfu) was counted and the titre of cells calculated for each dilution. The excised phagemid library was amplified by inoculating a single colony of *E. coli* XLOLR in 10 mL of LB medium in a 50 mL centrifuge tube following incubation overnight at 150 rpm at 37°C. The culture was spun down for 10 min at 3500 rpm and the pellet was resuspended in 10 mM $MgSO_4$ to an OD_{600} of 1.0 and then 500 µL of cells were added to 100 mL NZY broth containing 0.2% (w/v) maltose in a 250 mL flask and incubated at 200 rpm at 37°C until an OD_{600} of 0.3 – 0.4 was reached. Then the cells were spun down for 10 min at 3500 rpm and resuspended in 10 mM $MgSO_4$ to an OD_{600} of 1.0. Excised phagemid (~$2x10^8$ phagemids) and *E. coli* XLOLR (~$2x10^9$ cells) were mixed in a 50 mL centrifuge tube and incubated for 15 min at 150 rpm, 37°C. The mixture was then added to 500 mL LB medium containing ampicillin and incubated at 200 rpm at 37°C until an OD_{600} of 0.3 – 0.4. Then the cells were spun down in a Beckman Coulter Avanti® J-E centrifuge fitted with a JLA-10,5 rotor for 10 min at 3500 rpm and the supernatant was decanted. Pellets were stored at -20°C. The plasmid DNA was isolated using a QIAFilter Plasmid Maxi Prep (QIAGEN 11/05) according to the manufacturer's protocol.

4.2.2 Yeast Transformation and Y2H Library Screening

The *AtCDC25* and *AtWEE1* bait plasmids were transformed into wild type *S. cerevisiae* YRG2 cells and assayed for activation of *HIS3* and *LacZ* reporter genes as described in sections 3.11.2 and 3.12, respectively. Prior to the Y2H library screening, a transformation efficiency test was performed to indicate the extent, to

which the transformation had to be scaled up, since a minimum of 1 – 2 x 10^6 transformants had to be screened (Van Criekinge and Beyaert, 1999). Re-transformation of YRG2 cells carrying the *AtCDC25* and *AtWEE1* bait plasmids, respectively, with the Y2H cDNA library was done by a high efficiency transformation method. A single yeast colony was used to inoculate 10 mL of SD medium containing 50 µL of an appropriate DO solution in a 100 mL flask and incubated overnight in a Gallenkamp orbital incubator at 160 rpm at 30°C. The titre of the culture was determined and the volume of overnight culture corresponding to 2.5 x 10^8 cells was calculated. This volume was added to pre-warmed YEPD medium in a 250 mL flask to give a final volume of 50 mL. The culture was incubated at 160 rpm at 30°C until it reached a cell density of 2 x 10^7 cells/mL. The cells were harvested by centrifugation in an MSE Centaur 2 centrifuge for 5 min at 3500 rpm and afterwards the cells were resuspended in 25 mL of sterile dH_2O. The cells were spun down and the supernatant removed. The cells were then resuspended in 900 µL sterile dH_2O, transferred to a microcentrifuge tube, spun down in an Eppendorf MiniSpin centrifuge for 1 min at full speed, resuspended in 100 mM LiAc to a final volume of 1 mL and incubated for 10 min at 30°C. For each transformation, 100 µL of LiAc cell suspension was transferred into fresh microcentrifuge tubes, spun down for 1 min at full speed and to the cell pellets the following components were added: 240 µL 50% PEG, 36 µL 1M LiAc, 50 µL 2 mg/mL salmon sperm ssDNA (Sigma). 1 µg of plasmid DNA and dH_2O were added to the mix to a final volume of 360 µL. The tubes were vortexed until the cell pellet was fully resuspended. To one tube, sterile dH_2O was added instead of DNA to serve as a negative control for the transformations. The mixture was incubated for 30 min at 30°C and heat-shocked for 30 min at 42°C. The cells were then spun down for 1 min at full speed and the transformation mixture removed. The cells were resuspended in 1 mL of sterile dH_2O. The transformation mixtures were diluted 10x and aliquots of 100 µL were plated onto SD agar plates containing 100 µL of an appropriate DO solution and incubated for 3 – 5 days at 30°C. Based on the outcome of the transformation efficiency test, the transformation was scaled up so a minimum of 1x 10^6 transformants were screened.

4.3 Results

As described previously, the Y2H technique is a relatively sensitive method for studying protein-protein interactions *in vivo* therefore this technique was used in the identification of interaction partners for AtCDC25 and AtWEE1. The identification of interaction partners for the two proteins could provide important information about the regulatory elements of the plant cell cycle and furthermore help to determine the exact function and involvement of these two proteins in the plant cell cycle.

Initially, bait plasmids containing the coding sequences *AtCDC25* and *AtWEE1*, respectively, were transformed into YRG2 cells. The transformed yeast cells were selected on SD agar plates containing trp DO solution and subsequently patched on SD agar plates containing his DO in order to check their ability to auto-activate the *HIS3* reporter gene. The transformants carrying the *AtCDC25* bait plasmid did not grow on SD agar plates containing his DO whereas the transformants carrying the *AtWEE1* bait plasmid did, indicating that this bait plasmid was capable of auto-activating the *HIS3* reporter gene. To circumvent auto-activation of the *HIS3* reporter gene, the transformants were grown on SD agar plates containing 40 mM 3-AT, which was found to inhibit the growth of the transformants on SD agar plates containing his DO. The transformants were verified for the presence *AtWEE1* bait plasmid and the *AtCDC25* bait plasmid by colony PCR using a gene-specific primer and a primer specific for the bait plasmid (*AtWEE1* (P44+P50) and *AtCDC25* (P44+P52)).

A transformation efficiency test was performed prior to the Y2H library screening. YRG2 cells that were initially transformed with the *AtCDC25* bait plasmid and the *AtWEE1* bait plasmid, respectively, were transformed with 1, 2 or 5 µg of the *A. thaliana* seedling root cDNA library, which previously had been prepared by *in vivo* excision of a phagemid library (4.2.1). Based on the number of colony forming units (cfu), the transformation efficiencies and degrees of scale-up were calculated. For the AtCDC25 library screen 1 µg of library DNA was used and the transformation mixture had to be scaled-up 50x and all the cell culture volumes and resuspension volumes had to be scaled-up 5x. For the AtWEE1 library screen 1 µg of library DNA was used and the transformation mixture had to be scaled-up 100x and all the cell culture volumes and resuspension volumes had to be scaled-up 10x. The transformed

yeast was resuspended in a final volume of 10 mL and 0.5 mL aliquots were plated onto 20 SD agar plates (140 mm) each containing 500 µL trp-leu-his DO for selection of transformants (as previously mentioned the target plasmid contains the *LEU2* gene and the bait plasmid contains the *TRP1* gene) and for assaying activation of the *HIS3* reporter gene. Furthermore, 40 mM 3-AT was added in the agar plates for selecting the yeast initially transformed with the *AtWEE1* bait plasmid to circumvent auto-activation of the *HIS3* reporter gene. After a week of incubation at 30°C, the SD agar plates were covered with a background growth of yeast and colonies that appeared through the background were assumed to be real transformants. These colonies were picked and patched onto a fresh SD agar plate containing trp-leu-his DO. Colonies were picked as they emerged over a period of three weeks. After two weeks heavy contamination was present on the AtCDC25 library screening plates and attempts were made to remove the contamination by exision of the regions of comtanimated agar from the plates. This resulted in the recovery of only 81 transformants that were found to activate the *HIS3* reporter gene. However, the AtWEE1 library screening resulted in more than 900 transformants that could activate the *HIS3* reporter gene. Using the filter lift assay, the double transformants were assayed for their ability to activate the transcription of the *LacZ* reporter gene, which gives rise to a blue coloration of the yeast when grown on medium containing X-β-gal. For the AtCDC25 library screening and the AtWEE1 library screen 9 and 82 transformants, respectively, activated transcription of the *lacZ* reporter gene. These transformants were patched onto fresh SD agar plates containing trp-leu DO and then used as templates in colony PCR using primers specific for the target plasmid (P52+P53) for the isolation the cDNA insert of the target plasmid. The cDNA inserts were then purified using Montage PCR cleanup products (Millipore) according to the manufacturer's protocol. The purified PCR products were sequenced by the sequencing facility at Cardiff University using primer P52. The sequences that were obtained from the sequencing were identified using the BLAST program (http://www.ncbi.nlm.nih.gov/BLAST/).

4.3.1 AtCDC25 Y2H Library Screening

The results obtained from the AtCDC25 library screening revealed seven different AtCDC25 interaction partners, of which one was identified three times. Using the Tair search engine (http://www.arabidopsis.org) the identified proteins were broadly divided into three functional groups (Table 6)

Table 6 – Proteins that interact with AtCDC25 in the Y2H library screen. The identified proteins are divided into groups, AGI numbers of the genes are given in the left column and the name of the genes encoding the proteins/ name of the proteins are given in the right column together with the number of hits in brackets.

1) Ribosomes/Protein biosynthesis	
At1g04270	40S ribosomal protein S15 (1)
At5g26830	Threonyl-tRNA synthetase (1)
2) Cell division	
At1g52410	Caldesmon-related protein (1)
3) Stess responses	
At2g15970	Putative cold-acclimation protein FL3-5A3 (3)
At3g32980	Peroxidase 32 PRXR3 (1)
At1g27130	Putative GST (1)
Other	
At1g22180	Phosphoglyceride transfer/SEC14 cytosolic factor family protein (1)

The functional groups were: 1) protein biosynthesis, 2) cell division and 3) plant stress responses. Unexpectedly, 14-3-3 proteins were not found to interact with AtCDC25 in the Y2H library screen suggesting that AtCDC25 does not interact with 14-3-3 proteins.

However, due to the heavy contamination of the AtCDC25 library screening plates, it is likely that the AtCDC25 library screen gives an incomplete picture of the proteins that interact with AtCDC25. Hence, many more AtCDC25 interacting proteins, possibly including 14-3-3s may remain to be discovered.

4.3.2 AtWEE1 Y2H Library Screening

The AtWEE1 library screen revealed 60 different AtWEE1 interaction partners, of which 11 were identified multiple times. Using the Tair search engine (http://www.arabidopsis.org) 42 of the identified proteins were broadly divided into six functional groups (Table 7).

Table 7 – Proteins that interact with AtWEE1 in the Y2H library screen. The identified proteins are divided into functional groups, AGI numbers of the genes are given in the left column and the name of the genes encoding the proteins/ name of the proteins are given in the right column together with the number of hits in brackets.

1) Transcription factors/ DNA or RNA binding proteins, histone modifications	
At2g18160	bZIP transcription factor GBF5 (2)
At1g04960	Simliar to bZIP transcription factor family proteins (2)
At4g00150	Transcription factor SCL6 (3)
At1g64570	Similar to DNA-binding protein (1)
At2g33610	SWIRM domain containing protein (1)
At5g13780	GCN5 related N-terminal acetyltransferase (1)
At4g14465	DNA binding protein (1)
At5g49400	Zinc knuckle (CCHC-type) family protein (1)
At1g56070	E2F (1)
2) Plant growth regulation and signal transduction	
At1g48480	Receptor kinase gene RLK1 (1)
At1g08980	IAA biosynthesis (1)
At3g22440	Hydroxyproline-rich glycoprotein family protein (1)
3) Stress responses/ detoxification/ pathogen responses	
At2g41300	Strictosidine synthase (3)
At3g56240	Copper chaperone ATX1 (3)
At2g30860	GST AtGSTF9 (2)
At2g30870	GST AtGSTF10 (1)
At1g06040	Zinc finger protein (1)
At2g37040	Phenylalanine ammonia-lyase 1 PAL1 (1)
At4g11650	Osmotin OSM34 (1)
At1g14730	Cytochrome B561 family protein (1)
At2g38730	Similar to Cyclophilin protein (1)
At1g18970	Germin-like protein (1)
At4g15610	Integral membrane family protein (1)
At4g23680	Major latex protein (MLP) related (1)
At5g60640	Protein disulfide isomerase-like (PDIL), Thioredoxin family protein (1)
4) Cell division/cell size/ cell wall and cell growth	
At1g05850	Chitinase AtCTL1 (2)
At3g09840	CDC48A (2)
At3g10220	Tubulin folding co-factor B (1)

At5g62350	Pectin methyl esterase inhibitor family Protein (1)
At4g24780	Pectate lyase family protein (1)
At3g61430	Aquaporin PIP1A (1)
At3g11070	Outer membrane protein OMP85 (1)
At3g16640	Tumour family protein (1)

5) Ribosomes/ protein biosynthesis

At4g01560	Brix domain protein (3)
At2g43970	La domain protein (2)
At1g07830	Ribosomal protein(1)
At1g54270	translation initiation factor(1)

6) Ubiquitin-mediated degradation

At5g57900	SKP1/SCF (1)
At5g23540	26S proteasome regulatory subunit (1)
At4g39600	F-box family protein(1)
At1g06630	F-box family protein(1)
At1g67340	F-box family protein(1)

Other

At1g28580	Lipase (1)
At1g29900	Carbamoylphosphate synthetase (1)
At2g05440	Glycine rich protein (1)
At3g03773	Glycine rich protein (1)
At2g10950	BSD domain containing protein (1)
At2g44100	Rab-specific GDP dissociation inhibitor (1)
At3g02090	Mitochondrial processing peptidase (1)
At3g02470	S-adenosylmethionine decarboxylase (1)
At3g07350	Unknown protein (1)
At3g55410	Mitochondrial protein, (1)
At2g40800	Mitochondrial protein (3)
At3g55440	Cytosolic triose phosphate isomerase (1)
At4g27870	Integral membrane family protein (1)
At4g31350	Predicted protein (1)
At5g03940	Chloroplast Signal Recognition Particle Subunit (1)
At4g22920	Chloroplast protein (1)
At5g35570	Chloroplast protein (1)
At5g43330	Cytosolic malate dehydrogenase (1)

The functional groups were: 1) transcription, RNA/DNA binding and histone modifications, 2) plant growth regulation and signal transduction, 3) stress responses, detoxification and pathogen responses, 4) cell division and cell growth 5) protein biosynthesis and 6) ubiquitin-mediated degradation. Neither in the AtWEE1 Y2H library screen, 14-3-3 proteins was identified as target proteins, which could suggest that AtWEE1 does not interact with 14-3-3 proteins.

4.4 Discussion

Although cell division in plants shares basic mechanisms with all eukaryotes, a more profound understanding of how the plant cell cycle is regulated is still needed. As in other eukaryotes, CDKs play a central role in plant cell cycle regulation and CDK activity is regulated by association with regulatory cyclin subunits. The activity of the CDK/cyclin complexes is further controlled by a variety of regulatory mechanisms including transcription, proteolysis, phosphorylation/dephosphorylation, interaction with regulatory proteins and intracellular trafficking. Wee1 kinases and Cdc25 phosphatases are important regulators of CDK activity and therefore also the G2/M transition, but how are the activities of Cdc25 and Wee1 regulated themselves?

In yeast and animals, Cdc25 and Wee1 activities are tightly regulated by multiple mechanisms including sub-cellular localization, phosphorylation status and ubiquitin-mediated degradation by the 26S proteasome (Michael and Newport, 1998; Goes and Martin, 2001; Donzelli *et al.*, 2002; Watanabe *et al.*, 2004; Watanabe *et al.*, 2005; Wang *et al.*, 2007). Phosphorylations of Cdc25 and Wee1 proteins are responsible for both positive and negative regulation the catalytic activity of the proteins and in addition the phosphorylations promote 14-3-3 binding (Dalal *et al.*, 1999; Furnari *et al.*, 1999; Wang *et al.*, 2000; Lee *et al.*, 2001; Rothblum-Oviatt *et al.*, 2001; Chen *et al.*, 2003b). In the cell cycle context, the majority of reports of Cdc25 and Wee1 interaction partners have been focussed on their interaction with 14-3-3 proteins. In addition to 14-3-3 proteins several other proteins, such as p42 MAPK and Pin1 in *X. laevis* (Patra *et al.*, 1999; Walter *et al.*, 2000), Hsp90 in *S. cerevisiae* (Aligue *et al.*, 1994) and Nim1/Cdr1 proteins in *S. pombe* (Parker *et al.*, 1993; Wu and Russell, 1993; Kanoh and Russell, 1998), have been identified to bind and inhibit Wee1 in a phosphorylation-dependent manner and thereby act as mitotic controls. Similarly, for Cdc25 several other proteins, such as Pim-1 and Prk in *H. sapiens* (Ouyang *et al.*, 1999; Bachmann *et al.*, 2006) and Pin1 in *X. laevis* (Crenshaw *et al.*, 1998), have been identified binding to Cdc25 in a phosphorylation-dependent manner and thereby promoting Cdc25 activity.

To elucidate if similar regulatory mechanisms exist for AtWEE1 and the putative AtCDC25 protein during the plant cell cycle, two Y2H library screens were performed using AtCDC25 and AtWEE1, respectively, as baits against an *A. thaliana*

seedling root cDNA library (Sorrell *et al.*, 2002). The seedling root cDNA library was used, since this tissue is rich in rapidly dividing cells and therefore biologically relevant for the proteins analyzed. AtWEE1 expression is up-regulated in proliferative tissues, such as seedling and flowers (Sorrell *et al.*, 2002), however the expression of AtCDC25 is more or less constant in rapidly dividing tissues and non-proliferative tissues (Sorrell *et al.*, 2005).

4.4.1 AtCDC25 interacts with Proteins involved in Cell Division and Stress Responses

AtCDC25 differs from the classical Cdc25 proteins identified in animals and yeast, since it consists of only the C-terminal catalytic domain (Landrieu *et al.* 2004; Sorrell *et al.*, 2005). In the classical Cdc25 protein, the N-terminal regulatory domain undergoes multiple phosphorylations that regulate protein sub-cellular localization, stability and catalytic activity (Gabrielli *et al.*, 1997; Dalal *et al.*, 1999). Despite this difference, AtCDC25 is considered to be a member of the Cdc25 family based on functional and structural data. Furthermore, it is evident that AtCDC25 induces a Cdc25-like effect in *S. pombe* resulting in a smaller mitotic cell size (Sorrell *et al.* 2005). However, neither the exact cellular function nor the regulatory network associated with this protein has been determined. The AtCDC25 protein shows sequence similarity to the *S. cerevisiae* arsenate reductase and it possess arsenate reductase activity (Bleeker *et al.*, 2006; Dhankher *et al.*, 2006). Therefore, it has been questioned whether AtCDC25 is a true ortholog of the classical Cdc25s (Boudolf *et al.*, 2006; Inze and De Veylder, 2006). However, that AtCDC25 should function as an arsenate reductase should not exclude it from being a plant CDC25, since it was recently shown that the *H. sapiens* CDC25A can be suppressed by arsenite (Lehmann and McCabe, 2007).

Although 14-3-3 proteins can interact with Cdc25s in several other organisms, 14-3-3 proteins were not identified in the AtCDC25 library screen. Using a motif scanning software (http://scansite.mit.edu/motifscan_seq.phtml) the protein sequence of AtCDC25 is found to contain only one putative 14-3-3 binding site located in the region of S20/S22. Therefore, AtCDC25 may actually interact with 14-3-3 proteins, but these transformants may have been lost due to the heavy contamination of the Y2H library screening plates resulting in an incomplete picture of the proteins

interacting with AtCDC25. Since the AtCDC25 protein only consists of the C-terminal catalytic domain it is possible that it has to interact with a second protein to become a complete plant Cdc25. It was possible that this protein could have been revealed in the Y2H library screen. However, none of the putative CDC25 interactors found in the Y2H library screening resemble the N-terminal regulatory domain from the classical Cdc25s. It is assumed that if this second protein exists that it could be revealed by a more complete Y2H screen. However, a BLAST search of the 400 amino acid N-terminal of *S. pombe* Cdc25 (including the regulatory domain of the protein) against the TIGR Plant Transcript Assemblies database (http://plantta.tigr.org), which includes transcripts from more than 215 plant species including the three fully sequenced genomes of *A. thaliana*, *O. sativa* and poplar, *Populus trichocarpa* (*P. trichocarpa*) (Childs *et al.*, 2007), did not identify any proteins with homology to this domain, making it questionable whether such a domain exists in plants.

Despite the contamination of the AtCDC25 Y2H library screening plates, a number of AtCDC25 interacting proteins were identified. In particular, a cold-acclimation protein similar to the cold-acclimation WCOR413 protein from wheat, *Triticum aestivum* (*T. aestivum*, Ta) was hit three times. However, whether these hits represent the same clone or different clones is not known due to incomplete sequencing of the target plasmids. Cold-regulated (*COR*) genes encode structural proteins protecting plants during low temperature stress and enzymes involved in the biosynthesis of different osmo-protectants and membrane lipids. Furthermore, *COR* genes regulate gene expression and are involved in signal transduction pathways (Breton *et al.*, 2003). No reports have previously been made of Cdc25 proteins involved in physiological stress responses, such as cold-acclimation, but it is evident that environmental signals, such as nutrient availability and physiological stresses, modulate the cell cycle and cell size of *S. pombe* (Kishimoto and Yamashita 2000). The findings presented here suggest a role for plant CDC25 in similar physiological stress responses. Another interesting putative AtCDC25 interacting protein hit once in the Y2H library screening is the caldesmon-related protein TONSOKU (TSK) associating protein 1 (TSA1). In synchronized cell cultures, TSA1 and TSK relocalize to the ends of spindle microtubules that are ahead of separating chromatids during metaphase and anaphase suggesting a possible involvement of TSK and TSA1 in

mitosis. *A. thaliana tsk* mutants are blocked at the G2/M transition suggesting that TSK is required for proper execution of mitosis (Suzuki *et al.*, 2005b; Suzuki *et al.*, 2005a). Again no reports have been made of Cdc25s interacting with caldesmon-related proteins, but it is evident from several species that Cdc25s indeed are involved in the regulation of the cell cycle at G2/M (Kumagai and Dunphy, 1991; Furnari *et al.*, 1997; Peng *et al.*, 1997; Sanchez *et al.*, 1997; Yang *et al.*, 1999; Zeng and Piwnica-Worms, 1999; Sorrell *et al.*, 2003; Sgarlata and Perez-Martin, 2005; Boutros *et al.*, 2006).

4.4.2 AtWEE1 interacts with Proteins from a Variety of Functional Groups

The AtWEE1 Y2H library screen revealed 60 different AtWEE1 interacting proteins of which 11 were identified more than once. Of particular interest was to elucidate if AtWEE1 shares similar cell cycle regulatory mechanisms as its homologues in other organisms. The AtWEE1 library screen did not reveal any 14-3-3 proteins interacting with AtWEE1 although the AtWEE1 protein sequence was found to contain five putative 14-3-3 binding sites with T15, S144, T247, S450 and S485 as the possible phosphorylation sites (http://scansite.mit.edu/motifscan_seq.phtml). It is therefore likely that AtWEE1 interacts with 14-3-3 proteins, but the reason for not identifying 14-3-3 proteins as AtWEE1 interaction partners in this Y2H library screen could be due to the inexhaustive nature of the Y2H technique.

Of particular interest, proteins involved in the ubiquitin-mediated degradation pathway were found, such as a SKP1/SCF protein, a 26S proteasome regulatory subunit and three F-box containing proteins. Although these proteins were only hit once they are considered to be very likely protein interaction partners for AtWEE1, since as previously mentioned the ubiquitin-mediated degradation is one way of regulating Wee1 protein levels in both yeast and animals (Michael and Newport, 1998; Goes and Martin, 2001; Watanabe *et al.*, 2004; Watanabe *et al.*, 2005). In *H. sapiens* Wee1 is down-regulated by phosphorylation-dependent degradation rather than direct inhibition by phosphorylation and the protein responsible for the ubiquination and degradation is a SKP1/Cul1/F-box protein (SCF) complex containing the F-box protein β-transducin repeat-containing protein 1/2 (β-TrCP1/2) (Watanabe *et al.*, 2004). In *S. cerevisiae* an F-box protein Met30 is responsible for the

substrate recognition in the SCF complex and thereby responsible for the ubiquitination-dependent degradation of Swe1 (Kaiser *et al.*, 1998). Likewise in *X. laevis* an SCF complex containing the putative F-box protein Trigger of mitotic entry 1 (Tome-1) is responsible for Wee1 degradation (Ayad *et al.*, 2003). Therefore, ubiquitin-mediated degradation is also considered to be a very likely regulatory mechamism for plant WEE1s.

Another interesting putative WEE1 interaction partner hit twice in the Y2H library screen is the AtCDC48A protein. Also in this case it is not known whether these hits represent the same clone or different clones due to incomplete sequencing of the target plasmids. AtCDC48 is a homologue of the mammalian AAA-ATPase, p97, which functions in cell division, membrane fusion and in proteasome- and ER-associated degradation of proteins (Woodman, 2003). In *A. thaliana* CDC48A was originally described as a cell division cycle protein based on functional complementation studies in *S. cerevisiae cdc48* mutants (Feiler *et al.*, 1995). In *S. cerevisiae* CDC48 is essential for cell cycle progression and is presumably involved in spindle pole body duplication or separation and in addition it participates in fusion of ER membranes (Frohlich *et al.*, 1995; Latterich *et al.*, 1995). AtCDC48A is highly expressed in proliferating cells of the vegetative shoot, root, floral inflorescence and flowers and in rapidly dividing cells. Recently, AtCDC48 was found to interact with *A. thaliana* somatic embryogenesis receptor-like kinase 1 (AtSERK1) together with At14-3-3λ (Rienties *et al.*, 2005) showing analogy to the mammalian p97, which can be phosphorylated by the JAK-2 kinase and dephosphorylated by the phosphatase PTPH1 in association with a 14-3-3 protein (Zhang *et al.*, 1997; Zhang *et al.*, 1999) Furthermore, AtCDC48 is involved in a membrane fusion pathway that operates at the cell division plane to mediate cytokinesis (Rancour *et al.*, 2002) and more recently the interaction between AtCDC48A and SERK1 was mapped to peripheral ER based membranes and the plasma membrane (Aker *et al.*, 2006). Based on the previously mentioned expression pattern, localization and cell cycle function AtCDC48A is considered to be plausible WEE1 interaction partner, which in concert with WEE1 could be involved in plant cell division. Interestingly, Baldin and Ducommun (1995) found HsWee1 to be localized at the mitotic equator during cell division and by the end of M phase it was exclusively associated with midbody bridges suggesting a role in cytokinesis. In addition to the AtCDC48 protein, a tubulin folding co-factor B was

hit once in the Y2H screen. Interestingly, *D. melanogaster* Wee1 binds and phosphorylates the γ-tubulin ring complex (γ-TURC) and Wee1 loss-of-function mutants show mitotic-spindle defects implying a function in spindle morphogenesis and positioning (Stumpff *et al.*, 2005). Furthermore, it was proposed that DmWee1 in cooperation with other kinases may coordinate many distinct cell-division events, such as spindle movements, chromosome segregation and cytokinesis, which further gives evidence for a possible role of AtWEE1 in cytokinesis.

In the Y2H library screen many other putative WEE1 interaction partners were identified among these several transcription factors, plant growth regulators, proteins involved in regulating/maintaining plant stress responses and proteins involved in cell growth/cell wall maintenance. The putative WEE1 interaction partners summarized in this section is selected based on multiple hits and their biological relevance/potential as WEE1 interacting proteins. However, it should be emphasized that whether the multiple hits represent the same clone or different clones is not known due to incomplete sequencing of the target plasmids. That WEE1 should interact with transcription factors is plausible during G2 to maintain transcription of key genes and thus counteract transcriptional shut down at mitosis. The transcription factor SCARECROW-LIKE 6 (SCL6), was hit three times in the Y2H library screen. SCL6 belongs to the GRAS protein family, which is unique to plants and is involved in diverse processes from hormone signalling to meristem maintenance and development. SCL loss-of-function plants are characterized by their aberrant root growth indicating the significance of SCL proteins in root development (Sabatini *et al.*, 2003; Bolle, 2004). Also AtWEE1 was implicated in normal root development by controlling root growth and lateral root initiation in *A. thaliana* plants (Siciliano, 2006; Chapter 7). Furthermore, the bZIP transcription factor GBF5 was also identified as a putative WEE1 interaction partner. GBF5 belongs to the S group of the *A. thaliana* bZIP protein family, which is the largest, but also the least characterized bZIP protein group in *A. thaliana.* There is evidence that gene transcription is up-regulated by light and that the proteins function in sucrose signalling (Rook *et al.*, 1998). In *Z. mays* homologues of the *A. thaliana* S group bZIP protein family were also induced after stress treatment (Kusano *et al.*, 1995), which could be the link between AtWEE1 and bZIP transcription factors. Finally, a GCN5-related acetyltransferase was hit once in the Y2H library screen, which further suggests that

AtWEE1 has a function in stress responses, since GCN5 proteins are involved in the regulation on stress response genes upon salt stress in *S. pombe* (Johnsson *et al.*, 2006). Furthermore, in *S. cerevisiae* a direct link between GCN5 and G2/M cell cycle arrest has been made, since the combined loss-of-function of the two acetyltransferases *GCN5* and *SAS3* resulted in an extensive, global loss of H3 acetylation leading to G2/M arrest (Howe *et al.*, 2001).

GSTs were also identified multiple times as putative AtWEE1 interaction partners, which could link WEE1 with regulation of stress responses in *A. thaliana*. AtGST9 was hit twice and AtGST10 once. Expression of plant GSTs is induced upon various stresses such as infection, wounding, heavy metals, cold, drought, plant hormones and senescence (Marrs, 1996; Moons, 2005). In a previous study by Wagner *et al.* (2002) *AtGST9* and *AtGST10* were shown to be among the highest constitutively expressed GSTs. However, their expression was not significantly induced upon exposure to diverse stress treatments, such as hormones, H_2O_2 or pathogens, suggesting that the respective proteins have house-keeping roles. Further relating WEE1 with regulation of plant stress responses a copper chaperone was hit three times in the Y2H screen. The *A. thaliana Copper CHaperone* (*AtCCH*) gene was originally identified by its ability to complement *S. cerevisiae anti-oxidant 1* (*atx1*) mutants and is normally expressed in root, leaves and inflorescences. Furthermore, *AtCCH* expression is up-regulated during leaf senescence suggesting a role for this protein in copper binding and/or transport during senescence (Himelblau *et al.*, 1998). In plants, nutrients are recycled and transported from the senescent tissue to other parts of the plant, where the nutrients can contribute to growth, which could be the basis for a putative interaction site for AtCCH and AtWEE1.

Finally, a chitinase-like protein, AtCTL1, was hit twice in the Y2H screen. Chitinase-like proteins have long been proposed to play roles in normal plant growth and development. Mutations in the *AtCTL1* gene resulted in a number of conspicuous phenotypes, such as aberrant shapes of cells with incomplete cell walls, reduced length and increased width of hypocotyls and roots and an increased number and length of root hairs (Zhong *et al.*, 2002) suggesting that this gene is necessary for proper root development. Apparently *AtWEE1* deficient plants do not display a mutant phenotype unless a stress response is triggered upon stress treatment (De Schutter *et al.*, 2007). However, over-expression of *AtWEE1* results in similar phenotypes as the

AtCTL1 mutants, such as a reduced root length and an increased number and length of root hairs (Siciliano, 2006; De Schutter *et al.*, 2007) suggesting that these proteins may act together to ensure proper root development.

The Y2H technique is a valuable and relatively fast primary screen for identifying protein interaction partners even if the proteins only interact transiently or weakly (Van Criekinge and Beyaert, 1999) and clearly the outcome of the Y2H library screens presented in this thesis result in the formation of many new hypotheses about the localization, regulation and function of AtCDC25 and AtWEE1. However, it is important to bear in mind that the Y2H technique also has potential draw-backs. 14-3-3 proteins were not identified in either of the Y2H library screens, however the actual possibility of 14-3-3 proteins interacting with AtCDC25 and AtWEE1 cannot be excluded. Y2H library screens are not always exhaustive and maybe a larger number of clones have to be screened in order to screen the library until saturation (Van Criekinge and Beyaert, 1999). More potential draw-backs of the technique could be that the detection of the interaction depends on its compartmentalization within the cell and the interaction of a protein with more than one protein is not always detectable. By assaying protein interactions in a heterologous system, another possible draw-back could be that some interactions depend on post-translational modifications that do not, or inappropriately, occur in yeast (Golemis *et al.*, 1999; Van Criekinge and Beyaert, 1999; Causier and Davies, 2002; Bhat *et al.*, 2006). Because of these potential draw-backs it is desirable to confirm the Y2H interactions by the use of additional *in vitro* or *in vivo* methods, such as co-immunoprecipitation and fluorophore-based methods.

4.5 Summary

To obtain a better understanding of how the plant cell cycle is regulated the Y2H technique was used for identifying protein interaction partners for AtCDC25 and AtWEE1. The AtCDC25 interacting proteins are involved in protein biosynthesis, cell division and plant stress responses and the AtWEE1 interacting proteins are involved in transcription, RNA/DNA binding and histone modifications, plant growth regulation, signal transduction, stress responses, detoxification, pathogen responses, cell division, cell growth, protein biosynthesis and ubiquitin-mediated degradation. The identification of interaction partners leads to many new hypotheses about the localization, regulation and function of AtCDC25 and AtWEE1

5 *A. thaliana* WEE1 and 14-3-3ω interact in *N. tabacum* BY-2 Cells

5.1 Introduction

In both yeast and animals, 14-3-3 proteins have an important role in cell cycle checkpoints. 14-3-3 proteins bind and protect the phosphorylations of both Wee1 and Cdc25 and thereby maintain their activation or inactivation, respectively (Forbes *et al.*, 1998; Lee *et al.*, 1999; Zeng and Piwnica-Worms, 1999; Graves *et al.*, 2001; Rothblum-Oviatt *et al.*, 2001). 14-3-3 proteins bind via high affinity phosphorylation-dependent binding motifs that are recognized by all 14-3-3 isoforms: RSXpSXP (mode I) and RXXXpSXP (mode II), where pS represents phosphoserine, although in some cases it can be replaced by a phosphothreonine (Yaffe *et al.*, 1997; Rittinger *et al.*, 1999). Recently, a C-terminal pS/pTX_{1-2} (mode III) binding motif was shown to have a role in re-directing proteins to the cell surface (Coblitz *et al.*, 2005; Shikano *et al.*, 2005).

From *S. pombe*, *X. laevis* and *H. sapiens* it is evident that 14-3-3 binding regulates cellular processes by modulating protein localization. The binding of 14-3-3 proteins to Cdc25 results in its sequesteration to cytoplasm, which prevents premature activation of the CDK (Zeng and Piwnica-Worms, 1999; Muslin and Xing, 2000; Graves *et al.*, 2001). Moreover, 14-3-3 proteins also regulate enzyme activity directly as shown in *H. sapiens* where binding of 14-3-3 proteins inhibits CDC25A and CDC25B activity by blocking its catalytic site and thereby preventing it from activating the CDK/cyclin complex (Conklin *et al.*, 1995; Forrest and Gabrielli, 2001; Chen *et al.*, 2003b). In *X. laevis* 14-3-3 proteins together with Chk1 have been shown to function as positive regulators of Wee1 and during mitosis the interaction between 14-3-3 and Wee1 proteins is reduced leading to a decrease in Wee1 kinase activity (Lee *et al.*, 2001). Similarly, *H. sapiens* Wee1 is also positively regulated by 14-3-3 proteins resulting in an increased Wee1 stability. Wee1 mutants lacking the ability to bind 14-3-3 proteins are less active in phosphorylating CDK and are therefore not efficient in inducing a G2 cell cycle delay (Wang *et al.*, 2000; Rothblum-Oviatt *et al.*, 2001).

If and how 14-3-3 proteins act in the plant cell cycle is as yet largely unknown. So far only a few reports have suggested that plant 14-3-3s are involved in cell cycle regulation. The *A. thaliana* 14-3-3 gene family is the largest and best characterized consisting of 15 isoforms, where 13 are translated isoforms and the remaining two are considered as pseudo-forms. In *A. thaliana* three 14-3-3 proteins (ω, λ and κ) interact with *S. pombe* Cdc25, however only the 14-3-3ω isoform complements a *S. pombe rad24* mutant and has elevated expression in tissues with rapidly dividing cells (Sorrell *et al.*, 2003). Also other 14-3-3 isoforms (μ, υ, χ and φ) from *A. thaliana* complement the lethal *S. cerevisiae bmh* double mutant (van Heusden *et al.*, 1996; Kuromori and Yamamoto, 2000). Finally, the *A. thaliana* 14-3-3ω isoform accumulates differentially in the cell nucleus in a cell cycle-dependent manner suggesting a role in cell division (Cutler *et al.*, 2000).

In the work reported in this chapter, the Y2H technique was used to discover if members of the Non-Epsilon 14-3-3 protein family interact with the two *A. thaliana* cell cycle proteins AtCDC25 and AtWEE1. The specificity of the interaction between AtWEE1 and At14-3-3ω was further confirmed *in vitro* in yeast by co-immunoprecipiation and *in vivo* in *N. tabacum* BY-2 cells by BiFC. Finally, 14-3-3 binding sites were identified in AtWEE1 and based on similar binding sites in mammals a putative 14-3-3ω binding site could be proposed. To investigate if the AtWEE1/At14-3-3ω interaction could be abolished, an AtWEE1 (S485A) mutant was constructed and analyzed by Y2H and BiFC.

5.2 Materials and Methods

5.2.1 Yeast Transformation and Reporter Gene Screening

For the Y2H screen, the target plasmids containing the coding sequences of At14-3-3ω, At14-3-3λ and At14-3-3κ, respectively, had previously been constructed by Dr. D. A. Sorrell (previous postdoctoral researcher in the laborstory of Drs. J. R. Dickinson, D. Francis and H. J. Rogers, Cardiff University) (Sorrell *et al.*, 2003) The remaining target plasmids containing the coding sequences of At14-3-3χ, At14-3-3φ, At14-3-3ν, At14-3-3υ and At14-3-3ψ, respectively, were constructed as follows: the coding sequences of At14-3-3χ, At14-3-3φ, At14-3-3ν, At14-3-3υ and At14-3-3ψ were amplified from cDNA with primers P32+P33 (pAD-Gal4-2.1 *At14-3-3χ*), P30+P31 (pAD-Gal4-2.1 *At14-3-3φ*), P26+P27 (pAD-Gal4-2.1 *At14-3-3ν*), P28+P29 (pAD-Gal4 2.1 *At14-3-3υ*) and P24+P25 (pAD-Gal4-2.1 *At14-3-3ψ*), respectively. The PCRs were performed using *Pfu* polymerase. All the forward cloning primers were designed to incorporate a *Nhe*I restriction site to the 5' end and the reverse cloning primers were designed to incorporate a *Bam*HI restriction site to the 3' end of the coding sequences. The PCR products were digested with *Nhe*I/*Bam*HI and ligated into empty pAD-Gal4-2.1 vectors, which had been prepared by digestion with *Nhe*I/*Bam*HI. This resulted in an in-frame N-terminal fusion of the coding sequences to the Gal4 activation domain in the pAD-Gal4-2.1 vector. The insertions were verified by sequencing using primers P52+P53.

Co-transformation of wild type YRG2 cells with the *At14-3-3* target plasmids and the *AtCDC25* and *AtWEE1* bait plasmids, respectively, and the reporter gene screening were performed as described in sections 3.11.2 and 3.12, respectively.

5.2.2 Protein Expression and Purification in *S. cerevisiae* and Co-immunoprecipitation

For the co-immunoprecipitation analysis two plasmids had to be constructed, one containing the coding sequence of *AtWEE1* and one containing the coding sequences of both *AtWEE1* and *At14-3-3ω*. The coding sequence of *AtWEE1* was PCR amplified from plasmid DNA (pTA7002 *AtWEE1*) with primers P16+P17 using *Pfx* polymerase. The primers were designed to incorporate a *Bam*HI restriction site to the 5' end and a *Sal*I restriction site to the 3' end of the coding sequences. The PCR product was

digested with *Bam*HI/*Sal*I and ligated into an empty pESC vector and a pESC *At14-3-3ω* vector (Sorrell *et al.*, 2003), which had been prepared by digestion with *Bam*HI/*Sal*I. This resulted in an in-frame C-terminal fusion of the coding sequence of *AtWEE1* to the c-myc epitope in MCS2 of the pESC vector. The insertion of *AtWEE1* into the pESC vectors was verified by sequencing using primers P36 – P39. The constructed plasmids were then transformed into *S. cerevisiae* YPH499 as described in section 3.11.2 and the transformants were selected on agar plates containing trp DO solution, since the pESC vector contains the *TRP1* gene as selectable marker in *S. cerevisiae*. Additionally, the transformants were verified for the presence of the pESC *AtWEE1* and pESC *AtWEE1/At14-3-3ω* plasmids by colony PCR using two gene specific primers (P16+P17).

Prior to protein expression, the transformed yeast cells were grown for two days at 30°C on SGR agar plates containing trp DO solution. A 2 cm^2 patch of yeast was used to inoculate 10 mL SG medium containing trp DO solution in a 50 mL flask. The culture was incubated overnight in a Gallenkamp orbital incubator at 160 rpm at 30°C. The overnight culture was used to inoculate fresh SG medium containing trp DO solution (app. 1.5 mL overnight culture/100 mL fresh SG medium). The culture was incubated at 160 rpm for 16 h at 30°C (to a cell density of $5x10^6$ cells/mL ~ OD_{600} 0.5). Cells were harvested by centrifugation in a Beckman Coulter Avanti® J-E centrifuge fitted with a JA-14 rotor for 5 min at 4000 rpm, 4°C and the pellet was resuspended in 1 mL of lysis buffer (50 mM HEPES pH 7.5, 100 mM NaCl, 10% glycerol, 60 mM β-glycerophosphate, 1 mM Na_3VO_4, 0.5 mM PMSF, 1x complete protease inhibitors (Roche)). Cells were transferred to 15 mL culture tubes and glass beads were added to just under the liquid surface. Tubes were vortexed in intervals of 30 s vortex and then 30 s ice app. 10 – 15 times. The liquid was then transferred to pre-chilled microcentrifuge tubes and centrifuged in a Beckman Coulter Allegra™ 21R centrifuge fitted with a F2402H rotor for 30 min at 14000 rpm, 4°C. The concentrations of the protein extracts were determined using a Bradford assay as described in section 3.16, aliquoted into pre-chilled microcentrifuge tubes, frozen in liquid N_2 and stored at -80°C.

For co-immunoprecipitations, 40 µL of Flag® resin (Sigma) were aliquoted into microcentrifuge tubes and centrifuged in an Eppendorf MiniSpin centrifuge for 30 sec at 3000 rpm, 4°C, The supernatant was removed and the resin was washed twice with

500 µL TBS buffer (50mM Tris-HCl pH. 7.5, 150mM NaCl). Then 0.5 – 1 mg protein extract was added and the volume was made up to 1 mL with lysis buffer. Samples were incubated with rotation overnight at 4°C. The supernatant was removed and the resin was washed three times with 1 mL TBS buffer. Bound proteins were eluted from resin by adding 50 µL 0.1 M glycine pH. 3.5 and subsequently incubated at room temperature for 5 min. The samples were flicked gently three times during the incubation period. Samples were then centrifuged for 30 s at 3000 rpm, 4°C and the supernatant was transferred to fresh microcentrifuge tubes containing 10 µL 0.5 M Tris-HCl pH. 7.4 and 1.5 M NaCl. Samples were either used immediately or stored at -20°C for a maximum of a week. For Western blotting 20 µL of each co-immunoprecipitated sample were used. Western blotting was performed as described in section 3.17.

5.2.3 Transformation of competent *A. tumefaciens*, transformation and maintenance of *N. tabacum* BY-2 Cells

Transgenic *N. tabacum* BY-2 cell cultures were made by *A. tumefaciens*-mediated transformation. Initially, calcium competent *A. tumefaciens* LBA4404 were prepared as described in section 3.10. The competent *A. tumefaciens* LBA4404 cells were transformed with appropriate plasmids by heat-shock transformation as follows: competent LBA4404 cells were thawed on ice and 1 µg of plasmid DNA was added. The mixture was frozen in liquid N_2 for 10 s before being heat-shocked for 5 min at 37°C. To the cells 1 mL of LB medium was added and the cells were incubated for 4 h at 30°C and 160 rpm in a Gallenkamp orbital incubator. Afterwards, the cells were centrifuged for 30 s at full speed in an Eppendorf MiniSpin centrifuge and resuspended in 100 µl of LB medium. Aliquots of 80 and 20 µL of the transformations were plated onto LB agar with appropriate selection. Plates were incubated for 3 – 4 days at 30°C.

A three day old sub-culture of *N. tabacum* BY-2 cells was used for the transformations. To 14 mL of culture 20 µM acetosyringon (Sigma) was added. Then 7 mL of acetosyringon-treated cells were co-cultivated with 100 µL of an overnight culture of *A. tumefaciens* LBA4404 (transformed with appropriate constructs) in 9 cm Petri dishes containing BY-2 agar without selection. Plates were wrapped in Nesco film and incubated in the dark for 2 days at 27°C. Cultures were washed three times

with 50 mL liquid BY-2 medium by centrifugation in an MSE Centaur 2 centrifuge for 5 min at 3000 rpm. After the final wash cells were resuspended in 10 mL BY-2 medium. Then 2.5 mL aliquots were plated onto BY-2 agar containing timentin for selection against the *A. tumefaciens* LBA4404 and hygromycin for selection of the transformed *N. tabacum* BY-2 cells. Plates were sealed with micropore tape and incubated at 27°C in the dark in a Gallenkamp orbital incubator. Hygromycin resistant calli were isolated after 3 – 4 weeks. Each individual callus was considered as an independent clone and was grown for a further two weeks on fresh BY-2 agar plates containing timentin and hygromycin. App. 2 mm^3 of each callus were then transferred to 8 mL BY-2 medium containing timentin and hygromycin and incubated in a Gallenkamp orbital incubator at 130 rpm at 27°C in the dark until cultures reached stationary phase (1-3 weeks). The transgenic *N. tabacum* BY-2 cultures were subsequently genotyped by PCR and checked for transcription of the transgene by RT-PCR as described in section 3.5.

Both wild-type and transgenic BY-2 cultures were sub-cultured on a weekly basis. Cultures were kept both in small- and large-scale cultures. The large-scale cultures were sub-cultured by transferring 3.5 mL of culture to 95 mL BY-2 medium containing hygromycin in a 300 mL flask. The small-scale cultures were sub-cultured by transferring 240 µL of culture to 8 mL of BY-2 medium containing hygromycin in a 25 mL flask. All cultures were incubated in the dark in a Gallenkamp orbital incubator at 130 rpm at 27°C.

5.2.4 BiFC

The vectors used for BiFC were kindly donated by Dr. J. Kudla, Münster University, Germany. As the negative control the pSPYNE 35S empty vector and the pSPYCE 35S empty vector were used and as a positive control the pSPYNE 35S *AtbZIP63* and the pSPYCE 35S *AtbZIP63* were used (Walter *et al.*, 2004). In addition, the following plasmids had to be constructed: pSPYNE 35S and pSPYCE 35S containing the coding sequence of *AtWEE1* and pSPYNE 35S and pSPYCE 35S containing the coding sequence of *At14-3-3ω*. The coding sequences of *AtWEE1* and *At14-3-3ω* were amplified from plasmid DNA (pTA7002 *AtWEE1* and pESC *At14-3-3ω*, respectively) with primers P18+P20 (pSPYNE 35S *AtWEE1*), P18+P19 (pSPYCE 35S *AtWEE1*), P21+P23 (pSPYNE 35S *At14-3-3ω*) and P21+P22 (pSPYCE 35S *At14-3-3ω*). The

PCRs were performed using *Pfx* polymerase. The pSPYNE 35S primers were designed to incorporate a *Spe*I restriction site to the 5' end and a *Kpn*I restriction site to the 3' end of the coding sequences. The pSPYCE 35S primers were designed to incorporate a *Spe*I restriction site to the 5' end and an *Xho*I restriction site to the 3' end of the coding sequences. The PCR products were digested with either *Spe*I/*Kpn*I or *Spe*I/*Xho*I and ligated into empty pSPYNE 35S and pSPYCE 35S vectors, which had been prepared by digestion with *Spe*I/*Kpn*I and *Spe*I/*Xho*I, respectively, resulting in an in-frame C-terminal fusion of the coding sequence of *AtWEE1* and *At14-3-3ω* to the 5' part of *YFP* in the pSPYNE 35S vector and in-frame C-terminal fusion of the coding sequence of *AtWEE1* and *At14-3-3ω* to the 3' part of *YFP* in the pSPYCE 35S vector. The insertions of *AtWEE1* and *At14-3-3ω* into the respective vectors were confirmed by sequencing using primers P36–P39 for *AtWEE1* and P34+P35 for *At14-3-3ω*.

The plasmids were transformed into *A. tumefaciens* EHA109 cells and the cells carrying the pSPYNE 35S plasmids were used for generating stable *N. tabacum* BY-2 transformants as described in section 5.2.3. In general the BiFC technique was performed by transient transformation of the stable *N. tabacum* BY-2 pSPYNE 35S cell lines with the *A. tumefaciens* EHA105 cells carrying the pSPYCE 35S plasmids. The technique was initiated by inoculating 10 mL of LB medium with a single colony of freshly streaked *A. tumefaciens* EHA105 containing appropriate plasmids. Cultures were incubated overnight in a Gallenkamp orbital incubator at 160 rpm at 30°C. Three day old sub-cultures of the stable *N. tabacum* BY-2 pSPYNE 35S cell lines were used for the transient transformations (prior to the transient transformation the stable *N. tabacum* BY-2 cell lines were sub-cultured without hygromycin at least twice). To 7 mL of the stable *N. tabacum* BY-2 pSPYNE 35S cell culture 200 µM acetosyringon was added. The acetosyringon-treated cells were then co-cultivated with 200 µL of the overnight *A. tumefaciens* EHA105 carrying the pSPYCE 35S constructs in Petri dishes containing BY-2 agar without selection. Plates were wrapped in Nesco film and incubated in the dark for 72 h at 27°C. Yellow fluorescence was assessed using a fluorescence microscope (Olympus BH2) equipped with a 530 nm filter. Images were colour adjusted using Adobe Photoshop® software.

5.2.5 Site-directed Mutagenesis

Site-directed mutagenesis was used in order to make an AtWEE1 (S485A) mutant. This was done by one base pair substitution, which was introduced in the AtWEE1 sequence by PCR using a modified QuickChange® Site-Directed Mutagenesis protocol (Stratagene, 2007). The primers used in the PCR were designed based on the following criteria: both primers must contain the desired mutation and have at least eight non-overlapping bases in the 3' end of the primer. The primers should be between 25 and 45 bases in length with a melting temperature ≥78°C (The melting temperature was calculated as follows: 81.5 + 0.41(%GC) – 675/N – %mismatch, where N is the primer length in bases and values for %GC and %mismatch are in whole numbers), the primers should have a minimum GC content of 40% and should terminate in one or more C or G bases (Zheng *et al.*, 2004; Stratagene 2007). For the mutagenesis PCR, *Pfu*Turbo® DNA polymerase (Stratagene) was used and the PCR reaction was set up by mixing 5 µL 10x cloned *Pfu* PCR buffer (200 mM Tris-HCl pH 8.8, 100 mM KCl, 100 mM $(NH_4)_2SO_4$, 20 mM $MgSO_4$, 1.0% Triton® X-100, 1 mg/mL nuclease-free BSA), 1.5 µL 10 mM dNTP, 1.25 µL of each 10 µM primer (P58+P59), 1 µL *Pfu*Turbo® DNA polymerase (2.5 U/µL). Template (20 ng) and dH_2O were added to a final volume of 50 µL. The PCR program was as follows: 1 cycle of initial denaturation for 30 s at 95°C; 16 cycles of denaturation for 30 s at 95°C; annealing for 1 min at 55°C; extension for 20 min at 68°C; 1 cycle of final extension for 1 h at 68°C. Afterwards, the PCR reactions were digested with 10 U *Dpn*I, which specifically digests the methylated template DNA, but not the newly synthesized DNA, for 1 h at 37°C and subsequently EtOH precipitated. The EtOH precipitation was done by adding 1/10 volume of 3 M KAc pH 4.8 and 2.5 volumes of 99% EtOH to the sample and subsequently exposing the sample to liquid N_2 for 10 s. Then the sample was centrifuged for 10 min at 14000 rpm and the supernatant discarded. The pellet was washed with 70% EtOH by centrifugation for 5 min at 14000 rpm. The pellet was then air dried and resuspended in 10 µL 10 mM Tris-HCl pH 7.5. The precipitated DNA was then transformed into *E. coli* DH5α cells as described in section 3.11.1. The S485A mutation was verified by sequencing of the original mutagenised plasmid and subsequently the *AtWEE1 (S485A)* coding sequence was amplified using the original cloning primers (60+61) and re-cloned into an empty pBD-Gal4-cam vector by the use of *Sal*I/*Eco*RI restriction sites. In order to test the

AtWEE1(S485A) mutant *in vivo* by BiFC, the coding sequence of *AtWEE1 (S485A)* was also inserted in the empty pSPYCE 35S vector as described in section 5.2.4. The insertion of *AtWEE1(S485A)* into the respective plasmids was confirmed by sequencing using primers P36 – P39.

5.3 Results

Although 14-3-3 proteins interact with both Wee1 and Cdc25 in several organisms it is not known whether 14-3-3 proteins interact with either WEE1s or CDC25s in plants. When AtWEE1 and AtCDC25 were used as baits in a Y2H screen against an *A. thaliana* root cDNA library, none of the *A. thaliana* 14-3-3 proteins were identified as interaction partners for either protein (Chapter 4) indicating that the mechanism of regulating WEE1 and CDC25 in plants might be different compared to the yeast and animal systems. However, three of the *A. thaliana* Non-Epsilon group 14-3-3 proteins (ω, κ and λ) had previously been shown to interact with SpCdc25 (Sorrell *et al.*, 2003) suggesting that these 14-3-3 proteins might have a role in regulating the cell cycle. Based on this it is very likely that the 14-3-3 proteins are interaction partners for both AtWEE1 and AtCDC25, even though they were not identified in the Y2H library screening. Therefore, the entire group of Non-Epsilon 14-3-3s (χ, ω, ψ, φ, υ, λ, ν and κ) were used as target proteins for AtWEE1 and AtCDC25 in a targeted Y2H screening.

5.3.1 AtWEE1 interacts with the *A. thaliana* Non-Epsilon 14-3-3s, whereas AtCDC25 does not

For the targeted Y2H screen, a positive control (SpCdc25 as bait against At14-3-3ω) and a negative control (LaminC as bait against At14-3-3ω) were used as previously described in Sorrell *et al.* (2003). The bait plasmids containing the coding sequences of *LaminC* (encoding a 163 amino acid fragment of LaminC) and *SpCdc25*, respectively, were transformed into YRG2 cells. Transformed yeast cells were selected on SD agar plates containing trp DO solution. Furthermore, the transformants were verified for the presence of the *LaminC* bait plasmid and the *SpCdc25* bait plasmid by colony PCR using a gene-specific primer and a primer specific for the bait plasmid (*LaminC* (P44+P46) and *SpCdc25* (P44+P45)). By plating the transformation mixes onto SD agar plates containing his DO solution, the bait plasmids were checked for their ability to auto-activate the *HIS3* reporter gene. The transformants carrying the *LaminC* bait plasmid did not grow on SD agar plates containing his DO solution, whereas the transformants carrying the *SpCdc25* bait plasmid did, indicating that the *SpCdc25* bait plasmid was capable of auto-activating the *HIS3* reporter gene as previously reported by Sorrell *et al.* (2003). The auto-activation of the *HIS3* reporter

gene was circumvented by the addition of 10 mM 3-AT in the growth medium. After the initial transformations of the *LaminC* and *SpCdc25* bait plasmids into YRG2 cells, these transformants were co-transformed with the *At14-3-3ω* target plasmid and used as controls in the further Y2H screening.

The transformants carrying the *AtCDC25* or *AtWEE1* bait plasmids, respectively, were co-transformed with the target plasmids containing the coding sequences for the Non-Epsilon 14-3-3χ, 14-3-3ω, 14-3-3ψ, 14-3-3φ, 14-3-3υ, 14-3-3λ, 14-3-3ν and 14-3-3κ, respectively. The double transformed yeast cells were selected on SD agar plates containing trp-leu DO solution. Furthermore, the transformants were verified for the presence of the correct bait and target plasmids by colony PCR (*LaminC* (P44+P46), *SpCdc25* (P44+P45), *AtWEE1* (P44+P50), *AtCDC25* (P44+P52), *At14-3-3λ* (P44+P49), *At14-3-3κ* (P44+P48), *14-3-3ω* (P44+P47), *14-3-3χ* (P44+P32), *14-3-3ψ* (P44+P24), *14-3-3φ* (P44+P30), *14-3-3υ* (P44+P28), and *14-3-3ν* (P44+P26)).

The transformant carrying the *LaminC* bait plasmid co-transformed with the *14-3-3ω* target plasmid did not grow on SD agar plates containing his DO solution implying that LaminC does not interact with 14-3-3ω. However, the transformant carrying the *SpCdc25* bait plasmid co-transformed with the *14-3-3ω* target plasmid did grow on SD agar plates containing his DO solution and 10 mM 3-AT implying that SpCdc25 interacts with 14-3-3ω. The transformants carrying the *AtWEE1* bait plasmid co-transformed with the 14-3-3χ, 14-3-3ω, 14-3-3ψ, 14-3-3φ, 14-3-3υ, 14-3-3λ, 14-3-3ν and 14-3-3κ target plasmids, respectively, did grow on SD agar plates containing his DO solution and 40 mM 3-AT implying that AtWEE1 interacts with all the Non-Epsilon 14-3-3 proteins. However, none of the transformants carrying the *AtCDC25* bait plasmid co-transformed with the 14-3-3χ, 14-3-3ω, 14-3-3ψ, 14-3-3φ, 14-3-3υ, 14-3-3λ, 14-3-3ν and 14-3-3κ, respectively, grew on SD agar plates containing his DO solution, suggesting that AtCDC25 does not interact with the Non-Epsilon 14-3-3s.

Additionally, the transformants were tested for transcriptional activation of the *lacZ* reporter gene using filter lift assays (Figure 11). The negative control transformant carrying the *LaminC* bait plasmid co-transformed with the *14-3-3ω* target plasmid did not give rise to blue coloration. This, together with the inability to grow on SD agar plates containing his DO solution confirmed that LaminC is not interacting with

14-3-3ω. Furthermore, YRG2 cells transformed with the *AtWEE1* bait plasmid alone was included in the filter lift assay to verify that the *AtWEE1* bait plasmid is not capable of auto-activating the *LacZ* reporter gene itself when grown under these conditions.

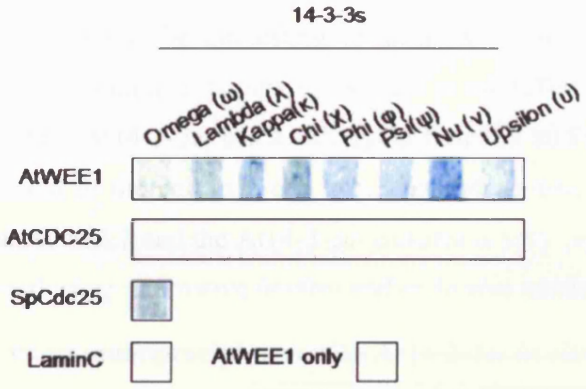

Figure 11 – Filter lift assay, in which the double transformants were assayed for their ability to drive the transcription of the *LacZ* reporter gene. First panel: AtWEE1/Non-Epsilon 14-3-3s; second panel: AtCDC25/Non-Epsilon 14-3-3s; third panel: SpCdc25/At14-3-3ω (positive control); fourth panel: LaminC/At14-3-3ω and AtWEE1 only (negative controls).

The transformant carrying the *SpCdc25* bait plasmid co-transformed with the *At14-3-3ω* target plasmid gave rise to a blue coloration (Figure 11). This confirms that SpCdc25 interacts with 14-3-3ω, which is consistent with previous findings by Sorrell *et al.* (2003). Furthermore, the transformants carrying the *AtCDC25* bait plasmid co-transformed with the 14-3-3χ, 14-3-3ω, 14-3-3ψ, 14-3-3φ, 14-3-3υ, 14-3-3λ, 14-3-3ν and 14-3-3κ target plasmids, respectively, did not give rise to a blue colour further suggesting that AtCDC25 does not interact with the Non-Epsilon 14-3-3s. In contrast, blue coloration of the transformants carrying the *AtWEE1* bait plasmid co-transformed with 14-3-3χ, 14-3-3ω, 14-3-3ψ, 14-3-3φ, 14-3-3υ, 14-3-3λ, 14-3-3ν and 14-3-3κ target plasmids occurred, respectively. The intensity of the blue colouration of the different transformants varied (Figure 11). However, this does not necessarily mean that the two proteins assayed in one transformant interact more strongly than two proteins assayed in another transformant, since a filter lift assay is a qualitative rather than quantitative assay. Activation of both the *LacZ* and *HIS3* reporter genes strongly indicates that AtWEE1 interacts with all the Non-Epsilon 14-3-3 proteins.

5.3.2 *In vitro* and *in vivo* Confirmation of the Interaction between AtWEE1 and At14-3-3ω

Based on the findings of cell cycle regulating interactions between Wee1 proteins and 14-3-3 proteins in several organisms (Wang *et al.*, 2000; Lee *et al.*, 2001; Rothblum-Oviatt *et al.*, 2001), it would be interesting to discover if 14-3-3 proteins exert a similar function in *A. thaliana*. Findings by Sorrell *et al.* (2003) and Cutler *et al.* (2000) have shown that At14-3-3ω has a cell cycle function and that this particular isoform is sublocalized in the cell in a cell cycle-dependent manner. Therefore, the interaction between AtWEE1 and the At14-3-3ω isoform is very probable, although it needs to be confirmed using alternative *in vitro* and/or *in vivo* methods.

5.3.2.1 AtWEE1 co-immunoprecipitates with At14-3-3ω *in vitro*

One way of confirming protein-protein interactions found in Y2Hs is to co-immunoprecipitate the two proteins *in vitro*. The Stratagene pESC yeast epitope tagging vector system, which is designed for expression and functional analysis of eukaryotic genes in *S. cerevisiae*, was used for the confirmation of the AtWEE1/ At14-3-3ω interaction. The vector contains the *GAL1* and *GAL10* yeast promoters in opposing orientation making it possible to introduce one or two cloned genes into a yeast strain under the control of repressible promoters. When two genes are co-expressed, protein-protein interactions can be confirmed by co-immunoprecipitations. The vector contains sequences encoding epitope peptides, c-myc or FLAG®, which can be specifically recognized by commercial monoclonal antibodies (Stratagene 12/05). The FLAG® epitope is located in multiple cloning site 1 (MCS1) and the c-myc epitope is located in MCS2 (Figure 12).

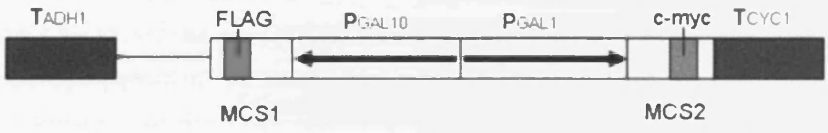

Figure 12 – Schematic diagram of the features of the pESC vector (not to scale). The *GAL1* and *GAL10* yeast promoters in opposing orientation and the two multiple cloning sites (MCS1 and MCS2), which contain the sequences for the FLAG® and the c-myc epitope tags, respectively. MCS1 is flanked by the *ADH1* terminator and the MSC2 is flanked by the *CYC1* terminator (Stratagene 12/05).

Proteins were produced in *S. cerevisiae* and used for the co-immunoprecipitation analysis (5.2.2). For Western blotting, 20 µL of FLAG® resin eluate was subjected to SDS-PAGE and duplicate Western blots were probed with FLAG and c-myc antibodies (Figure 13A). A band of 56 kDa corresponding to the size of AtWEE1 was detected in the AtWEE1 c-myc/At14-3-3ω FLAG eluate and in the AtWEE1 c-myc+At14-3-3ω FLAG eluate with the c-myc antibody, indicating that AtWEE1 binds to At14-3-3ω. In the AtWEE1 c-myc/At14-3-3ω FLAG extract, the two recombinant proteins were produced simultaneously in *S. cerevisiae*, whereas in the AtWEE1 c-myc+At14-3-3ω FLAG the two proteins were produced separately and mixed together prior to the co-immunoprecipitation. The 56 kDa band corresponding to the size of AtWEE1 was not present in the control co-immunoprecipitations (AtWEE1 c-myc only or At14-3-3ω FLAG only). However, a band of 29 kDa corresponding to the size of At14-3-3ω was detected in all co-immunoprecipitation eluates except in the AtWEE1 c-myc only control.

Figure 13 – Co-immunoprecipitation analysis of AtWEE1 and At14-3-3ω A) FLAG and c-myc antibody-probed Western blots of FLAG immunoprecipitated proteins extracted from yeast transformants carrying: At14-3-3ω FLAG only, AtWEE1 c-myc only, AtWEE1 c-myc/14-3-3 FLAG and AtWEE1 c-myc+14-3-3 FLAG. In the AtWEE1 c-myc/At14-3-3ω FLAG extract the two proteins were produced simultaneously in the same *S. cerevisiae* cell, whereas in the AtWEE1 c-myc+At14-3-3ω FLAG the two proteins were produced separately and mixed together prior to the co-immunoprecipitation. B) FLAG and c-myc antibody-probed Western blots of FLAG immunoprecipitated proteins extracted from yeast transformants carrying: At14-3-3ω FLAG only and At14-3-3ω FLAG mixed with 1 mg of an *A. thaliana* protein extract.

To investigate if At14-3-3ω could also bind to native AtWEE1, 1 mg of a total protein extract from *A. thaliana* was mixed together with the protein extract from the At14-3-3ω expressing *S. cerevisiae* transformant and added to the FLAG® resin (Figure 13B). An antibody raised against plant WEE1 was used to probe the Western blot and a band of app. 56 kDa corresponding to the size of AtWEE1 was detected in

the At14-3-3ω FLAG extract mixed with the *A. thaliana* protein extract, indicating that At14-3-3ω not only binds to AtWEE1 produced in *S. cerevisiae*, but also binds to native AtWEE1 from *A. thaliana*. Furthermore, a band of 29 kDa corresponding to the size of At14-3-3ω was detected in all eluates confirming the presence of At14-3-3ω.

5.3.2.2 AtWEE1 interacts with At14-3-3ω *in vivo* in *N. tabacum* BY-2 Cells

In addition to the *in vitro* confirmation of the AtWEE1/At14-3-3ω interaction, the interaction was also confirmed *in vivo* in *N. tabacum* BY-2 cells using BiFC. The BiFC technique takes advantage of splitting the yellow fluorescent protein (YFP) in two and fusing one part to one protein (X) and the other to a second protein (Y). If the two proteins interact the two parts of YFP will be brought in close proximity and give rise to a yellow fluorescent BiFC complex (Figure 14A).

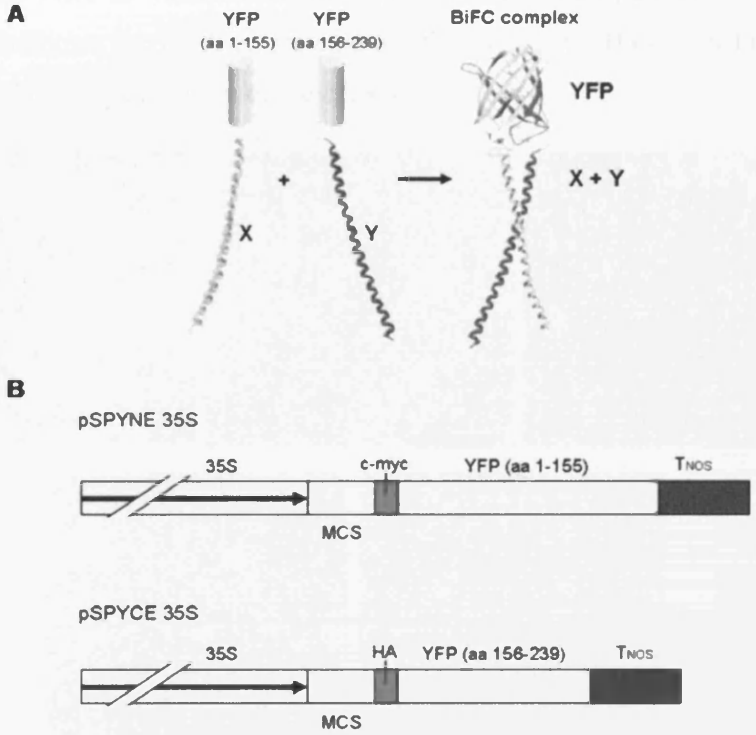

Figure 14 – A) Schematic diagram of the BiFC technique. The yellow fluorescent protein (YFP) is split in two and one part is fused to a protein (X) and the other part is fused to a protein (Y). If the two proteins interact the two parts of YFP will be brought in close proximity and give rise to a yellow fluorescent BiFC complex (Hu *et al.*, 2002). B) Schematic diagram of the features of the BiFC vectors, pSPYNE 35S and pSPYCE 35S (not drawn to scale). The vectors have in common the 35S promoter, MCS and the *NOS* terminator. In addition, the pSPYNE 35S contains a c-myc tag and the N-terminal part of YFP (aa 1-155). The pSPYCE 35S contains a HA tag and the C-terminal part of YFP (aa 156-239) (Adapted from Walter *et al.*, 2004).

The BiFC system used was previously developed by Walter *et al.* (2004). It consists of two vectors, pSPYNE 35S and pSPYCE 35S. In common the two vectors have a 35S promoter, MCS and a *NOS* terminator. In addition, the pSPYNE 35S contains a c-myc tag and the N-terminal part of YFP (aa 1 – 155). The pSPYCE 35S contains an HA tag and the C-terminal part of YFP (aa 156 – 239) (Figure 14B).

Stable *N. tabacum* BY-2 cell lines carrying pSPYNE 35S empty vector, pSPYNE 35S AtbZIP63, pSPYNE 35S AtWEE1 and pSPYNE 35S At14-3-3ω, respectively, were generated and subsequently genotyped by PCR (data not shown). The transcription of the transgene was checked by RT-PCR using gene-specific primers. The phenotypes of the cell lines that showed presence and transcription of the transgene were assessed by light microscopy using an Olympus BH2 microscope (Figure 15). In addition to performing RT-PCR to verify the transcription of the transgene, PCR was also performed directly on the RNA extracted from the transgenic BY-2 cell lines to rule out genomic DNA contamination of the cDNA.

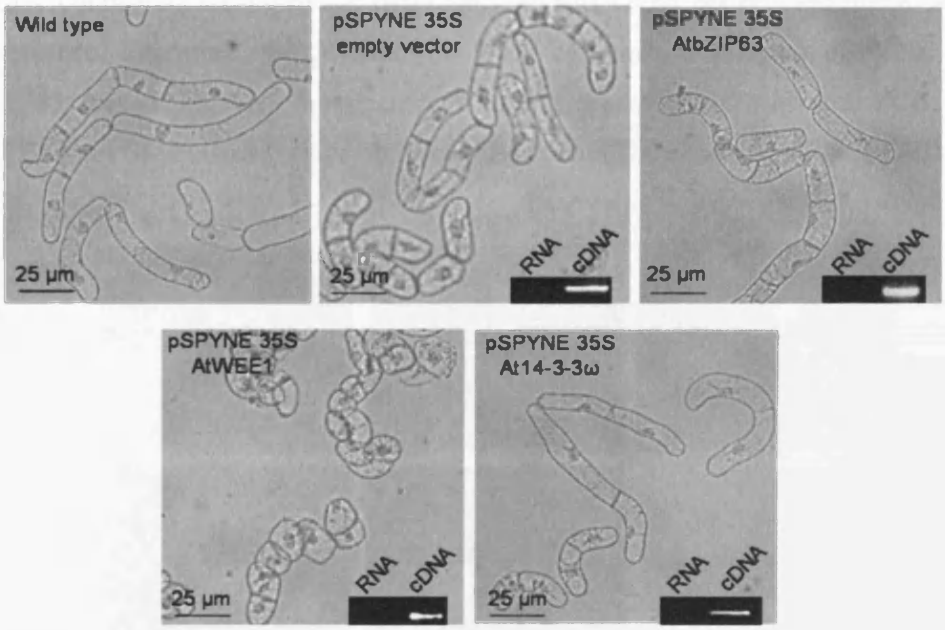

Figure 15 – Light microscope images of the cell phenotypes of wild type and transgenic *N. tabacum* BY-2 cell lines including RT-PCR data on cDNA from the transgenic lines verifying the transcripton of the transgene and PCR data on RNA for ruling out genomic DNA contamination of the cDNA. The transgenic cells carrying the pSPYNE 35S empty vector, pSPYNE 35S *AtbZIP63*, pSPYNE 35S *At14-3-3ω* shares the same cell phenotype as wild type cells, whereas the transgenic cells carrying pSPYNE 35S *AtWEE1* has a small cell phenotype as previously described (Siciliano, 2006).

For analysis of the AtWEE1/At14-3-3ω interaction only the *N. tabacum* BY-2 cell line carrying pSPYNE 35S *At14-3-3ω* was used, since the cell line carrying the pSPYNE 35S *AtWEE1* showed a small cell phenotype compared to wild type and the other transgenic *N. tabacum* BY-2 cell lines. This phenotype is thought to be caused by the constitutive over-expression of AtWEE1 by the 35S promoter and has previously been described by Siciliano (2006).

The BiFC analyses were performed as described in section 5.2.4 by *A. tumefaciens*-mediated transient transformation of the stable *N. tabacum* BY-2 pSPYNE 35S cell cultures. As a negative control for all the BiFC experiments the pSPYNE 35S and pSPYCE 35S empty vectors were used and as the positive control pSPYNE 35S *AtbZIP63* and pSPYCE 35S *AtbZIP63* were used. The bZIP63 proteins form nuclear localized homodimers by transiently transforming both constructs into *Nicotiana benthamiana* (*N. benthamiana,* Nb) leaves and *A. thaliana* cell culture-derived protoplasts (Walter *et al.*, 2004). However, in the BiFC system presented here the negative control consisting of the two empty vectors could not be used due to auto-fluorescence. Therefore, the *N. tabacum* BY-2 cell culture carrying pSPYNE 35S *AtbZIP63* mixed with *A. tumefaciens* EHA105 transformed with pSPYCE 35S *AtWEE1* were used instead, since no fluorescence could be observed (Figure 16II).

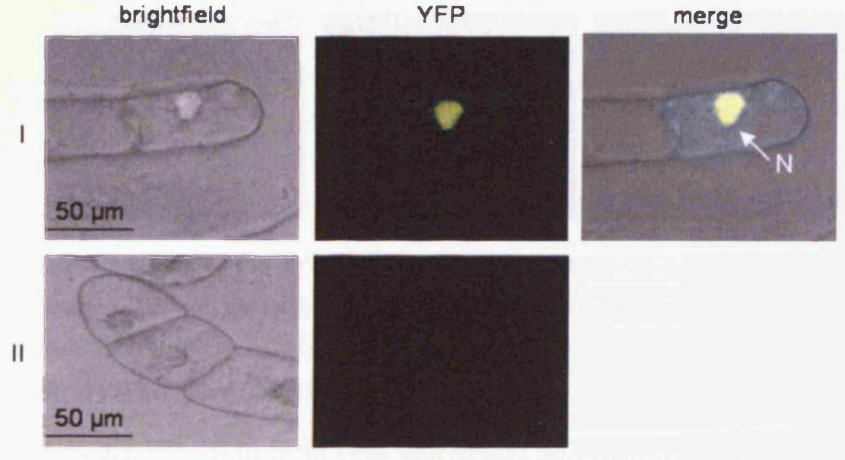

Figure 16 – I) BiFC analysis of the AtbZIP63/AtbZIP63 homodimerization (positive control) by transient *A. tumefaciens*-mediated transformation of the pSPYNE 35S *AtbZIP63* BY-2 cell line with pSPYCE 35S *AtbZIP63*. Yellow fluorescence could be detected only in the nucleus (N). II) BiFC analysis of AtbZIP63/AtWEE1 (negative control) by transient *A. tumefaciens*-mediated transformation of the pSPYNE 35S *AtbZIP63* BY-2 cell line with pSPYCE 35S *AtWEE1*. No yellow fluorescence could be detected.

For the positive control, fluorescence was observed exclusively in the nucleus (Figure 16I). This is consistent with the findings of Walter *et al.* (2004) and implies that the BiFC system is also functional in the transgenic *N. tabacum* BY-2 cell system with a transformation efficiency of 1:200 cells. The *N. tabacum* BY-2 cell culture carrying pSPYNE 35S *At14-3-3ω* was mixed with *A. tumefaciens* EHA105 transformed with pSPYCE 35S *AtWEE1* and after 72 h yellow fluorescence could be observed in the nucleus, cytoplasm, cell wall and at the cell plate (Figure 17I-III). These observations suggest a dynamic interaction between AtWEE1 and At14-3-3ω, which might be influenced by the cell cycle phase.

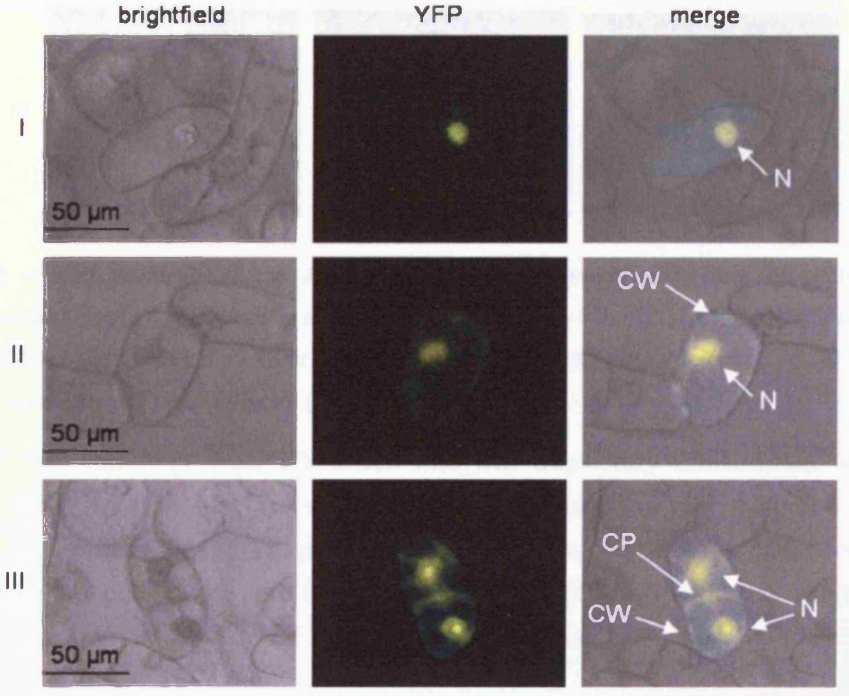

Figure 17 – BiFC analysis of the AtWEE1/At14-3-3ω interaction by transient *A. tumefaciens*-mediated transformation of the pSPYNE 35S At14-3-3ω BY-2 cell line with pSPYCE 35S AtWEE1. Yellow fluorescence could be detected in the nucleus (N) (I, II and III), cell wall (CW) (II and III) and at the cell plate (CP) (III).

14-3-3 proteins are known to form both hetero and homodimers with each monomer forming a phospho-peptide binding groove (Obsil *et al.*, 2001, Aitken, 2002; Ferl, 2004). The specific composition of 14-3-3 dimers within a given cell is thought to be important for the ability of 14-3-3 protein family to act as modulators or adapters that facilitate the interaction of distinct components of signalling pathways. Therefore, it was investigated if and where At14-3-3ω homodimerizes *in vivo*.

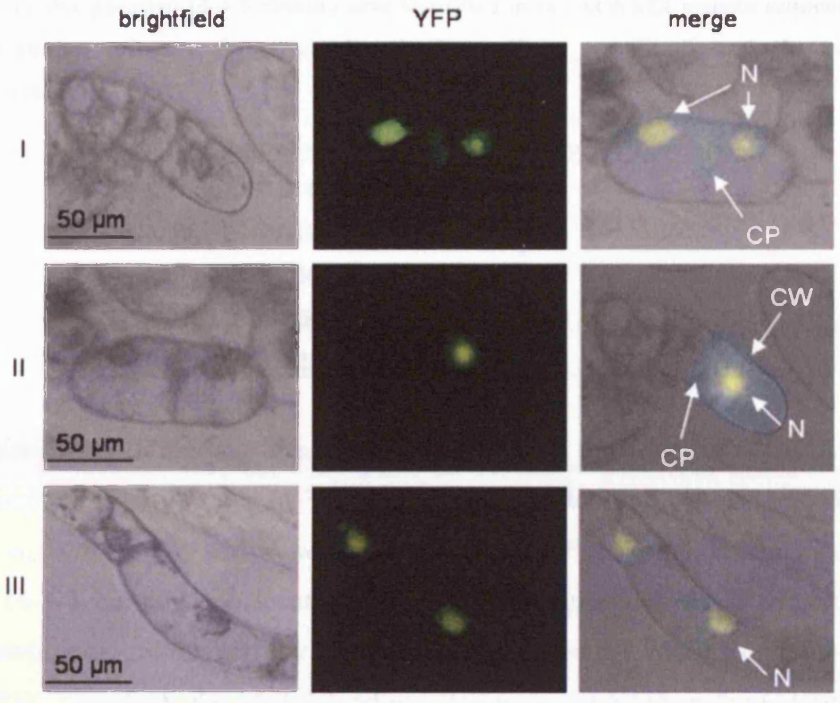

Figure 18 – BiFC analysis of the At14-3-3ω/At14-3-3ω homodimerization by transient *A. tumefaciens*-mediated transformation of the pSPYNE 35S At14-3-3ω BY-2 cell line with pSPYCE 35S At14-3-3ω. After 72 h yellow fluorescence could be detected in the nucleus (N) (I, II and III) and in the cell plate (CP) and cell wall (CW) (I and II).

The pSPYNE 35S *At14-3-3ω* BY-2 cell line was transiently transformed with the pSPYCE 35S *At14-3-3ω* plasmid and yellow fluorescence was observed in the nucleus of the BY-2 cells (Figure 18I-III). Furthermore, fluorescence could be detected at the cell plate and in the cell wall coinciding with the sub-cellular localization pattern of the AtWEE1/At14-3-3ω interaction.

5.3.3 Identification of a putative AtWEE1/At14-3-3ω Interaction Site

Using a motif scanning software (http://scansite.mit.edu/motifscan_seq.phtml) five putative 14-3-3 binding motifs were identified in the protein sequence of AtWEE1 (Table 8). The binding sites identified by the motif scanning software are mode I (RSXpSXP) 14-3-3 binding sites only. Residues T15, S144, T247, S450 and S485 are the predicted phosphorylation sites within these binding motifs.

Table 8 – The five putative 14-3-3 binding sites identified in the AtWEE1 protein sequence using a motif scanning software (http://scansite.mit.edu/motifscan_seq.phtml) and the predicted phosphorylation sites.

Sequence of putative 14-3-3 binding site	Phosphorylation site
TLLAKRK**pT**QGTIKTR	T15
SKRCRQE**pS**FTGNHSN	S144
DGLSRYL**pT**DFHEIRO	T247
LTESRNQ**pS**LNIKEGK	S450
RDPKRRP**pS**ARELLDH	S485

The putative 14-3-3 binding site located at S485 in the C-terminal of AtWEE1 displays high similarity to the 14-3-3 binding sites located at S549/S558/S559 found in *X. laevis*, *M. musculus* and *H. sapiens*, respectively (Figure 19). Furthermore, a C-terminal 14-3-3 binding site located at S642 in *H. sapiens* Wee1 is important for Wee1 protein localization, activity and stability (Wang *et al.*, 2000; Rothblum-Oviatt at al., 2001). Therefore, the 14-3-3 binding site located at S485 in the C-terminal of AtWEE1 was predicted to be the most likely binding site for At14-3-3ω.

Figure 19 – Alignment of the 14-3-3 binding motifs located at S485 in *A. thaliana*, S558 in *M. musculus*, S559 in *H. sapiens* and S549 in *X. laevis*. Alignment was made in Workbench (http://www.workbench.sdsc.edu) using the Clustal W alignment tool showing conserved residues (blue and *), conserved strong group residues (green and :), black residues are residues with no consensus. Arrow indicate the predicted phosphorylation sites within these binding motifs

To investigate if the AtWEE1/At14-3-3ω interaction could be abolished, an AtWEE1 (S485A) mutant was constructed by site-directed mutagenesis. Specific primers were designed to introduce a base pair change resulting in the S485A mutation and the mutagenesis was performed as described in section 5.2.5. In order to test if the AtWEE1 (S485A) is incapable of interacting with At14-3-3ω *in vivo*, the following plasmids were constructed: a pBD-Gal4-cam *AtWEE1(S485A)* to use in a Y2H screen and a pSPYNE 35S *AtWEE1(S485A)* to use in a BiFC analysis.

The pBD-Gal4-cam *AtWEE1 (S485A)* plasmid was co-transformed with pAD Gal4 2.1 At14-3-3ω into wild type *S. cerevisiae* YRG2 cells and selected on SD agar plates

containing trp-leu DO solution. Furthermore, the transformants were verified for the presence of the bait and target plasmids by colony PCR using primers *AtWEE1* (P44+P50) and *14-3-3ω* (P44+P47). The transformants were subsequently checked for activation of the *HIS3* and *LacZ* reporter genes. As controls in these experiments the transformants carrying the *AtWEE1* and *AtWEE1(S485A)* bait plasmids and the *AtWEE1/At14-3-3ω* double transformant were used. Initially, the *AtWEE1(S485A)* bait plasmid was tested for its ability to auto-activate the *HIS3* reporter gene. The transformants did not grow on SD agar containing his DO solution and therefore did not auto-activate the *HIS3* reporter gene. As previously found, the *AtWEE1/ At14-3-3ω* double transformant was capable of growing on SD agar plates containing his DO solution and 40 mM 3-AT. However, growth could not be observed when the WEE1 (S485A)/At14-3-3ω transformant was grown on SD agar plates containing his DO solution suggesting that the S485A mutation of AtWEE1 abolishes At14-3-3ω binding. Additionally, the transformants were tested for transcriptional activation of the *LacZ* reporter gene using a filter lift assay and a quantitative liquid ONPG assay (Figure 20A and B). The transformant carrying the *AtWEE1* and *AtWEE1(S485A)* bait plasmids only were not capable of activating the *LacZ* reporter gene, since *β-galactosidase* activity could not be detected either in the filter lift assay or in the ONPG assay. The *AtWEE1/At14-3-3ω* double transformant was capable of activating the *LacZ* reporter gene resulting in blue colouration of the yeast in the filter lift assay, as previously shown, and *β-galactosidase* activity was detected in the ONPG assay. For the *AtWEE1(S485A)/At14-3-3ω* double transformant, *β-galactosidase* activity could not be detected either in the filter lift assay or in the ONPG assay. This together with its inability to activate the *HIS3* reporter gene suggests that the S485A mutation of AtWEE1 is sufficient for abolishing At14-3-3ω binding.

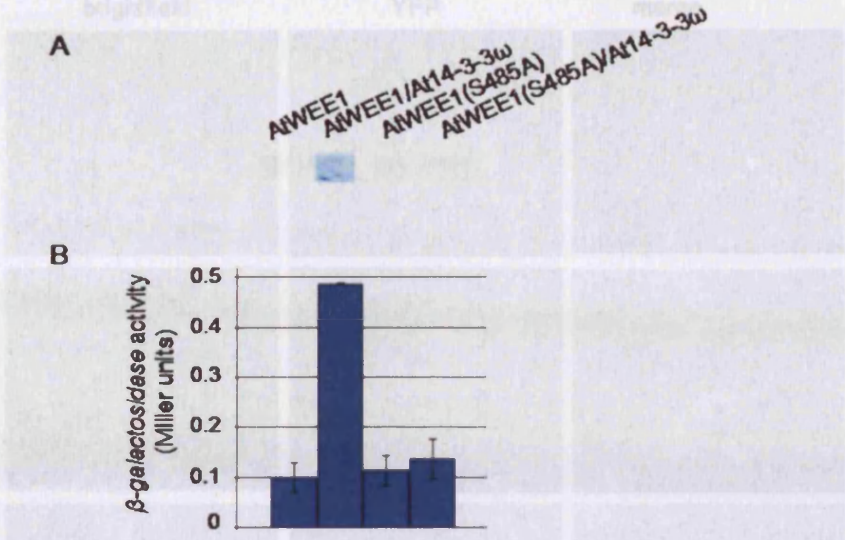

Figure 20 – *LacZ* reporter gene screening A) Filter lift assay, from left AtWEE1 only, AtWEE1/At14-3-3ω, AtWEE1 (S485A) only and AtWEE1 (S485A)/At14-3-3ω. B) Quantitative ONPG assay, from left AtWEE1 only, AtWEE1/At14-3-3ω, AtWEE1 (S485A) only and AtWEE1 (S485A)/At14-3-3ω.

In the Y2H system the AtWEE1/At14-3-3ω interaction was abolished by a S485A mutation in the 14-3-3 binding site of AtWEE1 indicating that the presence of S485 is vital for At14-3-3ω binding.

To test if the interaction was also abolished *in vivo A. tumefaciens* transformed with pSPYCE 35S *AtWEE1 (S485A)* was mixed with the *N. tabacum* BY-2 cell culture carrying pSPYNE 35S *At14-3-3ω*. Unexpectedly, fluorescence was observed after 72 h (Figure 21I – III) indicating that S485A mutation of WEE1 is not sufficient to abolish 14-3-3 binding *in vivo*. Fluorescence was detected in the nucleus, but not in the cell wall or cell plate, which could suggest that the AtWEE1 (S485A) mutation affects the binding of At14-3-3ω resulting in a nuclear localization of AtWEE1.

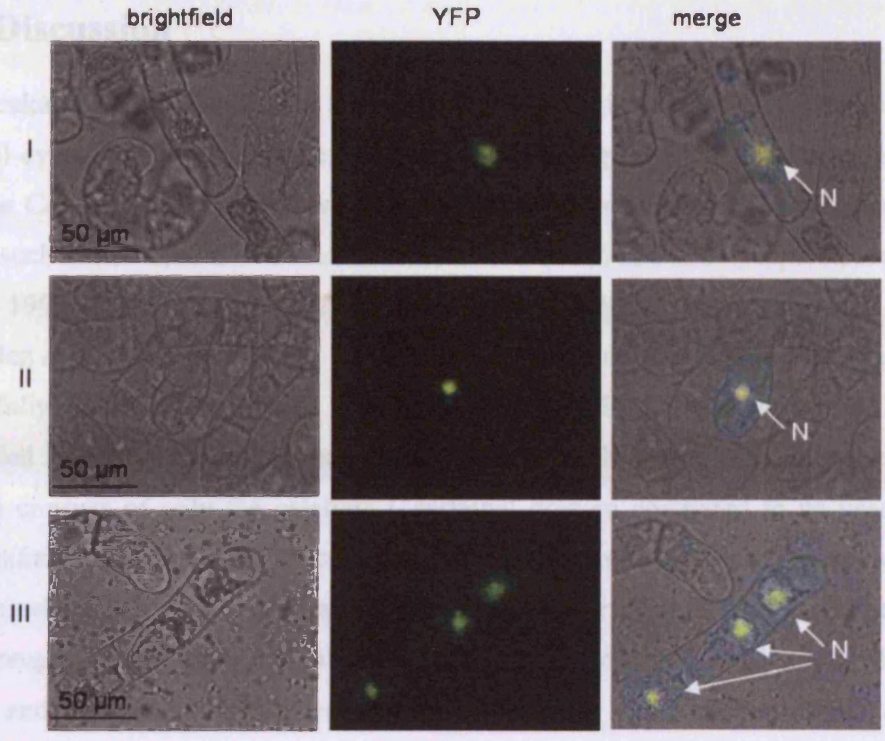

Figure 21 – BiFC analysis of the AtWEE1 (S485A)/At14-3-3ω interaction by transient *A. tumefaciens*-mediated transformation of the pSPYNE 35S At14-3-3ω BY-2 cell line with pSPYCE 35S AtWEE1(S485A). After 72 h yellow fluorescence could be detected in the nucleus (N) (I, II and III).

5.4 Discussion

In all eukaryotes the progression from G2 into M phase is a major transition point of the cell cycle. The two key proteins regulating this progression are the Wee1 kinase and the Cdc25 phosphatase. Wee1 kinases have been identified in a wide range of plants such as *Z. mays*, *A. thaliana, O. sativa*, *L. esculentum* and *S. lycopersicum* (Sun *et al.*, 1999; Sorrell *et al.*, 2002; Vandepoele *et al.*, 2002; Gonzalez *et al.*, 2004; Gonzalez *et al.*, 2007; Guo *et al.*, 2007). However, a homologue to the Cdc25 has not been fully identified in higher plants. A putative CDC25 homologue has been identified in *A. thaliana*, which possesses *in vitro* phosphatase activity. However, the protein consists of only the catalytic C-terminal domain compared to its yeast and mammalian homologues, which consist of both a C-terminal catalytic domain and an N-terminal regulatory domain (Landrieu *et al.*, 2004; Sorrell *et al.*, 2005). During cell cycle progression in both animals and yeast, the activity and localization of both Cdc25 and Wee1 are greatly affected by the binding of 14-3-3 proteins (Dalal *et al.*, 1999; Kumagai and Dunphy, 1999; Zeng and Piwnica-Worms, 1999; Wang *et al.*, 2000; Lee *et al.*, 2001; Rothblum-Oviatt *et al.*, 2001; Chen *et al.*, 2003b).

A direct involvement of 14-3-3 proteins in regulating WEE1 and CDC25 localization and activity in the plant cell cycle have not previously been reported and only a few reports suggest that plant 14-3-3s are involved in cell cycle regulation (Cutler *et al.*, 2000; Kuromori and Yamamoto, 2000; Sorrell *et al.*, 2003). Y2H library screens were made using AtCDC25 and AtWEE1 as bait in an *A. thaliana* seedling root cDNA library (Chapter 4) to discover protein interaction partners for these two proteins that could help to determine the exact functions for these two proteins and help to draw parallels between the plant cell cycle and cell cycles in other eukaryotes. Unexpectedly, 14-3-3 proteins were not identified as interaction partners for either AtWEE1 or the putative AtCDC25 suggesting that these proteins do not interact with 14-3-3 proteins. This would indeed distinguish the *A. thaliana* CDC25 and WEE1 from other eukaryotic homologues. However, an analysis of the protein sequences of AtCDC25 and AtWEE1 revealed that putative 14-3-3 binding sites were present in both sequences. The AtCDC25 and AtWEE1 sequences contained one and five putative 14-3-3 binding sites, respectively. Based on the previous findings by Sorrell *et al.* (2003), who showed using Y2H that *A. thaliana* Non-Epsilon group 14-3-3ω, λ

and κ interact with SpCdc25, the Non-Epsilon 14-3-3s from *A. thaliana* were investigated as putative interaction partners for AtCDC25 and AtWEE1.

In the Y2H screen, AtCDC25 was found not to interact with any of the Non-Epsilon 14-3-3 proteins since the double transformants were incapable of activating the transcription of either the *HIS3* or the *LacZ* reporter gene. In the last decade, several reports have shown that 14-3-3 protein binding to *S. pombe*, *H. sapiens* and *X. laevis* Cdc25 proteins is an important regulatory feature of the cell cycle. When Cdc25 is bound by 14-3-3 proteins it is sequestered to the cytoplasm and the 14-3-3 binding retains Cdc25 in the cytoplasm and thereby keeps Cdc25 away from its substrate (Zeng and Piwnica-Worms, 1999; Graves *et al.*, 2001; Uchida *et al.*, 2004). This clearly implies that binding of 14-3-3 proteins to Cdc25 is crucial for proper execution and regulation of the cell cycle, which might question the cell cycle function of the putative *A. thaliana* CDC25. However, the lack of the N-terminal regulatory domain of AtCDC25 could be the reason for the protein not interacting with 14-3-3 proteins. The binding of 14-3-3 proteins to *H. sapiens* CDC25B and *S. pombe* Cdc25 occurs at specific 14-3-3 binding sites located in the N-terminal regulatory domain (Zeng and Piwnica-Worms, 1999; Uchida *et al.*, 2004; Boutros *et al.*, 2006; Uchida *et al.*, 2006). As previously mentioned, it is possible that the missing N-terminal regulatory domain may be found as a separate protein that has to interact with the C-terminal part of AtCDC25 in order for AtCDC25 to act as fully functional plant CDC25. Because of the putative AtCDC25 and the inability to identify full-length CDC25 homologues in higher plants, it has been speculated that in higher plants the *CDC25* gene might have become redundant and consequently lost through evolution (Boudolf *et al.*, 2006). Interestingly, Budolf *et al.* (2006) reports a striking number of functional parallels between the *A. thaliana* CDKB1;1 and the *D. melanogaster* CDC25 suggesting that the acquisition of B-type CDKs and the possible disappearance of CDC25 in plants might be associated. This would indeed make plants distinct from other eukaryotic species and suggest that plants would have a different method of counteracting the WEE1 kinase activity in the regulation of the plant cell cycle.

In the Y2H screen, AtWEE1 was found to interact with all the Non-Epsilon 14-3-3 isoforms, which is not surprising, since the members of the *A. thaliana* Non-Epsilon 14-3-3 protein family display high sequence conservation of 70 – 90% both at the nucleotide and protein level (Wu *et al.*, 1997a, Appendix A). In *H. sapiens* and

X. laevis 14-3-3 proteins function as positive regulators of Wee1 by protecting the activating phosphorylation and thereby stabilizing the activity of Wee1 (Wang *et al.*, 2000; Lee *et al.*, 2001; Rothblum-Oviatt *et al.*, 2001). This suggests that binding of 14-3-3 proteins to Wee1 is important not only for maintaining the G2 arrest of the cells, but also for driving the cells more efficiently into mitosis. Of the Non-Epsilon 14-3-3 isoforms interacting with AtWEE1, 14-3-3ω is of particular interest, since this isoform was previously shown to have cell cycle function because of its ability to rescue an *S. pombe rad24*⁻ mutant (Sorrell *et al.*, 2003) and furthermore this isoform was shown to shuttle between the cytoplasm and nucleus in a cell cycle-dependent manner (Cutler *et al.*, 2000).

The specificity of the interaction between AtWEE1 and At14-3-3ω was confirmed *in vitro* by co-immunoprecipitation of recombinant proteins produced in *S. cerevisiae*. In addition, recombinant At14-3-3ω bound to AtWEE1 from a total protein extract from *A. thaliana* seedlings further adding evidence of the specificity of the interaction. The interaction was also confirmed *in vivo* using the BiFC technique in *N. tabacum* BY-2 cell cultures. So far the BiFC technique has proven to be very valuable for analyzing protein-protein interactions in a wide-range of plant tissues and cell types in onion, *Allium cepa* (*A. cepa*, Ac), *O. sativa*, *A. thaliana* and *N. tabacum* (Bracha-Drori *et al.*, 2004; Walter *et al.*, 2004; Diaz *et al.*, 2005; Stolpe *et al.*, 2005; Xie *et al.*, 2006). So far the technique has been implemented in whole plant leaves by leaf infiltration techniques or in plant cell-derived protoplasts by transient transformation, which makes the BiFC system implemented in this work, the first report of a functional BiFC system in plant cell culture. Besides confirming specific protein-protein interactions *in vivo* in the native environment of the proteins, this technique also reveals valuable information concering the sub-cellular localization of the specific protein interaction in actively dividing cells. The BiFC technique was successfully implemented in transgenic *N. tabacum* BY-2 cell lines by *A. tumefaciens*-mediated transient transformation. Besides confirming the AtWEE1/At14-3-3ω interaction, the localization of the interaction was mapped to the nucleus, cell wall and at the cell plate indicating a dynamic interaction between AtWEE1 and At14-3-3ω, which may very well be influenced by the cell cycle phase.

Findings in *X. laevis* suggest that the role of 14-3-3 binding is to keep Wee1 evenly distributed in the nucleus (Lee *et al.*, 2001). However in *H. sapiens*, Wee1 is localized

both in the nucleus and in the cytoplasm upon 14-3-3 binding (Rothblum-Oviatt *et al.*, 2001) consistent with the localization of the AtWEE1/At14-3-3ω interaction presented here. It is likely that the interaction between AtWEE1 and At14-3-3ω is weak or transient and thus only occurring at specific times during the cell cycle *e.g.* during cell cycle regulation or in response to stress. The BiFC technique makes it possible to monitor transient or weak interactions due to the irreversibility of the formed BiFC complexes (Hu *et al.*, 2002; Walter *et al.*, 2004; Bhat *et al.*, 2006). Previously, At14-3-3ω was shown to shuttle between cytoplasm and nucleus in a cell cycle-dependent manner. The At14-3-3ω protein accumulates in the nucleus just after completion of nuclear division and relocalizes to the cytoplasm shortly before completion of cytokinesis (Cutler *et al.*, 2000). Furthermore, in the work presented here At14-3-3ω was found to homodimerize primarily in the nucleus, which could imply that in the *N. tabacum* BY-2 cells At14-3-3ω monomers bind to AtWEE1 and when 14-3-3ω is not required for binding to AtWEE1 it homodimerises in the nucleus. In *A. thaliana* it is very likely that At14-3-3ω, in addition to the formation of homodimers, will form heterodimers with other 14-3-3 isoforms possibly altering both function and specificity of At14-3-3ω, since the dimerisation of 14-3-3 proteins results in two binding pockets in the dimer allowing it to interact with two motifs simultaneously (Liu *et al.*, 1995; Yaffe *et al.*, 1997; Rittinger *et al.*, 1999; Obsil *et al.*, 2001, Ferl, 2004). The interaction between proteins is greatly influenced by time/space constraints and it is possible that two proteins, although able to interact, are never in close proximity to each other within the cell. The two proteins could be expressed in different cell types or even if they are expressed in the same cell they could be located in different sub-cellular compartments (Van Criekinge and Beyaert, 1999). To date no reports have been made of the sub-cellular localization or eventual shuttling of AtWEE1 between cytoplasm and nucleus in a cell cycle-dependent manner. However, it is evident from *H. sapiens* that the sub-cellular localization of Wee1 is regulated during the cell cycle. Wee1 is located in the nucleus during interphase and is relocalized to the cytoplasm when the cell undergoes mitosis (Baldin and Ducommun, 1995).

The 14-3-3 protein interaction site of Wee1 in both *H. sapiens* and *X. laevis* has been mapped to the well conserved C-terminal catalytic domain and mutations of the phosphorylation site within these 14-3-3 binding motifs abolished 14-3-3 protein

binding and also affected Wee1 activity and stability (Wang *et al.*, 2000; Lee *et al.*, 2001; Rothblum-Oviatt *et al.*, 2001). In order to map the site of interaction between AtWEE1 and At14-3-3ω, the protein sequence of AtWEE1 was screened for the presence of 14-3-3 binding sites. Five mode I 14-3-3 protein binding sites were identified, of which one at S485 showed high similarity to the above mentioned 14-3-3 binding sites reported for both *H. sapiens* and *X. laevis* Wee1s. Therefore, this was predicted to be the most likely binding site for At14-3-3ω. A Y2H screen showed that the AtWEE1(S485A) mutant was not longer capable of interacting with At14-3-3ω suggesting that the 14-3-3 protein binding site located at S485 is the binding site for At14-3-3ω and that the S485 residue is vital for 14-3-3 binding. To investigate if the binding of At14-3-3ω to AtWEE1 was abolished or if the At14-3-3ω binding affinity was primarily decreased, a quantitative ONPG assay was performed, which further indicated that the interaction between AtWEE1 and At14-3-3ω was abolished by the S485A mutation. However, when the AtWEE1(S485A) mutant was tested by BiFC *in vivo* in the *N. tabacum* BY-2 cells the situation proved to be different. Yellow fluorescence was observed for the AtWEE1(S485A)/At14-3-3ω transformant, which indeed was unexpected, since the interaction was found to be abolished in the Y2H screen. This finding strongly emphasizes the significance and necessity of confirming protein-protein interactions identified in Y2H screens in their native environment. However, in the case of the AtWEE1(S485A)/At14-3-3ω, transformant fluorescence was detected in the nucleus and not in the cell wall or cell plate, which could suggest that the AtWEE1 (S485A) mutation affects the binding of At14-3-3ω resulting in a nuclear localization of AtWEE1. It has not been previously reported in other organisms if 14-3-3 protein binding affects the sub-cellular localization of Wee1. However, it is evident from *S. pombe*, *H. sapiens* and *X. laevis* that 14-3-3 binding causes cytoplasmic localization of Cdc25 (Dalal *et al.*, 1999; Zeng and Piwnica-Worms, 1999; Kumagai and Dunphy, 1999; Yang *et al.*, 1999; Boutros *et al.*, 2006; Uchida *et al.*, 2006).

An explanation for why the interaction is abolished in the Y2H system and not in the BiFC system could be that the protein expression in the BiFC system is driven by the strong constitutive 35S promoter resulting in high levels of the expressed proteins within the transformed cells (Bracha-Drori *et al.*, 2004; Walter *et al.*, 2004; Ohad *et al.*, 2007). This could potentially result in two proteins that do not actually physical

interact coming into close proximity, causing the restoration of the YFP (BiFC complex) and hence YFP fluorescence. However, no reports have been made of this occurrence in other systems and hence this is unlikely to be the explanation for the observed fluorescence indicating interaction between AtWEE1(S485A) and At14-3-3ω *in vivo*. This is further supported by the AtbZIP63 and AtWEE1 protein pair (used as negative control in all BiFC experiments), which does not cause fluorescence although the two proteins are expressed under identical conditions as the AtWEE1(S485A) and At14-3-3ω protein pair. A more plausible explanation for the abolition of the AtWEE1(S485A)/At14-3-3ω interaction in the Y2H system is that the binding affinity is reduced, but not in fact abolished. A similar finding was made in *S. pombe*, where mutations of all the putative phosphorylation sites within the three 14-3-3 binding motifs of Cdc25 was found to reduce, but not eliminate 14-3-3 binding and the triple mutant was only partially impaired in its ability to arrest cell cycle progression in response to a DNA replication block (Zeng and Piwnica-Worms, 1999). Expression of the proteins in the Y2H system is driven by a truncated 410 bp version of the *S. cerevisiae ADH1* promoter and expression from this promoter leads to low or in some cases very low levels of fusion protein expression (Santangelo and Tornow, 1990; Ruohonen *et al.*, 1991; Legrain *et al.*, 1994). A low level of protein expression in the Y2H system together with a decreased binding affinity of At14-3-3ω to the AtWEE1(S485S) mutant protein compared to the wild type WEE1 could be a likely reason for not detecting activation of neither the *HIS3* nor the *LacZ* reporter gene. In the BiFC system both proteins are being over-expressed by the 35S promoter and it might complicate the detection/quantification of proteins with decreased binding affinity. In the *N. tabacum* BY-2 cell cultures, which better reflect the native environment of the proteins analyzed, there could be additional proteins/factors present, which might influence or maybe even promote an interaction between AtWEE1(S485A) and At14-3-3ω.

At this time there is no clear and straight forward answer to why the S485A mutation of AtWEE1 is sufficient for abolishing the interaction between AtWEE1 and At14-3-3ω in the Y2H system and not in the BiFC system. From the findings presented in this thesis, it is evident that the S485A mutation of WEE1 does not abolish 14-3-3ω binding *in vivo*. However, the findings suggest that the S485A mutation of AtWEE1 affects the sub-cellular localization of the interaction, which

possibly could be a consequence of a decreased At14-3-3ω binding to AtWEE1(S485A).

5.5 Summary

In plants, the *A. thaliana* 14-3-3 protein family is the largest and best characterized. It consists of 13 translated proteins divided into the Epsilon and Non-Epsilon subgroups. In several eukaryotic species 14-3-3 proteins are important key regulators of both Cdc25 and Wee1 proteins. Three of the Non-Epsilon 14-3-3 isoforms interact with *S. pombe* Cdc25 and therefore the entire group of Non-Epsilon 14-3-3s was investigated as possible interaction partners for AtWEE1 and AtCDC25 in a targeted Y2H screening. AtCDC25 did not interact with the Non-Epsilon group 14-3-3s, whereas AtWEE1 did interact with all members. The specific interaction between the At14-3-3ω isoform and AtWEE1 was confirmed *in vivo* by co-immunoprecipitation and *in vivo* by BiFC. A putative 14-3-3 binding site was identified in AtWEE1 and a S485A mutant of AtWEE1 was constructed. When this mutant was used in a Y2H screen against At14-3-3ω, the interaction was abolished indicating that S485 is vital for the binding of 14-3-3ω to AtWEE1. However, *in vivo* the S485A mutation was not sufficient to abolish the interaction between AtWEE1 and At14-3-3ω, which reflects the need to confirm protein-protein interactions in their native environment.

6 WEE1 Protein Level and Kinase Activity in synchronized *N. tabacum* BY-2 Cells

6.1 Introduction

The timing of cell exit from G2 and entry into mitosis is dependent on phosphorylation and dephosphorylation of threonine 14 and tyrosine 15 of the ATP-binding cleft of the CDKs. In animals, the negative regulation is exerted by the Wee1, Mik1 and Myt1 kinases, which catalyze the inhibitory phorphorylations of CDKs. In both animals and yeast these inhibitory phosphorylations are removed by positive regulators of the cell cycle, namely the Cdc25 dual-specificity phosphatases. However, entry into mitosis appears to be determined by a balance between the activities of Cdc25 and Wee1 (Kumagai and Dunphy, 1991; Lee *et al.*, 2001).

Originally, Wee1 was identified from *S. pombe* by its ability to phosphorylate the M-phase promoting factor (MPF) on tyrosine 15 and thereby causing mitotic delay (Nigg, 1995). Myt1, which is a membrane-associated Wee1 homologue found in *X. laevis* and *H. sapiens*, preferentially phosphorylates threonine 14 and, to a lesser extent, tyrosine 15 (Mueller *et al.*, 1995; Liu *et al.*, 1997). The Wee1/Mik1-type kinases have been identified in a number of eukaryotes, such as *S. cerevisiae*, *H. sapiens*, *D. melanogaster*, *X. laevis*, and *M. musculus* (Parker and Piwnica-Worms, 1992; Booher *et al.*, 1993; Honda at al., 1995; McGowan and Russell, 1995; Mueller *et al.*, 1995). To date no Myt1 or Mik1 kinases have been identified in plants, in contrast to the Wee1 kinase, which has been identified in a variety of plants, such as *Z. mays*, *A. thaliana*, *O. sativa*, *L. esculentum* and *S. lycopersicum* (Sun *et al.*, 1999; Sorrell *et al.*, 2002; Vandepoele *et al.*, 2002; Gonzalez *et al.*, 2004; Gonzalez *et al.*, 2007; Guo *et al.*, 2007). The Wee1/Mik1 kinases range in size from the 68 kDa Wee1 from *X. laevis* (Mueller *et al.*, 1995) to the 107 kDa Swe1 in *S. cerevisiae* (Booher *et al.*, 1993). Plant WEE1s are however smaller in size ranging from 44 – 58 kDa. Consistent with Wee1s from other eukaryotes (Mueller *et al.*, 1995; Aligue *et al.*, 1997), the highest degree of sequence variation in the plant WEE1s occurs in the N-terminal domain, whereas the C-terminal domain, which includes the kinase domain, is more conserved (Appendix A). Recently, the first two functional analyses of plant

WEE1s were published. In *A. thaliana* WEE1 was shown not to be rate-limiting for cell cycle progression or endoreduplication under normal growth conditions. However, upon DNA damage and replication blockage, AtWEE1 was found to be a critical target for ATM/ATR signalling (De Schutter *et al.*, 2007). In addition, findings by Gonzalez *et al.* (2007) show that *S. lycopersicum* WEE1 participates in cell size control and in the onset of endoreduplication in tomato fruit development. All in all this might suggest that plant WEE1 kinases have multiple functional roles within the cell.

During the last decade much effort has been put into the discovery of how the Wee1 kinase activity is regulated in yeast and animals. It has become evident that the Wee1 kinase activity is regulated in multiple ways by protein abundance, phosphorylation status and protein degradation. In *S. pombe* the Wee1 transcript level is stable during the cell cycle, however the abundance of Wee1 protein undergoes moderate oscillation (Aligue *et al.*, 1997), which suggests either translational regulation or regulation by proteolytic degradation of the Wee1 protein. The *S. cerevisiae* Swe1 and *X. laevis* Wee1 proteins are regulated by ubiquitin-mediated degradation, whereas in *H. sapiens* Wee1 is regulated both by phosphorylation and degradation (Kaiser *et al.*, 1998; Michael and Newport, 1998; Goes and Martin, 2001; Watanabe *et al.*, 2004; Watanabe *et al.*, 2005). That Wee1 activity is also regulated by phosphorylation status is evident from *S. pombe* where phosphorylation of Wee1 by the protein kinase Chk1 positively regulates Wee1 activity (O'Connell *et al.*, 1997) and conversely Wee1 phosphorylation by Nim1 inhibits Wee1 kinase activity *in vitro* (Parker *et al.*, 1993; Wu and Russell, 1993). *X. laevis* and *H. sapiens* 14-3-3 proteins are also known to regulate Wee1 activity by binding and stabilizing active Wee1 (Wang *et al.*, 2000; Lee *et al.*, 2001; Rothblum-Oviatt *et al.*, 2001). Finally in *X. laevis* and yeast, Wee1 undergoes extensive hyperphosphorylation during mitosis resulting in a decrease in kinase activity (Harvey and Kellogg, 2003; Mueller *et al.*, 1995; Tang *et al.*, 1993).

To obtain a better knowledge of the behaviour of the plant WEE1 during the cell cycle, a newly synthesized antibody raised against an NtWEE1 peptide was used for monitoring WEE1 protein levels in a synchronized wild type *N. tabacum* BY-2 cell culture. Furthermore, WEE1 kinase inhibition assay was established and used to investigate if NtWEE1 has an inhibitory effect on CDK activity *in vitro*. Furthermore, protein levels and kinase activity were monitored in a transgenic *N. tabacum* BY-2

cell line carrying pTA7002 *AtWEE1*, in which *A. thaliana WEE1* can be expressed under a dexamethasone-inducible promoter (Siciliano, 2006).

6.2 Materials and Methods

6.2.1 Recombinant Protein Expression and Purification

The pET15B vector system was used for the production of recombinant NtWEE1 and At14-3-3ω proteins. Initially, two vector constructs were made containing the coding sequence of *NtWEE1* and *At14-3-3ω*, respectively. The coding sequence of *NtWEE1* was PCR amplified from plasmid DNA (pTA7002 *NtWEE1*) with primers P56+P57 using *Pfu* polymerase and similarly the coding sequence of *At14-3-3ω* was PCR amplified from plasmid DNA (pAD-Gal4-2.1 *At14-3-3ω*) with primers P54+P55. Primers were designed to incorporate an *Nde*I restriction site to the 5' end and a *Bam*HI restriction site to the 3' end of the coding sequences. The PCR products were digested with *Nde*I/*Bam*HI and ligated into an empty pET15B vector, which had been prepared by digestion with *Nde*I/*Bam*HI. This resulted in an in-frame N-terminal fusion of the coding sequence of *NtWEE1* and *At14-3-3ω*, respectively, to an HIS_6 tag. The insertions of *NtWEE1* and *At14-3-3ω* into the pET15B vectors were verified by sequencing using primers P40–P43 (*NtWEE1*) and primers P34+P35 (*At14-3-3ω*). The constructed plasmids were then transformed into *E. coli* DE3 Rosetta pLysS cells. The empty pET15B vector and the *E. coli* DE3 Rosetta pLysS cells were kindly provided by Dr. P. Kille, Cardiff University. Transformants were verified for the presence of pET15B *NtWEE1* and pET15B *At14-3-3ω* plasmids by colony PCR using gene-specific primers (*NtWEE1* (P56+P57) and *At14-3-3ω* (P54+P55)).

Initially, two or three transformants from each transformation were screened for protein expression by picking single colonies and inoculating 5 mL LB medium with appropriate selection. Cultures were incubated overnight in a Gallenkamp orbital incubator at 200 rpm, 37°C. The overnight cultures were used for inoculating 5 mL of fresh LB medium to an OD_{600} of 0.05 – 0.1 (app. 1:20 dilution of overnight culture). Cultures were then incubated at 37°C, 200 rpm until reaching an OD_{600} of 0.4 (app. 2 – 3 hours). To fresh centrifuge tubes, 2.5 mL of each culture was transferred and stored on ice. In the remaining cultures, protein expression was induced by adding IPTG to a final concentration of 0.5 mM and cultures were incubated for an additional 3 hours. Then all cultures were harvested by centrifugation in an MSE Centaur 2 centrifuge for 10 min at 4000 rpm. The pellets were resuspended in 50 – 100 µL 2x SDS loading buffer. The protein induction was checked by SDS-PAGE and Western

blotting as described in section 3.17. The transformant showing the highest recombinant protein expression were selected for the further protein expression and purification experiments.

For the recombinant protein production and purification experiment, a single freshly streaked colony was used for inoculation of 10 mL LB medium with appropriate selection. Cultures were incubated overnight in a Gallenkamp orbital incubator at 200 rpm, 37°C. The overnight cultures were used to inoculate 100 mL of fresh LB medium to an OD_{600} of 0.05 – 0.1 (app. 1:20 dilution of overnight culture). Cultures were then incubated at 37°C, 200 rpm until an OD_{600} of 0.4 (app. 2 – 3 hours). Protein expression was induced by adding IPTG to a final concentration of 0.5 mM and cultures were incubated overnight at 22°C. The next day the cells were harvested by centrifugation in a Beckman Coulter Avanti® J-E centrifuge fitted with a JA-14 rotor for 15 min at 6000 rpm, 4°C. The supernatant was discarded and the pellet was resuspended in 2 mL lysis buffer (50 mM NaH_2PO_4, 300 mM NaCl, 10 mM imidazole pH 8.0). Lysozyme was added to the cells to a final concentration of 1 mg/mL and the cells were incubated on ice for 1 h. Samples were then sonicated (exponential tip, 10 µm amplitude) in a Soniprep 150 sonicator (MSE) for three times 30 s with 30 s on ice between each sonication. After sonication the samples were transferred to pre-chilled microcentrifuge tubes and centrifuged in a Beckman Coulter Allegra™ 21R centrifuge fitted with a F2402H rotor for 30 min at 13000 rpm, 4°C. The supernatant was transferred to a fresh microcentrifuge tube and the recombinant proteins were purified according to the Novagen His-Bind® Kit manual (Novagen, 2006). His beads were prepared by washing three times with 4 volumes binding buffer (0.5 M NaCl, 5 mM imidazole, 20 mM Tris-HCl pH 7.9). One volume is equivalent to the settled bed volume of the beads, *e.g.* 100 µL His beads equals 50 µL settled bed volume. After the final wash the beads were resuspended in 2 volumes of binding buffer and combined with 1 mL of the lysed cell extract. The cell extract and beads were mixed by inversion and then incubated for 30 min at 4°C with rotation. The samples were then spun down in an Eppendorf MiniSpin centrifuge for 3 min at 2000 rpm, 4°C. The supernatant was removed and the beads were washed three times with a total of 20 – 30 volumes wash buffer (0.25 M NaCl, 30 mM imidazole, 10 mM Tris-HCl pH 7.9). After the final wash the beads were resuspended in 1 volume elution buffer (0.25 M NaCl, 0.5 M imidazole, 10 mM Tris-HCl pH 7.9) and incubated for 20 min at 4°C

with rotation. The samples were then spun down for 3 min at 2000 rpm, 4°C and the supernatant was transferred to fresh microcentrifuge tubes. The purity of the recombinant proteins was analyzed by SDS-PAGE. The remaining protein samples were aliquoted, frozen in liquid N_2 and stored at -80°C.

6.2.2 Synchronization of *N. tabacum* BY-2 Cell Culture

Wild type and transgenic *N. tabacum* BY-2 cultures were synchronized using aphidicolin (Sigma), a reversible inhibitor of DNA polymerase α (Nagata *et al.*, 1992). By the addition of aphidocolin, any cell that is replicating its nuclear DNA will be arrested and all other cells will be unable to enter S phase. On the 7th day following sub-culture 20 mL of *N. tabacum* BY-2 cell cultures were transferred to 95 ml of fresh BY-2 liquid medium and added aphidicolin in dimethyl sulphoxide (DMSO) to a final concentration of 5 µg/L. Cell cultures were incubated in the dark in a Gallenkamp orbital incubator at 130 rpm, 27°C. After 24 h incubation, the cells were released from the aphidicolin block by washing with 1 L fresh BY-2 liquid medium. The cells were decanted into a funnel with a fused-in sintered glass filter (Baird and Tatlock No. 1) to which 1000 ml of fresh medium was added in 100 ml aliquots. The flow rate of the washing medium was regulated by a Hoffman clamp attached to silicon tubing connected to the bottom of the funnel. The washing procedure was of exactly 15 min duration in order to achieve a high rate of mitotic synchrony. The cells were then resuspended in 95 ml of fresh BY-2 liquid medium and incubated as previously described.

6.2.3 Dexamethasone-induction of *AtWEE1* expression in *N. tabacum* BY-2 Cells

For induction of *AtWEE1* expression in the transgenic *N. tabacum* BY-2 cell cultures carrying pTA7002 *AtWEE1*, 30 µM dexamethasone (Sigma) was added to the cells and incubated as previously described. At hourly intervals (for 9 – 12 hours depending on the experiment) 20 µL of the cell culture was mixed with 1 µL Hoechst stain in 2% Triton X-100 and the mitotic index (the sum of prophase, anaphase, metaphase, and telophase mitotic figures as a percentage of all cells) was scored on a minimum of 300 cells. Additionally, aliquots of 5 mL of the cell culture were removed and harvested by centrifugation in an MSE Centaur 2 centrifuge for 5 min at

3000 rpm. The cell pellets were frozen in liquid N_2, ground to a fine powder using a pre-cooled pestle and mortar and stored at -80°C. Total protein was extracted from the ground tissue as described in section 3.15.

6.2.4 CDK and WEE1 Immunoprecipitations and Kinase Assay

Immunoprecipitations of CDK and WEE1 from *N. tabacum* BY-2 cell culture protein extracts and kinase assays were performed as described in section 3.18.

6.3 Results

To gain a better knowledge of the behavior of the WEE1 protein in a synchronized *N. tabacum* BY-2 cell culture, the *N. tabacum* WEE1 protein level and kinase activity were monitored. The work presented in this chapter is based on the application of a newly synthesized NtWEE1 antibody (Sigma), which was raised against the DADAADGDNKDFILC peptide located in the N-terminal regulatory domain of *N. tabacum* WEE1 (Appendix D).

6.3.1 The NtWEE1 Antibody recognizes both native *N. tabacum* and *A. thaliana* WEE1 Proteins

The specificity of the NtWEE1 antibody was tested by immunodetection of WEE1 proteins in protein extracts obtained from a wild type *N. tabacum* BY-2 cell culture and from wild type *A. thaliana* seedlings and cell culture by Western blotting (Figure 22). A band of 56 kDa corresponding to the size of NtWEE1 was detected in the *N. tabacum* BY-2 cell culture protein extract. Additionally, bands of similar sizes were detected in both *A. thaliana* seedling and cell culture protein extract showing that the NtWEE1 antibody cross-reacts with the AtWEE1 protein and can therefore be used for detecting native AtWEE1 as well as native NtWEE1 protein.

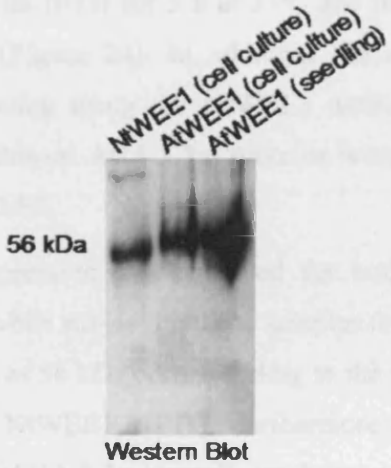

Figure 22 – Immunodetection of WEE1 in protein extracts from wild type *N. tabacum* BY-2 cell culture and wild type *A. thaliana* seedling material and cell culture by Western blotting using the NtWEE1 antibody.

6.3.2 Recombinant *N. tabacum* WEE1 inhibits CDK Activity *in vitro*

Previously, it was shown that *Z. mays* and *S. lycopersicum* WEE1 proteins control CDK activity *in vitro* by their ability to inhibit substrate phosphorylation of the CDKs (Sun *et al.*, 1999; Gonzalez *et al.*, 2007). Therefore, the CDK inhibitory activity of NtWEE1 was investigated using a WEE1 kinase inhibition assay. The basic principle of the assay is to test if the addition of NtWEE1 to a mixture of purified CDK and histone H1 substrate can inhibit the ability of CDKs to phosphorylate histone H1 *in vitro* (Figure 23). The total CDK activity in this assay is interpreted as the inverse of WEE1 activity as previously demonstrated for *H. sapiens* Wee1 by McGowan and Russell, 1995.

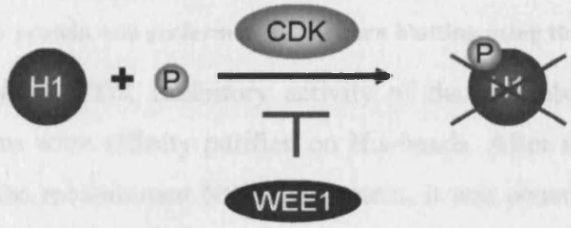

Figure 23 – The principle of the 'WEE1 kinase inhibition assay'. The addition of WEE1 protein to a mixture of purified CDKs and a histone H1 substrate can inhibit the CDK phosphorylation of histone H1 *in vitro*.

For the assay, recombinant NtWEE1 proteins were produced in *E. coli.* Protein expression was induced with IPTG for 3 h at 37°C and the induction was confirmed by SDS-PAGE analysis (Figure 24). In addition, the recombinant proteins were subjected to Western blotting using the NtWEE1 antibody. As a control for the protein expression, recombinant At14-3-3ω proteins were expressed in an identical experiment to that of NtWEE1.

IPTG-induced protein expression was observed for both NtWEE1 (56 kDa) and At14-3-3ω (29 kDa) and when subjecting these samples to Western blotting using the NtWEE1 antibody, a band of 56 kDa corresponding to the size of the NtWEE1 protein was only observed in the NtWEE1 +IPTG. Furthermore, the NtWEE1 antibody did not cross react with the At14-3-3ω protein implying a specific detection of the NtWEE1 protein by the antibody.

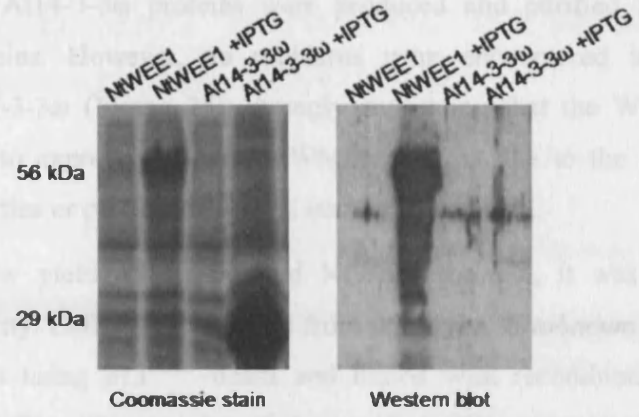

Figure 24 – Recombinant NtWEE1 and At14-3-3ω proteins produced in *E. coli*. IPTG-induced protein expression was confirmed by SDS-PAGE analysis and immunodetection of the recombinant NtWEE1 protein was performed by Western blotting using the NtWEE1 antibody.

For the analysis of the CDK inhibitory activity of the recombinant NtWEE1, the recombinant proteins were affinity purified on His-beads. After several unsuccessful attempts to purify the recombinant NtWEE1 protein, it was observed that the protein produced formed inclusion bodies (data not shown). To circumvent this, the IPTG induction was performed overnight at 22°C. Although the optimized conditions were applied, the yield of purified NtWEE1 protein remained at a very low level (Figure 25).

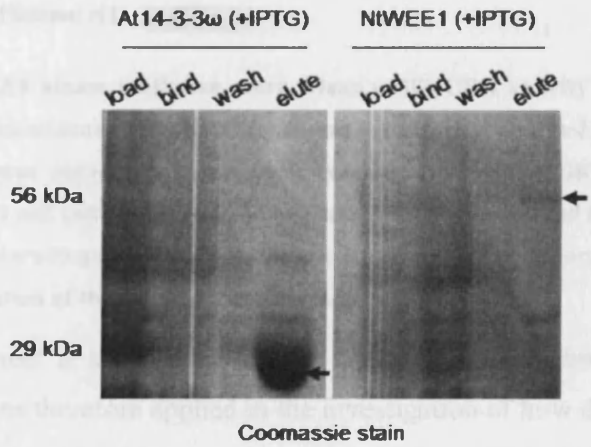

Figure 25 – Affinity purification of recombinant NtWEE1 and At14-3-3ω proteins. Aliquots of proteins were sampled before loading proteins onto the beads (load), after binding proteins onto the beads (bind), after the first wash of the beads (wash) and from the elution of proteins from the beads (elute). Samples were analyzed by SDS-PAGE.

As a control, At14-3-3ω proteins were produced and purified identically to the NtWEE1 proteins. However, no problems were encountered in producing and purifying At14-3-3ω (Figure 25); strongly suggesting that the WEE1 proteins are more difficult to express and purify. Whether this is due to the size of NtWEE1, physical properties or protein stability is currently unknown.

Despite the low yield of the purified NtWEE1 protein, it was tested for CDK inhibitory activity. CDKs were purified from wild type *N. tabacum* BY-2 cell culture protein extracts using $p13^{SUC1}$ beads and mixed with recombinant NtWEE1 in a kinase assay buffer. The activity of the purified CDKs alone was quantified and normalized to 100%. Addition of recombinant NtWEE1 resulted in a 5-fold decrease in CDK activity (Figure 26). This shows that the recombinant NtWEE1 protein produced in *E. coli* possesses kinase activity and similarly to other WEE1 kinases, NtWEE1 can negatively regulate CDK activity *in vitro*.

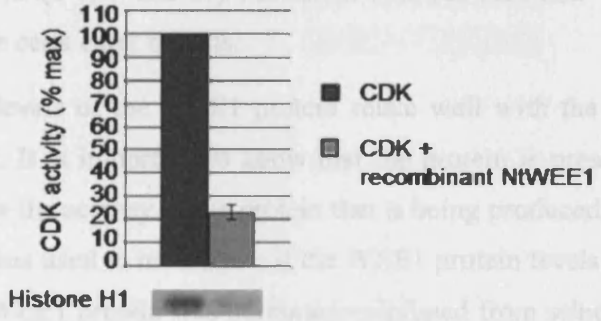

Figure 26 – The WEE1 kinase inhibition assay. Mean (±SE) CDK activity based on a replicate experiment (n=2). Recombinant HIS_6-NtWEE1 fusion protein produced in *E. coli* and purified by affinity purification was added to a kinase assay reaction containing CDKs purified from wild type *N. tabacum* BY-2 cell culture protein extracts using $p13^{SUC1}$ beads and histone H1 substrate. A representative autoradiograph is shown below histogram. The incorporation of ^{32}P was assayed by quantification of the bands on the autoradiograph.

From this experiment it is evident that the WEE1 kinase inhibition assay is fully functional and it was therefore applied in the investigation of how the native NtWEE1 protein level and kinase activity correlates in a synchronized wild type *N. tabacum* BY-2 cell culture.

6.3.3 Wild type WEE1 Protein Level and Kinase Activity in synchronized *N. tabacum* BY-2 Cells

For the first four hours after releasing the wild type *N. tabacum* BY-2 cells from the aphidicolin block mitotic cells were not observed. However, from the fifth hour until the ninth hour the mitotic index increased and peaked at 37% followed by a decrease in mitotic index (Figure 27A).

Proteins were extracted from all the samples and the WEE1 protein levels were analyzed in every second sample (hours 1, 3, 5, 7, 9 and 11) by Western blotting using the NtWEE1 antibody (Figure 27B). Consistent with the mitotic index, the WEE1 protein levels increased just after the release from the aphidicolin block where none or a low percentage of the cells were mitotic (hours 1, 3 and 5). However, as the mitotic index increased, meaning that increasingly more cells enter mitosis, the WEE1 protein level decreased (hours 7, 9 and 11) consistent with the idea that WEE1 is no longer required when the cells enter mitosis.

The timing and levels of the WEE1 protein relate well with the progression of the cells into mitosis. It is important to know that the protein is present, but even more important to know the activity of the protein that is being produced. The WEE1 kinase inhibition assay was used to investigate if the WEE1 protein levels and kinase activity relates native NtWEE1 protein was immunoprecipitated from selected samples (hours 1, 4, 6, 8 and 10) and mixed with CDKs purified from wild type *N. tabacum* BY-2 cell culture protein extracts using $p13^{SUC1}$ beads and histone H1 as substrate in a kinase assay buffer. The WEE1 kinase activity was expressed as the reciprocal of CDK activity and indeed the WEE1 protein activity related with the protein level (Figure 27B and C). The WEE1 kinase activity was maximal in early S phase (hour 1) and decreased by 46% as the cells progressed into G2 (hour 4). As the mitotic index increased (hours 6, 8 and 10) the WEE1 kinase activity further decreased by 45% reaching a minimum.

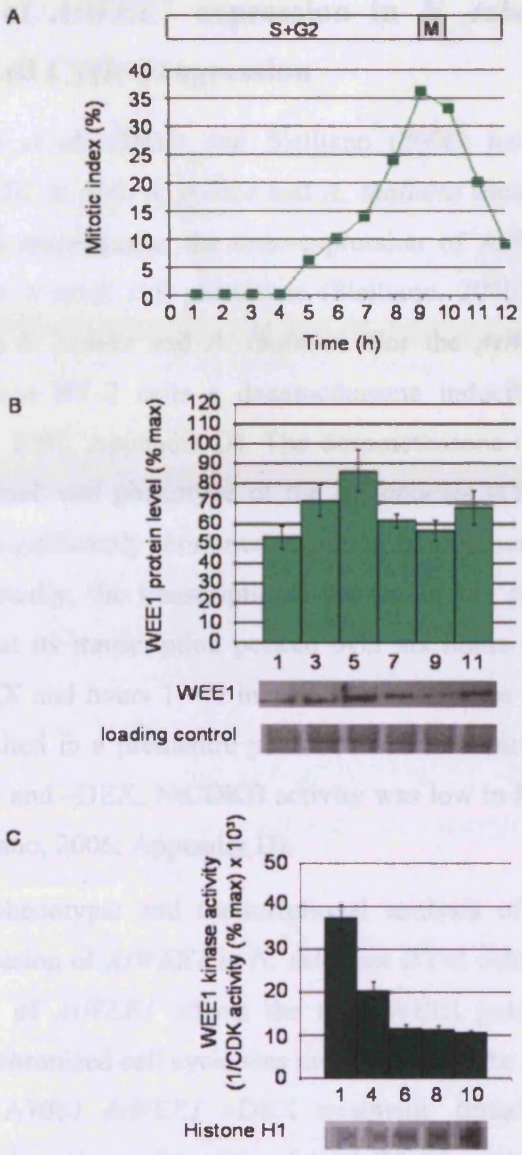

Figure 27 – WEE1 protein level and kinase activity in a synchronized wild type *N. tabacum* BY-2 cell culture A) Mitotic index profile calculated as the sum of prophase, anaphase, metaphase, and telophase mitotic figures as a percentage of minimum 300 cells. The corresponding cell cycle phases are shown above the mitotic index graph. B) Immunodetection of NtWEE1 protein extracted from synchrony samples and subjected to Western blotting using the NtWEE1 antibody. Histogram displays mean (± SE) WEE1 expression levels (n=2). A representative Western blot and a Coomassie stain loading control are shown below the histogram. C) WEE1 kinase inhibition assay. Histogram displays the mean (±SE) WEE1 kinase activity levels (n=2). The incorporation of ^{32}P was assayed by quantification of the bands on the autoradiograph and WEE1 kinase activity was expressed as the reciprocal of CDK activity (1/CDK activity (% max) x 10^3). A representative autoradiograph is shown below histogram.

6.3.4 Induction of *AtWEE1* expression in *N. tabacum* BY-2 Cells perturbs Cell Cycle Progression

Findings by Sorrell *et al.* (2002) and Siciliano (2006) have shown that over-expression of AtWEE1 in both *S. pombe* and *A. thaliana* cause a large mitotic cell phenotype. However surprisingly, the over-expression of AtWEE1 in *N. tabacum* BY-2 cells results in a small cell phenotype (Siciliano, 2006) conflicting with the previous findings in *S. pombe* and *A. thaliana*. For the *AtWEE1* over-expression studies in *N. tabacum* BY-2 cells a dexamethasone inducible system was used (Aoyama and Chua, 1997; Appendix D). The dexamethasone (+DEX) treatment not only resulted in a small cell phenotype of the *N. tabacum* BY-2 cells, but also the duration of G2 was significantly shortened, resulting in a premature entry of the cells into mitosis. Additionally, the transcriptional pattern of the endogeneous NtWEE1 was perturbed so that its transcription peaked over six hours instead of four hours (hours 1 – 4 in –DEX and hours 1 – 6 in +DEX). Finally, the induction of *AtWEE1* over-expression resulted in a premature peak of NtCDKB activity in early S phase, whereas in wild type and –DEX, NtCDKB activity was low in S phase and peaked in early/mid G2. (Siciliano, 2006; Appendix D).

In support of the phenotypic and transcriptional analysis of the dexamethasone-inducible over-expression of *AtWEE1* in *N. tabacum* BY-2 cells, the extent to which this over-expression of *AtWEE1* affects the total WEE1 protein level and kinase activity during a synchronized cell cycle was investigated in the *N. tabacum* BY-2 cell culture carrying pTA7002 *AtWEE1* ±DEX treatment. Initially, the induction of AtWEE1 was tested by immunodetection of total WEE1 protein in protein extracts obtained from non-synchroneous *N. tabacum* BY-2 cell culture carrying pTA7002 *AtWEE1* ±DEX treatment (Figure 28). Upon DEX addition, a 4-fold increase in the total WEE1 protein level was detected proving that the DEX treatment indeed induces *AtWEE1* over-expression and furthermore demonstrating the ability of the NtWEE1 antibody to detect both NtWEE1 and AtWEE1 proteins.

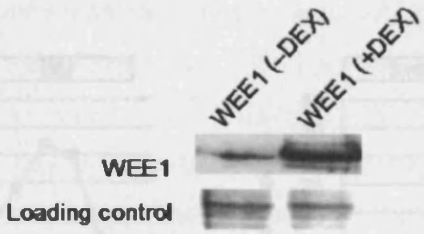

Figure 28 – Immunodetection of total WEE1 in protein extracts from *N. tabacum* BY-2 cell culture carrying pTA7002 *AtWEE1* ±DEX treatment by Western blotting using the NtWEE1 antibody. Equal loadings were confirmed by Coomassie staining.

For the synchronization experiments, duplicate transgenic *N. tabacum* BY-2 cultures carrying pTA7002 *AtWEE1* were synchronized by a 24 h aphidicolin treatment. After releasing the cells from the aphidicolin block, 30 µM DEX was added to one culture for induction of *AtWEE1* expression. Aliquots from each culture were sampled every hour and the mitotic index was scored on a minimum of 300 cells (Figure 29A). The mitotic index profile of –DEX resembled the one of wild type except for a slightly earlier increase in the peak in the mitotic index. From the fourth hour until the eigth hour the mitotic index increased and peaked at 32%. In +DEX the mitotic peak occurred prematurely at the fifth hour consistent with a shortened G2 confirming the previous findings by Siciliano (2006).

Proteins were extracted from all the samples and the WEE1 protein levels were analyzed in every second sample (hours 1, 3, 5, 7, 9 and 11 for –DEX and hours 1, 3, 5, 7 and 9 for +DEX) by Western blotting using the NtWEE1 antibody (Figure 29B). In –DEX, the WEE1 protein levels increased just after the release from the aphidicolin block and remained high while the mitotic index increased (hours 1, 3 and 5). However, as the majority of the cells entered mitosis, the WEE1 protein level decreased (hours 7, 9 and 11). Compared to wild type (Figure 27B) the decrease in WEE1 protein was more subtle in –DEX, which could be due to the transgenic nature of the culture. However, a similar trend as the one in wild type was observed for –DEX showing that the WEE1 protein level is minimal when the cells enter mitosis.

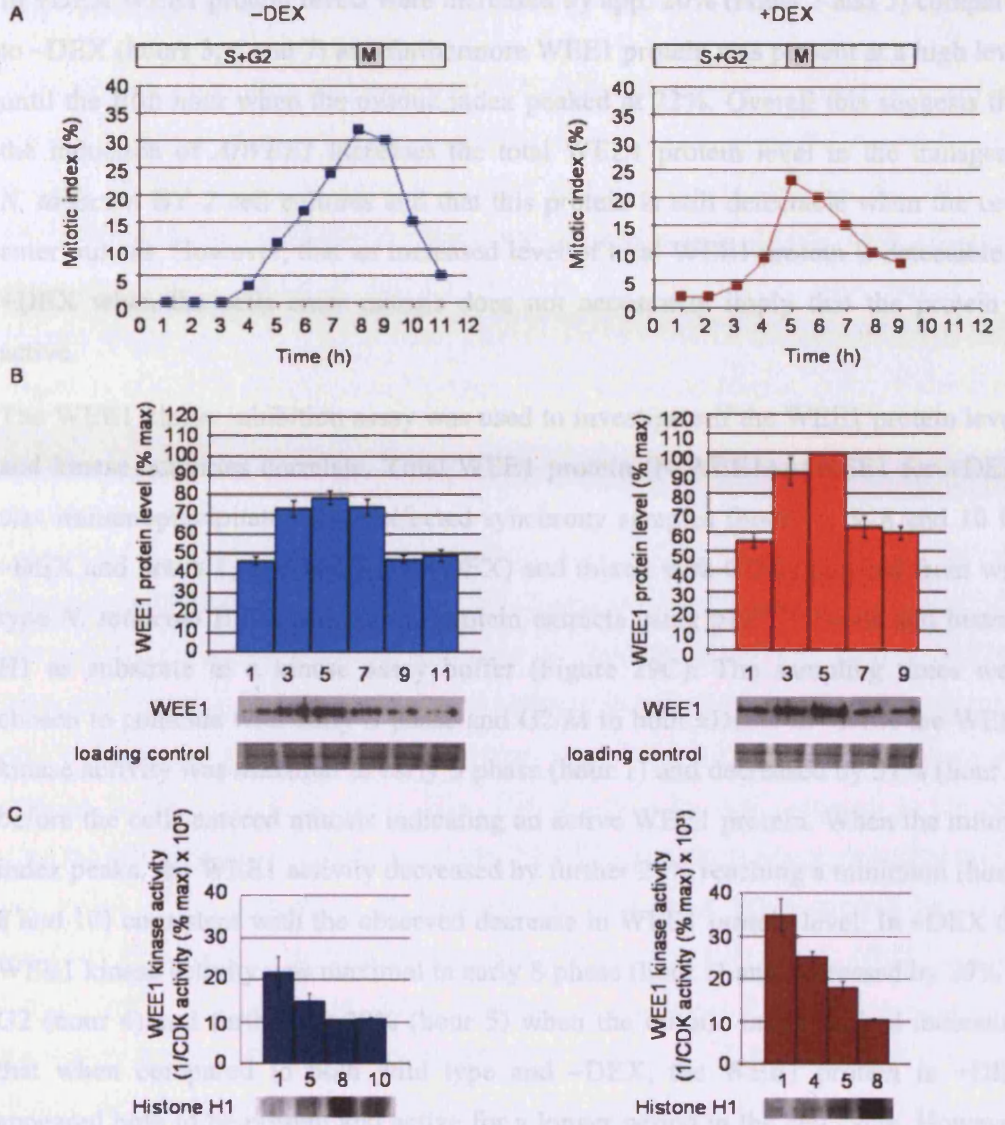

Figure 29 – WEE1 protein level and kinase activity in a synchronized transgenic *N. tabacum* BY-2 cell culture carrying pTA7002 AtWEE1. Left: –DEX. Right: +DEX. A) Mitotic index profile was calculated as the sum of prophase, anaphase, metaphase, and telophase mitotic figures as a percentage of minimum 300 cells. The corresponding cell cycle phases are shown above the mitotic index graph. B) Immunodetection of NtWEE1 protein (Total WEE1 (NtWEE1+AtWEE1) for +DEX). Proteins were extracted from synchrony samples and subjected to Western blotting using the NtWEE1 antibody. Histogram displays mean (± SE) WEE1 expression levels (n=3). A representative Western blot and a Coomassie stain loading control are shown below the histogram. C) WEE1 kinase inhibition assay. Histogram displays the mean (±SE) WEE1 kinase activity levels (n=2). The incorporation of ^{32}P was assayed by quantification of the bands on the autoradiograph and WEE1 kinase activity was expressed as the reciprocal of CDK activity (1/CDK activity (% max) x 10^3). A representative autoradiograph is shown below histogram.

In +DEX WEE1 protein levels were increased by app. 20% (hours 3 and 5) compared to –DEX (hours 3, 5 and 7) and furthermore WEE1 protein was present at a high level until the fifth hour when the mitotic index peaked at 22%. Overall this suggests that the induction of *AtWEE1* increases the total WEE1 protein level in the transgenic *N. tabacum* BY-2 cell cultures and that this protein is still detectable when the cells enter mitosis. However, that an increased level of total WEE1 protein is detectable in +DEX when the cells enter mitosis does not necessarily imply that the protein is active.

The WEE1 kinase inhibition assay was used to investigate if the WEE1 protein levels and kinase activities correlate. Total WEE1 protein (NtWEE1+AtWEE1 for +DEX) was immunoprecipitated from selected synchrony samples (hours 1, 5, 8 and 10 for –DEX and hours 1, 4, 5 and 8 for +DEX) and mixed with CDKs purified from wild type *N. tabacum* BY-2 cell culture protein extracts using $p13^{SUC1}$ beads and histone H1 as substrate in a kinase assay buffer (Figure 29C). The sampling times were chosen to coincide with early S phase and G2/M in both ±DEX. In –DEX the WEE1 kinase activity was maximal in early S phase (hour 1) and decreased by 31% (hour 5) before the cells entered mitosis indicating an active WEE1 protein. When the mitotic index peaks, the WEE1 activity decreased by further 27% reaching a minimum (hours 8 and 10) consistent with the observed decrease in WEE1 protein level. In +DEX the WEE1 kinase activity was maximal in early S phase (hour 1) and decreased by 29% in G2 (hour 4) and further by 28% (hour 5) when the mitotic index peaked indicating that when compared to both wild type and –DEX, the WEE1 protein in +DEX appeared both to be present and active for a longer period in the cell cycle. However, also in +DEX the cells entry into mitosis is accompanied by a decrease in both WEE1 protein and kinase activity levels.

6.4 Discussion

Only limited knowledge exists of how plant cells are effectively driven into mitosis. Guided by studies of model systems, notably *S. pombe*, *X. laevis* and *H. sapiens*, it is evident that the timing of mitosis in yeast and animals depends on the inhibitory phospho-regulation of CDKs by Wee1 and the mechanism driving cells efficiently into mitosis is an organized interplay between cell size control, gene transcription, protein levels and last, but not least, protein activity (McGowan and Russell, 1995; Aligue *et al.*, 1997; Michael and Newport, 1998; Goes and Martin, 2001; Watanabe *et al.*, 2004; Watanabe *et al.*, 2005).

In the work presented here, a newly synthesized NtWEE1 antibody was used for the first time to provide new information about plant WEE1 protein levels and activity during the cell cycle using *N. tabacum* BY-2 cells as a model system. Siciliano (2006) showed that in a synchronized wild type *N. tabacum* BY-2 cell culture *NtWEE1* transcript increases during S phase and peaks in late S phase and here the NtWEE1 protein level was found to follow the same trend by increasing during S phase and peaking in late S/early G2 phase. The NtWEE1 protein level decreases as the cells progress into mitosis, which suggests that NtWEE1 protein might be degraded during this phase of the cell cycle. In both animals and yeast Wee1 protein levels are regulated by ubiquitin-mediated degradation (Michael and Newport, 1998; Goes and Martin, 2001; Watanabe *et al.*, 2004; Watanabe *et al.*, 2005). Furthermore, the protein expression pattern of NtWEE1 corresponds to findings in *S. pombe* where the Wee1 protein is present throughout the cell cycle, but undergoes moderate oscillation with the Wee1 protein level peaking in the phases corresponding to S and G2 (Aligue *et al.*, 1997).

The activity of the NtWEE1 protein was assessed by its ability to inhibit CDK phosphorylation of histone H1 in a newly established WEE1 kinase inhibition assay. Initially, the assay was applied to show that recombinant NtWEE1 produced in *E. coli* has CDK inhibitory activity as previously shown for *Z. mays* and *S. lycopersicum* WEE1s (Sun *et al.*, 1999; Gonzalez *et al.*, 2007). Using the NtWEE1 antibody NtWEE1 was immunoprecipitated from protein extracts obtained from samples of a synchronized wild type *N. tabacum* BY-2 cell culture and mixed with purified CDKs and histone H1 substrate in a kinase assay buffer. Correlating with the observed

changes in WEE1 protein levels, NtWEE1 activity decreases markedly as the cells enter the G2 phase, which is also consistent with the published data from *H. sapiens* showing that active WEE1 protein is not required when cells progress into mitosis (McGowan and Russell, 1995). Hence both NtWEE1 protein levels and kinase activity are sensitive markers of the onset of mitosis in *N. tabacum* BY-2 cells.

As previously mentioned, the Wee1 protein was originally isolated as a negative regulator of cell division in *S. pombe* by having a well-defined role in delaying entry into mitosis until the cell reaches a critical cell size (Fantes and Nurse, 1977). A similar role in mitotic delay and cell size control has also been proposed for the *S. cerevisiae* Swe1 (Jorgensen *et al.*, 2002; Harvey and Kellogg, 2003). In general, loss of Wee1 function leads to a premature entry of cells into mitosis resulting in a small cell size. Whereas over-expression of Wee1 has the opposite effect leading to a large cell phenotype due to a delay of mitotic entry (Russell and Nurse, 1987; Sun *et al.*, 1999; Walter *et al.*, 2000; Sorrell *et al.*, 2002; Harvey and Kellogg, 2003). These findings link Wee1 activity with both timing of entry into mitosis and cell size regulation. Sorrell *et al.* (2002) and Siciliano (2006) showed that over-expression of *AtWEE1* in both *S. pombe* and *A. thaliana* causes large cell phenotypes. Similarly, over-expression of *SlWEE1* in *N. tabacum* BY-2 cells results in a large cell phenotype as a consequence of a lengthening of the G2 phase (Gonzalez *et al.*, 2004). However, surprisingly the over-expression of *AtWEE1* in *N. tabacum* BY-2 cells results in a small cell phenotype as a consequence of a shortened G2 phase releasing the cells prematurely into mitosis (Siciliano, 2006). The small mitotic cell phenotype indeed resembles the phenotypes of Wee1 loss-of-function mutants described in both yeast and animals (Walter *et al.*, 2000; Harvey and Kellogg, 2003). More recently, it was also reported in *S. lycopersicum*, where anti-sense *SlWEE1* plants display a reduced mitotic cell size, which is caused by a shortening of G2 and a coincident premature entry into mitosis. This finding was further supported by an increase in CDK kinase activity caused by the impairment of SlWEE1 kinase activity (Gonzalez *et al.*, 2007). Additionally, the small mitotic cell phenotype also resembles the phenotype of Cdc25 phosphatase gain-of-function mutants, which was shown by Orchard *et al.* (2005) by the over-expression of *S. pombe Cdc25* in *N. tabacum* BY-2 cells. The over-expression of *AtWEE1* did not only result in a shortening of G2 and a premature entry of the cells into mitosis, but also in a perturbation in the transcription pattern of the

endogeneous *NtWEE1*. Its transcriptional peak was extended from four to six hours resulting in the presence of the endogeneous *NtWEE1* transcript in M phase (Siciliano, 2006; Appendix D). The transcription of *AtWEE1* was found to increase during S phase and decrease during M phase as previously shown for the *S. lycopersicum* WEE1 when over-expressed in *N. tabacum* BY-2 cells (Gonzalez *et al.*, 2004). Another consequence of the induction of *AtWEE1* over-expression was a premature peak of NtCDKB activity in early S phase compared to wild type and the –DEX control, where the NtCDKB activity peaks in early/mid G2 (Joubes *et al.*, 2000; Sorrell *et al.*, 2001; Siciliano, 2006; Appendix D). Overall this could indicate that the perturbation/shift in the transcription of the endogeneous *NtWEE1* triggers the premature peak of NtCDKB activity, which is no longer inhibited by NtWEE1 and therefore forces the cells prematurely into mitosis. That CDKB is implicated in promoting mitotic cell division coincides with findings by Boudolf *et al.* (2004) showing that plants expressing a dominant negative *CDKB1* undergo enhanced endoreduplication and that CDKB1 activity is necessary for inhibiting the endocycle.

Based on the previous findings, the reduced mitotic cell phenotype was suggested to be due to a transcriptional effect of the *AtWEE1* over-expression. If both NtWEE1 and AtWEE1 transcripts are being translated into active protein, it would result in an elevated level of active WEE1 protein. In the work presented in this thesis it was indeed confirmed that the over-expression of *AtWEE1* increases the pool of total WEE1 protein in the cells (Figure 28). In the synchronized *N. tabacum* BY-2 cells +DEX the total WEE1 protein level was increased by app. 20% in both S and G2. Moreover, the elevated WEE1 protein level could still be detected at the G2/M border. The WEE1 kinase activity was also found to be increased by app. 37% in +DEX (hour 1) compared to –DEX (hour 1) (Figure 29C) suggesting that the WEE1 kinase activity in +DEX originates from both AtWEE1 and NtWEE1. At this time it is not possible to distinguish between the AtWEE1 and NtWEE1 kinase activities using this WEE1 kinase assay. The fluctuation in total WEE1 protein level in –DEX resembled the one of wild type, which showed that as the number of mitotic cells increases, both WEE1 protein and kinase activity decreases consistent with minimal WEE1 kinase activity during mitosis. Since the NtWEE1 protein level peaks when the kinase activity is at its minimum (hour 7) (Figure 29B and C) it might indicate an inactivation of WEE1 protein before its degradation. The mechanism that causes the inactivation of

NtWEE1 protein is not currently known, but it is plausible that the mechanism could either be inhibitory phosphorylations/deactivating dephosphorylations or binding of inhibitor proteins (Parker *et al.*, 1993; Tang *et al.*, 1993; McGowan and Russell, 1995; O'Connell *et al.*, 1997; Harvey and Kellogg, 2003). If the elevated WEE1 protein level in +DEX exceeds a specific threshold level within the cell it could be possible that the protein is targeted for degradation. Depending on the rate of degradation of the WEE1 protein this could very well be the force that drives the cells prematurely into mitosis strongly suggesting that in plants as well as other eukaryotes WEE1 protein level and activity controls G2/M and the cells entry into mitosis.

6.5 Summary

To gain a better knowledge of the behavior of the plant WEE1 during the cell cycle, NtWEE1 protein level and kinase activity was monitored in a synchronized wild type *N. tabacum* BY-2 cell culture. This showed that as the number of mitotic cells increases, the WEE1 protein decreases and so does the activity of the WEE1 protein consistent with the idea that WEE1 kinase activity is no longer required when cells enter mitosis. In addition, WEE1 protein level and kinase activity was also monitored in a transgenic *N. tabacum* BY-2 cell line over-expressing *AtWEE1*. The over-expression of *AtWEE1* caused a number of effects, such as a premature entry of the cells into mitosis, an increase in total WEE1 protein level and finally a presence of active WEE1 protein at the G2/M transition point. These findings clearly show that WEE1 protein and kinase activity are regulated in a cell cycle-dependent manner and indeed are sensitive indicators of the G2/M transition.

7 Perturbation of *AtWEE1* alters the Stress Response of *A. thaliana* Plants

7.1 Introduction

The Wee1 protein was originally isolated as a negative regulator of cell division in *S. pombe*. Loss of Wee1 function resulted in a smaller cell size, due to premature entry into mitosis and conversely, an increased Wee1 expression resulted in an enlarged cell size, due to delayed entry into mitosis (Fantes and Nurse, 1977; Russell and Nurse, 1987). These findings linked Wee1 activity with both timing of entry into mitosis and regulation of cell size. Wee1 kinases have been widely reported in plants (Sun *et al.*, 1999; Sorrell *et al.*, 2002; Vandepoele *et al.*, 2002; Gonzalez *et al.*, 2004; Gonzalez *et al.*, 2007; Guo *et al.*, 2007). Consistent with the original findings in *S. pombe*, over-expression of both *A. thaliana* and *Z. mays* WEE1s in *S. pombe* causes a significant increase in mitotic cell size (Sun *et al.*, 1999; Sorrell *et al.*, 2002). *AtWEE1* expression is confined to proliferative tissues of *A. thaliana* (Sorrell *et al.*, 2002) and the AtWEE1 protein can phosphorylate CDKs (Shimotohno *et al.*, 2006) suggesting a similar function of the plant *WEE1* to its homologues in other organisms. *Wee1* deficiency in yeast, *X. laevis*, *D. melanogaster* and *M. musculus* causes a premature entry into mitosis leading to embryo lethality in the latter organism (Price *et al.*, 2000; Walter *et al.*, 2000; Kellogg, 2003; Tominaga *et al.*, 2006). Some organisms encode multiple Wee1-related kinases that have similar functions to those of Wee1 *e.g.* XlWee2, SpMik1 and the vertebrate Myt1 (Lundgren *et al.*, 1991; Mueller *et al.*, 1995; Leise and Mueller, 2002). The function of the SpMik1 kinase partially overlaps the function of SpWee1, however only loss of Wee1 function results in a smaller cell size (Lundgren *et al.*, 1991; Kellogg, 2003).

In contrast to yeast and animals, the DNA damage response in plants is only beginning to be understood. In *A. thaliana* most work on DNA damage response has been done by analysis of loss-of-function mutants. Recently, the first insights into the role of DNA replication and damage checkpoints in plants were revealed by the characterization of the *A. thaliana* knock-out mutants in genes encoding the ATM and ATR kinases (Garcia *et al.*, 2003; Culligan *et al.*, 2004). ATM deficient plants are

primarily hypersensitive to DNA-damaging agents, such as γ-irradiation, but rather insensitive to replication blocking agents, such as HU or aphidicolin (Garcia *et al.*, 2003). In contrast, ATR mutants are hypersensitive to replication blocking agents but only mildly sensitive toward γ-irradiation (Culligan *et al.*, 2004). These findings strongly indicate that the *ATM/ATR* genes have a central role in the response to both stress-induced and developmentally programmed DNA damage and that the DNA checkpoint signalling pathways are well-conserved in higher eukaryotes. In *A. thaliana*, the WEE1 kinase was recently shown to be a downstream target for the ATR/ATM signaling cascade. Moreover, analysis of *A. thaliana wee1* deficient mutants showed that in contrast to the small cell phenotype and embryo lethality reported for *wee1* deficiency in other organisms, *WEE1* deficient plants were viable and have no distinctive phenotype when grown under standard conditions (Inze and De Veylder, 2006; De Schutter *et al.*, 2007). However, exposing the *AtWEE1* deficient plants to HU triggers a hypersensitivity response, as previously reported for both *Wee1* deficient yeast and *D. melanogaster* (Murakami and Nurse, 1999; Price *et al.*, 2000; Asano *et al.*, 2005). HU treatment of *AtWEE1* deficient plants results in a reduced primary root length phenotype, which is consistent with the phenotypes of *AtWEE1* over-expressing *A. thaliana* plants (Siciliano, 2006) indicating that AtWEE1 could have a role as negative cell cycle regulator capable of delaying mitotic entry of cells. Although, a putative *A. thaliana* CDC25 was only recently identified, studies of positive regulation of the plant cell cycle have been performed by over-expressing *S. pombe* Cdc25 in *A. thaliana* and *N. tabacum* plants, which resulted in an increase in lateral root formation (McKibbin *et al.*, 1998; N. Spadafora unpublished results). Recently, it was shown that the over-expression of the putative AtCDC25 in *A. thaliana* plants did not result in an obvious phenotype similar to that of plants over-expressing SpCdc25 (N. Spadafora, unpublished results) suggesting that AtCDC25 might not be a target of the DNA damaging signalling cascade.

To obtain a better knowledge of the role of *AtWEE1* during plant development, three independent *wee1* T-DNA insertion lines were phenotypically and biochemically characterized both when grown under standard conditions and when exposed to the DNA replication blocking agent, HU.

7.2 Materials and Methods

7.2.1 *A. thaliana* Seed Stocks

Name	Description	Origin
Col-0	Wild type	Lab collection
wee1-1 (SALK_147968) [1,2]	T-DNA insertion line	NASC, UK
wee1-3 (GABI_006C10) [1]	T-DNA insertion line	NASC, UK
wee1-5 (GABI_270E05) [1,2]	T-DNA insertion line	NASC, UK

[1] Lines were fully characterized in the work presented in this thesis

[2] Lines were previously characterized and published by De Schutter *et al.* 2007 (*wee1-1* and *wee1-5* lines characterized in this thesis correspond to the *wee1-2* (partially characterized) and *wee1-1* (fully characterized) lines, respectively, reported in De Schutter *et al.* (2007))

7.2.2 Sterilization and Growth of *A. thaliana* Seeds

Wild type and transgenic *A. thaliana* seeds (ecotype Columbia 0) were sterilized by adding 1 mL of bleach solution (sodium hypochlorite 5.65% – 6% (Fisher Scientific) and dH_20 (1:10)) to each tube containing seeds. The tubes were inverted thoroughly and allowed to settle for 5 min. Then the majority of the bleach solution was pipetted off and 1 mL of EtOH mix (EtOH, dH_2O and bleach (7:2:1)) was added to each tube. The tubes were inverted and flicked thoroughly and allowed to settle for 5 min. The seeds were then washed three times in 1 mL of dH_2O. Then the seeds were spread onto a sterile filter paper (Whatman Grade 1) and transferred using sterile forceps to a Petri dish containing MS agar (4.708 g/L MS basic salts (Duchefa), 30 g/L sucrose, 10 g/L agar). For selection of transgenic plants, seeds were germinated on MS agar plates containing 20 μg/mL hygromycin. To induce germination, the seeds were stratified by placing the plates at 4°C for 24 – 48 h. Plates were then transferred to a Sanyo growth cabinet, where seeds were germinated and seedlings grown at 22°C with 16 h light and 8 h dark per day.

7.2.3 *A. thaliana* Root Phenotype Analysis and Feulgen Staining

Root phenotype analysis was performed on 10 day old wild type and transgenic *A. thaliana* seedlings. Initially, the primary root length was measured and afterwards the seedlings were fixed directly on the MS agar plate by adding 8 mL fixative (EtOH: glacial acetic acid (3:1)). Plates were left at room temperature for 30 min and

then the fixative was decanted. Plates were wrapped in cling film and stored for 24 h at 4°C. After 24 h seedlings were stained with Feulgen reagent (BDH Chemicals Ltd.). Seedlings were washed for 5 min by adding 8 mL of dH_20 directly on the agar plate and afterwards the dH_2O was decanted and 8 mL of 5 M HCl was added to the agar plate. Seedlings were incubated for 25 min at room temperature and subsequently washed twice with 8 mL ice-cold dH_20 for 5 min. After the wash, 8 mL of Feulgen stain was poured onto the plate and the seedlings were incubated for 2 h at room temperature. Roots were analyzed by light microscopy using an Olympus BH2 microscope equipped with a 10x objective and the number of lateral roots and lateral root primordia were scored. If seedlings could not be analyzed on the same day, the agar plates were stored at 4°C until analysis.

7.2.4 DNA Extraction and Genotyping of *A. thaliana*

Genomic DNA was extracted from single leaves as described in Edwards *et al.* (1991) by grinding the tissue for 10 s in a microcentrifuge tube using a pestle, then 400 µL of Edwards extraction buffer (200 mM Tris-HCl pH 7.5, 250 mM NaCl, 25 mM EDTA, 0.5% SDS) was added and the sample was vortexed for 5 s followed by centrifugation in an Eppendorf MiniSpin centrifuge for 1 min at full speed. 300 µL of the supernatant was transferred to a fresh tube and added 300 µL room temperature isopropanol. The sample was inverted, incubated at room temperature for 2 min and centrifuged for 5 min at full speed in an Eppendorf MiniSpin centrifuge. The supernatant was decanted and the pellet was air dried for 30 min. The pellet was resuspended in 80 µL TE buffer (10 mM Tris-HCl pH 7.6, 1 mM EDTA). The genomic DNA was checked by using 1 – 5 µL as template in a PCR. The remaining DNA was stored at -20°C. Genotyping of *A. thaliana* seedlings was performed by PCR as described in section 3.5.

7.2.5 RNA Extraction, cDNA Synthesis and Semi-quantitative PCR

Total RNA was extracted from *A. thaliana* seedlings and cDNA was synthesized as described in sections 3.13 and 3.14, respectively. Transcript levels were analyzed using semi-quantitative RT-PCR. Initially, the optimum number of cycles (where the PCR product increases linearly with the number of cycles) was determined for both 18S rRNA (for normalization of cDNA content) and WEE1 (target gene). PCRs were performed as described in section 3.5 using cDNA as template and primers P14+P15

(18S rRNA) and primers P8+P9 (*AtWEE1*). A sample from each PCR was removed every second cycle between cycles 16 and 40. Samples were analyzed by agarose gel electrophoresis and the intensities of the bands were quantified and plotted against the number of cycles. The number of cycles corresponding to the linear part of the plot was determined for each gene. For the 18S rRNA and *AtWEE1* PCR amplifications 22 and 40 cycles, respectively, were necessary. PCRs were performed using this number of cycles and the samples were analyzed by agarose gel electrophoresis. For each sample the intensity of the band obtained from the *AtWEE1* PCR was normalized against the intensity of the 18S rRNA PCR.

7.2.6 Protein Extraction and Western Blotting

Total protein was extracted from *A. thaliana* seedlings and analyzed by Western blotting as described in sections 3.15 and 3.17, respectively.

7.2.7 CDK and WEE1 Immunoprecipitations and Kinase Assay

Immunoprecipitations of CDK and WEE1 from *A. thaliana* seedling protein extracts and kinase assays were performed as described in section 3.18.

7.3 Results

7.3.1 Identification and Analysis of *wee1* T-DNA Lines

Several collections of *A. thaliana* plant lines with large segments of DNA randomly inserted in the genome have been generated (Krysan *et al.*, 1996; Krysan *et al.*, 1999), and today more than 300,000 such lines can be obtained from stock centres.

Three *A. thaliana* T-DNA insertion lines potentially carrying insertions in the *WEE1* gene were identified using the Salk Institute Genomic Analysis Laboratory (SIGnAL) T-DNA Express search engine (http://signal.salk.edu/cgi-bin/tdnaexpress). These lines were designated *wee1-1, wee1-3 and wee1-5*. The *wee1-1* line originates from the SALK collection of T-DNA insertion lines (Alonso *et al.*, 2003). This insertion allele is predicted to carry the T-DNA insertion in the second exon. The *wee1-3* and *wee1-5* lines originate from the GABI-Kat collection of T-DNA insertion lines (Rosso *et al.*, 2003). These insertion alleles are predicted to carry the T-DNA insertion in the 5'-UTR and in seventh intron, respectively (Figure 30A). Initially, seeds from all lines were grown on MS agar plates and after two weeks leaf material was harvested and seedlings were genotyped (Figure 30B). Genotyping was done by PCR using primers specific for the wild type allele (*wee1-1* (P1+P4a), *wee1-3* (P1+P2) and *wee1-5* (P4b+P3)) and a PCR using a primer specific for the insertion allele and a gene-specific primer (*wee1-1* (P1+P5), *wee1-3* (P6+P2), *wee1-5* (P4b+P6)). PCR products of the expected sizes were obtained for all lines confirming the positions of the T-DNA insertions. For all lines, seedlings were obtained that were homozygous for the insertion, which subsequently were checked for the presence of transcript (Figure 30C). For this purpose RNA was extracted and cDNA synthesised from seven day old homozygous seedlings. In order to analyze transcription both upstream and downstream of the insertion the following regions were amplified: PCR1 (P7+P9), PCR2 (P8+P10), PCR3 (P11+P13) and PCR4 (P12+P13) (Figure 30A).

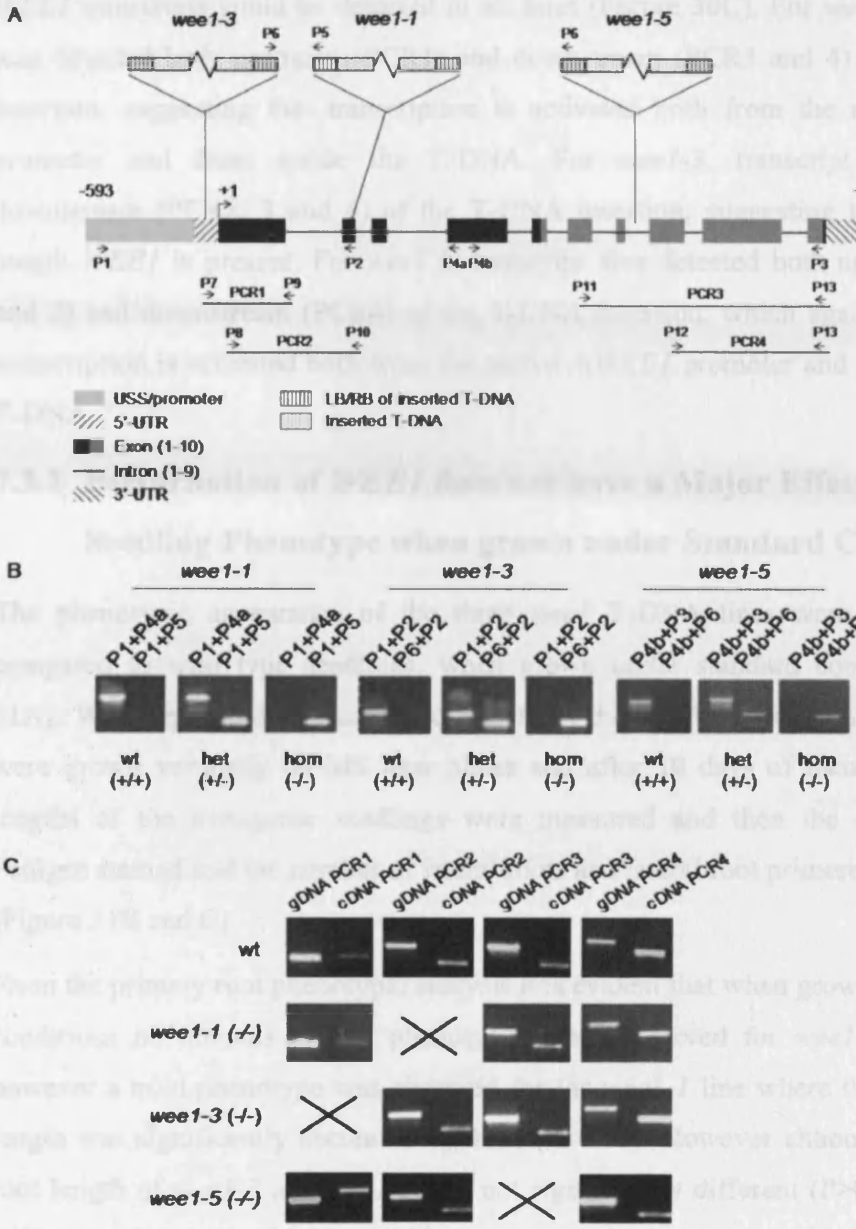

Figure 30 – Genotyping of wee1 T-DNA lines. A) Schematic diagram of the WEE1 gene (to scale) with USS/promoter (light grey), 5'-UTR (forward tilted stripes), exons (black (encoding the N-terminal regulatory domain) and grey (encoding the C-terminal catalytic domain)), introns (black lines) and 3'-UTR (backward tilted stripes). The relative positions of the three *wee1* insertions are shown as well as the orientation of the left border of the T-DNA (P5 and P6). Primers used for genotyping (numbered arrows) and the PCRs performed in the transcriptional analysis of the *wee1* T-DNA lines (PCR1 (P7+P8), PCR2 (P8+P10), PCR3 (P11+P13) and PCR4 (P12+P13)) are shown. B) Genotyping PCRs of the three *wee1* alleles made on gDNA. C) Transcriptional analysis of *wee1* T-DNA lines. B) Transcriptional analysis of the three *wee1* alleles made on both gDNA and cDNA. Crosses (X) denotes PCRs that could not be performed.

WEE1 transcripts could be detected in all lines (Figure 30C). For *wee1-1*, transcript was detected both upstream (PCR1) and downstream (PCR3 and 4) of the T-DNA insertion, suggesting that transcription is activated both from the native *AtWEE1* promoter and from inside the T-DNA. For *wee1-3*, transcript was detected downstream (PCR2, 3 and 4) of the T-DNA insertion, suggesting that that a full-length *WEE1* is present. For *wee1-5*, transcript was detected both upstream (PCR1 and 2) and downstream (PCR4) of the T-DNA insertion, which again suggests that transcription is activated both from the native *AtWEE1* promoter and from inside the T-DNA.

7.3.2 Perturbation of *WEE1* does not have a Major Effect on the Seedling Phenotype when grown under Standard Conditions

The phenotypic appearance of the three *wee1* T-DNA lines were examined and compared to wild type seedlings, when grown under standard conditions (Figure 31A). Wild type seedlings and seedlings from the *wee1-1*, *wee1-3* and *wee1-5* line were grown vertically on MS agar plates and after 10 days of incubation the root lengths of the transgenic seedlings were measured and then the seedlings were Feulgen stained and the number of lateral roots and lateral root primordia was counted (Figure 31B and C).

From the primary root phenotypic analysis it is evident that when grown under normal conditions no obvious mutant phenotypes were observed for *wee1-3* and *wee1-5* however a mild phenotype was observed for the *wee1-1* line where the primary root length was significantly decreased by 15% ($P<0.05$). However although the primary root length of *wee1-3* and *wee1-5* was not significantly different ($P>0.05$) to that of wild type, they had a highly significant increase in the total number of lateral roots and lateral root primordia per mm primary root length of 45% ($P<0.001$) and 56% ($P<0.001$), respectively, when compared to wild type. This resulted in a higher ratio of total number of lateral roots and lateral root primordia per mm primary root in *wee1-3* and *wee1*-5 of 0.32 and 0.35, respectively, compared to wild type, where the ratio was 0.17, thus indicating a faster lateral root initiation in *wee1-3* and *wee1-5*. *wee1-1* was found to have a strongly significant decrease in the total number of lateral roots and lateral root primordia of 45% ($P<0.01$) compared to wild type, which thereby resulted in a decreased ratio of total number of lateral roots and lateral root

primordia per mm primary root of 0.11 suggesting a slower lateral root initiation compared to that of wild type.

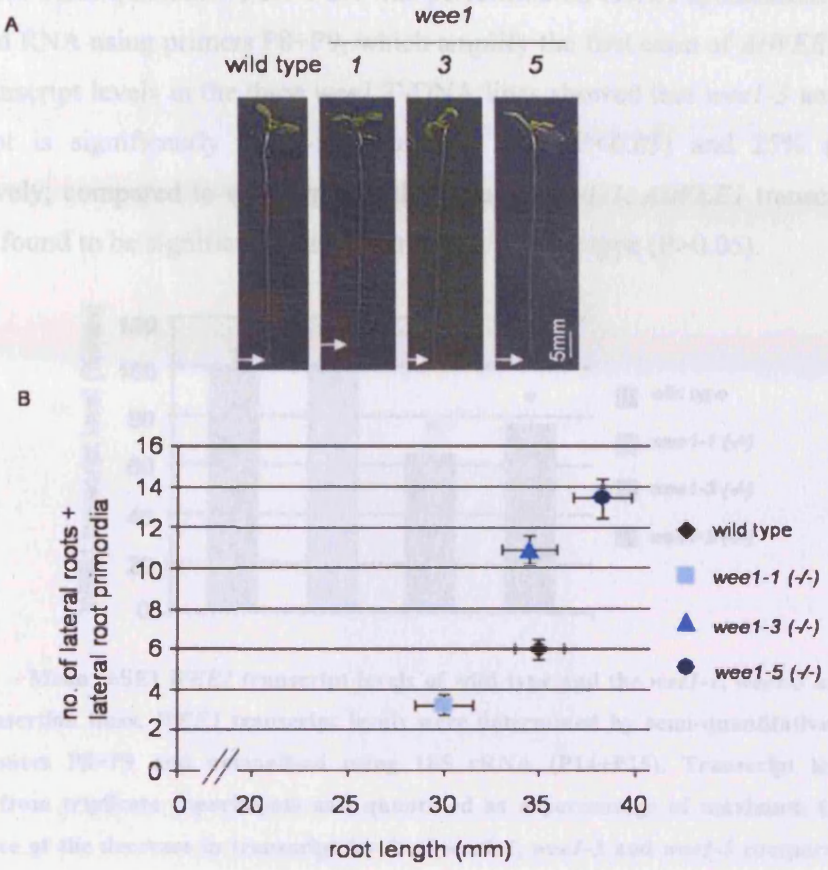

C

	Primary root length (±SE) (mm)	No. of replications (n)	Student's t-test (P)
wild type	35.00 (± 1.3)	20	–
wee1-1 (-/-)	30.00 (± 1.5)	20	<0.05
wee1-3 (-/-)	34.50 (± 1.4)	20	>0.05
wee1-5 (-/-)	38.30 (± 1.5)	20	>0.05

	No. of lateral roots + lateral root primordia	No. of replications (n)	Student's t-test (P)
wild type	5.95 (± 0.5)	20	–
wee1-1 (-/-)	3.20 (± 0.5)	20	<0.01
wee1-3 (-/-)	10.90 (± 0.7)	20	<0.001
wee1-5 (-/-)	13.40 (± 1.0)	20	<0.001

Figure 31 – Root phenotype of *wee1-1*, *wee1-3* and *wee1-5* compared to wild type. A) Wild type, *wee1-1*, *wee1-3* and *wee1-5* seedlings grown on MS agar plates. Bar represent 5 mm. B) The sum of the mean (±SE) number of lateral roots and lateral root primordia as a function of the mean (±SE) root length for wild type, *wee1-1*, *wee1-3* and *wee1-5* seedlings grown on MS agar plates. C) Mean (±SE) primary root length and mean (±SE) number of lateral roots and lateral root primordia, number of replicates and Student's t-test data.

For the analysis of the *WEE1* transcript levels in wild type and *wee1-1*, *wee1*-3 and *wee1-5*, seeds were germinated on MS agar, grown for 7 days and harvested for RNA extraction. Semi-quantitative RT-PCR was performed on cDNA synthesized from the extracted RNA using primers P8+P9, which amplify the first exon of *AtWEE1* (Figure 32). Transcript levels in the three *wee1* T-DNA lines showed that *wee1-3* and *wee1-5* transcript is significantly down-regulated by 35% ($P<0.05$) and 25% ($P<0.05$), respectively, compared to wild type. In the case of *wee1-1*, *AtWEE1* transcript level was not found to be significantly different to that of wild type ($P>0.05$).

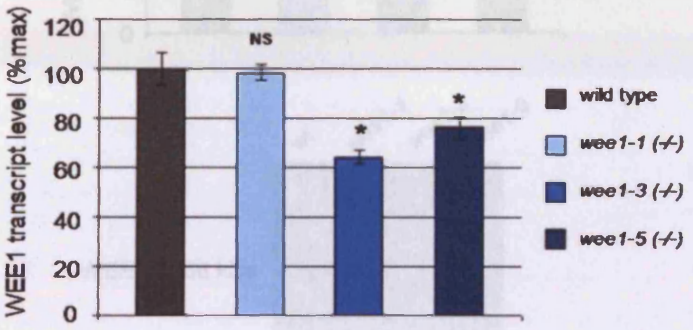

Figure 32 – Mean (±SE) *WEE1* transcript levels of wild type and the *wee1-1*, *wee1-3* and *wee1-5* T-DNA insertion lines. *WEE1* transcript levels were determined by semi-quantitative RT-PCR using primers P8+P9 and normalized using 18S rRNA (P14+P15). Transcript levels were obtained from triplicate experiments and quantified as a percentage of maximum (n=3). The significance of the decrease in transcript levels of *wee1-1*, *wee1-3* and *wee1-5* compared to wild type transcript levels was assessed by Student's t-test (NS not significant, * $P<0.05$)

AtWEE1 protein levels were detected by Western blotting using an antibody raised against a peptide in the N-terminal regulatory domain of NtWEE1 protein (amino acids 89 – 101 encoded in the first exon of the *NtWEE1* gene, which corresponds to amino acids 74 – 85 encoded in the first exon of AtWEE1 gene), which was found to cross-react with the AtWEE1 protein as shown in 6.3.1. As expected from the transcript levels, the wee1 protein levels were highly significantly down-regulated in *wee1-3* and *wee1-5* by 70% ($P<0.01$) and 60% ($P<0.01$), respectively, when compared to wild type (Figure 33). For *wee1-1* a 30% ($P<0.01$) decrease in protein level was observed, which was also a significant down-regulation compared to wild type AtWEE1 protein levels suggesting that although transcript is produced in comparable levels to wild type, the T-DNA insertion in the second exon of *WEE1* could result in

an inefficient translation of the protein or in a reduced stability of the produced protein.

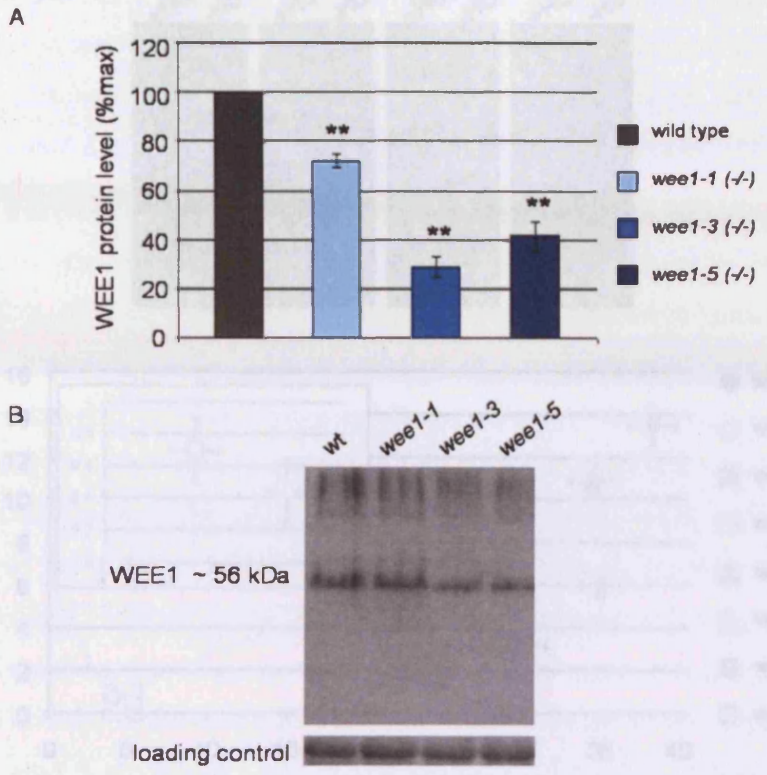

Figure 33 – WEE1 protein levels of wild type and the *wee1-1*, *wee1-3* and *wee1-5* T-DNA insertion lines. A) Mean (±SE) WEE1 protein levels were determined by Western blotting of samples obtained from triplicate experiments and the intensity of the bands were quantified as a percentage of maximum (n=3). The significance of the decrease in protein levels of *wee1-1*, *wee1-3* and *wee1-5* compared to wild type protein levels was assessed by Student's t-test (P<0.01). B) Representative Western blot and the corresponding Coomassie stain loading control.**

7.3.3 Perturbation of *WEE1* causes Plants to exhibit an Increased Hypersensitivity Response upon HU Treatment

In *D. melanogaster*, yeast and *A. thaliana Wee1* deficient mutants are extremely sensitive towards HU presumably reflecting a requirement for Wee1 activity for a fully functional DNA replication checkpoint (Murakami and Nurse, 1999; Price *et al.*, 2000; Asano *et al.*, 2005). HU arrests cells during S-phase by inhibition of ribonucleotide reductase (RNR) and thereby directly blocks DNA replication (Eklund *et al.*, 2001).

A

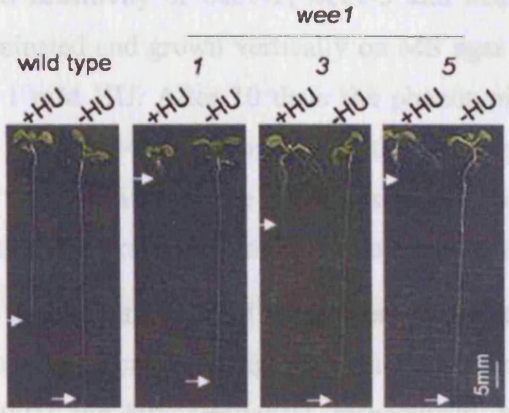

B

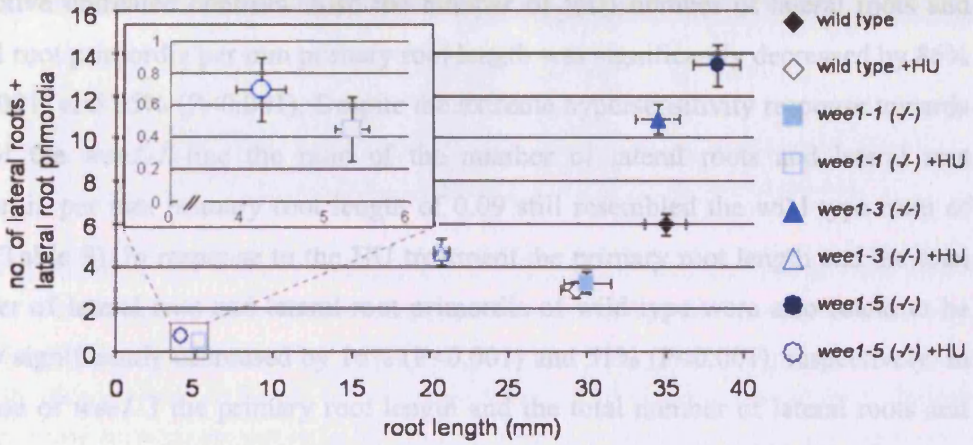

C

	Primary root length (±SE) (mm)		No. of replications (n)		Students t-test (P)
	-HU	+HU	-HU	+HU	
wild type	35.00 (± 1.3)	29.25 (± 0.9)	20	20	<0.001
wee1-1 (-/-)	30.00 (± 1.5)	5.30 (± 0.2)	20	20	<0.001
wee1-3 (-/-)	34.50 (± 1.4)	20.75 (± 0.5)	20	20	<0.001
wee1-5 (-/-)	38.30 (± 1.5)	4.20 (± 0.3)	20	20	<0.001

	No. of lateral roots + lateral root primordia		No. of replications (n)		Students t-test (P)
	-HU	+HU	-HU	+HU	
wild type	5.95 (± 0.5)	2.90 (± 0.4)	20	20	<0.001
wee1-1 (-/-)	3.20 (± 0.5)	0.45 (± 0.2)	20	20	<0.001
wee1-3 (-/-)	10.90 (± 0.7)	4.65 (± 0.6)	20	20	<0.001
wee1-5 (-/-)	13.40 (± 1)	0.70 (± 0.2)	20	20	<0.001

Figure 34 – Root phenotype of *wee1-1*, *wee1-3* and *wee1-5* compared to wild type. A) Wild type, *wee1-1*, *wee1-3* and *wee1-5* seedlings grown on MS agar plates with (+HU) and without 1 mM HU (-HU). Bar represent 5 mm. B) The sum of the mean (±SE) number of lateral roots and lateral root primordia as a function of the mean (±SE) root length (±HU). The inserted graph represents a close-up of the *wee1-1* and *wee1-5* +HU. C) Mean (±SE) primary root length and mean (±SE) number of lateral roots and lateral root primordia, number of replicates and Student's t-test data.

To investigate the HU sensitivity of *wee1-1*, *wee1-3* and *wee1-5* compared to wild type, seeds were germinated and grown vertically on MS agar plates in the presence or in the absence of 1 mM HU. After 10 days the phenotypical appearance of the plants was assessed (Figure 34A). Additionally, the primary root lengths of the transgenic seedlings were measured, the seedlings were Feulgen stained and the number of lateral roots and lateral root primordia was counted (Figure 34B and C).

Upon HU treatment *wee1-1* and *wee1-5* lines were found to exhibit an extreme hypersensitive response resulting in a highly significant decrease in primary root length of 80% ($P<0.001$) and 89% ($P<0.001$), respectively, when compared to the respective untreated controls. Also the number of total number of lateral roots and lateral root primordia per mm primary root length was significantly decreased by 86% ($P<0.001$) and 95% ($P<0.001$). Despite the extreme hypersensitivity response towards HU of the *wee1-1* line the ratio of the number of lateral roots and lateral root primordia per mm primary root length of 0.09 still resembled the wild type ratio of 0.10 (Table 9). In response to the HU treatment the primary root length and the total number of lateral root and lateral root primordia of wild type were also found to be highly significantly decreased by 16% ($P<0.001$) and 51% ($P<0.001$), respectively. In the case of *wee1-3* the primary root length and the total number of lateral roots and lateral root primordia were also highly significantly decreased by 40% ($P<0.001$) and 57% ($P<0.001$), respectively. Furthermore, the ratios of total number of lateral roots and lateral root primordia per mm primary root of *wee1-3* and *wee1-5* of 0.22 and 0.17, respectively, were still increased with app. 50% compared to wild type, which was also found for the seedlings not treated with HU. It is therefore evident that HU treatment affects the root morphogenesis in both wild type and *wee1* T-DNA lines by decreasing the lateral root production.

Table 9 – Ratio of total number of lateral roots and lateral root primordia per mm primary root length in wild type, *wee1-1*, *wee1-3* and *wee1-5*

	Ratio of total number of lateral roots + lateral root primordia / mm primary root length	
	–HU	+HU
wild type	0.17	0.10
wee1-1	0.11	0.09
wee1-3	0.32	0.22
wee1-5	0.35	0.17

For the analysis of the *WEE1* transcriptional response to HU, wild type and *wee1-1*, *wee1-3* and *wee1-5* seeds were germinated on MS agar, grown for 6 days and subsequently transferred onto MS agar supplemented with 1 mM HU. Seedlings were exposed to the HU for 24 hours and harvested for RNA extraction. Semi-quantitative RT-PCR was performed on cDNA synthesized from the extracted RNA using primers P8+P9, which amplify the first exon of *AtWEE1* (Figure 35).

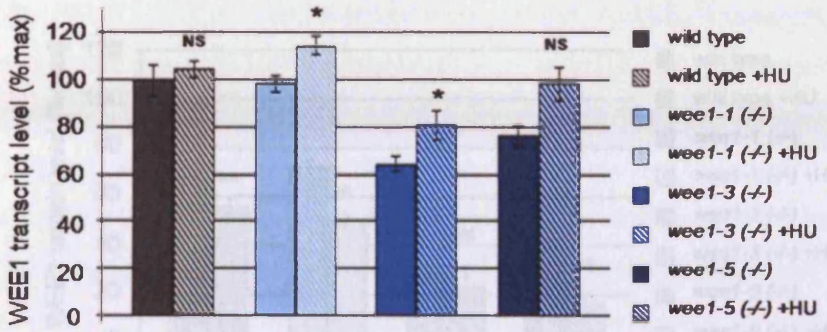

Figure 35 – Mean (±SE) *WEE1* transcript levels of wild type and the *wee1-1*, *wee1-3* and *wee1-5* T-DNA insertion lines after 24 hours treatment with 1 mM HU (+HU) compared to the non-treated controls (–HU) (Figure 32). *WEE1* transcript levels were determined by semi-quantitative RT-PCR using primers P8+P9 and normalized using 18S rRNA. Transcript levels were obtained from triplicate experiments and quantified as a percentage of maximum (n=3). The significance of the increase in transcript levels of *wee1-1*, *wee1-3* and *wee1-5* compared to wild type transcript levels was assessed by Student's t-test (NS not significant, * P<0.05)

In wild type seedlings the *WEE1* transcript levels were not significantly up-regulated (P>0.05) after 24 hours of treatment with 1 mM HU. However, in the case of *wee1-1* and *wee1-3* the *WEE1* transcripts were found to be significantly up-regulated by 15% (P<0.05) and 20% (P<0.05), respectively. Although a 20% increase in *WEE1* transcript level was observed for *wee1-5* this increase was not statistically significant (P>0.05). However, it is evident that the standard error bars of *wee1-5* ±HU *AtWEE1* transcript levels do not overlap (Figure 35), so it is likely that the 20% increase may be significant. The increase was found to be not significant in the Student's t-test because of the number of replications of the experiments. The *AtWEE1* transcript analysis was based on an average of triplicate experiments, which is the minimum number of replications needed for a Student's t-test.

Total protein was extracted from the harvested seedling material and AtWEE1 protein levels were detected by Western blotting using an NtWEE1 antibody as previously described in 7.3.2 (Figure 36A and B). Based on the somewhat up-regulated transcript levels upon HU treatment, it could be expected that the protein levels of the HU treated seedlings would be up-regulated as well. However, upon HU treatment wild type and *wee1-1* WEE1 protein levels were found to be significantly decreased by 44% ($P<0.01$) and 30% ($P<0.05$), respectively.

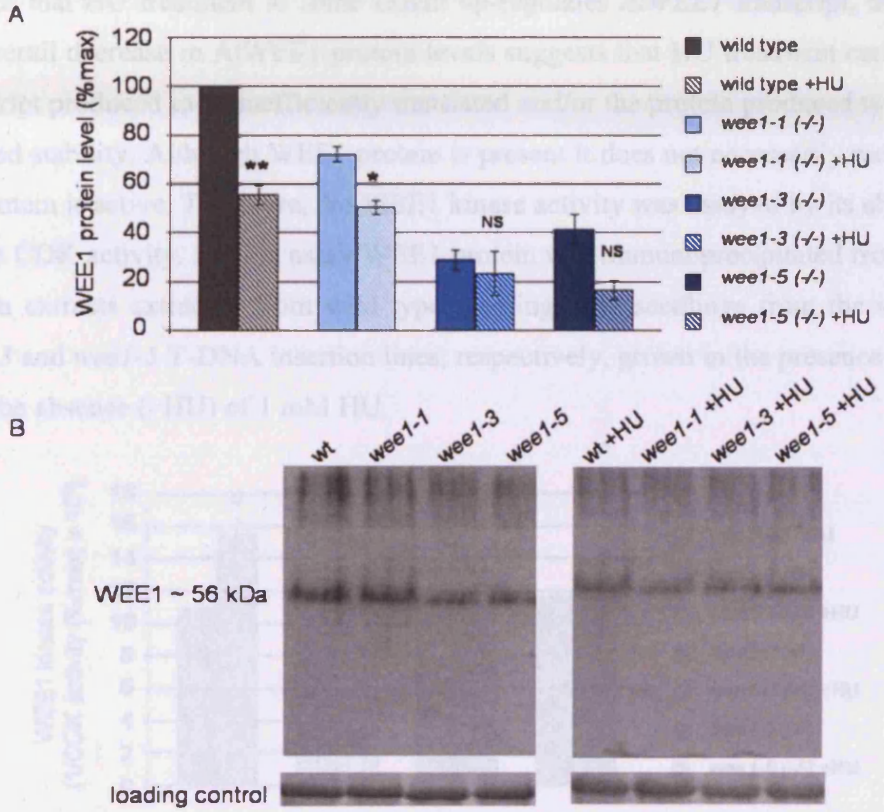

Figure 36 – Mean (±SE) *WEE1* protein levels of wild type and the *wee1-1*, *wee1-3* and *wee1-5* T-DNA insertion lines after 24 hours treatment with 1 mM HU (+HU) compared to the non-treated controls (–HU) (Figure 33). A) WEE1 protein levels were determined by Western blotting of samples obtained from triplicate experiments and the intensity of the bands were quantified as a percentage of maximum (n=3). The significance of the decrease in protein levels of *wee1-1*, *wee1-3* and *wee1-5* compared to wild type protein levels was assessed by Student's t-test (NS not significant, * $P<0.05$, ** $P<0.01$). B) Representative Western blots and the corresponding Coomassie stain loading controls.

Although the WEE1 protein levels were decreased by 18% ($P>0.05$) and 60% ($P>0.05$) in *wee1-3* and *wee1-5*, respectively, upon HU treatment, these decreases

were found not to be statistically significant compared to the untreated controls. In the case of *wee1-5*, it is evident that the standard error bars of AtWEE1 protein levels ±HU do not overlap (Figure 36A), so in this case it is likely that the 60% decrease may be significant. Again the decrease was probably found to be not significant in the Student's t-test because of the number of replications of the experiments. The AtWEE1 protein level determination was based on an average of triplicate experiments. From the analysis of the *AtWEE1* transcript and protein levels it is evident that HU treatment to some extent up-regulates *AtWEE1* transcript, however the overall decrease in AtWEE1 protein levels suggests that HU treatment causes the transcript produced to be inefficiently translated and/or the protein produced to have a reduced stability. Although WEE1 protein is present it does not necessarily mean that the protein is active. Therefore, the WEE1 kinase activity was assayed by its ability to inhibit CDK activity. For the assay WEE1 protein was immunoprecipitated from total protein extracts extracted from wild type seedlings and seedlings from the *wee1-1*, *wee1-3* and *wee1-5* T-DNA insertion lines, respectively, grown in the presence (+HU) or in the absence (–HU) of 1 mM HU.

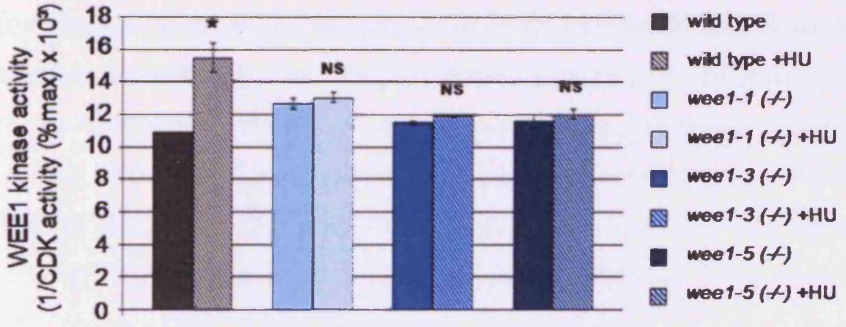

Figure 37 – Mean (±SE) *WEE1* kinase activity levels of wild type and the *wee1-1*, *wee1-3* and *wee1-5* T-DNA insertion lines after 24 hours treatment with 1 mM HU (+HU) compared to non-treated controls (–HU). WEE1 protein was immunoprecipitated from total protein extracts from wild type seedlings and seedlings from the *wee1-1*, *wee1-3* and *wee1-5* T-DNA insertion lines, respectively, and mixed with CDKs purified from wild type *A. thaliana* seedling protein extracts using $p13^{SUC1}$ beads and histone H1 as substrate in a kinase assay buffer. Samples obtained from duplicate experiments (n=2) and the intensity of the bands were quantified and WEE1 kinase activity was expressed as the reciprocal of CDK activity (1/CDK activity x 10^3). The significance of the changes in WEE1 kinase activity of *wee1-1*, *wee1-3* and *wee1-5* ±HU was assessed by Student's t-test (NS not significant, * P<0.05)

The immunoprecipitated WEE1 protein was mixed with CDKs purified from wild type *A. thaliana* seedling protein extracts using $p13^{SUC1}$ beads and histone H1 as substrate in a kinase assay buffer (Figure 37). From the WEE1 kinase activity measurements it is evident that the WEE1 kinase activity in wild type seedlings increased significantly by 30% ($P<0.05$) compared to the un-treated control. In contrast the kinase activity of *wee1-1*, *wee1-3* and *wee1-5* was not significantly increased ($P>0.05$ in all cases) upon HU treatment suggesting that the WEE1 protein produced in these lines is not activated by HU treatment and that these lines might not be capable of inducing a checkpoint. It is notable that the basal WEE1 kinase activity of *wee1-1* (–HU) is increased by 14% compared to the basal WEE1 kinase activity of wild type (–HU), however this increase was found not to be significant ($P>0.05$).

7.4 Discussion

To study the role of *AtWEE1* during plant development three *A. thaliana* T-DNA insertion lines potentially carrying insertions in the *WEE1* gene were analyzed. The insertion alleles were predicted to carry the T-DNA insertion in the second exon (*wee1-1*), in the 5'-UTR (*wee1-3*) and in the seventh intron (*wee1-5*). The T-DNA insertions were confirmed by PCR and genotyping revealed that seedlings homozygous for the insertion allele could be obtained from all three lines potentially resulting in *WEE1* deficient mutants. In yeast, *Wee1* loss-of-function causes cells to enter mitosis before sufficient growth has occurred resulting in daughter cells that are smaller than normal (Kellogg 2003) and more crucially in *M. musculus Wee1* deficiency causes embryo lethality (Tominaga *et al.*, 2006). Concurrent and independently of the work presented in this thesis, two of these lines (*wee1-1* and *wee1-5*) were characterized and published by De Schutter *et al.* (2007). The findings showed that these two lines were deficient in *WEE1* transcript and for the *wee1* T-DNA line corresponding to *wee1-5*, the truncated version of the AtWEE1 protein was over-expressed in *S. pombe*, which resulted in an inability of the cells to induce cell cycle arrest, thus demonstrating that a complete WEE1 kinase domain is necessary for WEE1 function. Interestingly, the *AtWEE1* deficient plants were reported to be viable and have no distinctive phenotype when grown under standard conditions (De Schutter *et al.*, 2007). To investigate whether the homozygous *wee1* T-DNA lines analyzed in the work were also *WEE1* deficient mutants, the lines were analyzed for the presence of *WEE1* transcript both upstream and downstream of the insertion sites (Figure 38). Surprisingly, *WEE1* transcript was detected in all lines however full-length *WEE1* transcript was only detected in wild type and *wee1-3*. The presence of transcript in the *wee1-1* and *wee1-5* lines counteracts the findings by De Schutter *et al.* (2007). However, in that report the characterized *wee1* T-DNA lines were not analyzed for the presence of either transcript upstream and downstream of the insertion. The absence of *WEE1* transcript was based exclusively on RT-PCR using primers that anneal to the coding sequence of *WEE1* flanking the T-DNA insertion site.

It is assumed that the transcription of *wee1-3* originates from the T-DNA insertion located in the 5'-UTR, which most likely separates the native *AtWEE1* promoter and

the *AtWEE1* gene. Therefore, this line might show an altered *WEE1* expression, since the gene is no longer transcribed from its original promoter.

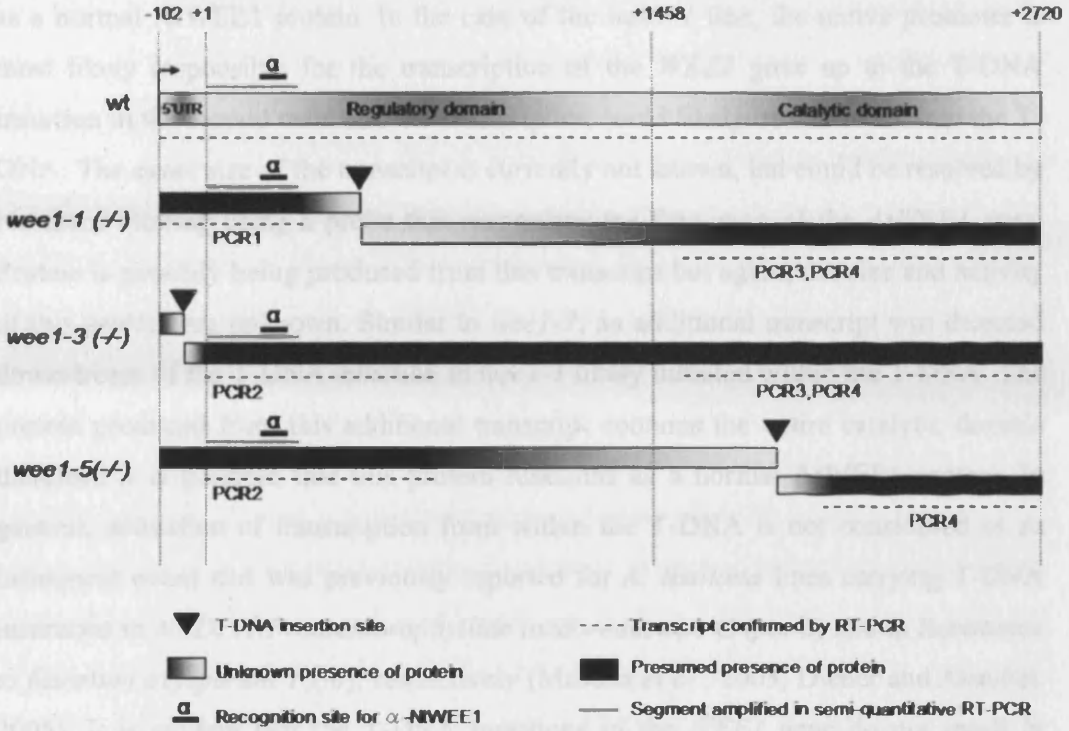

Figure 38 – Models of wild type and the *wee1* T-DNA lines *wee1-1*, *wee1-3* and *wee1-5* showing the 5'UTR, the N-terminal regulatory domain and the C-terminal catalytic domain including the T-DNA insertion sites (black triangles), the recognition site for the NtWEE1 antibody (solid black lines), the segment (exon 1) amplified in semi-quantitative RT-PCR (solid grey lines) and the parts of *AtWEE1* transcript that have been confirmed by RT-PCR (dashed lines). Solid black bars represent the presumed WEE1 protein present in the *wee1-1*, *wee1-3* and *wee1-5* lines and the grey graduated bars represent WEE1 protein, which presence is unknown.

In the case of *wee1-5*, in which the insertion is located in the seventh exon, the activation of transcription is likely to originate from the native promoter possibly resulting in a truncated transcript and protein. It is likely that the function of trunctated protein is different to the function of the wild type AtWEE1 protein. The transcript detected downstream of the insertion is probably initiated within the T-DNA, which could result in the production of a protein corresponding to the C-terminal part of the WEE1 protein. However, since the transcript is not produced from the native *AtWEE1* promoter it cannot be assumed that the transcriptional regulation resembles that of wild type *AtWEE1* gene. Furthermore, the peptide

produced from this transcript could potentially posses catalytic function. However, due to the absence of the regulatory domain, it is unlikely that this peptide functions as a normal AtWEE1 protein. In the case of the *wee1-1* line, the native promoter is most likely responsible for the transcription of the *WEE1* gene up to the T-DNA insertion in the second exon and the transcription could likely be continued into the T-DNA. The exact size of the transcript is currently not known, but could be resolved by Northern blotting using a probe that recognizes the first exon of the *AtWEE1* gene. Protein is possibly being produced from this transcript but again, the size and activity of this protein are unknown. Similar to *wee1-5*, an additional transcript was detected downstream of the T-DNA insertion in *wee1-1* likely initiated within the T-DNA. The protein produced from this additional transcript contains the entire catalytic domain therefore it is possible that this protein functions as a normal AtWEE1 protein. In general, activation of transcription from within the T-DNA is not considered as an infrequent event and was previously reported for *A. thaliana* lines carrying T-DNA insertions in *NADPH:Protochlorophyllide oxidoreductase C* (*porC*) and in *Resistance to fusarium oxysporum 1*(*rfo*), respectively (Masuda *et al.*, 2003; Diener and Ausubel, 2005). It is evident that the T-DNA insertions in the *WEE1* gene do not result in *WEE1* deficient mutants, but rather in independent plant lines carrying a perturbed version of the *WEE1* gene.

According to De Schutter *et al.* (2007), the *wee1* T-DNA lines have no distinctive phenotype when grown under standard conditions. However, it is evident from the analyses performed in this work that the *wee1-1* line has a significantly reduced primary root length of 15% ($P<0.05$) compared to wild type. This could be an effect of the transcription driven from the T-DNA insertion in the second exon, since it is evident from *S. pombe* that truncation of the N-terminal domain of Wee1 interferes with the timing of mitosis (Aligue *et al.*, 1997). Moreover, phosphorylation of the N-terminal domain of SpWee1 dramatically reduces Weel activity suggesting that the N-terminal domain is necessary for negative regulation of Wee1 (Tang *et al.*, 1993). Interestingly, the short primary root phenotype is also found in plants constitutively over-expressing *AtWEE1*, which were found to have an average decrease in primary root length of 20% ($P<0.001$) when compared to wild type (data not shown). In the *AtWEE1* over-expressing plants, the delayed primary root growth could possibly be the consequence of the elevated levels AtWEE1 causing the cells to arrest in G2 by

inactivating the CDK/cyclin complex. Similar findings were previously reported in plants over-expressing the *A. thaliana* SUC1/CKS1 homologue, AtCKS1, where reduction in the primary root growth was found to be caused by prolonged cell cycle duration (De Veylder *at al.*, 2001a). In the *wee1-1* line the ratio of total number of lateral roots and lateral root primordia per mm primary root was found to be 0.10, which is a significant decrease of app. 50% ($P<0.01$) compared to wild type. Also in the plants constitutively over-expressing *AtWEE1* this ratio is found to significantly decrease by app. 60% ($P<0.001$) compared to wild type (data not shown). Interestingly, Himanen *et al.* (2002) suggested a role for the *A. thaliana* CDK inhibitor *KRP2* in root branching, since over-expression of this gene reduced the number of lateral roots by 60%. On a similar basis, this could link *AtWEE1* with lateral root initiation and root branching. Although the primary root phenotype of the *wee1-3* and *wee1-5* lines is not significantly different ($P>0.05$) to that of wild type a closer examination showed that the ratio of total number of lateral roots and lateral root primordia per mm primary root length was 0.32 and 0.34, respectively. This is a highly significant increase of app. 50% ($P<0.001$) compared to wild type, suggesting that the root branching pattern in these lines is similar to what would be expected for plants free of *WEE1* suppression, such as CDC25 over-expressing plants. Previous studies of positive regulation of the plant cell cycle have shown that the over-expression of *S. pombe Cdc25* in both *A. thaliana* and *N. tabacum* plants increases the lateral root production (McKibbin *et al.*, 1998; N. Spadafora unpublished results), which is indeed observed for *wee1-3* and *wee1-5*.

Semi-quantitative RT-PCR analysis was performed using primers that amplify the first exon of *AtWEE1* (Figure 38). The analysis indicated that the *wee1-1* line produces *WEE1* transcript at a comparable level to wild type, however the *WEE1* transcript level in *wee1-3* and *wee1-5* was found to be significantly down-regulated by 35% and 25%, respectively ($P<0.05$). In the case of *wee1-1* it should be emphasized that although the transcript is produced from the native *AtWEE1* promoter, *AtWEE1* is only transcribed up to the T-DNA insertion thereafter most likely transcription continues into the T-DNA. Furthermore, the analysis suggests that the transcriptional activation from the T-DNA insertion in the 5'-UTR of the *wee1-3* line either down-regulates the transcription of *AtWEE1* or reduces the stability of the produced *AtWEE1* transcript. In the case of *wee1-5*, the T-DNA insertion in the seventh intron,

resulting in a truncated transcript, could reduce the stability of the transcript. The phenotype of the *wee1-1* line resembles the one of a *WEE1* over-expressing line suggesting a possible up-regulation of the *WEE1* transcript produced downstream of the T-DNA insertion relative to WEE1 transcript in wild type plants. To investigate if this was causing the WEE1 over-expressing phenotype of the *wee1-1* line, semi-quantitative RT-PCR was performed using primers (P11+P13) which amplify the sequence encoding the catalytic domain of AtWEE1 (PCR3) (Figure 38). Surprisingly, *wee1-1* was found to produce this transcript at a comparable level to wild type (data not shown) suggesting that another reason has to be sought for the *wee1-1* phenotype.

The AtWEE1 protein levels of wild type, *wee1-1*, *wee1-3* and *wee1-5* lines were determined by Western blotting using an NtWEE1 antibody that recognizes amino acids 74 – 85 of AtWEE1 protein encoded by nucleotides 222 – 255 in the first exon of the *AtWEE1* gene (Figure 38). Consistent with the down-regulated transcript levels, *wee1-3* and *wee1-5* were also found to have significantly down-regulated protein levels of 70% ($P<0.01$) and 60% ($P<0.01$), respectively, when compared to the wild type WEE1 protein level. Although the *WEE1* transcript level of *wee1-1* was comparable to that of wild type, the protein level was found to be significantly down-regulated by 30% ($P<0.01$) suggesting a reduced stability of the produced protein. However, it could have been expected that the T-DNA insertion in the second exon of *AtWEE1* would have a stabilizing effect on the WEE1 protein, since an analysis of *H. sapiens* Wee1 showed that the N-terminal domain contains a degradation signal that regulates the normal turn-over and thereby the stability of the protein (Wang *et al.*, 2000).

Although the *wee1* T-DNA lines were found to both transcribe and translate *WEE1*, it does not necessarily imply that the protein is functional. WEE1 proteins were immunoprecipitated from proteins extracted from seven day old seedlings. The kinase activity of the immunoprecipitated WEE1 proteins was assessed by their ability to inhibit the ability of CDK to phosphorylate histone H1 *in vitro*. Surprisingly, the *wee1-1*, *wee1-3* and *wee1-5* lines were found to have similar basal levels of WEE1 kinase activity as that of wild type although the *wee1* T-DNA lines showed strongly significant reductions in AtWEE1 protein levels compared to wild type. A reason for this observation could be that the basal level of AtWEE1 activity is actually a

minimum activity level that is present under standard growth conditions. This is consistent with De Schutter *et al.* (2007), who showed that both wild type and a *wee1* T-DNA line (the *wee1-5* line in this thesis) grown under standard conditions was not capable of mediating tyrosine phosphorylation of CDKs, which is regarded as a measure for WEE1 kinase activity (Parker and Piwnica-Worms, 1992).

Previous reports have shown that *wee1* mutants in yeast, *D. melanogaster* and now also in *A. thaliana* exhibit an extreme sensitivity towards HU presumably reflecting a requirement for *Wee1* activity for a fully functional DNA replication checkpoint (Murakami and Nurse, 1999; Price *et al.*, 2000; Asano *et al.*, 2005). Therefore, the DNA damage response in *wee1-1*, *wee1-3* and *wee1-5* was assessed by a 24 h exposure of seedlings to 1 mM HU. Consistent with De Schutter *et al.* (2007), the *wee1-1*, *wee1-3* and *wee1-5* lines exhibited an extreme sensitivity towards HU resulting in a highly significant decrease in primary root length of 80% ($P<0.001$), 40% ($P<0.001$) and 89% ($P<0.001$), respectively, when compared to untreated controls. The *wee1* T-DNA lines were found to be more responsive towards HU treatment than wild type, in which the primary root length decreased by only 15% ($P<0.001$). The extreme hypersensitivity response of the *wee1-1* and *wee1-5* line suggests that the T-DNA insertions located in the second exon and in the seventh intron, respectively, have a more prominent effect on the stress response of the plants compared to the *wee1-3* line, where the insertion is in the 5'-UTR, which presumably only perturbs the *WEE1* expression and does not result in truncation or perturbation of transcript or protein. Also the ratio of total number of lateral roots and lateral root primordia per mm primary root found to be significantly decreased by 18% ($P<0.001$), 31% ($P<0.001$) and 51% ($P<0.001$) in *wee1-1*, *wee1-3*, *wee1-5*, respectively, compared with a 41% ($P<0.001$) decrease in the ratio for wild type. This clearly implies that HU treatment affects root development in both wild type and the *wee1* T-DNA lines by decreasing the lateral root production and thereby minimizing the roots exposure to HU.

De Schutter *et al.* (2007) showed that in wild type *A. thaliana* cell cultures *AtWEE1* is transcriptionally activated upon HU treatment in an ATM/ATR-dependent manner thereby making *AtWEE1* a downstream target gene of the ATM/ATR signalling cascade. However, in the work presented in this thesis, wild type *AtWEE1* was not found to be significantly up-regulated upon HU treatment. This could probably be due

to the concentration of HU used in the experiment, since it is possible HU activates *AtWEE1* transcription in a dose-dependent manner. The fact that the RT-PCR was performed on cDNA synthesized from RNA extracts obtained from whole *A. thaliana* seedlings could also be a reason for not observing increased *AtWEE1* transcript levels, since De Schutter *et al.* (2007) showed that *AtWEE1* expression upon HU treatment was confined to the root apical meristem, which only constitutes a small fraction of a whole seedling. However, the transcript levels of the *wee1-1*, *wee1-3* and *wee1-5* lines were increased by 15% – 20%, respectively, when compared to untreated controls. This suggests that the perturbation of *AtWEE1* greatly influences the plants response towards HU and because an increase in *AtWEE1* transcript level was observed in *wee1-1*, it could be speculated that the HU treatment influences regulatory elements of the native *AtWEE1* promoter, since it is evident that only the first exon of the *AtWEE1* gene was analyzed in the semi-quantitative RT-PCR analysis. However, although the transcript was found to be up-regulated, surprisingly this did not result in a corresponding up-regulation of protein levels. In the *wee1-1*, *wee1-3* and *wee1-5* lines, the AtWEE1 protein levels were reduced by 30%, 18% and 60%, respectively, suggesting that proteins with reduced stability are produced from these transcripts. Also in wild type, the AtWEE1 protein level was significantly decreased by 44% ($P<0.01$) upon HU treatment despite the fact that the transcript level was not affected upon HU treatment. In the case of the *wee1* T-DNA lines it could be speculated that the *WEE1* transcripts result in the production of unstable transcripts, inefficient translation of transcripts or that the proteins produced are less stable and more easily degraded. In yeast, *X. laevis* and *H. sapiens* protein degradation is one of the main ways of regulating Wee1 protein levels within the cells (Michael and Newport, 1998; Sia *et al.*, 1998; Goes and Martin, 2001; Watanabe *et al.*, 2004; Watanabe *et al.*, 2005). For both wild type and the *wee1* T-DNA insertion lines to maintain the response towards HU it is necessary to increase the transcription of *WEE1* in order to compensate for the rapid turn-over of WEE1 protein. The WEE1 kinase activity of wild type and the *wee1* T-DNA lines was assayed upon HU treatment and consistent with the findings by De Schutter *et al.* (2007) the WEE1 kinase activity of wild type was found to significantly increase by 30% ($P<0.05$), indicating that WEE1 kinase activity rather than WEE1 protein level is a determinant for checkpoint control. However, upon HU treatment enhanced WEE1 activities were not observed for the

wee1 T-DNA lines suggesting that the WEE1 proteins produced in these lines are not activated by HU treatment. As a consequence, these lines might not be capable of activating G2 arrest leading to the dramatic reduction in primary root length and decreases the lateral root production.

7.5 Summary

To obtain a better knowledge of the role of *AtWEE1* during normal plant development three independent *wee1* T-DNA lines carrying perturbed versions of the *wee1* gene were analyzed. Generally, under normal growth conditions the *wee1* T-DNA lines do not have an obvious mutant phenotype, but by closer examination it is evident that the root development is affected. Exposure of the *wee1* T-DNA lines to HU triggers a hypersensitivity response resulting in a reduced primary root phenotype and a decrease in lateral root production. A clear pattern combining phenotype, transcript, protein and kinase activity levels in the three *wee1* T-DNA lines could not be easily made. However, it is evident that the position of the T-DNA actually greatly affects all of these parameters.

8 General Discussion and Perspectives

The basis of the work presented in this thesis was to investigate the function of a plant cell cycle checkpoint and attempt to link known features of the yeast and mammalian G2/M model to the plant model. Of particular interest was to obtain a better knowledge of the mechanisms that regulate AtCDC25 and AtWEE1 activities by identifying interaction partners for the two proteins (Chapter 4 and 5). In addition greater insights into the role of WEE1 in cell cycle regulation and plant development were obtained by an investigation of the biochemistry of *N. tabacum* WEE1 during the cell cycle of synchronized *N. tabacum* BY-2 cells and by a phenotypic and biochemical characterization of three independent *A. thaliana* plant lines carrying T-DNA insertions in the *WEE1* gene (Chapter 6 and 7).

In the following sections the main findings from the different chapters of this thesis are summarized and discussed including perspectives for future work.

8.1 Regulation of *A. thaliana* CDC25 and WEE1

In yeast and animals, Cdc25 and Wee1 activities are tightly regulated by multiple mechanisms including sub-cellular localization, phosphorylation status and protein degradation. In *S. cerevisiae* Swe1 activity is regulated at the protein level by ubiquitin-mediated degradation (Sia *et al.*, 1998) whereas in *S. pombe* Wee1 is mainly down-regulated by phosphorylation (Parker *et al.*, 1993; Tang *et al.*, 1993; Wu and Russell, 1993; Kanoh and Russell, 1998). In *X. laevis*, Cdc25 and Wee1 protein levels are regulated by degradation only, whereas *H. sapiens* Cdc25 and Wee1 are regulated by both phosphorylation and degradation (Michael and Newport, 1998; Goes and Martin, 2001; Donzelli *et al.*, 2002; Watanabe *et al.*, 2004; Watanabe *et al.*, 2005; Wang *et al.*, 2007).

Interaction between proteins is of great importance in order for these regulatory mechanisms to occur. In some cases one mechanism may lead to another as in *H. sapiens* where phosphorylation of Wee1 leads to ubiquitin-mediated degradation of the protein (Watanabe *et al.*, 2004). It is evident from both animals and yeast that phosphorylations of Cdc25s and Wee1s also form protein binding sites for 14-3-3 proteins, which stabilizes the activity and/or alters the sub-cellular localization of the proteins (Dalal *et al.*, 1999; Furnari *et al.*, 1999; Chen *et al.*, 2003b). To investigate if

similar regulatory mechanisms exist for *A. thaliana* WEE1 and CDC25 protein during the plant cell cycle, two Y2H library screens were performed using AtCDC25 and AtWEE1, respectively, as baits against an *A. thaliana* seedling root cDNA library.

The AtCDC25 library screening resulted in the discovery of only seven interaction partners, due to heavy contamination of the screening plates. In summary, the proteins identified in the AtCDC25 Y2H screen could be divided into three functional groups: 1) protein biosynthesis, 2) cell division and 3) plant stress responses. In relation to plant stress responses, a cold-acclimation protein similar to the *T. aestivum* cold-acclimation WCOR413 was hit three times. It is not evident from other organisms that Cdc25 proteins are involved in physiological stress responses, such as cold-acclimation, however environmental signals, such as nutrient availability and physiological stresses, modulate the cell cycle and cell size of *S. pombe* (Kishimoto and Yamashita 2000). In relation to cell division the caldesmon-related protein, TSK-associating protein 1, TSA1, was hit once. *A. thaliana tsk* mutants are blocked at the G2/M transition suggesting that TSK is required for proper execution of the cell cycle (Suzuki *et al.*, 2005b; Suzuki *et al.*, 2005a). This complements the proposed function of AtCDC25 as a mitosis promoting factor involved in the G2/M checkpoint. However, at this point it is still questionable if AtCDC25 is a true CDC25 in higher plants, since its role as a functional protein tyrosine phosphatase remains to be demonstrated *in vivo* (Landrieu *et al.*, 2004). Furthermore, AtCDC25 is structurally different compared to the classical Cdc25 proteins identified in animals and yeast since it consists of only the C-terminal catalytic domain (Landrieu *et al.* 2004; Sorrell *et al.*, 2005). The classical Cdc25 proteins are phosphorylated in the N-terminal regulatory domain and these phosphorylations are crucial for the regulation of Cdc25 sub-cellular localization, stability and catalytic activity (Gabrielli *et al.*, 1997; Dalal *et al.*, 1999). It is possible that AtCDC25 has to interact with a second protein to become a complete plant Cdc25 and that this protein could have been revealed in the Y2H library screen. However, none of the putative CDC25 interaction partners identified in the library screen resemble the N-terminal regulatory domain from the classical Cdc25s. It is assumed that if a second protein exists it might be revealed by a more exhaustive Y2H screen. Alternatively, it could be revealed by introducing an affinity-tagged version of the putative AtCDC25 into *A. thaliana* plants or cell culture and thereby use the affinity-tag to co-immunoprecipitate AtCDC25 together with its *in*

vivo interaction partners. The proteins interacting with AtCDC25 could then be identified by mass spectrometry.

The AtWEE1 Y2H library screen revealed 60 different AtWEE1 interacting proteins of which 42 of the proteins could be divided into six functional groups: 1) transcription, RNA/DNA binding and histone modifications, 2) plant growth regulation and signal transduction, 3) stress responses, detoxification and pathogen responses, 4) cell division and cell growth 5) protein biosynthesis and 6) protein degradation. Of the 42 proteins, 10 proteins were identified more than once. Of particular interest was to elucidate if AtWEE1 shares similar cell cycle regulatory mechanisms as its homologues in other organisms. Therefore, the main groups of AtWEE1 interaction partners relevant to putative regulatory and functional pathways were mapped (Figure 39) and summarized in the following text:

In *H. sapiens* Wee1 is predominantly located in the nucleus in interphase (Baldin and Ducommun, 1995), during which it potentially could interact with DNA binding proteins (DBPs) and transcription factors (TFs). To date, it is not evident from other eukaryotic species if and how Wee1 could have a role in transcriptional regulation. However, it is a plausible assumption that Wee1 proteins could interact directly with both DBPs and TFs to maintain transcription of key genes during the cell cycle. In late S/G2, it is evident from *H. sapiens* that Wee1 relocalizes to the cytoplasm (Katayama *et al.*, 2005), which could also be the case for AtWEE1. In the cytoplasm WEE1 could interact with proteins involved in stress responses and DNA damage. If AtWEE1 relocates to the cytoplasm, its activity can also be regulated by plant growth regulators (PGRs). Since proteins involved in protein biosynthesis were identified as AtWEE1 interaction partners it suggests that AtWEE1 influences protein biosynthesis and possibly affects the levels of specific proteins in the cell. The underlying mechanism for this hypothesis is not known. However, previous findings by Suda *et al.* (2000) showed that in response to protein synthesis inhibition, *S. pombe* cells have a mechanism to induce G2 delay by positively regulating Wee1.

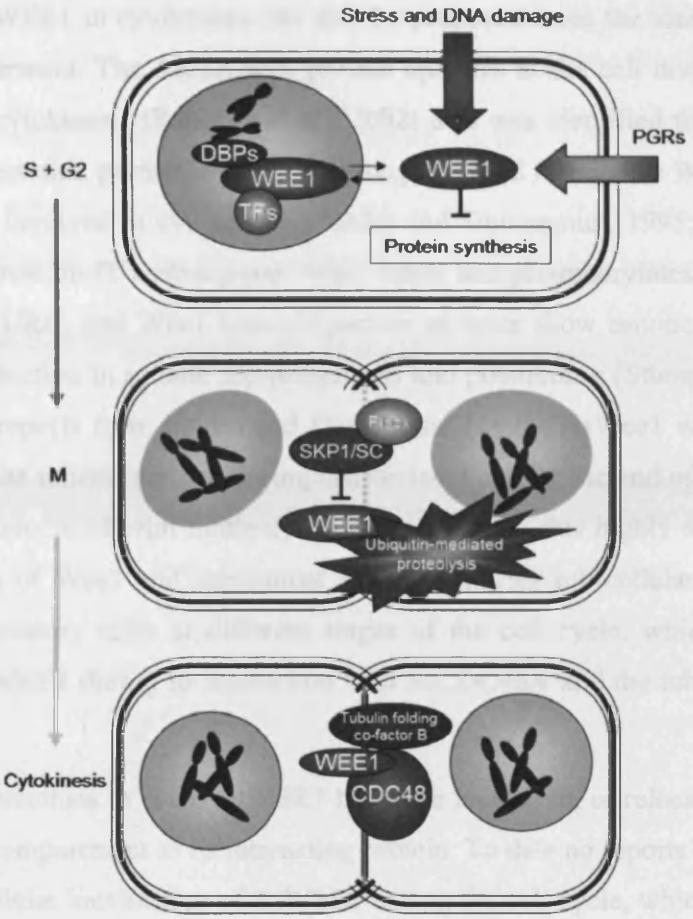

Figure 39 – Putative regulatory and functional pathways for AtWEE1 during the cell cycle. In S phase AtWEE1 is possibly predominantly located in the nucleus, where it could interact with DNA binding proteins (DBPs) and transcription factors (TFs) to maintain transcription of key genes. In late S/G2 AtWEE1 possibly relocates to the cytoplasm, where its activity could be affected by stress, DNA damage and plant growth regulators (PGRs). At this stage AtWEE1 could also interact with proteins involved in protein biosynthesis and thereby affect the levels of specific proteins the cell. In M phase, when WEE1 is not longer needed, it is possible that WEE1 is targeted for degradation by its interaction with a SCF protein complex. A role for AtWEE1 in mitotic spindle morphogenesis and cytokinesis could also be suggested by its interaction with a tubulin folding co-factor and AtCDC48.

As previously mentioned, protein degradation is an important regulatory mechanism of Wee1 proteins in both yeast and animals (Michael and Newport, 1998; Sia *et al.*, 1998; Watanabe *et al.*, 2004; Watanabe *et al.*, 2005). Interestingly, proteins involved in ubiquitin-mediated degradation, such as SKP1, a 26S proteasome subunit and several F-box proteins, were also identified as AtWEE1 interacting proteins implying that AtWEE1 activity is also regulated by protein degradation.

A role of AtWEE1 in cytokinesis can also be proposed from the identified AtWEE1 interaction partners. The AtCDC48A protein operates at the cell division plane as a mediator of cytokinesis (Rancour *et al.*, 2002) and was identified three times as an AtWEE1 interaction partner. Both *D. melanogaster* and *H. sapiens* Wee1s have been shown to be involved in cytokinesis (Baldin and Ducommun, 1995; Stumpff *et al.*, 2005). Moreover, in *D. melanogaster* Wee1 binds and phosphorylates the tubulin ring comples, γ-TURC, and Wee1 loss-of-function mutants show mitotic-spindle defects implying a function in spindle morphogenesis and positioning (Stumpff *et al.*, 2005). In the early reports from Baldin and Ducommun (1995) HsWee1 was shown to be restricted to the mitotic equator during cell division and by the end of M phase it was exclusively associated with midbody bridges. All in all this highly suggests that the relocalization of Wee1 and subsequent association with sub-cellular structures may play key regulatory roles at different stages of the cell cycle, which indeed could apply for AtWEE1 during its interaction with AtCDC48A and the tubulin folding co-factor.

For these interactions to occur AtWEE1 has to be located in, or relocated to the same, sub-cellular compartment as its interacting protein. To date no reports have been made of the sub-cellular localization of AtWEE1 during the cell cycle, which could provide useful information about AtWEE1 in relation to the previously described putative interaction partners. The sub-cellular localization of AtWEE1 could be investigated in plant cells by WEE1 fused to a fluorescent protein or by immunolocalization. Immunolocalization studies investigating Wee1 sub-cellular localization have previously been performed in both *S. pombe* and *H. sapiens* using Wee1 antibodies. These studies elegantly showed that both Wee1 proteins are predominantly localized in the nucleus during mitosis (Baldin and Ducommun, 1995; Wu *et al.*, 1996; Aligue *et al.*, 1997).

Although the outcome of the Y2H library screens presented in this thesis result in the formation of many new hypotheses about the localization, regulation and function of AtCDC25 and AtWEE1, it is important to bear in mind that the Y2H technique is solely based on transcriptional activation of reporter genes in the nucleus of *S. cerevisiae* and that proteins assayed in a heterologous system not necessarily have the correct post-translational modifications and/or sub-cellular localization (Golemis *et al.*, 1999; Van Criekinge and Beyaert, 1999; Causier and Davies, 2002; Bhat *et al.*,

2006). It is therefore necessary to confirm the interactions by the use of additional *in vivo* techniques, such as co-immunoprecipitation or fluorophore-based methods.

8.2 Involvement of 14-3-3 Proteins in the Plant Cell Cycle

During cell cycle progression in both animals and yeast, the activity and localization of both Cdc25 and Wee1 are greatly affected by the binding of 14-3-3 proteins (Dalal *et al.*, 1999; Kumagai and Dunphy, 1999; Zeng and Piwnica-Worms, 1999; Wang *et al.*, 2000; Lee *et al.*, 2001; Rothblum-Oviatt *et al.*, 2001; Uchida *et al.*, 2004). Although 14-3-3 proteins were not identified in either of the Y2H library screens, the possibility of 14-3-3 proteins interacting with AtCDC25 and AtWEE1 could not be excluded. Y2H library screens are not exhaustive and it is possible that a larger number of clones would have had to be screened in order to screen the library until saturation (Van Criekinge and Beyaert, 1999). Therefore, targeted Y2H screens were performed against the members of the *A. thaliana* Non-Epsilon 14-3-3 protein group against AtCDC25 and AtWEE1 baits, respectively, which established the first link between 14-3-3 proteins, AtCDC25 and AtWEE1 in the plant cell cycle. Previously only a few reports have suggested that plant 14-3-3s were involved in cell cycle regulation based on their sub-cellular localization or ability to complement yeast 14-3-3 mutants (van Heusden *et al.*, 1996; Cutler *et al.*, 2000; Kuromori and Yamamoto, 2000; Sorrell *et al.*, 2002; Paul *et al.*, 2005).

Surprisingly, none of the Non-Epsilon 14-3-3 proteins interacted with AtCDC25. As previously mentioned, a plausible explanation for this observation could be the absence of the N-terminal regulatory domain of AtCDC25. In *H. sapiens* all three CDC25 isoforms are phosphorylated *in vivo* in the N-terminal domain and those phosphorylations are critical for CDC25 localization and for both positive and negative regulation of CDC25 catalytic activity by protein degradation and 14-3-3 protein binding (Baldin *et al.*, 1997; Gabrielli *et al.*, 1997; Donzelli *et al.*, 2002; Bulavin *et al.*, 2003; Boutros *et al.*, 2006). The fact that AtCDC25 does not interact with any of the Non-Epsilon 14-3-3 proteins analyzed contradicts the proposed 'sticky' nature of the 14-3-3 proteins, however it also further questions cell cycle function of the putative plant CDC25, since studies in both yeast and animals have made it evident that 14-3-3 binding to Cdc25 is crucial for proper execution and regulation of the cell cycle (Zeng and Piwnica-Worms, 1999; Graves *et al.*, 2001;

Uchida *et al.*, 2004). Because of the inability to identify full-length CDC25 homologues in higher plants, it has been speculated that in higher plants the *CDC25* gene has been lost through evolution (Boudolf *et al.*, 2006). However, this would make plants distinct from other eukaryotic species and another method of counteracting the WEE1 kinase activity in the regulation of the plant cell cycle would have to be sought.

In contrast to AtCDC25, AtWEE1 interacted with all members of Non-Epsilon 14-3-3 protein group, which is maybe not so surprising, since the members of the Non-Epsilon 14-3-3 protein group display high sequence conservation of 70 – 90% both at the nucleotide and protein level (Wu *et al.*, 1997a, Appendix A). Additionally, based on the rather similar expression and localization patterns of the different isoforms (section 1.2.6.2, Table 4) it is not unlikely that they exert similar functions within the cell. Because of the multiple *A. thaliana* 14-3-3 isoforms it is possible that WEE1 interacts with both 14-3-3 hetero- and homodimers, which could influence the activity and/or sub-cellular localization of WEE1 differently. To date analyses of *A. thaliana* 14-3-3 proteins have concerned the expression pattern and sub-cellular localization of the individual 14-3-3 proteins (Bihn *et al.*, 1997; Cutler *et al.*, 2000; DeLille *et al.*, 2001; Paul *et al.*, 2005). The hetero- and homodimerisation patterns of the *A. thaliana* 14-3-3 isoforms have not been investigated although this could be of interest in relation to their binding to AtWEE1. The interaction between the different 14-3-3 monomers and their sub-cellular localization could be mapped using the BiFC technique as shown in the work presented in this thesis where 14-3-3ω proteins were found to homodimerize in the nucleus, cell plate and cell wall.

The specificity of interaction between AtWEE1 and At14-3-3ω was successfully confirmed *in vitro* by co-immunoprecipitation of proteins produced in *S. cerevisiae* and it was also shown that the At14-3-3ω protein produced in *S. cerevisiae* was capable of binding to AtWEE1 from an *A. thaliana* total protein extract. However, due to the issue of confirming protein interactions in an environment different from the native environment of the proteins, it was desired to confirm the interaction *in vivo* in a plant system (Bhat *et al.*, 2006; Ohad *et al.*, 2007). The BiFC technique was selected for *in vivo* confirmation of the interaction between AtWEE1 and At14-3-3ω. The BiFC analyses presented in this thesis were performed in *N. tabacum* BY-2 cells making this the first report of the implementation of the technique in plant cell

cultures. The interaction was successfully confirmed in the *N. tabacum* BY-2 cells and the interaction could be mapped to the nucleus, cytoplasm, cell wall and at the cell plate indicating a dynamic interaction between AtWEE1 and At14-3-3ω, which may well be influenced by the cell cycle phase. Again information about the sub-cellular localization of AtWEE1 would be useful, since it is evident that binding of 14-3-3 proteins can alter the sub-cellular localization of the target protein.

After the identification of a protein-protein interaction, the next challenging step is to determine the biological function of the interaction. Since this is the first report proving an interaction between WEE1 and 14-3-3 proteins in plants, a putative function of this interaction has to be derived from studies of interactions between 14-3-3s and both Cdc25 and Wee1 primarily in the *X. laevis* and *H. sapiens* model systems. That 14-3-3 protein binding should affect the sub-cellular localization of Wee1 has not been reported, whereas it is evident from *S. pombe*, *H. sapiens* and *X. laevis* that 14-3-3 binding causes cytoplasmic localization of Cdc25 (Dalal *et al.*, 1999; Zeng and Piwnica-Worms, 1999; Kumagai and Dunphy, 1999; Yang *et al.*, 1999; Boutros *et al.*, 2006; Uchida *et al.*, 2006). Cdc25 mutants incapable of binding 14-3-3 proteins were found to be retained in the nucleus suggesting that 14-3-3 protein binding is necessary for sequestering Cdc25 into the cytoplasm and thereby keeping it away from its substrate (Zeng and Piwnica-Worms, 1999; Graves *et al.*, 2001; Uchida *et al.*, 2004). In *X. laevis* it is suggested that the role of 14-3-3 binding is to keep Wee1 evenly distributed in the nucleus (Lee *et al.*, 2001), whereas in *H. sapiens* Wee1 localization upon 14-3-3 binding is mapped to both nucleus and cytoplasm (Rothblum-Oviatt *et al.*, 2001), which is consistent with the localization of the AtWEE1/At14-3-3ω interaction reported in this thesis. Wee1 mutants incapable of binding 14-3-3 proteins have been found to have a poor ability to induce a cell cycle delay as a result of a decreased kinase activity (Wang *et al.*, 2000; Lee *et al.*, 2001; Rothblum-Oviatt *et al.*, 2001). It was attempted to construct an AtWEE1 mutant incapable of binding to At14-3-3ω by mutating S485 in a putative 14-3-3 binding site of AtWEE1. In the Y2H system, the AtWEE1(S485A) mutant was incapable of interacting with At14-3-3ω, however in the BiFC system the interaction was still present. For the AtWEE1(S485A)/At14-3-3ω transformant, fluorescence was detected in the nucleus and not in the cell wall or cell plate, which suggest that the AtWEE1 (S485A) mutation affects the binding of At14-3-3ω resulting in a nuclear localization

of AtWEE1. It is therefore likely that the AtWEE1/At14-3-3ω interaction is not eliminated in the Y2H system, but merely reduced. In *S. pombe* the mutation of the phosphorylation sites of three putative 14-3-3 protein binding sites of Cdc25 resulted in a reduction, but not an elimination of 14-3-3 binding ability. Additionally, the triple mutant was partially impaired in its ability to arrest cell cycle progression in response to HU treatment (Zeng and Piwnica-Worms, 1999). It is a possibility that the sub-cellular localization of the AtWEE1(S485A)/At14-3-3ω interaction is altered as a consequence of a decreased At14-3-3ω binding to AtWEE1(S485A). Moreover, it cannot be excluded that the AtWEE1(S485A) mutant will have an altered stress response towards DNA damaging agents and/or DNA replication blocking agents as previously described for the SpCdc25 triple mutant.

The work presented in this thesis encourages further analysis of the specific consequences of the AtWEE1/At14-3-3ω interaction investigating if and how 14-3-3 binding affects the biochemical properties of WEE1 with regards to protein half life, activity and stability and furthermore if and how the 14-3-3 binding affects the sub-cellular localization of WEE1. If the AtWEE1(S485A) mutant has a reduced At14-3-3ω binding ability the necessity for At14-3-3ω in the cell cycle checkpoint could be investigated by assessing the ability of AtWEE1(S485A) to induce a cell cycle checkpoint.

8.3 *In vivo* Function of WEE1 in the Plant Cell Cycle

As well as identifying the mechanisms that regulate WEE1 activity it is also of great importance to identify the function of WEE1 and consequences of WEE1 activity in plants. Recently, functional analyses of a range of plant WEE1s have provided solid evidence for the involvement of WEE1 in cell size control and in plant root development (Sun *et al.*, 1999; Sorrell *et al.*, 2002; Gonzalez *et al.*, 2004; De Schutter *et al.*, 2007; Gonzalez *et al.*, 2007).

The work presented in this thesis is the first report of WEE1 protein levels and kinase activity during the plant cell cycle. The activity of the WEE1 kinase is assayed by its inhibitory effect on CDK activity using WEE1 protein immunoprecipitated from whole *A. thaliana* plant protein extracts or from *N. tabacum* BY-2 cell cultures. This type of kinase assay was originally established by McGowan and Russell (1995) for analyzing the CDK inhibitory ability of *H. sapiens* Wee1. The WEE1 kinase assay

was initially performed using recombinant NtWEE1, which was found to inhibit CDK activity as previously shown for *Z. mays* and *S. lycopersicum* WEE1s (Sun *et al.*, 1999; Gonzalez *et al.*, 2007). In synchronized wild type *N. tabacum* BY-2 cells the NtWEE1 protein level increases during S phase and peaks in late S/early G2 phase. As the cell progress into mitosis the NtWEE1 protein level decreases, which suggests that NtWEE1 protein might be degraded during this phase of the cell cycle. In both animals and yeast Wee1 protein levels are regulated by ubiquitin-mediated degradation (Michael and Newport, 1998; Goes and Martin, 2001; Watanabe *et al.*, 2004; Watanabe *et al.*, 2005). The activity of NtWEE1 decreases markedly as the cells enter the G2 phase, consistent with the observed changes in WEE1 protein levels and the published data from *H. sapiens* showing that active WEE1 protein is not required when cells progress into mitosis (McGowan and Russell, 1995). Hence both NtWEE1 protein levels and kinase activity are sensitive markers of the onset of mitosis in *N. tabacum* BY-2 cells.

As mentioned, the Wee1/Mik1-type kinases are the main kinases responsible for the phosphorylation of tyrosine 15 of CDKs and have been identified in both yeast and animals (Parker and Piwnica-Worms, 1992; Booher *et al.*, 1993; Honda at al., 1995; McGowan and Russell, 1995; Mueller *et al.*, 1995). However, the Myt1 kinase has only been identified in *X. laevis* and *H. sapiens* and preferentially phosphorylates threonine 14 and, to a lesser extent, tyrosine 15 (Mueller *et al.*, 1995; Liu *et al.*, 1997). To date only Wee1 kinases have been identified in plants (Sun *et al.*, 1999; Sorrell *et al.*, 2002; Vandepoele *et al.*, 2002; Gonzalez *et al.*, 2004; Gonzalez *et al.*, 2007; Gou *et al.*, 2007) and therefore it is considered as the main kinase phosphorylating tyrosine 15 of plant CDKs. Of course, it cannot be excluded that other currently unknown kinases phosphorylate plant CDKs however it is known that in *A. thaliana* WEE1 interacts with and phosphorylates CDKA (Shimothono *et al.*, 2006; De Schutter *et al.*, 2007). A specific depletion of WEE1 gene product *in vivo* by *e.g.* RNAi would enable the investigation of whether other kinases act in concert with WEE1.

Over-expression of *AtWEE1* in *S. pombe* and *A. thaliana* delays cell cycle progression resulting in a large mitotic cell phenotype (Sorrell *et al.*, 2002; Siciliano, 2006), However, the exact opposite effect was obtained when *AtWEE1* was over-expressed in *N. tabacum* BY-2 cells, where it resulted in a small mitotic cell phenotype as a consequence of a shortened duration of G2 phase. The small mitotic cell phenotype

indeed resembles the phenotypes of Wee1 loss-of-function mutants described in yeast, animals and plants (Walter *et al.*, 2000; Harvey and Kellogg, 2003, Gonzalez *et al.*, 2007). Over-expression of *SlWEE1* in *N. tabacum* BY-2 cells results in an increased cell size phenotype as a consequence of a lengthening of G2 as expected for WEE1 over-expressing cells (Gonzalez *et al.*, 2007). A possible explanation for the different phenotypes of the *WEE1* over-expressing cells could be that *N. tabacum* WEE1 is phylogenetically closer related to *S. lycopersicum* WEE1 than *A. thaliana* WEE1 (Appendix D). Interestingly, over-expression of *N. tabacum WEE1* in *N. tabacum* BY-2 cells also results in a lengthening of G2, but the cells show no significant difference in mitotic cell size (Appendix D).

In addition to the small mitotic cell size phenotype, the over-expression of *AtWEE1* was found to perturb the transcriptional pattern of the endogeneous NtWEE1 resulting in the presence of *NtWEE1* transcript during mitosis, which together with the introduction of *AtWEE1* transcripts could be the reason for the small mitotic cell phenotype. If both NtWEE1 and AtWEE1 transcripts are being translated into active protein, it would result in an elevated level of active WEE1 protein. It is possible that if the elevated WEE1 protein level exceeds a specific threshold level within the cell the translated protein would be targeted for degradation. Depending on the rate of degradation of the WEE1 protein this could very well be the force that drives the cells prematurely into mitosis. Therefore, the WEE1 protein levels and kinase activity in the presence and absence of *AtWEE1* over-expression were monitored in synchronized *N. tabacum* BY-2 cells. The induction of *AtWEE1* over-expression caused the WEE1 protein level to increase by 20% in S/G2 and the WEE1 kinase activity increased correspondingly indicating that the measured WEE1 kinase activity originated from both AtWEE1 and NtWEE1. Furthermore, upon induction of *AtWEE1* expression WEE1 protein and kinase activity were present until the G2/M transition. The overall findings indicate that both WEE1 protein levels and kinase activity are cell cycle-regulated strongly suggesting that in plants, as well as other eukaryotes, WEE1 protein level and activity controls G2/M and the cells entry into mitosis (McGowan and Russell, 1995; Aligue *et al.*, 1997; Michael and Newport, 1998; Goes and Martin, 2001; Watanabe *et al.*, 2004; Watanabe *et al.*, 2005).

The *AtWEE1* over-expression resulted in a premature peak of NtCDKB activity in early S phase, whereas in wild type and in the absence of *AtWEE1* over-expression

NtCDKB activity peaks in G2/M (Mironov *et al.*, 1999; Sorrell *et al.*, 2001). NtCDKA activity remained constant both in the presence and absence of *AtWEE1* over-expression consistent with the NtCDKA activity levels in wild type *N. tabacum* cells (Sorrell *et al.*, 2001; Siciliano, 2006; Appendix D). This indicates that *AtWEE1* over-expression might perturb the mechanism that normally ensures that CDKB remains inactive until S/G2. It is evident that *AtWEE1* over-expression causes both WEE1 protein and kinase activity to be increased in late S and G2 phase and that the WEE1 protein is a mixture of AtWEE1 and NtWEE1 proteins. Therefore, the premature NtCDKB activity could potentially be caused by AtWEE1 competing with NtWEE1 for the NtCDKB substrate or be caused by a perturbation of regulatory proteins that normally negatively regulate CDKs at G1/S. Such regulatory proteins could be the KRP proteins, which were previously shown to interact with CYCDs, CDKA and CDKB proteins (Wang *et al.*, 1998; Lui *et al.*, 2000; De Veylder *et al.*, 2001b; Jasinski *et al.*, 2002; Verkest *et al.*, 2005; Nakai *et al.*, 2006). Putative proteins involved in the regulation of NtCDKB activity could be discovered by the identification of NtCDKB interaction partners and by subsequent biochemical analysis of potential kinases that could phosphorylate NtCDKB.

In addition to the studies of plant WEE1 in cell size regulation, studies of *AtWEE1* function *in planta* shows that over-expression of *AtWEE1* influences plant root development by decreasing primary root growth and lateral root initiation (Siciliano, 2006). A possible explanation for these findings could be that over-expression of WEE1 increases CDK inactivation thereby resulting in a mitotic delay. Plants over-expressing the *A. thaliana* SUC1/CKS1 homologue, AtCKS1, were found to have a similar phenotype and the reduction in the primary root growth caused by prolonged cell cycle duration (De Veylder *at al.*, 2001a). In contrast the over-expression of AtCYCA, which would promote CDK activation, in *A. thaliana* plants was found to result in longer primary roots as a consequence of an accelerated cell cycle (Doerner *et al.*, 1996).

The work presented in this thesis includes phenotypical and biochemical analyses of three independent *A. thaliana* plant lines carrying T-DNA insertions in the *WEE1* gene. This work was performed concurrent with recent work published by De Schutter *et al.* (2007). Two of the three *wee1* T-DNA lines (*wee1-1* and *wee1-5*) presented in this thesis were also characterized by De Schutter *et al.* (2007) and contradicting the

findings presented in this thesis both lines were found to be deficient in *WEE1* transcript and not to have mutant phenotypes when grown under standard conditions. However, De Schutter *et al.* (2007) only investigated the presence of the full-length *WEE1* transcript in the *wee1* T-DNA lines analyzed. As described in Chapter 7, the *wee1-1* line showed high phenotypic similarity to *AtWEE1* over-expressing lines by having a reduced primary root length and a reduced total number of lateral roots and lateral root primordia, suggesting that the T-DNA insertion in the second exon of *WEE1* might have an over-all up-regulating effect on *WEE1*. This is supported by findings in *S. pombe* showing that phosphorylation of the N-terminal domain Wee1 dramatically reduces Wee1 activity suggesting that the N-terminal domain is necessary for negative regulation of Wee1. Furthermore, truncation of the N-terminal domain of SpWee1 interferes with the timing of mitosis (Tang *et al.*, 1993; Aligue *et al.*, 1997). In contrast the *wee1-3* and *wee1-5* lines have normal primary root length with a 50% increase in total number of lateral roots and lateral root primordia and in addition the transcript and protein are significantly down-regulated compared to wild type, suggesting that these T-DNA insertions may have a down-regulating effect on *WEE1*. The phenotype is indeed similar to the one of *S. pombe Cdc25* over-expressed in *A. thaliana* and *N. tabacum* plants, which also resulted in an increase of the lateral root production (McKibbin *et al.*, 1998; N. Spadafora unpublished results).

As previously reported for both yeast and *D. melanogaster* Wee1 loss-of-function mutants (Murakami and Nurse, 1999; Price *et al.*, 2000; Asano *et al.*, 2005), all three T-DNA lines analyzed showed a hypersensitivity response towards HU suggesting that cells were not capable of inducing G2 arrest. It is evident that *WEE1* must be perturbed by the T-DNA insertions, since the *wee1* T-DNA lines generally show a more extreme hypersensitivity response compared to wild type. As a consequence of the HU treatment the plants had a reduced primary root length and production of lateral roots, which could reflect a way of minimizing the area of root exposed to HU. Another consequence of the HU treatment is an up-regulation of WEE1 transcript in the *wee1-3* and *wee1-5* lines. However, the protein levels were found to be down-regulated suggesting that the *WEE1* transcript might result in the production of unstable transcript, inefficient translation of transcript or that the protein produced is less stable and more easily degraded. Protein degradation is one of the main mechanisms of down-regulating Wee1 protein levels in yeast, *X. laevis* and *H. sapiens*

(Michael and Newport, 1998; Sia *et al.*, 1998; Goes and Martin, 2001; Watanabe *et al.*, 2004; Watanabe *et al.*, 2005). Although wild type *WEE1* was not transcriptionally regulated upon HU treatment the protein level was still found to be down-regulated. Consistent with De Schutter *et al.* 2007 the WEE1 kinase activity of wild type was found to increase by 30%, which suggests that WEE1 kinase activity, rather than WEE1 protein level, is a determinant for checkpoint control. However, upon HU treatment enhanced WEE1 activities were not observed for the *wee1* T-DNA lines suggesting that the WEE1 protein produced in these lines is not activated by HU treatment.

Based on the phenotypic and biochemical analysis of the three independent *wee1* T-DNA lines it proved to be difficult to form a clear pattern of phenotype, transcript, protein and kinase activity levels in the three *wee1* T-DNA lines (Chapter7; Appendix B). However, it is evident that the position of the T-DNA insertion in the *WEE1* gene greatly affects all of these parameters. The *wee1* T-DNA lines characterized in the work presented in this thesis functions merely as a tool in the investigation of the function of *AtWEE1* in the plant cell cycle. Moreover the different properties of the individual *wee1* T-DNA insertion lines reflect the necessity of analyzing more than one T-DNA insertion line for a desired gene. Furthermore, each T-DNA line contains an average of one to two T-DNA insertions (http://signal.salk.edu/tdna_FAQs.html), which could also strongly influence the observed phenotypes. Finally, T-DNA insertion lines often do not provide a genuine knock-out of gene function and therefore other methods, such as RNAi or artificial microRNA technology have to be used. An advantage of these technologies compared to T-DNA insertions lines would be that the expression of the small interference RNAs can be driven by specific promoters in order to target the knock-out/knock-down to specific organs/tissues of the plant (Schwab *et al.*, 2006) and furthermore different degrees of knock-down can be obtained for the analyzed gene.

8.4 Regulation of the Plant Cell Cycle

The basis of the work presented in this thesis was to investigate the function of a plant cell cycle checkpoint and investigate how the known features of the yeast and animal G2/M model apply to the plant model (Figure 40).

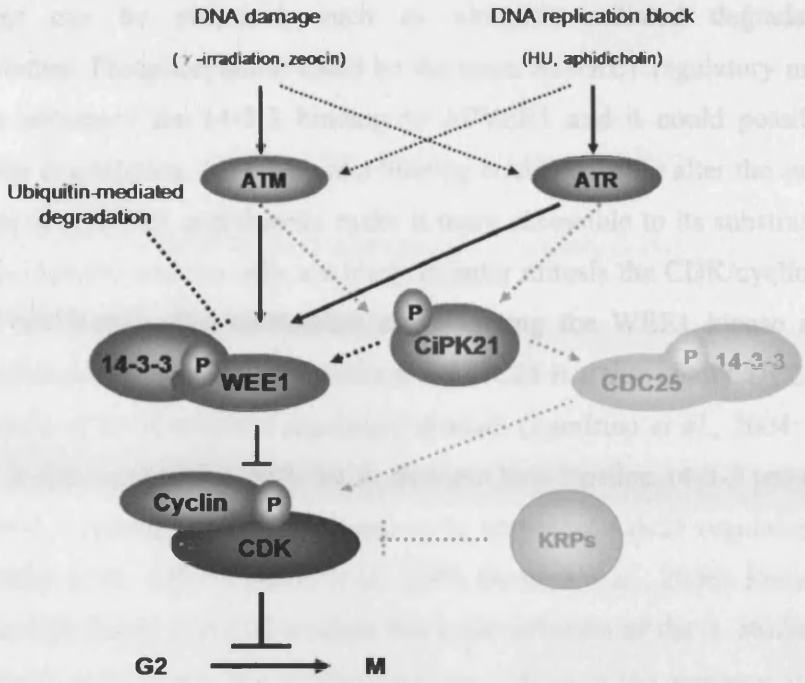

Figure 40 – Reviewed model of the plant G2/M transition. Faded areas and grey dashed arrows indicate putative not experimentally confirmed pathways. Black dashed arrows indicate putative experimentally confirmed pathways. Black arrows indicate experimentally confirmed pathways (Adapted from Menges *et al.*, 2005; Inze and De Veylder, 2006; De Schutter *et al.*, 2007). The ATM and ATR kinases are activated by various DNA stresses (γ-irradiation, zeocin, HU and aphidicholin) and induce the expression of WEE1. Putative mechanisms regulating WEE1 could be ubiquitin-mediated degradation and phosphorylation. The signalling cascade that operates between ATM/ATR and WEE1 is currently unknown, but a putative plant Chk1 protein, CiPK21, has been proposed and shown to interact with WEE1. 14-3-3 proteins bind to the active WEE1, which then negatively phosphorylates the CDK/cyclin complex leading to arrest of the cells in G2/M. It is still unknown if the putative CDC25 phosphatase is the WEE1 counteracting mechanism, since its functional role has not been demonstrated *in vivo* and it does not interact with the Non-Epsilon 14-3-3 protein group. Also it is currently unknown if other proteins, such as members of the KRP protein family, could compensate *WEE1* function.

In plants, it is currently known that upon DNA stress, *WEE1* expression is rapidly and strongly induced in an ATM/ATR-dependent manner resulting in the inactivation of CDKs and subsequent arrest of the cells in G2 (De Schutter *et al.*, 2007). However, the signalling cascade that operates between ATM/ATR and WEE1 has not been described. A putative Chk1/2 has not been identified in plants. However, recently light has been shed on the *A. thaliana* CiPK21 protein as a potential protein kinase regulating the signalling cascade downstream ATM/ATR. AtCiPK21 was found to interact with AtWEE1 in a Y2H screen (Appendix C). Putative WEE1 regulatory

mechanisms can be proposed, such as ubiquitin-mediated degradation and phosphorylation. Phosphorylation could be the main AtWEE1 regulatory mechanism since it is necessary for 14-3-3 binding to AtWEE1 and it could possibly target AtWEE1 for degradation. 14-3-3 protein binding could probably alter the sub-cellular localization of AtWEE1 and thereby make it more accessible to its substrates. When the DNA is repaired and the cells are ready to enter mitosis the CDK/cyclin complex has to be reactivated. The mechanism counteracting the WEE1 kinase activity is currently unknown. It is still questionable if AtCDC25 is a true plant CDC25 because of the absence of an N-terminal regulatory domain (Landrieu *et al.*, 2004; Sorrell *et al.*, 2005). It does not interact with the *A. thaliana* Non-Epsilon 14-3-3 protein group, although 14-3-3 proteins have been found to be important Cdc25 regulators in other species (Baldin *et al.*, 1997; Bulavin *et al.*, 2003; Boutros *et al.*, 2006). From the work presented in this thesis, it is also evident that a perturbation of the *A. thaliana WEE1* gene causes the cells to progress prematurely into mitosis in the presence of HU. This results in an arrest of primary root growth suggesting a loss of *WEE1* function. However, unlike yeast and animal *Wee1* loss-of-function mutants (Price *et al.*, 2000; Kellogg, 2003; Tominaga *et al.*, 2006), loss of *WEE1* function in *A. thaliana* is not lethal and the plants only show a slight mutant phenotype when grown under standard conditions, which could suggest a mechanism compensating *WEE1* function. This mechanism could be performed by members of the KRP protein family, which were recently shown to interact with plant-specific CDKBs and inhibit their kinase activity (Nakai *et al.*, 2006). The role of plant WEE1s in cell size regulation is also evident from the analysis of *AtWEE1* over-expression in *N. tabacum* BY-2 cells, where WEE1 protein level and kinase activity indeed are regulated in a cell cycle-dependent manner and act as sensitive indicators of the G2/M transition.

References

Abraham, J., Kelly, J., Thibault, P. and Benchimol, S. (2000). Post-translational modification of p53 protein in response to ionizing radiation analyzed by mass spectrometry. *J Mol Biol* **295**, 853-64.

Abrahams, S., Cavet, G., Oakenfull, E. A., Carmichael, J. P., Shah, Z. H., Soni, R. and Murray, J. A. (2001). A novel and highly divergent *Arabidopsis* cyclin isolated by complementation in budding yeast. *Biochim Biophys Acta* **1539**, 1-6.

Aitken, A. (2002). Functional specificity in 14-3-3 isoform interactions through dimer formation and phosphorylation. Chromosome location of mammalian isoforms and variants. *Plant Mol Biol* **50**, 993-1010.

Aker, J., Borst, J. W., Karlova, R. and de Vries, S. (2006). The *Arabidopsis thaliana* AAA protein CDC48A interacts in vivo with the somatic embryogenesis receptor-like kinase 1 receptor at the plasma membrane. *J Struct Biol* **156**, 62-71.

al-Khodairy, F., Fotou, E., Sheldrick, K. S., Griffiths, D. J., Lehmann, A. R. and Carr, A. M. (1994). Identification and characterization of new elements involved in checkpoint and feedback controls in fission yeast. *Mol Biol Cell* **5**, 147-60.

Aligue, R., Akhavan-Niak, H. and Russell, P. (1994). A role for Hsp90 in cell cycle control: Wee1 tyrosine kinase activity requires interaction with Hsp90. *EMBO J* **13**, 6099-106.

Aligue, R., Wu, L. and Russell, P. (1997). Regulation of *Schizosaccharomyces pombe* Wee1 tyrosine kinase. *J Biol Chem* **272**, 13320-5.

Alonso, J. M., Stepanova, A. N., Leisse, T. J., Kim, C. J., Chen, H., Shinn, P., Stevenson, D. K., Zimmerman, J., Barajas, P., Cheuk, R. *et al.* (2003). Genome-wide insertional mutagenesis of *Arabidopsis thaliana*. *Science* **301**, 653-7.

Alsterfjord, M., Sehnke, P. C., Arkell, A., Larsson, H., Svennelid, F., Rosenquist, M., Ferl, R. J., Sommarin, M. and Larsson, C. (2004). Plasma membrane H(+)-ATPase and 14-3-3 isoforms of *Arabidopsis* leaves: evidence for isoform specificity in the 14-3-3/H(+)-ATPase interaction. *Plant Cell Physiol* **45**, 1202-10.

Aoyama, T. and Chua, N. H. (1997). A glucocorticoid-mediated transcriptional induction system in transgenic plants. *Plant J* **11**, 605-12.

Asano, S., Park, J. E., Sakchaisri, K., Yu, L. R., Song, S., Supavilai, P., Veenstra, T. D. and Lee, K. S. (2005). Concerted mechanism of Swe1/Wee1 regulation by multiple kinases in budding yeast. *EMBO J* **24**, 2194-204.

Ayad, N. G., Rankin, S., Murakami, M., Jebanathirajah, J., Gygi, S. and Kirschner, M. W. (2003). Tome-1, a trigger of mitotic entry, is degraded during G1 via the APC. *Cell* **113**, 101-13.

Azumi, Y., Liu, D., Zhao, D., Li, W., Wang, G., Hu, Y. and Ma, H. (2002). Homolog interaction during meiotic prophase I in *Arabidopsis* requires the SOLO DANCERS gene encoding a novel cyclin-like protein. *EMBO J* **21**, 3081-95.

Bachmann, M., Huber, J. L., Athwal, G. S., Wu, K., Ferl, R. J. and Huber, S. C. (1996). 14-3-3 proteins associate with the regulatory phosphorylation site of spinach leaf nitrate reductase in an isoform-specific manner and reduce dephosphorylation of Ser-543 by endogenous protein phosphatases. *FEBS Lett* **398**, 26-30.

Bachmann, M., Kosan, C., Xing, P. X., Montenarh, M., Hoffmann, I. and Moroy, T. (2006). The oncogenic serine/threonine kinase Pim-1 directly phosphorylates and activates the G2/M specific phosphatase Cdc25C. *Int J Biochem Cell Biol* **38**, 430-43.

Baek, K., Brown, R. S., Birrane, G. and Ladias, J. A. (2007). Crystal structure of human cyclin K, a positive regulator of cyclin-dependent kinase 9. *J Mol Biol* **366**, 563-73.

Baldin, V., Cans, C., Knibiehler, M. and Ducommun, B. (1997). Phosphorylation of human CDC25B phosphatase by CDK1-cyclin A triggers its proteasome-dependent degradation. *J Biol Chem* **272**, 32731-4.

Baldin, V. and Ducommun, B. (1995). Subcellular localisation of human wee1 kinase is regulated during the cell cycle. *J Cell Sci* **108 (Pt 6)**, 2425-32.

Barroco, R. M., De Veylder, L., Magyar, Z., Engler, G., Inze, D. and Mironov, V. (2003). Novel complexes of cyclin-dependent kinases and a cyclin-like protein from *Arabidopsis thaliana* with a function unrelated to cell division. *Cell Mol Life Sci* **60**, 401-12.

Bhat, R. A., Lahaye, T. and Panstruga, R. (2006). The visible touch: *in planta* visualization of protein-protein interactions by fluorophore-based methods. *Plant Methods* **2**, 12.

Bihn, E. A., Paul, A. L., Wang, S. W., Erdos, G. W. and Ferl, R. J. (1997). Localization of 14-3-3 proteins in the nuclei of *arabidopsis* and maize. *Plant J* **12**, 1439-45.

Bleeker, P. M., Hakvoort, H. W., Bliek, M., Souer, E. and Schat, H. (2006). Enhanced arsenate reduction by a CDC25-like tyrosine phosphatase explains increased phytochelatin accumulation in arsenate-tolerant *Holcus lanatus*. *Plant J* **45**, 917-29.

Bolle, C. (2004). The role of GRAS proteins in plant signal transduction and development. *Planta* **218**, 683-92.

Booher, R. N., Deshaies, R. J. and Kirschner, M. W. (1993). Properties of *Saccharomyces cerevisiae* wee1 and its differential regulation of p34CDC28 in response to G1 and G2 cyclins. *EMBO J* **12**, 3417-26.

Bordo, D. and Bork, P. (2002). The rhodanese/Cdc25 phosphatase superfamily. Sequence-structure-function relations. *EMBO Rep* **3**, 741-6.

Boudolf, V., Inze, D. and De Veylder, L. (2006). What if higher plants lack a CDC25 phosphatase? *Trends Plant Sci* **11**, 474-9.

Boudolf, V., Vlieghe, K., Beemster, G. T., Magyar, Z., Torres Acosta, J. A., Maes, S., Van Der Schueren, E., Inze, D. and De Veylder, L. (2004). The plant-specific cyclin-dependent kinase CDKB1;1 and transcription factor E2Fa-DPa control the balance of mitotically dividing and endoreduplicating cells in *Arabidopsis*. *Plant Cell* **16**, 2683-92.

Boutros, R., Dozier, C. and Ducommun, B. (2006). The when and wheres of CDC25 phosphatases. *Curr Opin Cell Biol* **18**, 185-91.

Bracha-Drori, K., Shichrur, K., Katz, A., Oliva, M., Angelovici, R., Yalovsky, S. and Ohad, N. (2004). Detection of protein-protein interactions in plants using bimolecular fluorescence complementation. *Plant J* **40**, 419-27.

Bradford, M. M. (1976). A rapid and sensitive method for the quantitation of microgram quantities of protein utilizing the principle of protein-dye binding. *Anal Biochem* **72**, 248-54.

Brandt, J., Thordal-Christensen, H., Vad, K., Gregersen, P. L. and Collinge, D. B. (1992). A pathogen-induced gene of barley encodes a protein showing high similarity to a protein kinase regulator. *Plant J* **2**, 815-20.

Bregman, D. B., Pestell, R. G. and Kidd, V. J. (2000). Cell cycle regulation and RNA polymerase II. *Front Biosci* **5**, D244-57.

Breton, G., Danyluk, J., Charron, J. B. and Sarhan, F. (2003). Expression profiling and bioinformatic analyses of a novel stress-regulated multispanning transmembrane protein family from cereals and *Arabidopsis*. *Plant Physiol* **132**, 64-74.

Bulavin, D. V., Higashimoto, Y., Demidenko, Z. N., Meek, S., Graves, P., Phillips, C., Zhao, H., Moody, S. A., Appella, E., Piwnica-Worms, H. *et al.* (2003). Dual phosphorylation controls Cdc25 phosphatases and mitotic entry. *Nat Cell Biol* **5**, 545-51.

Burnette, W. N. (1981). "Western blotting": electrophoretic transfer of proteins from sodium dodecyl sulfate--polyacrylamide gels to unmodified nitrocellulose and radiographic detection with antibody and radioiodinated protein A. *Anal Biochem* **112**, 195-203.

Capasso, H., Palermo, C., Wan, S., Rao, H., John, U. P., O'Connell, M. J. and Walworth, N. C. (2002). Phosphorylation activates Chk1 and is required for checkpoint-mediated cell cycle arrest. *J Cell Sci* **115**, 4555-64.

Causier, B. and Davies, B. (2002). Analysing protein-protein interactions with the yeast two-hybrid system. *Plant Mol Biol* **50**, 855-70.

Chan, T. A., Hermeking, H., Lengauer, C., Kinzler, K. W. and Vogelstein, B. (1999). 14-3-3Sigma is required to prevent mitotic catastrophe after DNA damage. *Nature* **401**, 616-20.

Chaudhri, M., Scarabel, M. and Aitken, A. (2003). Mammalian and yeast 14-3-3 isoforms form distinct patterns of dimers in vivo. *Biochem Biophys Res Commun* **300**, 679-85.

Chen, F., Li, Q., Sun, L. and He, Z. (2006). The rice 14-3-3 gene family and its involvement in responses to biotic and abiotic stress. *DNA Res* **13**, 53-63.

Chen, I. P., Haehnel, U., Altschmied, L., Schubert, I. and Puchta, H. (2003a). The transcriptional response of *Arabidopsis* to genotoxic stress - a high-density colony array study (HDCA). *Plant J* **35**, 771-86.

Chen, L., Liu, T. H. and Walworth, N. C. (1999). Association of Chk1 with 14-3-3 proteins is stimulated by DNA damage. *Genes Dev* **13**, 675-85.

Chen, M. S., Ryan, C. E. and Piwnica-Worms, H. (2003b). Chk1 kinase negatively regulates mitotic function of Cdc25A phosphatase through 14-3-3 binding. *Mol Cell Biol* **23**, 7488-97.

Chen, Z., Fu, H., Liu, D., Chang, P. F., Narasimhan, M., Ferl, R., Hasegawa, P. M. and Bressan, R. A. (1994). A NaCl-regulated plant gene encoding a brain protein homology that activates ADP ribosyltransferase and inhibits protein kinase C. *Plant J* **6**, 729-40.

Childs, K. L., Hamilton, J. P., Zhu, W., Ly, E., Cheung, F., Wu, H., Rabinowicz, P. D., Town, C. D., Buell, C. R. and Chan, A. P. (2007). The TIGR Plant Transcript Assemblies database. *Nucleic Acids Res* **35**, D846-51.

Citovsky, V., Lee, L. Y., Vyas, S., Glick, E., Chen, M. H., Vainstein, A., Gafni, Y., Gelvin, S. B. and Tzfira, T. (2006). Subcellular localization of interacting proteins by bimolecular fluorescence complementation in planta. *J Mol Biol* **362**, 1120-31.

Clontech. (02/07). Yeast Protocols Handbook.

Coblitz, B., Shikano, S., Wu, M., Gabelli, S. B., Cockrell, L. M., Spieker, M., Hanyu, Y., Fu, H., Amzel, L. M. and Li, M. (2005). C-terminal recognition by 14-3-3 proteins for surface expression of membrane receptors. *J Biol Chem* **280**, 36263-72.

Cockcroft, C. E., den Boer, B. G., Healy, J. M. and Murray, J. A. (2000). Cyclin D control of growth rate in plants. *Nature* **405**, 575-9.

Colasanti, J., Tyers, M. and Sundaresan, V. (1991). Isolation and characterization of cDNA clones encoding a functional p34cdc2 homologue from Zea mays. *Proc Natl Acad Sci U S A* **88**, 3377-81.

Conklin, D. S., Galaktionov, K. and Beach, D. (1995). 14-3-3 proteins associate with cdc25 phosphatases. *Proc Natl Acad Sci U S A* **92**, 7892-6.

Crenshaw, D. G., Yang, J., Means, A. R. and Kornbluth, S. (1998). The mitotic peptidyl-prolyl isomerase, Pin1, interacts with Cdc25 and Plx1. *EMBO J* **17**, 1315-27.

Culligan, K., Tissier, A. and Britt, A. (2004). ATR regulates a G2-phase cell-cycle checkpoint in *Arabidopsis thaliana*. *Plant Cell* **16**, 1091-104.

Cutler, S. R., Ehrhardt, D. W., Griffitts, J. S. and Somerville, C. R. (2000). Random GFP::cDNA fusions enable visualization of subcellular structures in cells of *Arabidopsis* at a high frequency. *Proc Natl Acad Sci U S A* **97**, 3718-23.

Dahl, M., Meskiene, I., Bogre, L., Ha, D. T., Swoboda, I., Hubmann, R., Hirt, H. and Heberle-Bors, E. (1995). The D-type alfalfa cyclin gene cycMs4 complements G1 cyclin-deficient yeast and is induced in the G1 phase of the cell cycle. *Plant Cell* **7**, 1847-57.

Dalal, S. N., Schweitzer, C. M., Gan, J. and DeCaprio, J. A. (1999). Cytoplasmic localization of human cdc25C during interphase requires an intact 14-3-3 binding site. *Mol Cell Biol* **19**, 4465-79.

Daugherty, C. J., Rooney, M. F., Miller, P. W. and Ferl, R. J. (1996). Molecular organization and tissue-specific expression of an *Arabidopsis* 14-3-3 gene. *Plant Cell* **8**, 1239-48.

Davies, B., Egea-Cortines, M., de Andrade Silva, E., Saedler, H. and Sommer, H. (1996). Multiple interactions amongst floral homeotic MADS box proteins. *EMBO J* **15**, 4330-43.

De Bondt, H. L., Rosenblatt, J., Jancarik, J., Jones, H. D., Morgan, D. O. and Kim, S. H. (1993). Crystal structure of cyclin-dependent kinase 2. *Nature* **363**, 595-602.

de Falco, G. and Giordano, A. (1998). CDK9 (PITALRE): a multifunctional cdc2-related kinase. *J Cell Physiol* **177**, 501-6.

De Schutter, K., Joubes, J., Cools, T., Verkest, A., Corellou, F., Babiychuk, E., Van Der Schueren, E., Beeckman, T., Kushnir, S., Inze, D. *et al.* (2007). *Arabidopsis* WEE1 kinase controls cell cycle arrest in response to activation of the DNA integrity checkpoint. *Plant Cell* **19**, 211-25.

Desai, U. J. and Pfaffle, P. K. (1995) Single-step purification of thermostable DNA polymerase expressed in *Escherichia coli*. *Biotechniques* **19**, 780-2.

de Vetten, N. C. and Ferl, R. J. (1995). Characterization of a maize G-box binding factor that is induced by hypoxia. *Plant J* **7**, 589-601.

De Veylder, L., Beeckman, T., Beemster, G. T., de Almeida Engler, J., Ormenese, S., Maes, S., Naudts, M., Van Der Schueren, E., Jacqmard, A., Engler, G. *et al.* (2002). Control of proliferation, endoreduplication and differentiation by the *Arabidopsis* E2Fa-DPa transcription factor. *EMBO J* **21**, 1360-8.

De Veylder, L., Beeckman, T., Beemster, G. T., Krols, L., Terras, F., Landrieu, I., van der Schueren, E., Maes, S., Naudts, M. and Inze, D. (2001a). Functional analysis of cyclin-dependent kinase inhibitors of *Arabidopsis*. *Plant Cell* **13**, 1653-68.

De Veylder, L., Beemster, G. T., Beeckman, T. and Inze, D. (2001b). CKS1At overexpression in *Arabidopsis thaliana* inhibits growth by reducing meristem size and inhibiting cell-cycle progression. *Plant J* **25**, 617-26.

De Veylder, L., Segers, G., Glab, N., Casteels, P., Van Montagu, M. and Inze, D. (1997). The *Arabidopsis* Cks1At protein binds the cyclin-dependent kinases Cdc2aAt and Cdc2bAt. *FEBS Lett* **412**, 446-52.

DeLille, J. M., Sehnke, P. C. and Ferl, R. J. (2001). The *arabidopsis* 14-3-3 family of signaling regulators. *Plant Physiol* **126**, 35-8.

Dhankher, O. P., Rosen, B. P., McKinney, E. C. and Meagher, R. B. (2006). Hyperaccumulation of arsenic in the shoots of *Arabidopsis* silenced for arsenate reductase (ACR2). *Proc Natl Acad Sci U S A* **103**, 5413-8.

Diaz, I., Martinez, M., Isabel-LaMoneda, I., Rubio-Somoza, I. and Carbonero, P. (2005). The DOF protein, SAD, interacts with GAMYB in plant nuclei and activates transcription of endosperm-specific genes during barley seed development. *Plant J* **42**, 652-62.

Diener, A. C. and Ausubel, F. M. (2005). RESISTANCE TO FUSARIUM OXYSPORUM 1, a dominant *Arabidopsis* disease-resistance gene, is not race specific. *Genetics* **171**, 305-21.

Doerner, P., Jorgensen, J. E., You, R., Steppuhn, J. and Lamb, C. (1996). Control of root growth and development by cyclin expression. *Nature* **380**, 520-3.

Donzelli, M., Squatrito, M., Ganoth, D., Hershko, A., Pagano, M. and Draetta, G. F. (2002). Dual mode of degradation of Cdc25 A phosphatase. *EMBO J* **21**, 4875-84.

Dougherty, M. K. and Morrison, D. K. (2004). Unlocking the code of 14-3-3. *J Cell Sci* **117**, 1875-84.

Dubois, T., Howell, S., Amess, B., Kerai, P., Learmonth, M., Madrazo, J., Chaudhri, M., Rittinger, K., Scarabel, M., Soneji, Y. *et al.* (1997). Structure and sites of phosphorylation of 14-3-3 protein: role in coordinating signal transduction pathways. *J Protein Chem* **16**, 513-22.

Edwards, K., Johnstone, C. and Thompson, C. (1991). A simple and rapid method for the preparation of plant genomic DNA for PCR analysis. *Nucleic Acids Res* **19**, 1349.

Eklund, H., Uhlin, U., Farnegardh, M., Logan, D. T. and Nordlund, P. (2001). Structure and function of the radical enzyme ribonucleotide reductase. *Prog Biophys Mol Biol* **77**, 177-268.

Elledge, S. J. (1996). Cell cycle checkpoints: preventing an identity crisis. *Science* **274**, 1664-72.

Elledge, S. J. and Harper, J. W. (1998). The role of protein stability in the cell cycle and cancer. *Biochim Biophys Acta* **1377**, M61-70.

Ellis, C., Turner, J. G. and Devoto, A. (2002). Protein complexes mediate signalling in plant responses to hormones, light, sucrose and pathogens. *Plant Mol Biol* **50**, 971-80.

Ezhevsky, S. A., Nagahara, H., Vocero-Akbani, A. M., Gius, D. R., Wei, M. C. and Dowdy, S. F. (1997). Hypo-phosphorylation of the retinoblastoma protein (pRb) by cyclin D:Cdk4/6 complexes results in active pRb. *Proc Natl Acad Sci U S A* **94**, 10699-704.

Fantes, P. and Nurse, P. (1977). Control of cell size at division in fission yeast by a growth-modulated size control over nuclear division. *Exp Cell Res* **107**, 377-86.

Fauman, E. B., Cogswell, J. P., Lovejoy, B., Rocque, W. J., Holmes, W., Montana, V. G., Piwnica-Worms, H., Rink, M. J. and Saper, M. A. (1998). Crystal structure of the catalytic domain of the human cell cycle control phosphatase, Cdc25A. *Cell* **93**, 617-25.

Feiler, H. S., Desprez, T., Santoni, V., Kronenberger, J., Caboche, M. and Traas, J. (1995). The higher plant *Arabidopsis thaliana* encodes a functional CDC48 homologue which is highly expressed in dividing and expanding cells. *EMBO J* **14**, 5626-37.

Ferl, R. J. (2004). 14-3-3 proteins: regulation of signal-induced events. *Physiol Plant* **120**, 173-178.

Ferl, R. J., Manak, M. S. and Reyes, M. F. (2002). The 14-3-3s. *Genome Biol* **3**. (http://genomebiology.com/2002/3/7/reviews/3010.1)

Ferreira, P. C., Hemerly, A. S., Villarroel, R., Van Montagu, M. and Inze, D. (1991). The *Arabidopsis* functional homolog of the p34cdc2 protein kinase. *Plant Cell* **3**, 531-40.

Fobert, P. R., Gaudin, V., Lunness, P., Coen, E. S. and Doonan, J. H. (1996). Distinct classes of cdc2-related genes are differentially expressed during the cell division cycle in plants. *Plant Cell* **8**, 1465-76.

Fogarty, P., Campbell, S. D., Abu-Shumays, R., Phalle, B. S., Yu, K. R., Uy, G. L., Goldberg, M. L. and Sullivan, W. (1997). The *Drosophila* grapes gene is related to checkpoint gene chk1/rad27 and is required for late syncytial division fidelity. *Curr Biol* **7**, 418-26.

Forbes, K. C., Humphrey, T. and Enoch, T. (1998). Suppressors of cdc25p overexpression identify two pathways that influence the G2/M checkpoint in fission yeast. *Genetics* **150**, 1361-75.

Ford, J. C., al-Khodairy, F., Fotou, E., Sheldrick, K. S., Griffiths, D. J. and Carr, A. M. (1994). 14-3-3 protein homologs required for the DNA damage checkpoint in fission yeast. *Science* **265**, 533-5.

Forrest, A. and Gabrielli, B. (2001). Cdc25B activity is regulated by 14-3-3. *Oncogene* **20**, 4393-401.

Francis, D. (2003). The interface between the cell cycle and programmed cell death in higher plants from division into death. Cambridge, Elsevier Ltd.

Francis, D. (2007). The plant cell cycle--15 years on. *New Phytol* **174**, 261-78.

Frohlich, K. U., Fries, H. W., Peters, J. M. and Mecke, D. (1995). The ATPase activity of purified CDC48p from *Saccharomyces cerevisiae* shows complex dependence on ATP-, ADP-, and NADH-concentrations and is completely inhibited by NEM. *Biochim Biophys Acta* **1253**, 25-32.

Fuerst, R. A., Soni, R., Murray, J. A. and Lindsey, K. (1996). Modulation of cyclin transcript levels in cultured cells of *Arabidopsis thaliana*. *Plant Physiol* **112**, 1023-33.

Fulop, K., Pettko-Szandtner, A., Magyar, Z., Miskolczi, P., Kondorosi, E., Dudits, D. and Bako, L. (2005). The *Medicago* CDKC;1-CYCLINT;1 kinase complex phosphorylates the carboxy-terminal domain of RNA polymerase II and promotes transcription. *Plant J* **42**, 810-20.

Furnari, B., Blasina, A., Boddy, M. N., McGowan, C. H. and Russell, P. (1999). Cdc25 inhibited in vivo and in vitro by checkpoint kinases Cds1 and Chk1. *Mol Biol Cell* **10**, 833-45.

Furnari, B., Rhind, N. and Russell, P. (1997). Cdc25 mitotic inducer targeted by chk1 DNA damage checkpoint kinase. *Science* **277**, 1495-7.

Gabrielli, B. G., Clark, J. M., McCormack, A. K. and Ellem, K. A. (1997). Hyperphosphorylation of the N-terminal domain of Cdc25 regulates activity toward cyclin B1/Cdc2 but not cyclin A/Cdk2. *J Biol Chem* **272**, 28607-14.

Garcia, V., Bruchet, H., Camescasse, D., Granier, F., Bouchez, D. and Tissier, A. (2003). AtATM is essential for meiosis and the somatic response to DNA damage in plants. *Plant Cell* **15**, 119-32.

Garcia, V., Salanoubat, M., Choisne, N. and Tissier, A. (2000). An ATM homologue from *Arabidopsis thaliana*: complete genomic organisation and expression analysis. *Nucleic Acids Res* **28**, 1692-9.

Gelperin, D., Weigle, J., Nelson, K., Roseboom, P., Irie, K., Matsumoto, K. and Lemmon, S. (1995). 14-3-3 proteins: potential roles in vesicular transport and Ras signaling in *Saccharomyces cerevisiae*. *Proc Natl Acad Sci U S A* **92**, 11539-43.

Genschik, P., Criqui, M. C., Parmentier, Y., Derevier, A. and Fleck, J. (1998). Cell cycle - dependent proteolysis in plants. Identification Of the destruction box pathway and metaphase arrest produced by the proteasome inhibitor mg132. *Plant Cell* **10**, 2063-76.

Goes, F. S. and Martin, J. (2001). Hsp90 chaperone complexes are required for the activity and stability of yeast protein kinases Mik1, Wee1 and Swe1. *Eur J Biochem* **268**, 2281-9.

Golemis, E. A., Serebriiskii, I. and Law, S. F. (1999). The yeast two-hybrid system: criteria for detecting physiologically significant protein-protein interactions. *Curr Issues Mol Biol* **1**, 31-45.

Gonzalez, N., Gevaudant, F., Hernould, M., Chevalier, C. and Mouras, A. (2007). The cell cycle-associated protein kinase WEE1 regulates cell size in relation to endoreduplication in developing tomato fruit. *Plant J* **51**, 642-55.

Gonzalez, N., Hernould, M., Delmas, F., Gevaudant, F., Duffe, P., Causse, M., Mouras, A. and Chevalier, C. (2004). Molecular characterization of a WEE1 gene homologue in tomato (*Lycopersicon esculentum Mill.*). *Plant Mol Biol* **56**, 849-61.

Grafi, G., Burnett, R. J., Helentjaris, T., Larkins, B. A., DeCaprio, J. A., Sellers, W. R. and Kaelin, W. G., Jr. (1996). A maize cDNA encoding a member of the retinoblastoma protein family: involvement in endoreduplication. *Proc Natl Acad Sci U S A* **93**, 8962-7.

Graves, P. R., Lovly, C. M., Uy, G. L. and Piwnica-Worms, H. (2001). Localization of human Cdc25C is regulated both by nuclear export and 14-3-3 protein binding. *Oncogene* **20**, 1839-51.

Guo, J., Song, J., Wang, F. and Zhang, X. S. (2007). Genome-wide identification and expression analysis of rice cell cycle genes. *Plant Mol Biol* **64**, 349-60.

Hanahan, D. (1983). Studies on transformation of *Escherichia coli* with plasmids. *J Mol Biol* **166**, 557-80.

Harris, H. (1999). The birth of the cell. New Haven, Yale University Press.

Hartwell, L. H., Culotti, J., Pringle, J. R. and Reid, B. J. (1974). Genetic control of the cell division cycle in yeast. *Science* **183**, 46-51.

Hartwell, L. H. and Weinert, T. A. (1989). Checkpoints: controls that ensure the order of cell cycle events. *Science* **246**, 629-34.

Harvey, S. L. and Kellogg, D. R. (2003). Conservation of mechanisms controlling entry into mitosis: budding yeast wee1 delays entry into mitosis and is required for cell size control. *Curr Biol* **13**, 264-75.

Hermeking, H. (2003). The 14-3-3 cancer connection. *Nat Rev Cancer* **3**, 931-43.

Hermeking, H., Lengauer, C., Polyak, K., He, T. C., Zhang, L., Thiagalingam, S., Kinzler, K. W. and Vogelstein, B. (1997). 14-3-3 sigma is a p53-regulated inhibitor of G2/M progression. *Mol Cell* **1**, 3-11.

Himanen, K., Boucheron, E., Vanneste, S., de Almeida Engler, J., Inze, D. and Beeckman, T. (2002). Auxin-mediated cell cycle activation during early lateral root initiation. *Plant Cell* **14**, 2339-51.

Himelblau, E., Mira, H., Lin, S. J., Culotta, V. C., Penarrubia, L. and Amasino, R. M. (1998). Identification of a functional homolog of the yeast copper homeostasis gene ATX1 from *Arabidopsis*. *Plant Physiol* **117**, 1227-34.

Honda, R., Tanaka, H., Ohba, Y. and Yasuda, H. (1995). Mouse p87wee1 kinase is regulated by M-phase specific phosphorylation. *Chromosome Res* **3**, 300-8.

Howe, L., Auston, D., Grant, P., John, S., Cook, R. G., Workman, J. L. and Pillus, L. (2001). Histone H3 specific acetyltransferases are essential for cell cycle progression. *Genes Dev* **15**, 3144-54.

Hrabak, E. M., Chan, C. W., Gribskov, M., Harper, J. F., Choi, J. H., Halford, N., Kudla, J., Luan, S., Nimmo, H. G., Sussman, M. R. *et al.* (2003). The *Arabidopsis* CDPK-SnRK superfamily of protein kinases. *Plant Physiol* **132**, 666-80.

Hu, C. D., Chinenov, Y. and Kerppola, T. K. (2002). Visualization of interactions among bZIP and Rel family proteins in living cells using bimolecular fluorescence complementation. *Mol Cell* **9**, 789-98.

Huntley, R., Healy, S., Freeman, D., Lavender, P., de Jager, S., Greenwood, J., Makker, J., Walker, E., Jackman, M., Xie, Q. *et al.* (1998). The maize retinoblastoma protein homologue ZmRb-1 is regulated during leaf development and displays conserved interactions with G1/S regulators and plant cyclin D (CycD) proteins. *Plant Mol Biol* **37**, 155-69.

Huntley, R. P. and Murray, J. A. (1999). The plant cell cycle. *Curr Opin Plant Biol* **2**, 440-6.

Inze, D. and De Veylder, L. (2006). Cell cycle regulation in plant development. *Annu Rev Genet* **40**, 77-105.

Jahn, T., Fuglsang, A. T., Olsson, A., Bruntrup, I. M., Collinge, D. B., Volkmann, D., Sommarin, M., Palmgren, M. G. and Larsson, C. (1997). The 14-3-3 protein interacts directly with the C-terminal region of the plant plasma membrane H(+)-ATPase. *Plant Cell* **9**, 1805-14.

Jarillo, J. A., Capel, J., Leyva, A., Martinez-Zapater, J. M. and Salinas, J. (1994). Two related low-temperature-inducible genes of *Arabidopsis* encode proteins showing high homology to 14-3-3 proteins, a family of putative kinase regulators. *Plant Mol Biol* **25**, 693-704.

Jarillo, J. A., Capel, J., Tang, R. H., Yang, H. Q., Alonso, J. M., Ecker, J. R. and Cashmore, A. R. (2001). An *Arabidopsis* circadian clock component interacts with both CRY1 and phyB. *Nature* **410**, 487-90.

Jasinski, S., Riou-Khamlichi, C., Roche, O., Perennes, C., Bergounioux, C. and Glab, N. (2002). The CDK inhibitor NtKIS1a is involved in plant development, endoreduplication and restores normal development of cyclin D3; 1-overexpressing plants. *J Cell Sci* **115**, 973-82.

Jeffrey, P. D., Russo, A. A., Polyak, K., Gibbs, E., Hurwitz, J., Massague, J. and Pavletich, N. P. (1995). Mechanism of CDK activation revealed by the structure of a cyclinA-CDK2 complex. *Nature* **376**, 313-20.

Jiang, K., Pereira, E., Maxfield, M., Russell, B., Goudelock, D. M. and Sanchez, Y. (2003). Regulation of Chk1 includes chromatin association and 14-3-3 binding following phosphorylation on Ser-345. *J Biol Chem* **278**, 25207-17.

Jin, J., Smith, F. D., Stark, C., Wells, C. D., Fawcett, J. P., Kulkarni, S., Metalnikov, P., O'Donnell, P., Taylor, P., Taylor, L. *et al.* (2004). Proteomic, functional, and domain-based analysis of in vivo 14-3-3 binding proteins involved in cytoskeletal regulation and cellular organization. *Curr Biol* **14**, 1436-50.

Johnsson, A., Xue-Franzen, Y., Lundin, M. and Wright, A. P. (2006). Stress-specific role of fission yeast Gcn5 histone acetyltransferase in programming a subset of stress response genes. *Eukaryot Cell* **5**, 1337-46.

Jones, D. H., Ley, S. and Aitken, A. (1995). Isoforms of 14-3-3 protein can form homo- and heterodimers in vivo and in vitro: implications for function as adapter proteins. *FEBS Lett* **368**, 55-8.

Jorgensen, P., Nelson, B., Robinson, M. D., Chen, Y., Andrews, B., Tyers, M. and Boone, C. (2002). High-resolution genetic mapping with ordered arrays of *Saccharomyces cerevisiae* deletion mutants. *Genetics* **162**, 1091-9.

Joubes, J., Chevalier, C., Dudits, D., Heberle-Bors, E., Inze, D., Umeda, M. and Renaudin, J. P. (2000). CDK-related protein kinases in plants. *Plant Mol Biol* **43**, 607-20.

Kaiser, P., Sia, R. A., Bardes, E. G., Lew, D. J. and Reed, S. I. (1998). Cdc34 and the F-box protein Met30 are required for degradation of the Cdk-inhibitory kinase Swe1. *Genes Dev* **12**, 2587-97.

Kanoh, J. and Russell, P. (1998). The protein kinase Cdr2, related to Nim1/Cdr1 mitotic inducer, regulates the onset of mitosis in fission yeast. *Mol Biol Cell* **9**, 3321-34.

Karlova, R., Boeren, S., Russinova, E., Aker, J., Vervoort, J. and de Vries, S. (2006). The *Arabidopsis* SOMATIC EMBRYOGENESIS RECEPTOR-LIKE KINASE1 protein complex includes BRASSINOSTEROID-INSENSITIVE1. *Plant Cell* **18**, 626-38.

Katayama, K., Fujita, N. and Tsuruo, T. (2005). Akt/protein kinase B-dependent phosphorylation and inactivation of WEE1Hu promote cell cycle progression at G2/M transition. *Mol Cell Biol* **25**, 5725-37.

Kellogg, D. R. (2003). Wee1-dependent mechanisms required for coordination of cell growth and cell division. *J Cell Sci* **116**, 4883-90.

Khadaroo, B., Robbens, S., Ferraz, C., Derelle, E., Eychenie, S., Cooke, R., Peaucellier, G., Delseny, M., Demaille, J., Van de Peer, Y. *et al.* (2004). The first green lineage cdc25 dual-specificity phosphatase. *Cell Cycle* **3**, 513-8.

Kishimoto, N. and Yamashita, I. (2000). Multiple pathways regulating fission yeast mitosis upon environmental stresses. *Yeast* **16**, 597-609.

Kolukisaoglu, U., Weinl, S., Blazevic, D., Batistic, O. and Kudla, J. (2004). Calcium sensors and their interacting protein kinases: genomics of the *Arabidopsis* and rice CBL-CIPK signaling networks. *Plant Physiol* **134**, 43-58.

Kong, L. J., Orozco, B. M., Roe, J. L., Nagar, S., Ou, S., Feiler, H. S., Durfee, T., Miller, A. B., Gruissem, W., Robertson, D. *et al.* (2000). A geminivirus replication protein interacts with the retinoblastoma protein through a novel domain to determine symptoms and tissue specificity of infection in plants. *EMBO J* **19**, 3485-95.

Krysan, P. J., Young, J. C. and Sussman, M. R. (1999). T-DNA as an insertional mutagen in *Arabidopsis*. *Plant Cell* **11**, 2283-90.

Krysan, P. J., Young, J. C., Tax, F. and Sussman, M. R. (1996). Identification of transferred DNA insertions within *Arabidopsis* genes involved in signal transduction and ion transport. *Proc Natl Acad Sci U S A* **93**, 8145-50.

Kumagai, A. and Dunphy, W. G. (1991). The cdc25 protein controls tyrosine dephosphorylation of the cdc2 protein in a cell-free system. *Cell* **64**, 903-14.

Kumagai, A. and Dunphy, W. G. (1999). Binding of 14-3-3 proteins and nuclear export control the intracellular localization of the mitotic inducer Cdc25. *Genes Dev* **13**, 1067-72.

Kumagai, A., Guo, Z., Emami, K. H., Wang, S. X. and Dunphy, W. G. (1998). The Xenopus Chk1 protein kinase mediates a caffeine-sensitive pathway of checkpoint control in cell-free extracts. *J Cell Biol* **142**, 1559-69.

Kuromori, T. and Yamamoto, M. (2000). Members of the *Arabidopsis* 14-3-3 gene family trans-complement two types of defects in fission yeast. *Plant Science* **158**, 155-161.

Kusano, T., Berberich, T., Harada, M., Suzuki, N. and Sugawara, K. (1995). A maize DNA-binding factor with a bZIP motif is induced by low temperature. *Mol Gen Genet* **248**, 507-17.

Landrieu, I., da Costa, M., De Veylder, L., Dewitte, F., Vandepoele, K., Hassan, S., Wieruszeski, J. M., Corellou, F., Faure, J. D., Van Montagu, M. *et al.* (2004). A small CDC25 dual-specificity tyrosine-phosphatase isoform in *Arabidopsis thaliana*. *Proc Natl Acad Sci U S A* **101**, 13380-5.

Latterich, M., Frohlich, K. U. and Schekman, R. (1995). Membrane fusion and the cell cycle: Cdc48p participates in the fusion of ER membranes. *Cell* **82**, 885-93.

Lee, J., Kumagai, A. and Dunphy, W. G. (2001). Positive regulation of Wee1 by Chk1 and 14-3-3 proteins. *Mol Biol Cell* **12**, 551-63.

Legrain, P., Dokhelar, M. C. and Transy, C. (1994). Detection of protein-protein interactions using different vectors in the two-hybrid system. *Nucleic Acids Res* **22**, 3241-2.

Lehmann, G. M. and McCabe, M. J., Jr. (2007). Arsenite slows S phase progression via inhibition of cdc25A dual specificity phosphatase gene transcription. *Toxicol Sci* **99**, 70-8.

Leise, W., 3rd and Mueller, P. R. (2002). Multiple Cdk1 inhibitory kinases regulate the cell cycle during development. *Dev Biol* **249**, 156-73.

Lew, D. J., Dulic, V. and Reed, S. I. (1991). Isolation of three novel human cyclins by rescue of G1 cyclin (Cln) function in yeast. *Cell* **66**, 1197-206.

Liu, D., Bienkowska, J., Petosa, C., Collier, R. J., Fu, H. and Liddington, R. (1995). Crystal structure of the zeta isoform of the 14-3-3 protein. *Nature* **376**, 191-4.

Liu, F., Stanton, J. J., Wu, Z. and Piwnica-Worms, H. (1997). The human Myt1 kinase preferentially phosphorylates Cdc2 on threonine 14 and localizes to the endoplasmic reticulum and Golgi complex. *Mol Cell Biol* **17**, 571-83.

Lopez-Girona, A., Kanoh, J. and Russell, P. (2001). Nuclear exclusion of Cdc25 is not required for the DNA damage checkpoint in fission yeast. *Curr Biol* **11**, 50-4.

Lu, G., DeLisle, A. J., de Vetten, N. C. and Ferl, R. J. (1992). Brain proteins in plants: an *Arabidopsis* homolog to neurotransmitter pathway activators is part of a DNA binding complex. *Proc Natl Acad Sci U S A* **89**, 11490-4.

Lu, G., Sehnke, P. C. and Ferl, R. J. (1994). Phosphorylation and calcium binding properties of an *Arabidopsis* GF14 brain protein homolog. *Plant Cell* **6**, 501-10.

Lui, H., Wang, H., Delong, C., Fowke, L. C., Crosby, W. L. and Fobert, P. R. (2000). The *Arabidopsis* Cdc2a-interacting protein ICK2 is structurally related to ICK1 and is a potent inhibitor of cyclin-dependent kinase activity in vitro. *Plant J* **21**, 379-85.

Lundgren, K., Walworth, N., Booher, R., Dembski, M., Kirschner, M. and Beach, D. (1991). mik1 and wee1 cooperate in the inhibitory tyrosine phosphorylation of cdc2. *Cell* **64**, 1111-22.

Ma, J. and Ptashne, M. (1987). A new class of yeast transcriptional activators. *Cell* **51**, 113-9.

Magyar, Z., Meszaros, T., Miskolczi, P., Deak, M., Feher, A., Brown, S., Kondorosi, E., Athanasiadis, A., Pongor, S., Bilgin, M. *et al.* (1997). Cell cycle phase specificity of putative cyclin-dependent kinase variants in synchronized alfalfa cells. *Plant Cell* **9**, 223-35.

Manak, M. S. and Ferl, R. J. (2007). Divalent cation effects on interactions between multiple *Arabidopsis* 14-3-3 isoforms and phosphopeptide targets. *Biochemistry* **46**, 1055-63.

Marrs, K. A. (1996). The Functions and Regulation of Glutathione S-Transferases in Plants. *Annu Rev Plant Physiol Plant Mol Biol* **47**, 127-158.

Masters, S. C., Pederson, K. J., Zhang, L., Barbieri, J. T. and Fu, H. (1999). Interaction of 14-3-3 with a nonphosphorylated protein ligand, exoenzyme S of *Pseudomonas aeruginosa*. *Biochemistry* **38**, 5216-21.

Masuda, T., Fusada, N., Oosawa, N., Takamatsu, K., Yamamoto, Y. Y., Ohto, M., Nakamura, K., Goto, K., Shibata, D., Shirano, Y. *et al.* (2003). Functional analysis of isoforms of NADPH: protochlorophyllide oxidoreductase (POR), PORB and PORC, in *Arabidopsis thaliana*. *Plant Cell Physiol* **44**, 963-74.

Matsuo, T., Yamaguchi, S., Mitsui, S., Emi, A., Shimoda, F. and Okamura, H. (2003). Control mechanism of the circadian clock for timing of cell division in vivo. *Science* **302**, 255-9.

Matsuoka, S., Huang, M. and Elledge, S. J. (1998). Linkage of ATM to cell cycle regulation by the Chk2 protein kinase. *Science* **282**, 1893-7.

Mazzurco, M., Sulaman, W., Elina, H., Cock, J. M. and Goring, D. R. (2001). Further analysis of the interactions between the Brassica S receptor kinase and three interacting proteins (ARC1, THL1 and THL2) in the yeast two-hybrid system. *Plant Mol Biol* **45**, 365-76.

McGowan, C. H. and Russell, P. (1995). Cell cycle regulation of human WEE1. *EMBO J* **14**, 2166-75.

McKibbin, R. S., Halford, N. G. and Francis, D. (1998). Expression of fission yeast cdc25 alters the frequency of lateral root formation in transgenic tobacco. *Plant Mol Biol* **36**, 601-12.

Meek, S. E., Lane, W. S. and Piwnica-Worms, H. (2004). Comprehensive proteomic analysis of interphase and mitotic 14-3-3-binding proteins. *J Biol Chem* **279**, 32046-54.

Menges, M., de Jager, S. M., Gruissem, W. and Murray, J. A. (2005). Global analysis of the core cell cycle regulators of *Arabidopsis* identifies novel genes, reveals multiple and highly specific profiles of expression and provides a coherent model for plant cell cycle control. *Plant J* **41**, 546-66.

Michael, W. M. and Newport, J. (1998). Coupling of mitosis to the completion of S phase through Cdc34-mediated degradation of Wee1. *Science* **282**, 1886-9.

Miller, J. (1972). Experiments in Molecular Genetics. New York, Cold Spring Harbor Laboratory Press.

Mironov, V. V., De Veylder, L., Van Montagu, M. and Inze, D. (1999). Cyclin-dependent kinases and cell division in plants- the nexus. *Plant Cell* **11**, 509-22.

Mitchison, J. M. (1971). The biology of the cell cycle. Cambridge, Cambridge University Press.

Moons, A. (2005). Regulatory and functional interactions of plant growth regulators and plant glutathione S-transferases (GSTs). *Vitam Horm* **72**, 155-202.

Moore, B. W. and Perez, V. J. (1967). Specific acid proteins in the nervous system. Englewood Cliffs, Prentice-Hall.

Moorhead, G., Douglas, P., Morrice, N., Scarabel, M., Aitken, A. and MacKintosh, C. (1996). Phosphorylated nitrate reductase from spinach leaves is inhibited by 14-3-3 proteins and activated by fusicoccin. *Curr Biol* **6**, 1104-13.

Morgan, D. O. (1997). Cyclin-dependent kinases: engines, clocks, and microprocessors. *Annu Rev Cell Dev Biol* **13**, 261-91.

Mueller, P. R., Coleman, T. R., Kumagai, A. and Dunphy, W. G. (1995). Myt1: a membrane-associated inhibitory kinase that phosphorylates Cdc2 on both threonine-14 and tyrosine-15. *Science* **270**, 86-90.

Murakami, H. and Nurse, P. (1999). Meiotic DNA replication checkpoint control in fission yeast. *Genes Dev* **13**, 2581-93.

Muslin, A. J., Tanner, J. W., Allen, P. M. and Shaw, A. S. (1996). Interaction of 14-3-3 with signaling proteins is mediated by the recognition of phosphoserine. *Cell* **84**, 889-97.

Muslin, A. J. and Xing, H. (2000). 14-3-3 proteins: regulation of subcellular localization by molecular interference. *Cell Signal* **12**, 703-9.

Nagata, T., Nemoto, Y. and Hasezewa, S. (1992). Tobacco BY-2 cell line as the 'HeLa' cell line in the cell biology of higher plants. *Int Rev Cytol* **132**, 1-30.

Nakagami, H., Sekine, M., Murakami, H. and Shinmyo, A. (1999). Tobacco retinoblastoma-related protein phosphorylated by a distinct cyclin-dependent kinase complex with Cdc2/cyclin D in vitro. *Plant J* **18**, 243-52.

Nakai, T., Kato, K., Shinmyo, A. and Sekine, M. (2006). *Arabidopsis* KRPs have distinct inhibitory activity toward cyclin D2-associated kinases, including plant-specific B-type cyclin-dependent kinase. *FEBS Lett* **580**, 336-40.

Nasmyth, K. (1993). Control of the yeast cell cycle by the Cdc28 protein kinase. *Curr Opin Cell Biol* **5**, 166-79.

Nigg, E. A. (1995). Cyclin-dependent protein kinases: key regulators of the eukaryotic cell cycle. *Bioessays* **17**, 471-80.

Novagen. (2006). Novagen His-Bind® Kit manual

Nurse, P. (1990). Universal control mechanism regulating onset of m-phase. *Nature* **344**, 503-508.

Nurse, P. (2000). A long twentieth century of the cell cycle and beyond. *Cell* **100**, 71-8.

Nurse, P., Thuriaux, P. and Nasmyth, K. (1976). Genetic control of the cell division cycle in the fission yeast *schizosaccharomyces pombe*. *Mol Gen Genet* **146**, 167-178.

O'Connell, M. J., Raleigh, J. M., Verkade, H. M. and Nurse, P. (1997). Chk1 is a wee1 kinase in the G2 DNA damage checkpoint inhibiting cdc2 by Y15 phosphorylation. *EMBO J* **16**, 545-54.

Obsil, T., Ghirlando, R., Klein, D. C., Ganguly, S. and Dyda, F. (2001). Crystal structure of the 14-3-3zeta:serotonin N-acetyltransferase complex. a role for scaffolding in enzyme regulation. *Cell* **105**, 257-67.

Ohad, N., Shichrur, K. and Yalovsky, S. (2007). The analysis of protein-protein interactions in plants by bimolecular fluorescence complementation. *Plant Physiol* **145**, 1090-9.

Ohta, M., Guo, Y., Halfter, U. and Zhu, J. K. (2003). A novel domain in the protein kinase SOS2 mediates interaction with the protein phosphatase 2C ABI2. *Proc Natl Acad Sci U S A* **100**, 11771-6.

Ohta, T., Okamoto, K., Isohashi, F., Shibata, K., Fukuda, M., Yamaguchi, S. and Xiong, Y. (1998). T-loop deletion of CDC2 from breast cancer tissues eliminates binding to cyclin B1 and cyclin-dependent kinase inhibitor p21. *Cancer Res* **58**, 1095-8.

Okamoto, K. and Sagata, N. (2007). Mechanism for inactivation of the mitotic inhibitory kinase Wee1 at M phase. *Proc Natl Acad Sci U S A* **104**, 3753-8.

Olivari, C., Albumi, C., Pugliarello, M. C. and De Michelis, M. I. (2000). Phenylarsine oxide inhibits the fusicoccin-induced activation of plasma membrane H(+)-ATPase. *Plant Physiol* **122**, 463-70.

Orchard, C. B., Siciliano, I., Sorrell, D. A., Marchbank, A., Rogers, H. J., Francis, D., Herbert, R. J., Suchomelova, P., Lipavska, H., Azmi, A. *et al.* (2005). Tobacco BY-2 cells expressing fission yeast cdc25 bypass a G2/M block on the cell cycle. *Plant J* **44**, 290-9.

Ouellet, F., Overvoorde, P. J. and Theologis, A. (2001). IAA17/AXR3: biochemical insight into an auxin mutant phenotype. *Plant Cell* **13**, 829-41.

Ouyang, B., Li, W., Pan, H., Meadows, J., Hoffmann, I. and Dai, W. (1999). The physical association and phosphorylation of Cdc25C protein phosphatase by Prk. *Oncogene* **18**, 6029-36.

Pan, S., Sehnke, P. C., Ferl, R. J. and Gurley, W. B. (1999). Specific interactions with TBP and TFIIB in vitro suggest that 14-3-3 proteins may participate in the regulation of transcription when part of a DNA binding complex. *Plant Cell* **11**, 1591-602.

Parker, L. L. and Piwnica-Worms, H. (1992). Inactivation of the p34cdc2-cyclin B complex by the human WEE1 tyrosine kinase. *Science* **257**, 1955-7.

Parker, L. L., Walter, S. A., Young, P. G. and Piwnica-Worms, H. (1993). Phosphorylation and inactivation of the mitotic inhibitor Wee1 by the nim1/cdr1 kinase. *Nature* **363**, 736-8.

Patra, D., Wang, S. X., Kumagai, A. and Dunphy, W. G. (1999). The xenopus Suc1/Cks protein promotes the phosphorylation of G(2)/M regulators. *J Biol Chem* **274**, 36839-42.

Paul, A. L., Sehnke, P. C. and Ferl, R. J. (2005). Isoform-specific subcellular localization among 14-3-3 proteins in *Arabidopsis* seems to be driven by client interactions. *Mol Biol Cell* **16**, 1735-43.

Peng, C. Y., Graves, P. R., Thoma, R. S., Wu, Z., Shaw, A. S. and Piwnica-Worms, H. (1997). Mitotic and G2 checkpoint control: regulation of 14-3-3 protein binding by phosphorylation of Cdc25C on serine-216. *Science* **277**, 1501-5.

Pines, J. (1995). Cyclins and cyclin-dependent kinases: a biochemical view. *Biochem J* **308 (Pt 3)**, 697-711.

Pines, J. (1999). Four-dimensional control of the cell cycle. *Nat Cell Biol* **1**, E73-9.

Porceddu, A., Stals, H., Reichheld, J. P., Segers, G., De Veylder, L., Barroco, R. P., Casteels, P., Van Montagu, M., Inze, D. and Mironov, V. (2001). A plant-specific cyclin-dependent kinase is involved in the control of G2/M progression in plants. *J Biol Chem* **276**, 36354-60.

Pozuelo Rubio, M., Geraghty, K. M., Wong, B. H., Wood, N. T., Campbell, D. G., Morrice, N. and Mackintosh, C. (2004). 14-3-3-affinity purification of over 200 human phosphoproteins reveals new links to regulation of cellular metabolism, proliferation and trafficking. *Biochem J* **379**, 395-408.

Price, D., Rabinovitch, S., O'Farrell, P. H. and Campbell, S. D. (2000). *Drosophila* wee1 has an essential role in the nuclear divisions of early embryogenesis. *Genetics* **155**, 159-66.

QIAGEN. (06/02). QIAquick® Spin handbook.

QIAGEN. (07/05). QIAprep® miniprep handbook.

QIAGEN. (11/05). QIAGEN® plasmid purification handbook.

Rancour, D. M., Dickey, C. E., Park, S. and Bednarek, S. Y. (2002). Characterization of AtCDC48. Evidence for multiple membrane fusion mechanisms at the plane of cell division in plants. *Plant Physiol* **130**, 1241-53.

Renaudin, J. P., Doonan, J. H., Freeman, D., Hashimoto, J., Hirt, H., Inze, D., Jacobs, T., Kouchi, H., Rouze, P., Sauter, M. *et al.* (1996). Plant cyclins: a unified nomenclature for plant A-, B- and D-type cyclins based on sequence organization. *Plant Mol Biol* **32**, 1003-18.

Rhind, N. and Russell, P. (2000). Chk1 and Cds1: linchpins of the DNA damage and replication checkpoint pathways. *J Cell Sci* **113 (Pt 22)**, 3889-96.

Rienties, I. M., Vink, J., Borst, J. W., Russinova, E. and de Vries, S. C. (2005). The *Arabidopsis* SERK1 protein interacts with the AAA-ATPase AtCDC48, the 14-3-3 protein GF14lambda and the PP2C phosphatase KAPP. *Planta* **221**, 394-405.

Rittinger, K., Budman, J., Xu, J., Volinia, S., Cantley, L. C., Smerdon, S. J., Gamblin, S. J. and Yaffe, M. B. (1999). Structural analysis of 14-3-3 phosphopeptide complexes identifies a dual role for the nuclear export signal of 14-3-3 in ligand binding. *Mol Cell* **4**, 153-66.

Roberts, M. R. (2003). 14-3-3 proteins find new partners in plant cell signalling. *Trends Plant Sci* **8**, 218-23.

Roberts, M. R. and Bowles, D. J. (1999). Fusicoccin, 14-3-3 proteins, and defense responses in tomato plants. *Plant Physiol* **119**, 1243-50.

Rook, F., Gerrits, N., Kortstee, A., van Kampen, M., Borrias, M., Weisbeek, P. and Smeekens, S. (1998). Sucrose-specific signalling represses translation of the *Arabidopsis* ATB2 bZIP transcription factor gene. *Plant J* **15**, 253-63.

Rosenquist, M., Alsterfjord, M., Larsson, C. and Sommarin, M. (2001). Data mining the *Arabidopsis* genome reveals fifteen 14-3-3 genes. Expression is demonstrated for two out of five novel genes. *Plant Physiol* **127**, 142-9.

Rosenquist, M., Sehnke, P., Ferl, R. J., Sommarin, M. and Larsson, C. (2000). Evolution of the 14-3-3 protein family: does the large number of isoforms in multicellular organisms reflect functional specificity? *J Mol Evol* **51**, 446-58.

Rossignol, P., Collier, S., Bush, M., Shaw, P. and Doonan, J. H. (2007). *Arabidopsis* POT1A interacts with TERT-V(I8), an N-terminal splicing variant of telomerase. *J Cell Sci* **120**, 3678-87.

Rosso, M. G., Li, Y., Strizhov, N., Reiss, B., Dekker, K. and Weisshaar, B. (2003). An *Arabidopsis thaliana* T-DNA mutagenized population (GABI-Kat) for flanking sequence tag-based reverse genetics. *Plant Mol Biol* **53**, 247-59.

Rothblum-Oviatt, C. J., Ryan, C. E. and Piwnica-Worms, H. (2001). 14-3-3 binding regulates catalytic activity of human Wee1 kinase. *Cell Growth Differ* **12**, 581-9.

Ruohonen, L., Penttila, M. and Keranen, S. (1991). Optimization of Bacillus alpha-amylase production by *Saccharomyces cerevisiae*. *Yeast* **7**, 337-46.

Russell, P. and Nurse, P. (1987). Negative regulation of mitosis by wee1+, a gene encoding a protein kinase homolog. *Cell* **49**, 559-67.

Sabatini, S., Heidstra, R., Wildwater, M. and Scheres, B. (2003). SCARECROW is involved in positioning the stem cell niche in the *Arabidopsis* root meristem. *Genes Dev* **17**, 354-8.

Sambrook, J. and Russell, D. W. (2001). Molecular Cloning: A Laboratory Manual. New York, Cold Spring Harbor Laboratory Press.

Sanchez, I. and Dynlacht, B. D. (2005). New insights into cyclins, CDKs, and cell cycle control. *Semin Cell Dev Biol* **16**, 311-21.

Sanchez, Y., Wong, C., Thoma, R. S., Richman, R., Wu, Z., Piwnica-Worms, H. and Elledge, S. J. (1997). Conservation of the Chk1 checkpoint pathway in mammals: linkage of DNA damage to Cdk regulation through Cdc25. *Science* **277**, 1497-501.

Santangelo, G. M. and Tornow, J. (1990). Efficient transcription of the glycolytic gene ADH1 and three translational component genes requires the GCR1 product, which can act through TUF/GRF/RAP binding sites. *Mol Cell Biol* **10**, 859-62.

Schagger, H. and von Jagow, G. (1987). Tricine-sodium dodecyl sulfate-polyacrylamide gel electrophoresis for the separation of proteins in the range from 1 to 100 kDa. *Anal Biochem* **166**, 368-79.

Schwab, R., Ossowski, S., Riester, M., Warthmann, N. and Weigel, D. (2006). Highly specific gene silencing by artificial microRNAs in *Arabidopsis*. *Plant Cell* **18**, 1121-33.

Segers, G., Gadisseur, I., Bergounioux, C., de Almeida Engler, J., Jacqmard, A., Van Montagu, M. and Inze, D. (1996). The *Arabidopsis* cyclin-dependent kinase gene cdc2bAt is preferentially expressed during S and G2 phases of the cell cycle. *Plant J* **10**, 601-12.

Sehnke, P. C., Chung, H. J., Wu, K. and Ferl, R. J. (2001). Regulation of starch accumulation by granule-associated plant 14-3-3 proteins. *Proc Natl Acad Sci U S A* **98**, 765-70.

Sehnke, P. C., DeLille, J. M. and Ferl, R. J. (2002a). Consummating signal transduction: the role of 14-3-3 proteins in the completion of signal-induced transitions in protein activity. *Plant Cell* **14 Suppl**, S339-54.

Sehnke, P. C., Henry, R., Cline, K. and Ferl, R. J. (2000). Interaction of a plant 14-3-3 protein with the signal peptide of a thylakoid-targeted chloroplast precursor protein and the presence of 14-3-3 isoforms in the chloroplast stroma. *Plant Physiol* **122**, 235-42.

Sehnke, P. C., Rosenquist, M., Alsterfjord, M., DeLille, J., Sommarin, M., Larsson, C. and Ferl, R. J. (2002b). Evolution and isoform specificity of plant 14-3-3 proteins. *Plant Mol Biol* **50**, 1011-8.

Sgarlata, C. and Perez-Martin, J. (2005). The cdc25 phosphatase is essential for the G2/M phase transition in the basidiomycete yeast *Ustilago maydis*. *Mol Microbiol* **58**, 1482-96.

Shikano, S., Coblitz, B., Sun, H. and Li, M. (2005). Genetic isolation of transport signals directing cell surface expression. *Nat Cell Biol* **7**, 985-92.

Shimotohno, A., Matsubayashi, S., Yamaguchi, M., Uchimiya, H. and Umeda, M. (2003). Differential phosphorylation activities of CDK-activating kinases in *Arabidopsis thaliana*. *FEBS Lett* **534**, 69-74.

Shimotohno, A., Ohno, R., Bisova, K., Sakaguchi, N., Huang, J., Koncz, C., Uchimiya, H. and Umeda, M. (2006). Diverse phosphoregulatory mechanisms controlling cyclin-dependent kinase-activating kinases in *Arabidopsis*. *Plant J* **47**, 701-10.

Shimotohno, A., Umeda-Hara, C., Bisova, K., Uchimiya, H. and Umeda, M. (2004). The plant-specific kinase CDKF;1 is involved in activating phosphorylation of cyclin-dependent kinase-activating kinases in *Arabidopsis*. *Plant Cell* **16**, 2954-66.

Sia, R. A., Bardes, E. S. and Lew, D. J. (1998). Control of Swe1p degradation by the morphogenesis checkpoint. *EMBO J* **17**, 6678-88.

Siciliano, I. (2006). Effect of the plant WEE1 on the cell cycle and development in *Arabidopsis thaliana* and *Nicotiana tabacum*. PhD thesis, School of Biosciences, Cardiff, Cardiff University.

Soni, R., Carmichael, J. P., Shah, Z. H. and Murray, J. A. (1995). A family of cyclin D homologs from plants differentially controlled by growth regulators and containing the conserved retinoblastoma protein interaction motif. *Plant Cell* **7**, 85-103.

Sorrell, D. A., Chrimes, D., Dickinson, J. R., Rogers, H. J. and Francis, D. (2005). The *Arabidopsis* CDC25 induces a short cell length when overexpressed in fission yeast: evidence for cell cycle function. *New Phytol* **165**, 425-8.

Sorrell, D. A., Combettes, B., Chaubet-Gigot, N., Gigot, C. and Murray, J. A. (1999). Distinct cyclin D genes show mitotic accumulation or constant levels of transcripts in tobacco bright yellow-2 cells. *Plant Physiol* **119**, 343-52.

Sorrell, D. A., Marchbank, A., McMahon, K., Dickinson, J. R., Rogers, H. J. and Francis, D. (2002). A WEE1 homologue from *Arabidopsis thaliana*. *Planta* **215**, 518-22.

Sorrell, D. A., Marchbank, A. M., Chrimes, D. A., Dickinson, J. R., Rogers, H. J., Francis, D., Grierson, C. S. and Halford, N. G. (2003). The *Arabidopsis* 14-3-3 protein, GF14omega, binds to the *Schizosaccharomyces pombe* Cdc25 phosphatase and rescues checkpoint defects in the rad24- mutant. *Planta* **218**, 50-7.

Sorrell, D. A., Menges, M., Healy, J. M., Deveaux, Y., Amano, C., Su, Y., Nakagami, H., Shinmyo, A., Doonan, J. H., Sekine, M. *et al.* (2001). Cell cycle regulation of cyclin-dependent kinases in tobacco cultivar Bright Yellow-2 cells. *Plant Physiol* **126**, 1214-23.

Squire, C. J., Dickson, J. M., Ivanovic, I. and Baker, E. N. (2005). Structure and inhibition of the human cell cycle checkpoint kinase, Wee1A kinase: an atypical tyrosine kinase with a key role in CDK1 regulation. *Structure* **13**, 541-50.

Stolpe, T., Susslin, C., Marrocco, K., Nick, P., Kretsch, T. and Kircher, S. (2005). *In planta* analysis of protein-protein interactions related to light signaling by bimolecular fluorescence complementation. *Protoplasma* **226**, 137-46.

Stratagene. (07/06). HybriZap 2.1® two hybrid undigested vector kit.

Stratagene. (12/05). pESC® yeast epitope tagging vector kit.

Stratagene. (2007). QuickChange® Site-Directed Mutagenesis Kit.

Stumpff, J., Kellogg, D. R., Krohne, K. A. and Su, T. T. (2005). *Drosophila* Weel interacts with members of the gammaTURC and is required for proper mitotic-spindle morphogenesis and positioning. *Curr Biol* **15**, 1525-34.

Suda, M., Yamada, S., Toda, T., Miyakawa, T. and Hirata, D. (2000). Regulation of Weel kinase in response to protein synthesis inhibition. *FEBS Lett* **486**, 305-9.

Sun, Y., Dilkes, B. P., Zhang, C., Dante, R. A., Carneiro, N. P., Lowe, K. S., Jung, R., Gordon-Kamm, W. J. and Larkins, B. A. (1999). Characterization of maize (*Zea mays L.*) Weel and its activity in developing endosperm. *Proc Natl Acad Sci U S A* **96**, 4180-5.

Suzuki, T., Nakajima, S., Inagaki, S., Hirano-Nakakita, M., Matsuoka, K., Demura, T., Fukuda, H., Morikami, A. and Nakamura, K. (2005a). TONSOKU is expressed in S phase of the cell cycle and its defect delays cell cycle progression in *Arabidopsis*. *Plant Cell Physiol* **46**, 736-42.

Suzuki, T., Nakajima, S., Morikami, A. and Nakamura, K. (2005b). An *Arabidopsis* protein with a novel calcium-binding repeat sequence interacts with TONSOKU/MGOUN3/BRUSHY1 involved in meristem maintenance. *Plant Cell Physiol* **46**, 1452-61.

Tang, Z., Coleman, T. R. and Dunphy, W. G. (1993). Two distinct mechanisms for negative regulation of the Weel protein kinase. *EMBO J* **12**, 3427-36.

Tassan, J. P., Jaquenoud, M., Fry, A. M., Frutiger, S., Hughes, G. J. and Nigg, E. A. (1995). In vitro assembly of a functional human CDK7-cyclin H complex requires MAT1, a novel 36 kDa RING finger protein. *EMBO J* **14**, 5608-17.

Tominaga, Y., Li, C., Wang, R. H. and Deng, C. X. (2006). Murine weel plays a critical role in cell cycle regulation and pre-implantation stages of embryonic development. *Int J Biol Sci* **2**, 161-70.

Torres Acosta, J. A., de Almeida Engler, J., Raes, J., Magyar, Z., De Groodt, R., Inze, D. and De Veylder, L. (2004). Molecular characterization of *Arabidopsis* PHO80-like proteins, a novel class of CDKA;1-interacting cyclins. *Cell Mol Life Sci* **61**, 1485-97.

Tzivion, G., Shen, Y. H. and Zhu, J. (2001). 14-3-3 proteins; bringing new definitions to scaffolding. *Oncogene* **20**, 6331-8.

Uchida, S., Kubo, A., Kizu, R., Nakagama, H., Matsunaga, T., Ishizaka, Y. and Yamashita, K. (2006). Amino acids C-terminal to the 14-3-3 binding motif in CDC25B affect the efficiency of 14-3-3 binding. *J Biochem* **139**, 761-9.

Uchida, S., Kuma, A., Ohtsubo, M., Shimura, M., Hirata, M., Nakagama, H., Matsunaga, T., Ishizaka, Y. and Yamashita, K. (2004). Binding of 14-3-3beta but not 14-3-3sigma controls the cytoplasmic localization of CDC25B: binding site preferences of 14-3-3 subtypes and the subcellular localization of CDC25B. *J Cell Sci* **117**, 3011-20.

Umeda, M., Shimotohno, A. and Yamaguchi, M. (2005). Control of cell division and transcription by cyclin-dependent kinase-activating kinases in plants. *Plant Cell Physiol* **46**, 1437-42.

Umen, J. G. and Goodenough, U. W. (2001). Control of cell division by a retinoblastoma protein homolog in *Chlamydomonas*. *Genes Dev* **15**, 1652-61.

Van't Hof, J. (1973). The regulation of cell division in higher plants. In *Brookhaven Synposium*, vol. 25, 152-165. Upton, New York, USA.

Van Criekinge, K. and Beyaert, R. (1999). Yeast Two-Hybrid: State of the Art. *Biol Proced Online* **2**, 1-38.

van Heusden, G. P., van der Zanden, A. L., Ferl, R. J. and Steensma, H. Y. (1996). Four *Arabidopsis thaliana* 14-3-3 protein isoforms can complement the lethal yeast *bmh1 bmh2* double disruption. *FEBS Lett* **391**, 252-6.

Vandepoele, K., Raes, J., De Veylder, L., Rouze, P., Rombauts, S. and Inze, D. (2002). Genome-wide analysis of core cell cycle genes in *Arabidopsis*. *Plant Cell* **14**, 903-16.

Verkest, A., Weinl, C., Inze, D., De Veylder, L. and Schnittger, A. (2005). Switching the cell cycle. Kip-related proteins in plant cell cycle control. *Plant Physiol* **139**, 1099-106.

Wagner, U., Edwards, R., Dixon, D. P. and Mauch, F. (2002). Probing the diversity of the *Arabidopsis* glutathione S-transferase gene family. *Plant Mol Biol* **49**, 515-32.

Walter, M., Chaban, C., Schutze, K., Batistic, O., Weckermann, K., Nake, C., Blazevic, D., Grefen, C., Schumacher, K., Oecking, C. *et al.* (2004). Visualization of protein interactions in living plant cells using bimolecular fluorescence complementation. *Plant J* **40**, 428-38.

Walter, S. A., Guadagno, S. N. and Ferrell, J. E., Jr. (2000). Activation of Wee1 by p42 MAPK in vitro and in cycling xenopus egg extracts. *Mol Biol Cell* **11**, 887-96.

Walworth, N., Davey, S. and Beach, D. (1993). Fission yeast chk1 protein kinase links the rad checkpoint pathway to cdc2. *Nature* **363**, 368-71.

Wang, B., Yang, H., Liu, Y. C., Jelinek, T., Zhang, L., Ruoslahti, E. and Fu, H. (1999). Isolation of high-affinity peptide antagonists of 14-3-3 proteins by phage display. *Biochemistry* **38**, 12499-504.

Wang, G., Kong, H., Sun, Y., Zhang, X., Zhang, W., Altman, N., DePamphilis, C. W. and Ma, H. (2004). Genome-wide analysis of the cyclin family in *Arabidopsis* and comparative phylogenetic analysis of plant cyclin-like proteins. *Plant Physiol* **135**, 1084-99.

Wang, H., Fowke, L. C. and Crosby, W. L. (1997). A plant cyclin-dependent kinase inhibitor gene. *Nature* **386**, 451-2.

Wang, H., Qi, Q., Schorr, P., Cutler, A. J., Crosby, W. L. and Fowke, L. C. (1998). ICK1, a cyclin-dependent protein kinase inhibitor from *Arabidopsis thaliana* interacts with both Cdc2a and CycD3, and its expression is induced by abscisic acid. *Plant J* **15**, 501-10.

Wang, R., He, G., Nelman-Gonzalez, M., Ashorn, C. L., Gallick, G. E., Stukenberg, P. T., Kirschner, M. W. and Kuang, J. (2007). Regulation of Cdc25C by ERK-MAP kinases during the G2/M transition. *Cell* **128**, 1119-32.

Wang, W. and Shakes, D. C. (1996). Molecular evolution of the 14-3-3 protein family. *J Mol Evol* **43**, 384-98.

Wang, Y., Jacobs, C., Hook, K. E., Duan, H., Booher, R. N. and Sun, Y. (2000). Binding of 14-3-3beta to the carboxyl terminus of Wee1 increases Wee1 stability, kinase activity, and G2-M cell population. *Cell Growth Differ* **11**, 211-9.

Watanabe, N., Arai, H., Iwasaki, J., Shiina, M., Ogata, K., Hunter, T. and Osada, H. (2005). Cyclin-dependent kinase (CDK) phosphorylation destabilizes somatic Wee1 via multiple pathways. *Proc Natl Acad Sci U S A* **102**, 11663-8.

Watanabe, N., Arai, H., Nishihara, Y., Taniguchi, M., Hunter, T. and Osada, H. (2004). M-phase kinases induce phospho-dependent ubiquitination of somatic Wee1 by SCFbeta-TrCP. *Proc Natl Acad Sci U S A* **101**, 4419-24.

Weinert, T. (1998). DNA damage checkpoints update: getting molecular. *Curr Opin Genet Dev* **8**, 185-93.

Wilker, E. W., Grant, R. A., Artim, S. C. and Yaffe, M. B. (2005). A structural basis for 14-3-3sigma functional specificity. *J Biol Chem* **280**, 18891-8.

Woodman, P. G. (2003). p97, a protein coping with multiple identities. *J Cell Sci* **116**, 4283-90.

Wu, K., Lu, G., Sehnke, P. and Ferl, R. J. (1997a). The heterologous interactions among plant 14-3-3 proteins and identification of regions that are important for dimerization. *Arch Biochem Biophys* **339**, 2-8.

Wu, K., Rooney, M. F. and Ferl, R. J. (1997b). The *Arabidopsis* 14-3-3 multigene family. *Plant Physiol* **114**, 1421-31.

Wu, L. and Russell, P. (1993). Nim1 kinase promotes mitosis by inactivating Wee1 tyrosine kinase. *Nature* **363**, 738-41.

Wu, L., Shiozaki, K., Aligue, R. and Russell, P. (1996). Spatial organization of the Nim1-Wee1-Cdc2 mitotic control network in *Schizosaccharomyces pombe*. *Mol Biol Cell* **7**, 1749-58.

Xie, Z., Zhang, Z. L., Zou, X., Yang, G., Komatsu, S. and Shen, Q. J. (2006). Interactions of two abscisic-acid induced WRKY genes in repressing gibberellin signaling in aleurone cells. *Plant J* **46**, 231-42.

Yaffe, M. B. (2002). How do 14-3-3 proteins work?-- Gatekeeper phosphorylation and the molecular anvil hypothesis. *FEBS Lett* **513**, 53-7.

Yaffe, M. B., Rittinger, K., Volinia, S., Caron, P. R., Aitken, A., Leffers, H., Gamblin, S. J., Smerdon, S. J. and Cantley, L. C. (1997). The structural basis for 14-3-3:phosphopeptide binding specificity. *Cell* **91**, 961-71.

Yamaguchi, M., Fabian, T., Sauter, M., Bhalerao, R. P., Schrader, J., Sandberg, G., Umeda, M. and Uchimiya, H. (2000). Activation of CDK-activating kinase is dependent on interaction with H-type cyclins in plants. *Plant J* **24**, 11-20.

Yang, J., Winkler, K., Yoshida, M. and Kornbluth, S. (1999). Maintenance of G2 arrest in the Xenopus oocyte: a role for 14-3-3-mediated inhibition of Cdc25 nuclear import. *EMBO J* **18**, 2174-83.

Zachos, G., Rainey, M. D. and Gillespie, D. A. (2003). Chk1-deficient tumour cells are viable but exhibit multiple checkpoint and survival defects. *EMBO J* **22**, 713-23.

Zeng, Y. and Piwnica-Worms, H. (1999). DNA damage and replication checkpoints in fission yeast require nuclear exclusion of the Cdc25 phosphatase via 14-3-3 binding. *Mol Cell Biol* **19**, 7410-9.

Zhang, S. H., Kobayashi, R., Graves, P. R., Piwnica-Worms, H. and Tonks, N. K. (1997). Serine phosphorylation-dependent association of the band 4.1-related protein-tyrosine phosphatase PTPH1 with 14-3-3beta protein. *J Biol Chem* **272**, 27281-7.

Zhang, S. H., Liu, J., Kobayashi, R. and Tonks, N. K. (1999). Identification of the cell cycle regulator VCP (p97/CDC48) as a substrate of the band 4.1-related protein-tyrosine phosphatase PTPH1. *J Biol Chem* **274**, 17806-12.

Zheng, L., Baumann, U. and Reymond, J. L. (2004). An efficient one-step site-directed and site-saturation mutagenesis protocol. *Nucleic Acids Res* **32**, e115.

Zhong, R., Kays, S. J., Schroeder, B. P. and Ye, Z. H. (2002). Mutation of a chitinase-like gene causes ectopic deposition of lignin, aberrant cell shapes, and overproduction of ethylene. *Plant Cell* **14**, 165-79.

Appendix A

Alignments

A. thaliana 14-3-3 proteins

Protein sequences of the *A. thaliana* 14-3-3 proteins were obtained from the NCBI database (http://www.ncbi.nlm.nih.gov). Non-Epsilon 14-3-3 proteins: At14-3-3 omega [AAA96253], At14-3-3 lambda [AAD51781], At14-3-3 kappa [AAD51783], At14-3-3 chi [AAA96254], At14-3-3 phi [AAB62224], At14-3-3 psi [AAA96252], At14-3-3 upsilon [AAB62225], At14-3-3 nu [AAD51783]. Epsilon 14-3-3 proteins: At14-3-3 omicron [AAG47840], At14-3-3 epsilon [AAD51785], At14-3-3 mu [AAD51784], At14-3-3 iota [AAK11271], At14-3-3 pi [AAO38438]. The alignment was made in Workbench (http://www.workbench.sdsc.edu) using the Clustal W alignment tool with conserved residues (blue and *), conserved strong group residues (green and :). Black residues are residues with no consensus.

```
At14-3-3omega          ------MASGREEFVYMAKLAEQAERYEEMVEFMEKVSA-AVDGDELTVEERNLLSVAYK 53
At14-3-3lambda         ----MAATLGRDQYVYMAKLAEQAERYEEMVQFMEQLVTGATPAEELTVEERNLLSVAYK 56
At14-3-3kappa          ----MATTLSRDQYVYMAKLAEQAERYEEMVQFMEQLVSGATPAGELTVEERNLLSGAYK 56
At14-3-3chi            -MATPGASSARDEFVYMAKLAEQAERYEEMVEFMEKVAK-AVDKDELTVEERNLLSVAYK 58
At14-3-3phi            MAAPPASSSAREEFVYLAKLAEQAERYEEMVEFMEKVAE-AVDKDELTVEERNLLSVAYK 59
At14-3-3psi            ----MS---TREENVYMAKLAEQAERYEEMVEFMEKVAK-TVDVEELSVEERNLLSVAYK 52
At14-3-3upsilon        ----MSSDSSREENVYLAKLAEQAERYEEMVEFMEKVAK-TVETEELTVEERNLLSVAYK 55
At14-3-3nu             ----MS--SSREENVYLAKLAEQAERYEEMVEFMEKVAK-TVDTDELTVEERNLLSVAYK 53
At14-3-3omicron        ------MENERAKQVYLAKLNEQAERYDEMVEAMKKVAA---LDVELTIEERNLLSVGYK 51
At14-3-3epsilon        ------MENEREKQVYLAKLSEQTERYDEMVEAMKKVAQ---LDVELTVEERNLVSVGYK 51
At14-3-3mu             ----MGSGKERDTFVYLAKLSEQAERYEEMVESMKSVAK---LNVDLTVEERNLLSVGYK 53
At14-3-3iota           -MSSSGSDKERETFVYMAKLSEQAERYDEMVETMKKVAR---VNSELTVEERNLLSVGYK 56
At14-3-3pi             ------MENEREKLIYLAKLGCQAGRYDDVMKSMRKVCE---LDIELSEEERDLLTTGYK 51
                                *   :*:***  *: **::::: *..:         :*: ***:*:: .**

At14-3-3omega          NVIGARRASWRIISSIEQKEESRGNDDHVTAIREYRSKIETELSGICDGILKLLDSRLIP 113
At14-3-3lambda         NVIGSLRAAWRIVSSIEQKEESRKNDEHVSLVKDYRSKVESELSSVCSGILKLLDSHLIP 116
At14-3-3kappa          NVIGSLRAAWRIVSSLEQKEESRKNEEHVSLVKDYRSKVETELSSICSGILRLLDSHLIP 116
At14-3-3chi            NVIGARRASWRIISSIEQKEESRGNDDHVSLIRDYRSKIETELSDICDGILKLLDTILVP 118
At14-3-3phi            NVIGARRASWRIISSIEQKEESRGNDDHVTTIRDYRSKIESELSKICDGILKLLDTRLVP 119
At14-3-3psi            NVIGARRASWRIISSIEQKEESKGNEDHVAIIKDYRGEIESELSKICDGILNVLEAHLIP 112
At14-3-3upsilon        NVIGARRASWRIISSIEQKEDSRGNSDHVSIIKDYRGKIETELSKICDGILNLLEAHLIP 115
At14-3-3nu             NVIGARRASWRIISSIEQKEESRGNDDHVSIIKDYRGKIETELSKICDGILNLLDSHLVP 113
At14-3-3omicron        NVIGARRASWRILSSIEQKEESKGNEQNAKRIKDYRTKVEEELSKICYDILAVIDKHLVP 111
At14-3-3epsilon        NVIGARRASWRILSSIEQKEESKGNDENVKRLKNYRKRVEDELAKVCNDILSVIDKHLIP 111
At14-3-3mu             NVIGSRRASWRIFSSIEQKEAVKGNDVNVKRIKEYMEKVELELSNICIDIMSVLDEHLIP 113
At14-3-3iota           NVIGARRASWRIMSSIEQKEESKGNESNVKQIKGYRQKVEDELANICQDILTIIDQHLIP 116
At14-3-3pi             NVMEAKRVSLRVISSIEKMEDSKGNDQNVKLIKGQQEMVKYEFFNVCNDILSLIDSHLIP 111
                       **: : *.: *:.**:*: *  : *. :.  ::     :: *:  :* .*: :::  *:*

At14-3-3omega          AAAS-GDSKVFYLKMKGDYHRYLAEFKTGQERKDAAEHTLAAYKSAQDIANAELAPTHPI 172
At14-3-3lambda         SAGA-SESKVFYLKMKGDYHRYMAEFKSGDERKTAAEDTMLAYKAAQDIAAADMAPTHPI 175
At14-3-3kappa          SATA-RESKVFYLKMKGDYHRYLAEFKSGDERKTAAEDAMIAYKAAQDVAVADLAPTHPI 175
At14-3-3chi            AAAS-GDSKVFYLKMKGDYHRYLAEFKSGQERKDAAEHTLTAYKAAQDIANSELAPTHPI 177
At14-3-3phi            ASAN-GDSKVFYLKMKGDYHRYLAEFKTGQERKDAAEHTLTAYKAAQDIANAELAPTHPI 178
At14-3-3psi            SASP-AESKVFYLKMKGDYHRYLAEFKAGAERKEAAESTLVAYKSASDIATAELAPTHPI 173
At14-3-3upsilon        AASL-AESKVFYLKMKGDYHRYLAEFKTGAERKEAAESTLVAYKSAQDIALADLAPTHPI 174
At14-3-3nu             TASL-AESKVFYLKMKGDYHRYLAEFKTGAERKEAAESTLVAYKSAQDIALADLAPTHPI 172
At14-3-3omicron        FATS-GESTVFYYKMKGDYFRYLAEFKSGADREEAADLSLKAYEAATSSASTELSTTHPI 170
At14-3-3epsilon        SSNA-VESTVFFYKMKGDYYRYLAEFSSGAERKEAADQSLEAYKAAVAAAENGLAPTHPV 170
At14-3-3mu             SASE-GESTVFFNKMKGDYYRYLAEFKSGNERKEAADQSLKAYEIATTAAEAKLPPTHPI 172
At14-3-3iota           HATS-GEATVFYYKMKGDYYRYLAEFKTEQERKEAAEQSLKGYEAATQAASTELPSTHPI 175
At14-3-3pi             STTTNVESIVLFNRVKGDYFRYMAEFGSDAERKENADNSLDAYKVAMEMAENSLVPTNMV 170
                        :    :: *:: ::****.**:*** :  :*:  *: :: .*: *   *   : .*: :
```

```
At14-3-3omega       RLGLALNFSVFYYEILNSPDRACNLAKQAFDEAIAELDTLGEESYKDSTLIMQLLRDNLT 232
At14-3-3lambda      RLGLALNFSVFYYEILNSSDKACNMAKQAFEEAIAELDTLGEESYKDSTLIMQLLRDNLT 235
At14-3-3kappa       RLGLALNFSVFYYEILNSSEKACSMAKQAFEEAIAELDTLGEESYKDSTLIMQLLRDNLT 235
At14-3-3chi         RLGLALNFSVFYYEILNSPDRACNLAKQAFDEAIAELDTLGEESYKDSTLIMQLLRDNLT 237
At14-3-3phi         RLGLALNFSVFYYEILNSPDRACNLAKQAFDEAIAELDTLGEESYKDSTLIMQLLRDNLT 238
At14-3-3psi         RLGLALNFSVFYYEILNSPDRACSLAKQAFDDAIAELDTLGEESYKDSTLIMQLLRDNLT 233
At14-3-3upsilon     RLGLALNFSVFYYEILNSSDRACSLAKQAFDEAISELDTLGEESYKDSTLIMQLLRDNLT 234
At14-3-3nu          RLGLALNFSVFYYEILNSPDRACSLAKQAFDEAISELDTLGEESYKDSTLIMQLLRDNLT 232
At14-3-3omicron     RLGLALNFSVFYYEILNSPERACHLAKRAFDEAIAELDSLNEDSYKDSTLIMQLLRDNLT 230
At14-3-3epsilon     RLGLALNFSVFYYEILNSPESACQLAKQAFDDAIAELDSLNEESYKDSTLIMQLLRDNLT 230
At14-3-3mu          RLGLALNFSVFYYEIMNAPERACHLAKQAFDEAISELDTLNEESYKDSTLIMQLLRDNLT 232
At14-3-3iota        RLGLALNFSVFYYEIMNSPERACHLAKQAFDEAIAELDTLSEESYKDSTLIMQLLRDNLT 235
At14-3-3pi          RLGLALNFSIFNYEIHKSIESACKLVKKAYDEAITELDGLDKNICEESMYIIEMLKFNLS 230
                    *********:* *** :: : ** :.*:*:::**:*** *.::  ::*  *:::*: **:

At14-3-3omega       LWTSDMQDDAA-DEIKEAA--APKPTEEQQ---------- 259
At14-3-3lambda      LWTSDMQEQMD-----EA---------------------- 248
At14-3-3kappa       LWTSDMQEQMD-----EA---------------------- 248
At14-3-3chi         LWASDMQDDVA-DDIKEAAPAAAKPADEQQS---------- 267
At14-3-3phi         LWTSDMQDESP-EEIKEAA--APKPAEEQKEI---------- 267
At14-3-3psi         LWTSDMTDEAG-DEIKEASKP-----DGAE---------- 255
At14-3-3upsilon     LWTSDLNDEAG-DDIKEAPKEVQKVDEQAQPPPSQ------ 268
At14-3-3nu          LWNSDINDEAGGDEIKEASKHEPEEGKPAETGQ-------- 266
At14-3-3omicron     LWTSDLEEGG------EQSKGHNQQDEN------------ 252
At14-3-3epsilon     LWTSDLNEEGD-----ERTKGADEPQDEN------------ 254
At14-3-3mu          LWTSDISEEGGDDAHKTNGSAKPGAGGDDAEVSIRDSFTRGKSN 276
At14-3-3iota        LWTSDLPEDGGEDNIKTEESKQEQAKPADATEN-------- 268
At14-3-3pi          TWTSGDGNGNK-----TDG---------------------- 245
```

Plant WEE1 proteins

Protein sequences of the plant WEE1 proteins were obtained from the NCBI database (http://www.ncbi.nlm.nih.gov). AtWEE1 [NP_171796], SlWEE1 [CAJ56085], ZmWEE1 [AAD52983], OsWEE1 [XP_464040]. The full-length NtWEE1 sequence was obtained from Dr. H. J. Rogers, Cardiff University. The alignment was made in Workbench (http://www.workbench.sdsc.edu) using the ClustalW alignment tool with conserved residues (blue and *), conserved strong group residues (green and :). Black residues are residues with no consensus.

```
AtWEE1          ---------MFEKN-GRTLLAKRKTQGTIKTRASKKIRKMEGTLERHSLLQFGQLSKISF 50
NtWEE1          ---------MKRKTLNRTSTPRRNNKSNTKRMNKGSLFTVGFSKVSLPPLPNQQQLQSSF 51
SlWEE1          ---------MERKTPNRTRRKQRSNQKSKKRMNKGSLSRHFTVGIAKPPLPNQQQLHSSL 51
ZmWEE1          ------------------------------------------------------------ 0
OsWEE1          MLRTKTPRPRGGKSRRATAAAGKERERERERERERGRSPSGELSLQLEHVSLFSFLADAPR 60


AtWEE1          ENRPSSNVASSAFQGLLDSD-----SSELRNQLGS---ADSDANCG---EKDFILSQDFF 99
NtWEE1          STLPLSN--PSRFQKLLDSEVLPPAQSNFPSILPS----NTDADAADGDNKDFILSQDFF 105
SlWEE1          SNVTLPN--PSRFQKLLDSDDLPPAQSQFSSVLPLNLDADDDADVADVAEKDFILSQDFF 109
ZmWEE1          ------------------------------------------------------------ 0
OsWEE1          EGAAAARTPFTPFEELLEGSCDPDPTPPPPLPPLQPQATPMDADEVVEEKDSGILSQDFF 120


AtWEE1          CTPDYITPDNQNLMSGLDISKD-HSPCPRSPVKLNTVKSKRCRQESFTGNHSNSTWSSKH 158
NtWEE1          CTPDYLTPDAPAICNGLDGNKDDCMPCPKSPEKLQTVARKRQRLAVKSATSLSSDFPGQQ 165
SlWEE1          CTPDYLTPDAPAICNGLDGDKDDYTPCPKSPEKLLSVSRKRPRLA--SVRPFSSDLSGQQ 167
ZmWEE1          CTPDYITPEMPQVANEFDDDDKENIPCPKSPEKSANPRSKRYRTDCSPKAREVTDFSFDH 60
OsWEE1          CTPDYITPDAPQLGSGFDAN-KENIPCPNSPEKSVC-RSKRYKRDCSPKGLGSNDIFDSQ 178
                *****:**:   : . :* . .   ***.** *      ** :   .    .   .:


AtWEE1          RVDEQENDDIDTDEVMGDKLQANQTERTG-YVSQAAVALRCRAMPPPCLKNPYVLNQSET 217
NtWEE1          QLADIPEDAFGSDETKSEKITESEKGHS--YVSQSAIALRYRVMPPPCIRNPYLRDASEI 223
SlWEE1          QPVDIPTDTFGTDEMKSEKISESEKGPS--YVSQSAIALRYRVMPPPCIRNPYLGDASEI 225
ZmWEE1          QITPVLFDSLTRDDSEEEQPKQPALEKRGGYVSQSAVALRCRVMPPPCVKNPYLNTDPCI 120
OsWEE1          WIAPVQFEGLD--DSEEEQLKESSSHKRGSYVSQSAVALRCRVMPPPCIRNPYLNTDHQI 178
                       : :   :   ::           ****:*:*** *.*****::***:


AtWEE1          ATDPFGHQRSKCASFLPVSTSGDGLSRYLTDFHEIRQIGAGHFSRVFKVLKRMDGCLYAV 277
NtWEE1          DVDPFGNRRSKCAGFNPVIFGNDGLSRYRSDFHEIEQIGTGNFSRVFKVLKRIDGCMYAV 283
SlWEE1          DADPFGNRRSKYPGFNPAISGNDGLSRYRTDFHEIEQIGSGNFSRVFKVFKRIDGCMYAV 275
ZmWEE1          DAAVYGGRQCNSAVFSPSIGG-NGLSRYRTDFHEIEKIGYGNFSVVFKVLNRIDGCLYAV 179
OsWEE1          DDNVFGGRQCKSSGFSPSVDG-DGLSRYRTDFHEIEQIGRGNFSVVFKVLKRIDGCLYAV 295
                   :* ::.: . * *   . :***** :*****.:** *:** ****::*:***:***


AtWEE1          KHSTRKLYLDSERRKAMMEVQALAALGFHENIVGYYSSWFENEQLYIQLELCDHSLSALP 337
NtWEE1          KHSTKQLHQDTDRRKALMEVQALAALGPHENVVGYYSSWFENEHLYIQMELCDHSLSN-- 341
SlWEE1          KHSTKQLHQDTDRRQALMEVQALAALGPHENVVGYYSSWFENEHLYIQMELCDHSLSN-- 333
ZmWEE1          KRSIKQLHNDMERRQAVKEVQAMAALGSHENIVRYFTSWFENEQLYIQMELCDRCLS--- 236
OsWEE1          KRSIRQLHNDRERRQAVKEVQALAALGCHENIVGYFTSWFENKQLFIQMELCDRCLS--- 352
                *:* ::*: * :**:*: ****:**** ***:* *::*****::*:**:****:.**


AtWEE1          KKSSLKVSEREILVIMHQIAKALHFVHEKGIAHLDVKPDNIYIKNGVCKLGDFGCATRLD 397
NtWEE1          KKYSKLSSEVAVLEAMYQVAKALQYIHQRGVAHLDVKPDNIYVKSGVYKLGDFGCATLLD 401
SlWEE1          KKYCKLFSEVEVLEAMYQVANALQFIHQRGVAHLDVKPDNIYVKNGVYKLGDFGCATLLD 393
ZmWEE1          MNRNQPVKRGEALELLYQICKGLDFMHERGIAHLDVKPDNIYVRNGIYKLGDFGCATLVN 296
OsWEE1          MDRNQPLKCGEALELLYQICKGLDFIHERGIAHLDVKPDNIYVRNGVYKLGDFGCATLID 412
                 .     .    *  ::*:.:.*.::*::*:*************:.*: ********* ::
```

```
AtWEE1          KSLPVEEGDARYMPQEILNEDYEHLDKVDIFSLGVTVYELIKGSPLTESRNQSLNIKEGK 457
NtWEE1          KSQPIEEGDARYMPQEILNENYDHLDKVDVFSLGAAIYELIRGSPLPESGPHFLNLREGK 461
SlWEE1          KSQPIEEGDARYMPQEILNENYDHLDKVDIFSLGAAIYELIRGSSLPESGPHFLNLREGK 453
ZmWEE1          RSLAIEDGDSRYMPPEMLNDKYEHLDKVDIFSLGAAVYELIRGTPLPESGSHFTSIREGK 356
OsWEE1          RSLAIEDGDSRYMPPEMLNDKYEHLDKVDIFSLGAAIYELIRGTQLPDSGPQFTSLREGK 472
                :* .:*:**:**** *:**:.*:******:****.::****:*: *.:*  :  .::***

AtWEE1          LPLLPGHSLQLQQLLKTMMDRDPKRRPSARELLDHPMFDRIRG----- 500
NtWEE1          LPLLPGHSLQFQNLLKVMMDPDPTRRPSAKDLVDNPIFERCQRNANK- 508
SlWEE1          LPLLPGHSLQFQNLLKAMMDPDPTRRPSAKGVVDNPIFERWQRNSNK- 500
ZmWEE1          IALLPGCPMQFQSLIKSMMDPDPVRRPSAKEILRHPSFDKLHKASSK- 403
OsWEE1          IALLPGCPMQFQSLIKSMMDPDPVRRPSAKEVLRHPIFDKLHKAPAKK 520
                :.**** .:*:*.*:* *** ** *****: :: :* *:: :
```

Appendix B

Data from the *wee1* T-DNA Insertion Lines

Raw data – primary root length ±HU

wild type		*wee1-1*		*wee1-3*		*wee1-5*	
–HU	+HU	–HU	+HU	–HU	+HU	–HU	+HU
40	30	15	5	35	20	35	5
30	30	20	5	20	20	25	5
25	30	30	4	35	25	30	6
30	25	25	5	40	20	35	5
45	35	40	4	40	20	25	2
35	30	35	6	35	20	45	5
35	25	20	5	35	20	35	3
30	30	35	6	30	20	40	7
45	40	20	5	35	20	40	4
40	30	35	8	45	25	40	4
30	30	30	8	25	20	40	3
35	25	40	5	30	20	45	5
30	25	30	5	40	20	40	5
35	30	30	5	35	25	40	3
45	30	30	5	35	20	40	3
30	30	30	5	45	20	45	5
35	30	30	5	30	25	45	3
35	20	35	5	30	15	45	3
40	30	35	5	40	20	40	4
30	30	35	5	30	20	35	4

Raw data – total number of lateral roots and lateral root primordia ±HU

wild type		*wee1-1*		*wee1-3*		*wee1-5*	
–HU	+HU	–HU	+HU	–HU	+HU	–HU	+HU
9	3	2	0	11	4	7	1
10	3	2	0	7	0	14	1
6	1	2	1	9	0	13	0
4	3	0	1	15	0	7	1
7	2	1	1	9	5	7	2
9	3	0	0	6	3	9	0
7	2	0	0	13	6	8	0
5	2	1	0	6	3	20	1
8	0	4	0	11	9	19	0
10	0	4	0	14	2	11	0
3	4	5	0	12	8	15	0
4	2	7	0	13	5	17	0
4	2	7	1	12	4	16	0
3	4	5	0	10	7	18	1
4	3	4	0	12	4	14	1
8	6	4	0	17	7	19	2
4	2	2	0	16	7	15	1
4	5	6	1	7	6	12	1
7	5	3	2	11	8	13	1
3	6	5	2	7	5	14	1

Mean (±SE) measurements of primary root length, lateral roots and lateral root primordia and the calculated ratio of lateral root and lateral root primordia per mm primary root length

	Primary root length (mm)		Lateral roots + lateral root primordia		Ratio (lateral roots + lateral root primordia/ mm primary root length)	
	–HU	+HU	–HU	+HU	–HU	+HU
wild type	35.00 (± 1.3)	29.25 (± 0.9)	5.95 (± 0.5)	2.90 (± 0.4)	0.17	0.10
wee1-1	30.00 (± 1.5)	5.30 (± 0.2)	3.20 (± 0.5)	0.45 (± 0.2)	0.11	0.09
wee1-3	34.50 (± 1.4)	20.75 (± 0.5)	10.90 (± 0.7)	4.65 (± 0.6)	0.32	0.22
wee1-5	38.30 (±1.5)	4.20 (± 0.3)	13.40 (± 1.0)	0.70 (± 0.2)	0.35	0.17

T-tests for primary root length (–HU) (P)

	wild type	*wee1-1*	*wee1-3*	*wee1-5*
wild type		0.0229	0.7606	0.0695
wee1-1			0.0298	5.5989E-05
wee1-3				0.0369
wee1-5				

T-tests for primary root length (±HU) (P)

	wild type +HU	*wee1-1* +HU	*wee1-3* +HU	*wee1-5* +HU
wild type –HU	0.0001			
wee1-1 –HU		1.5109E-12		
wee1-3 –HU			6.9508E-09	
wee1-5 –HU				1.1111E-15

T-tests for lateral root + lateral root primordia (-HU) (P)

	wild type	*wee1-1*	*wee1-3*	*wee1-5*
wild type		0.0058	3.9352E-06	6.9038E-06
wee1-1			1.2645E-09	8.5243E-11
wee1-3				0.0004
wee1-5				

T-tests for lateral root + lateral root primordia (±HU) (P)

	wild type +HU	*wee1-1* +HU	*wee1-3* +HU	*wee1-5* +HU
wild type –HU	0.0007			
wee1-1 –HU		3.1245E-05		
wee1-3 –HU			1.5431E-05	
wee1-5 –HU				4.2271E-11

Mean (±SE) *AtWEE1* transcript levels, AtWEE1 protein levels and kinase activity

	Transcript		Protein		Kinase activity	
	–HU	+HU	–HU	+HU	–HU	+HU
wild type	100.00 (± 6.6)	104.51 (± 1.5)	100 (± 0.0)	55.60 (± 4.3)	10.94 (± 0.3)	15.53 (± 0.9)
wee1-1	98.39 (± 3.2)	114.59 (± 4.0)	72.06 (± 2.6)	50.38 (± 2.7)	12.68 (± 0.3)	13.03 (± 0.3)
wee1-3	64.38 (± 2.8)	80.61 (± 6.0)	28.65 (± 3.8)	23.43 (± 8.7)	11.52 (± 0.1)	11.93 (± 0.1)
wee1-5	76.23 (± 4.3)	98.48 (± 7.1)	41.51 (± 5.8)	16.56 (± 3.9)	11.63 (± 0.4)	12.02 (± 0.3)

T-tests for *WEE1* transcript level (–HU) (P)

	wild type	*wee1-1*	*wee1-3*	*wee1-5*
wild type		0.8513	0.0160	0.0264
wee1-1			0.0065	0.0236
wee1-3				0.0129
wee1-5				

T-tests for *WEE1* transcript level (±HU) (P)

	wild type +HU	*wee1-1* +HU	*wee1-3* +HU	*wee1-5* +HU
wild type –HU	0.5820			
wee1-1 –HU		0.0113		
wee1-3 –HU			0.0516	
wee1-5 –HU				0.0828

T-tests for *WEE1* protein level (–HU) (P)

	wild type	*wee1-1*	*wee1-3*	*wee1-5*
wild type		0.0075	0.0027	0.0101
wee1-1			0.0112	0.0642
wee1-3				0.1294
wee1-5				

T-tests for *WEE1* protein level (±HU) (P)

	wild type +HU	*wee1-1* +HU	*wee1-3* +HU	*wee1-5* +HU
wild type –HU	0.0099			
wee1-1 –HU		0.0187		
wee1-3 –HU			0.4336	
wee1-5 –HU				0.1199

T-tests for *WEE1* kinase level (–HU) (P)

	wild type	*wee1-1*	*wee1-3*	*wee1-5*
wild type		0.0792	0.2952	0.3440
wee1-1			0.2048	0.0577
wee1-3				0.8743
wee1-5				

T-tests for *WEE1* kinase level (±HU) (P)

	wild type +HU	*wee1-1* +HU	*wee1-3* +HU	*wee1-5* +HU
wild type –HU	0.0125			
wee1-1 –HU		0.0903		
wee1-3 –HU			0.2952	
wee1-5 –HU				0.6145

Appendix C

A. thaliana WEE1 interacts with CDKA1, CDKB2;1 and CiPK21, a putative *A. thaliana* CHK1 Protein, in a Y2H Screen

Introduction

The DNA damage checkpoint in both yeast and animals is defined as a signal transduction pathway that delays entry into mitosis in the presence of damaged DNA to preserve genomic integrity (Hartwell and Weinert, 1989). In yeast and animals DNA damage is sensed by the RAD and ATM/ATR proteins, respectively (Elledge, 1996; Weinert, 1998; Abraham, 2000), resulting in down-stream phosphorylation and activation of the Chk1/2 kinases. The Chk kinases are conserved in yeast and animals (Walworth *et al.* 1993; al-Khodairy *et al.* 1994; Fogarty *et al.*, 1997; Sanchez *et al.*, 1997; Kumagai *et al.*, 1998; Zachos *et al.*, 2003) and are responsible for the *in vivo* activation of Wee1 proteins and deactivation of Cdc25 proteins (Peng *et al.*, 1997; Wang *et al.*, 2000; Forrest and Gabrielli, 2001; Rothblum-Oviatt *et al.*, 2001; Chen *et al.*, 2003b).

The signalling pathway between ATM/ATR and WEE1 has not yet been described in plants. However, recently was suggested that a member of the CiPK family could act as the protein kinases regulating the signalling cascade down-stream ATM/ATR. The CiPK protein family in *A. thaliana* consists of 25 members, of which several have been shown to be involved in Ca^{2+} signalling (Hrabak *et al.*, 2003; Kolukisaoglu *et al.*, 2004). CiPK proteins consist of a conserved kinase domain and a plant-specific NAF domain, which mediates the interaction with the CBL calcium sensor proteins and, interestingly, the plant CIPK proteins possess a third domain, a protein phosphatase interaction (PPI) motif, which is similar to the *S. pombe* and *H. sapiens* Chk1 kinase (Ohta *et al.*, 2003). In a recent report by Rossignol *et al.* (2007) it was shown that the *A. thaliana* Protection of telomeres 1A (POT1A) protein, which is a regulator of telomeric length, interacts with AtCiPK21.

To elucidate a potential role for AtCiPK21 in the plant cell cycle, it was investigated if AtCiPK21 interacts with AtWEE1 in a Y2H screen. In addition to CiPK21, it was also investigated if AtWEE1 interacts with CDKA1 and AtCDKB2;1.

Materials and Methods

Yeast Transformation and Reporter Gene Screening

For the Y2H screen the target plasmids containing the coding sequences of *AtCiPK21*, *AtCDKA1* and *AtCDKB2;1*, respectively, were kindly donated by Dr. J. Doonan, John Innes Centre, UK. Co-transformation of wild type YRG2 cells with the *AtWEE1* bait plasmid and the target plasmids and the reporter gene screening were performed as described in sections 3.11.2 and 3.12, respectively.

Results

Wild type *S. cerevisiae* YRG2 cells were co-transformed with the *AtWEE1* bait plasmid and the target plasmids containing the coding sequences for *AtCiPK21*, *AtCDKA1* and *AtCDKB2;1*, respectively. The double transformants were selected on SD agar plates containing trp-leu DO solution and 40 mM 3-AT and tested for transcriptional activation of the *HIS3* and *LacZ* reporter genes (Figure C1A and B).

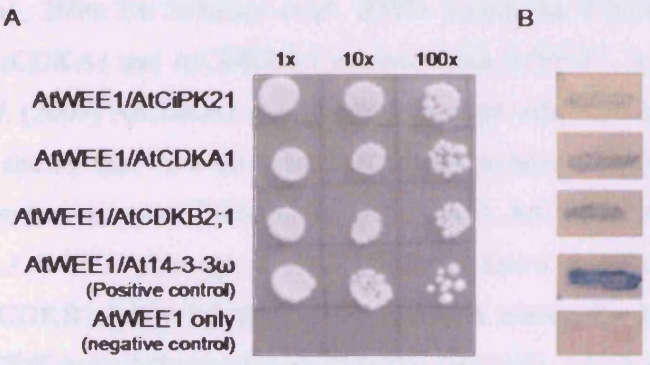

Figure C1 – Transcriptional activation of Y2H reporter genes YRG2 cells co-transformed with *AtWEE1* bait plasmid and *AtCiPK21*, *AtCDKA1*, *AtCDKB2;1* and *At14-3-3ω* (positive control) target plasmids, respectively, and YRG2 cells transformed with *AtWEE1* only (negative control). A) Activation of the *HIS3* reporter gene assayed by adding a 1x, 10x and 100x dilution of the transformants onto SD agar containing his DO and 40 mM 3-AT. B) Activation of the *LacZ* reporter gene assayed by filter lifts of the transformants.

The transformant carrying the *AtWEE1* bait plasmid and the *At14-3-3ω* target plasmid (Chapter 5) was used as a positive control for the Y2H and was found to activate both the *HIS3* and *LacZ* reporter genes. YRG2 cells transformed with the *AtWEE1* bait plasmid alone was included in the Y2H to verify that the *AtWEE1* bait plasmid is

incapable of auto-activating the *HIS3* or the *LacZ* reporter gene itself when grown under these conditions.

The transformants carrying the *AtWEE1* bait plasmid co-transformed with the *AtCiPK21*, *AtCDKA1* and *AtCDKB2;1* target plasmids, respectively, did grow on SD agar plates containing his DO solution and 40 mM 3-AT implying that AtWEE1 interacts with all of the above mentioned proteins. Furthermore, the double transformants were all found to give rise to a blue colouration in the filter lift assay further implying that the proteins interact resulting in a transcriptional activation of the *LacZ* reporter gene.

Discussion

The signalling cascade between ATM/ATR and WEE1 has not yet been described in plants, whereas in recent years the knowledge of the proteins involved in the signalling cascade down-stream of WEE1 has increased (Menges *et al.*, 2005; Shimotohno *et al.*, 2006; De Schutter *et al.*, 2007). Using the Y2H technique it was investigated if AtCDKA1 and AtCDKB2;1 interacts with AtWEE1. In agreement with De Schutter *et al.* (2007) AtCDKA1 was found to interact with AtWEE1. Furthermore, it was recently shown that AtWEE1 directly phosphorylates CDKA1 *in vitro* in a tyrosine 15-dependent manner (Shimotohno *et al.*, 2006). AtCDKB2;1 was also found to interact with AtWEE1, although it was previously found that AtWEE1 does not interact with AtCDKB1;1 (De Schutter *et al.*, 2007). A reason for this could be that the two B-type CDK have different functions in the cell cycle, which is also suggested from the expression patterns of *AtCDKB1* and *AtCDKB2* genes. In *A. thaliana* the expression of *CDKB1* peaks in S phase, whereas the expression of *CDKB2* peaks in G2/M (Menges *et al.*, 2005). So far, no reports have suggested a link between WEE1 with CDKB1 in S phase. Furthermore, the interaction between AtWEE1 and AtCDKB2;1 highlights the importance of assaying all members of a given protein family, here AtCDKB, rather than simply extending findings for one protein to the entire family.

Recently, CiPK proteins have become interesting in relation to the plant cell cycle. They contain a PPI motif similar to the *S. pombe* and *H. sapiens* Chk1 kinases (Ohta *et al.*, 2003) and since no Chk1 proteins have so far been identified in plants, it was

suggested that CiPK proteins could be the link between ATM/ATR and WEE1. AtCiPK21 was found to interact with AtWEE1 in a Y2H screen indicating a function of this protein in the plant cell cycle. However, it is necessary to confirm the interaction by additional *in vitro* and *in vivo* methods, such as co-immunoprecipitation and fluorophore-based methods, such as FRET and BiFC. If the interaction can be confirmed, it is further necessary to investigate, by the use of *in vitro* kinase assays, if CiPK21 phosphorylates and hence activates WEE1. In the case that CiPK21 proves to be the protein linking ATM/ATR and WEE1 signalling cascade, it would be interesting to investigate if CiPK21 is a target for 14-3-3 protein binding. In both *S. pombe* and *H. sapiens* 14-3-3 proteins bind to active Chk1 in a phosphorylation-dependent manner and thereby stabilize Chk1 activity and ensure its nuclear localization in the case of DNA damage (Chen *et al.*, 1999; Capasso *et al.*, 2002; Jiang *et al.*, 2003).

Appendix D

CDKB and WEE1 kinase regulate mitotic timing in BY-2 cells

Paper submitted to The Plant Journal on the 14th of November 2007

The author of this thesis has contributed to the paper with the following experimental work:

- Transcript levels of *AtWEE1* and *NtWEE1*
- Testing of the NtWEE1 antibody including recombinant protein production (Chapter 7)
- Protein levels and kinase activity of WEE1 (Chapter 7)

The Plant Journal

the plant journal

CDKB and WEE1 kinase regulate mitotic timing in BY-2 cells

Journal:	*The Plant Journal*
Manuscript ID:	TPJ-01017-2007
Manuscript Type:	Full Paper
Date Submitted by the Author:	14-Nov-2007
Complete List of Authors:	Siciliano, Ilario; Cardiff University, School of Biosciences Lentz-Grønlund, Anne; Cardiff University, School of Biological Sciences Spadafora, Natasha; Cardiff University, School of Biosciences Herbert, Robert; Worcester University, Applied Sciences, Geography and Archaeology Bitonti, M; Calabria University, Ecology Francis, Dennis; Cardiff University, School of Biosciences Rogers, Hilary; Cardiff University, School of Biosciences
Key Words:	Arabidopsis thaliana, , cell size, , BY-2 cell line, , CDKA/B, , Nicotiana tabacum, WEE1

SUBMITTED MANUSCRIPT

CDKB and WEE1 kinase regulate mitotic timing in BY-2 cells

Ilario Siciliano[1], Anne Lentz- Grønlund[1,2], Natasha Spadafora[1,2], Robert J. Herbert[2], M. Beatrice Bitonti[3], Dennis Francis[1*], Hilary J. Rogers[1*]

[1]School of Biosciences, Cardiff University, Main Building, Park Place, Cardiff. CF10 3TL, UK, [2]Department of Applied Sciences, Geography and Archaeology, University of Worcester, Henwick Grove, Worcester, UK. [3] Department of Ecology, University of Calabria, Arcavacata di Rende (Cosenza), Italy.

*for correspondence. Fax (0)29 2087 4305; e-mail francisdf@cardiff.ac.uk; rogershj@cardiff.ac.uk)

12 **Summary**

13 **Expressing the *Arabidopsis* cell cycle gene, *Arath;WEE1*, either in**
14 ***Schizosaccharomyces pombe* or *Arabidopsis thaliana* induced**
15 **elongated cells fuelling the idea that expressing this gene in BY-2 cells**
16 **would induce large cell sizes. We found the exact opposite. Either**
17 **constitutive or dexamethasone (DEX)-inducible expression of**
18 ***Arath;WEE1* induced small mitotic cell areas of 2300 – 2,500 μm^2 in five**
19 **independent transgenic lines compared with 2800 – 3,200 μm^2 in**
20 **controls. When expression of *Arath;WEE1* was induced, G2 was**
21 **shortened to 0.5 h with a compensatory increase in G1 duration. The**
22 **expression profile of the endogenous *Nicta;WEE1* was perturbed only**
23 **qualitatively; this cannot be attributed to an increase in WEE1**
24 **expression *per se* because when *Nicta; WEE1* was induced, there was a**
25 **2 hour delay in the peak of synchronous mitoses and no reduction in**
26 **mitotic cell area. In the inducible line ± DEX, WEE1 protein and kinase**
27 **levels were sensitive markers of the G2/M transition and induction of**
28 ***Arath;WEE1* did not affect a high level of WEE1 kinase in early S-phase.**
29 **In the normal cell cycle, WEE1 kinase activity was inversely related to**
30 **CDKB but not CDKA activity; *Arath;WEE1* expression induced maximal**
31 **Nicta;CDKB activity in early S-phase. Our data indicate that the timing of**
32 **CDKB but not CDKA activity is either acutely sensitive or central to a**
33 **cell size control mechanism. Moreover the data also support the**
34 **hypothesis that WEE1 kinase is a negative regulator of CDKB activity**
35 **during a normal cell cycle in BY-2 cells.**

36 **WC94 2**

Keywords: ***Arabidopsis thaliana*****, cell size, BY-2 cell line, CDKA/B,** ***Nicotiana tabacum, WEE1***

Word counts

Abstract	242
Introduction	633
Results	2318
Discussion	1153
Methods	1349
Legends	1189
Sub- TOTAL	**6885**
References	1105
TOTAL	**8064**

figures interpolated as appropriate

Introduction

The cell cycle is conserved in all eukaryotes where the key transitions, G1/S and G2/M are regulated by cyclin-dependent kinases (CDKs). These complexes comprise the CDK and cyclin as the catalytic and activating sub units, respectively (Krek and Nigg, 1991). In animals, there are several different CDKs each one functioning, at different stages of the cell cycle (Gould and Nurse, 1989). In plants, over 120 cyclins and over 30 CDK-related genes are classified into A through to F (DeWitte and Murray, 2003); the CDKB family is unique to plants. In *Arabidopsis*, CDKA;1 activity peaks at G1/S and G2/M whilst CDKB2;1 peaks at G2/M (Joubes *et al.*, 2000). In tobacco BY-2 cells, CDKA activity is relatively constant from S-phase to mitosis whilstB-type activity peaks in mid G2 (Sorrell*et al.*, 2001).

In fission yeast (*Schizosaccaharomyces pombe*), a single CDK encoded by *cdc2* associates with different cell cycle-specific cyclins to regulate both G1/S and G2/M (Nurse and Bisset, 1981; Gould and Nurse, 1989; Nurse, 1990). Cdc2 is phosphoregulated in G2, negatively by Spwee1 kinase and positively by Spcdc25 phosphatase (Nurse, 1990). A partial *WEE1* homologue was cloned in maize and inhibits CDK activity *in vitro* (Sun *et al.*, 1999) whilst a full length *WEE1* expressed only in meristematic regions was cloned in *Arabidopsis* (Sorrell *et al.*, 2002). *Arath;WEE1* participates in the DNA damage checkpoint, and insertion lines of WEE1 are hypersensitive to DNA damaging agents (De Schutter *et al.*, 2007). However its role in a normal cell cycle remains to be fully characterised especially since the insertion lines grow and develop normally. This is in contrast to *wee*$^{-/-}$ mice that die early during embryo development (Tominaga *et al*, 2006).

Expression of both *Arath;WEE1* and *ZmWEE1* in fission yeast resulted in a long cell phenotype mirroring the effect of *SpWee1*^{oe} (Russell and Nurse 1987; Sun *et al.*, 1999; Sorrell *et al.*, 2002), suggesting a possible role for plant WEE1 in cell size regulation. WEE1 transcripts were high during endoreduplication both in the endosperm of *Zea mays* (Sun et al., 1999) and in tomato fruit (Gonzalez et al, 2004) suggesting a role for WEE1 in this process. In tomato, a reduction in WEE1 levels using antisense, resulted in smaller fruit with reduced cell size, a lower ploidy level and a reduction in the levels of Y15 phosphorylated CDKA accompanied by a reduction in CDKA activity (Gonzalez *et al.*, 2007). They concluded that in wild type fruit, WEE1 negatively regulates CDKA activity to control cell size acting through a regulation of cell expansion and, or endoreduplication. However in these systems, neither WEE1 protein nor WEE1 kinase activity from plant protein extracts were measured and linked to cell cycle phase. The most comprehensive study of WEE kinase activity during the cell cycle was for HeLa cells where WEE1 kinase activity was detected during interphase but not in mitosis (McGowan and Russell, 1995). In these assays, native WEE1 was pulled down using human WEE1 antibody and then used in histone H1 kinase assays (McGowan and Russell, 1995).

Given the known cell cycle effect of *Arath;WEE1* expression in *S. pombe*, we aimed to examine its effects on cell size *in planta* and to resolve how WEE1, at the protein and kinase levels, might be regulating the plant cell cycle. We raised an antibody against tobacco WEE1 and used a similar approach to that of McGowan and Russell (1995) to provide, for the first time, measurements of WEE1 protein and WEE1 kinase activity during a plant cell

cycle. Expression of *Arath;WEE1* in tobacco cells resulted in an unexpected reduction in cell size and perturbation of the cell cycle. We investigated these effects at the levels of WEE1 transcript, protein, and kinase activity to offer a model about how WEE1 regulates entry into mitosis in a normal and a perturbed cell cycle.

Results

Arath;WEE1^{OE} in Arabidopsis results in an increase in epidermal cell length in root apical meristems

Given *Arath;WEE1's* induction of an elongated fission yeast phenotype, we tested whether the same effect would be induced in *Arabidopsis*. Indeed, there was a significant increase in epidermal cell length in root meristems in *Arath;WEE1^{OE}* plants from 3.96 ± 0.61 in WT, to 5.50 ± 0.83 µm (n=50; $P < 0.001$). However, this is a limited approach because mitotic cells could not be distinguished from interphase cells. To study *Arath;WEE1's* effects on mitotic cell size and the cell cycle, we expressed it in the tobacco BY-2 cell line which is free from developmental constraints and might obviate gene silencing. BY-2 cells were transformed with *Arath;WEE1* regulated either by a constitutive attenuated 35S promoter (Orchard et al. 2005) or a dexamethasone (DEX) inducible promoter (Ayoama and Chua, 1997). All cell lines were synchronised at the G1/S boundary with aphidicolin, and DEX was added to the inducible lines immediately following release from the aphidicolin block.

***Arath;WEE1* expression in BY-2 cells induces a reduction in mitotic cell size**

Constitutive expression of *Arath;WEE1* was detected in three independent lines (Fig. 1A) and in two inducible lines within 15 min of addition of DEX (referred to here on as +DEX) (line 1 Fig. 1B). Expression of *Arath;WEE1* was not detected in the absence of DEX (referred to here on as -DEX) in any of the i-WEE1 lines tested (data not shown) indicating that the promoter's inducibility was under tight control.

When *Arath;WEE1* was expressed constitutively in three independent transformed lines (c-WEE1 lines 2, 6 and 10), significant reductions in mitotic cell size were detected compared with the comparable Empty Vector-c- 10 (Fig. 1C). *Arath;WEE1* expression +DEX in line i-WEE1-1, and i-WEE1-6 induced significant reductions in mitotic cell area and compared with

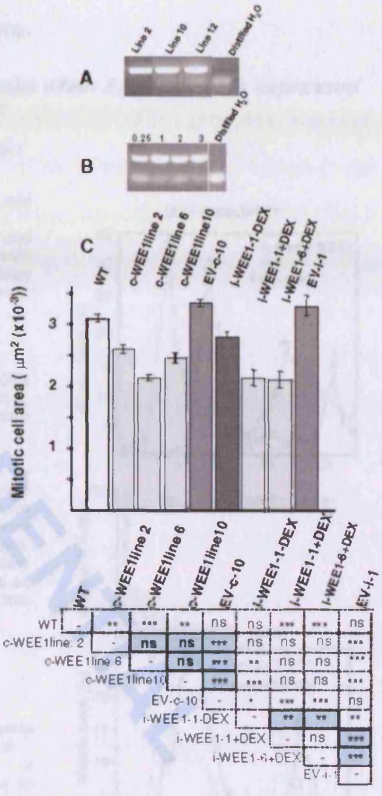

Figure 1. Constitutive or induced expression of *Arath;WEE1* in BY-2 cells results in a small mitotic cell size.

(A) RT-PCR expression of *Arath;WEE1* in three constitutively expressing BY-2 lines: 2, 10 and 12.

(B) *Arath;WEE1* expression in line 1 induced by Dexamethasone (DEX), first detected after 15 min of DEX.

(C) Mean mitotic cell area (µm² ±SE) in wild type (WT), constitutively (c) expressing WEE1 lines: 2, 6 and 10, empty vector (EV), inducible (i) lines 1 and 6 ±DEX and corresponding empty vector line EV-i-1 (n=300). Below is a matrix that compares all treatments by t-tests. Shaded boxes mark the strictly valid statistical comparisons. *P <05, **P <0.01, ***<0.001, ns not significant. There were no significant differences in mitotic cell size within treatments.

both i-WEE1-1-DEX ($P < 0.02$) and, the inducible empty vector, EV-i-1 ($P < 0.001$). Thus, the induction of small cellsfollowing *Arath;WEE1* expression was the exact converse of our predictions.

G2 shortens in synchronised BY-2 cells when Arath;WEE1 is expressed

Figure 2. Constitutive or inducible Arath;WEE1 expressing BY-2 cells have a short G2

Mitotic indices following synchronisation with and removal of aphidicolin in:
(A) : constitutive (c) - *Arath; WEE1* line 10 (----) and its corresponding Empty Vector (EV-c-10) (♦ solid lines). ↓ mark cell cycle durations for constitutively expressing *Arath;WEE1* and EV line 10, respectively; representative data from replicate experiments;

(B) in the inducible (i)- *Arath; WEE1* line 1 +DEX (grey dashed lines) or -DEX (black lines) at time 0. arrows mark the cell cycle times; representative data from replicate experiments.

BY2 cells blocked in late G1 and S-phase by aphidicolin and then released show an initial rise in the curve when cells trapped at the end of S-phase during the aphidicolin block, are the first to traverse G2 and enter mitosis following removal of the block. The first peak is when the bulk of synchronised cells enter mitosis; this point in time minus S-phase is an alternative measure of G2. Either way, G2 is less than 1 hour in the +DEX treatment, and 4 h -DEX.

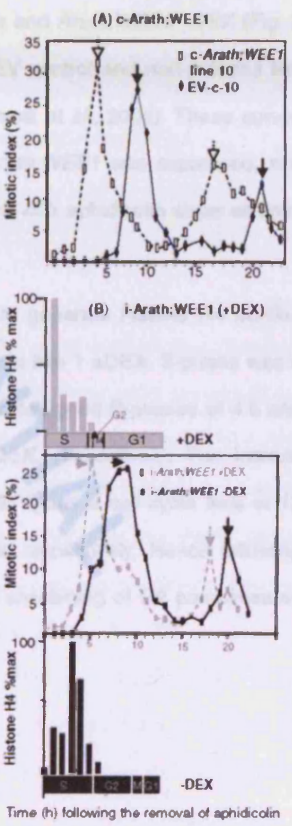

Above and below cell cycle plots for the inducible lines, are mean histone H4 expression profiles from semi quantitative RT-PCR as percentages of maximum expression ± DEX, used to calculate S-phase (4.5 h +DEX, 5.5 h –DEX). SEM was <3 %. throughout (n=3). M-phase duration was calculated from the average mitotic index for each treatment (M) using formulae of Nachtwey and Cameron (1968) which account for exponential growth: $dM = C/\ln 2 \times \ln(M+1)$. G1 is calculated by difference. All phase durations are in hours rounded up or down to the nearest 0.5 h

i-Arath;WEE1	S-phase	G2	M	G1	C
+ DEX	4.5	0.5	1	7	13
- DEX	5.5	4.0	1	1.5	12

144 To examine whether small mitotic cell size impacted on the cell cycle,
145 mitotic indices were charted following synchronisation with aphidicolin (Fig. 2).
146 In these curves, the highest mitotic index value is when the bulk of
147 synchronised (G1/S) cells enter mitosis as confirmed by microdensitometry
148 (Orchard *et al.*, 2005). For both constitutive (Fig. 2A), and inducible
149 *Arath;WEE1* lines +DEX (Fig. 2B), the mitotic index curve rose sooner (1-2h)
150 and peaked earlier (4-5 h) than empty vector and *Arath;WEE1* –DEX (Fig. 2
151 A and B). Cell cycle phase lengths for the EV control and non-induced line
152 were comparable to previous data (e.g. Orchard *et al.*, 2005). These curves
153 are consistent with a shortened G2 when *Arath;WEE1* was expressed, and
154 the effect cannot be ascribed to the treatment with aphidicolin since all lines
155 ±DEX were synchronised in the same way.

156 Semi-quantitative RT-PCR was used to generate histone H4 profiles
157 used to measure S-phase duration in inducible line 1 ±DEX. S-phase was 4
158 to 5h +DEX and 5 to 6 h –DEX (Fig. 2B); we assigned S-phases of 4.5 and
159 5.5 h for the inducible line +DEX and –DEX, respectively. The interval
160 between peaks (indicated by arrows in Fig. 2) spans a cell cycle time of 13
161 and 12 h in the +DEX and -DEX treatments, respectively. Hence following
162 *Arath;WEE1* expression, there was an 8-fold shortening of G2 compensated
163 by a 4.7-fold lengthening of G1 (Fig. 2).

164 ***Inter-specific differences at the amino acid level between the regulatory***

165 ***domain in Arath;WEE1 and Nicta;WEE1***

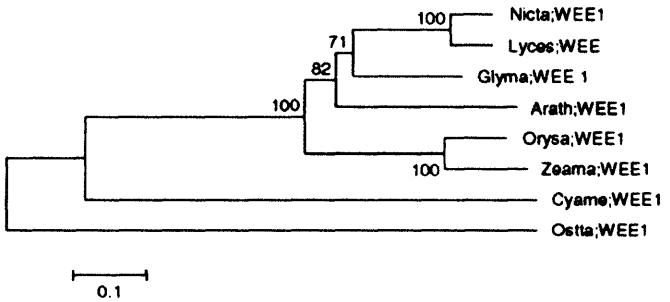

Figure 3. Phylogenetic tree showing relationship between the six available higher plant and two algal WEE1 sequences.

The tree was constructed using the Neighbour-joining algorithm, boot strap values are indicated above branches. Nicta;WEE1, *Nicotiana tabacum*; Zeama;WEE1, *Zea mays* (AAD52983); Arath;WEE1, *Arabidopsis thaliana* (CAD28679), Glyma;WEE1, *Glycine max* (AAS 13373), Orysa;WEE1, *Oryza sativa* (XP_464040); Lyces;WEE1, *Lycopersicon esculentum* (AM180939); Cyame;WEE1, *Cyanidioschyzon merolae;* (CMT590C); Ostta;WEE1, *Ostreococcys tauri* (AY675101)

166 The induction of *Arath;WEE1* leads to a small instead of a predicted
167 large cell size phenotype. We next asked whether there were any significant
168 differences between the Arabidopis and tobacco WEE1 genes. The 508
169 amino acid ORF of *Nicta;WEE1* was cloned using degenerate primers
170 followed by 3' and 5' RACE and compared to other available WEE1 amino
171 acid sequences from tomato, maize, soybean, Arabidopsis and rice, and two
172 alga, *Cyanidioschyzon merolae* and *Ostreococcys tauri* (Fig. 3).
173 Overall, the *Nicta;WEE1* amino acid sequence was most closely related to the
174 tomato sequence (95%) and most distant from the algal ones, (67 and 64%
175 respectively). In humans, *Xenopus* and fission yeast catalytic activity of WEE1
176 is located in the C-terminal domain while the N-terminal domain has a
177 regulatory function (Lee *et al*, 2001; McGowan and Russell, 1995; Rothblum-

178 Oviatt et al, 2001). A comparison of the putative protein kinase domain of
179 Nicta;WEE1 (amino acids 283 -508) to the equivalent region of Arath;WEE1
180 revealed 70% similarity whereas the N-terminal regions (amino acids 1-282)
181 were considerably less similar (49%, Fig. 4). Likewise, comparisons between
182 animal *WEE1* genes (e.g. Xenopus and human) reveal a higher similarity
183 within the catalytic domain (60%) compared to the N- terminal regulatory
184 domain (56%).
185
186

187

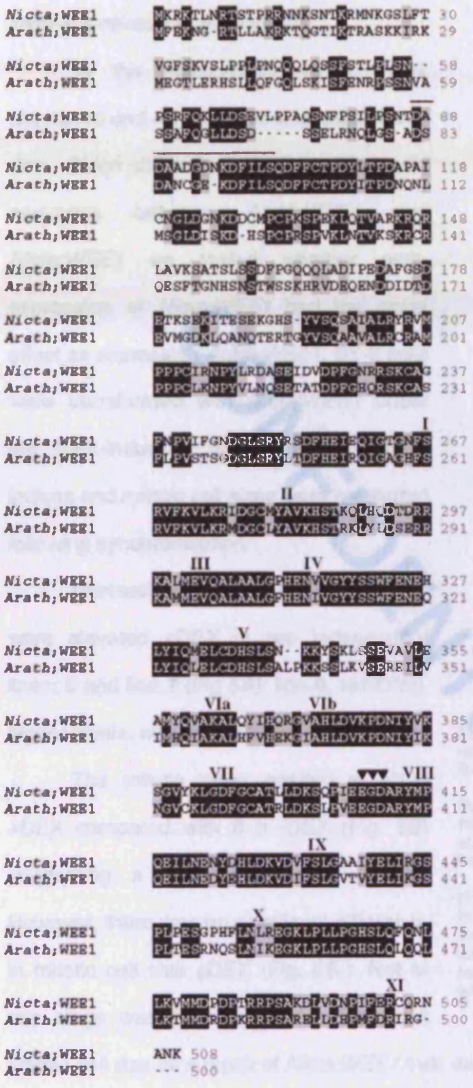

Figure 4. Alignment of Nicta;WEE1 and Arath;WEE1 predicted amino acid sequences showing conserved (black) and similar (grey) residues. Roman numerals indicate kinase sub domains in catalytic domain. Inverted closed triangles, 'EGD' Motif conserved in most WEE1 sequences. The line above the Nicta;WEE1 sequence indicates the peptide used to raise an antibody.

G2 lengthens when tobacco WEE1 is over-expressed in BY-2 cells,

In the *Arath;WEE1* +DEX , G2 shortened and cells divided at a reduced cell size. Given differences in the amino acid sequence between *Arath;WEE1* and *Nicta;WEE1* we tested whether over-expression of *Nicta;WEE1* had the same effect as expressing *Arath;WEE1*. BY-2 cells were transformed with *Nicta;WEE1* under the DEX-inducible promoter, and mitotic indices and mitotic cell sizes were measured following synchronisation.

Expression levels of *Nicta;WEE1* were elevated +DEX in two independent lines: 6 and line 7 (Fig 5A): line 6, exhibiting higher levels, was used subsequently

The mitotic index peaked at 10 h +DEX compared with 8 h -DEX (Fig. 5B) suggesting a 2 h lengthening of G2. However, there was no significant difference in mitotic cell size ±DEX (Fig. 6B.). Not at any stage was there evidence of a small mitotic cell size as a result of *Nicta;WEE1* over expression.

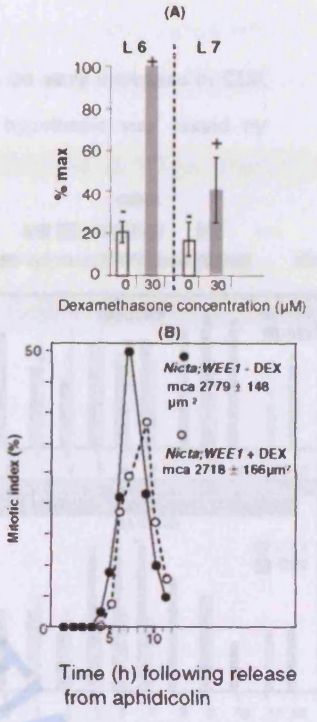

Figure 5. *Nicta;WEE1* over expression does not induce a small mitotic size phenotype but G2 lengthens.

(A). Mean (±SE) expression levels of *Nicta;WEE1* by semi-quantitative RT PCR, ±DEX (µM) as a percentage of max. in two transgenic lines: (L6 and L7). n = 3

(B). Mitotic indices in the *Nicta;WEE1* inducible line 6 ± 30 µM DEX (µM) following synchronisation with aphidicolin. DEX was added at time 0, and 500 cells were scored per sampling time. Mean (±SE), mitotic cell areas (mca) are added. (n= 48)

Expression of Arath;WEE1 results in a premature increase in Nicta;CDKB1 activity

For premature cell division there ought to be early increases in CDK activity driving cells into early mitoses. This hypothesis was tested by measuring kinase activity of both Nicta;CDKA;1 (referred to here, as CDKA) and Nicta;CDKB;1 (referred to here as CDKB) in the inducible *Arath;WEE1* line 1 ± DEX.

Both CDKA and CDKB activities in the –DEX (Fig. 6) were highly comparable to published CDKA and B activity during the cell cycle of BY-2 wild type cells (Sorrell *et al.*, 2001). At 1 h CDKA activity ±DEX was highest (Fig. 6A, early S-phase) but thereafter dropped. Only at 4 h was there a significant difference between treatments (1.4-fold) favouring CDKA +DEX (late S-phase, Fig. 6A). Hence, ±DEX CDKA activity was relatively constant although both dropped in G1.

At 1 h (early S-phase), CDKB activity was significantly higher

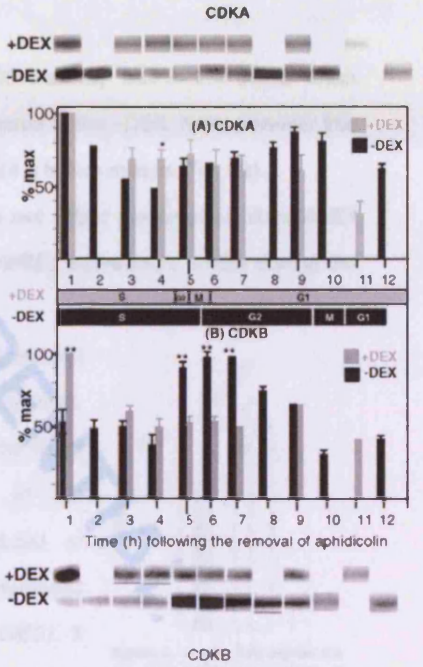

Figure 6. Nicta;CDKB1 kinase activity is premature when *Arath;WEE1* is expressed in BY-2 cells

Mean histone H1 kinase activities (±SE) of (A) CDKA ±DEX and (B) CDKB ± DEX. Immunoprecipitates in triplicate experiments were quantified as a percentage of maximum. Protein extracts for these assays were sampled from the same experiment used for generate mitotic index curves in Fig. 2 and phase durations are carried over. Between-treatment differences were assessed using the Student's t test: * $P < 0.05$, ** $P = 0.02$-0.05 Where error bars are absent, variation about the mean was <5%. (n=3). Above and below are gel images from one of the three replicates.

(1.92-fold) in +DEX compared with –DEX (Fig. 6B). Thereafter, CDKB +DEX fell to, and then levelled out at approximately 60% of max. until sample time 11 (late G1) when it decreased to 40% of max. Conversely, CDKB -DEX was low during early S-phase but peaked between 5-7 h (late S to mid G2), where it was significantly higher than the corresponding values in the +DEX treatment (1.63 – 1.96-fold, Fig. 6B).

Thus the major difference in CDK activity was in the CDKB which peaked prematurely in the +DEX compared to the –DEX. Note, however that in both +DEX and –DEX, CDKB peaked 4 h before mitosis (Fig. 6B).

Arath;WEE1 expression does not affect the level of Nicta;WEE1 expression but it perturbs the Nicta;WEE1 expression profile during the cell cycle

Premature entry into mitosis at a reduced cell size could be regulated at the transcriptional, protein or activity levels (or all three). Our initial hypothesis was that transcription of the *Nicotiana tabacum WEE1* was inhibited or suppressed when *Arath;*WEE1 was expressed resulting in overall reduced levels of *WEE1*. If so, a putative negative regulation of CDKs normally imposed by *Nicta;WEE1* would be removed. To test this hypothesis, we measured *Nicta;WEE1* expression in exponentially growing cells of inducible line 1 +DEX compared to WT using semi-quantitative RT-PCR and *Nicta;*WEE1 - specific PCR primers. The overlap of standard error bars between treatments

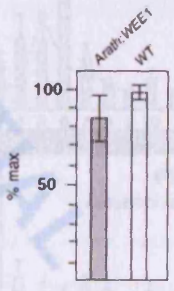

Figure 7. Mean (±SE) expression of *Nicta;WEE1* (percentage of max) by semi-quantitative RT-PCR in three day old cultures in BY-2 cells in which *Arath;WEE1* (+DEX) was induced for 12 h compared with wild type of comparable age. n = 3

indicates a null effect of *Arath;WEE1* transcripts on the level of *Nicta;WEE1* transcripts (Fig. 7). Hence, transcriptional silencing of *Nicta;WEE1* is a very unlikely mechanism by which *Arath;WEE1* expression was exerting its effects in BY-2 cells.

Next we tested whether the timing of *Nicta;WEE1* transcription was affected when *Arath;WEE1* was expressed during a synchronised cell cycle. Semi - quantitative RT-PCR charted the pattern of *Nicta;WEE1* tra nscription ± DEX, using *Nicta;WEE1*specific primers. This method has been validated in our lab. for obtaining patterns of gene expression from a variety of systems (Wagstaff *et al.* 2002; 2005; Parfitt *et al.*, 2005; Orchard *et al.*, 2005). Also, the *Arath;WEE1* expression was measured through the cell cycle using *Arath; WEE1* specific primers. Samples were taken from the same

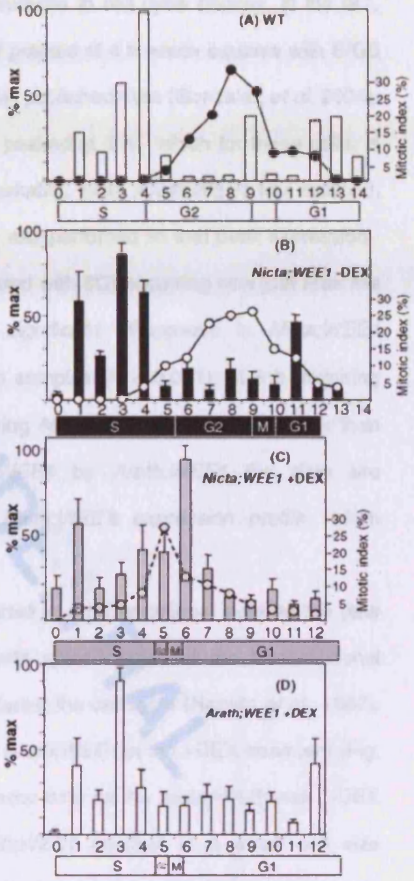

Figure 8. Expression of *Arath;WEE1* disrupts *Nicta;WEE1* expression profile during synchronised cell cycles. (A) WT (representative data and mitotic index), and mean expression level (±SE) (%max). (B) *Nicta;WEE1* – DEX;(C) *Nicta;WEE1* +DEX; (D) *Arath;WEE1* induced in BY-2 cells. Excluding 4 (A), n = > 3 and < 6. Line plots of mitotic index in (B) and (C), are from Fig. 2.

287 experiments / lines used for both histone H4 analysis and mitotic index scores
288 allowing us to relate transcriptional patterns to cell cycle phases. In the WT,
289 the expression profile of *Nicta;WEE1* peaked at 4 h which equates with S/G2
290 (Fig. 8a) and is highly comparable with published data (Gonzalez *et al.* 2004).
291 Minus DEX, *Nicta;WEE1* transcripts peaked at 3 h, which for these cells, is
292 mid-to-late S -phase (Fig. 8B). Remarkably, when *Arath;WEE1* was induced,
293 the pattern of *Nicta;WEE1* expression was perturbed so that peak expression
294 shifted from 3 to 6 h (Fig. 8B compared with 8C) occurring now just after the
295 mitotic peak. There were highly significant differences in *Nicta;WEE1*
296 transcription ±DEX in the 3 and 6 h samples ($P < 0.001$), at 3 h favouring
297 *Nicta;WEE1*-DEX, and at 6 h favouring *Nicta;WEE* +DEX. Thus, rather than
298 transcriptional inhibition of *Nicta;WEE1* by *Arath;WEE1* the data are
299 consistent with a perturbation of *Nicta;WEE1's expression profile* when
300 *Arath;WEE1* was expressed.
301 Induction of *Arath;WEE1* resulted in a transcriptional peak at 3 h (late
302 S-phase, Fig. 8D), in agreement with other studies of the transcriptional
303 pattern driven by the 35S promoter during the cell cycle (Nagata *et al.*, 1987).
304 Note that the transcriptional peak for *Arath;WEE1* in the +DEX treatment (Fig.
305 8D) occurred at approximately the same time as the *Nicta;WEE1* peak -DEX
306 (Fig. 8B). Since induction of *Arath;WEE1* resulted in a small cell size
307 phenotype we conclude that the mechanism for this perturbation is at least in
308 part due to a disruption of the normal pattern of native WEE1 transcription.

Expression of Arath;WEE1 in BY2 cells increases the overall amount of WEE1 protein.

One explanation for the aberrant results in the transformed cell line is that although transcripts of *Arath;WEE1* are produced, they are not translated. To test this hypothesis we raised an antibody to a peptide from the regulatory domain of the Nicta;WEE1 protein sequence (Fig 4). Although the antibody was raised to Nicta;WEE1 it does detect a single band of the correct MW for both Arabidopsis and tobacco WEE1 proteins on a Western blot (Fig 9A). The specificity of the antibody was further tested by expressing recombinant Nicta;WEE1 in *E. coli* (Fig 9B) WEE1 protein levels in a 3-day old culture of the induced *Arath;WEE1* cell line were

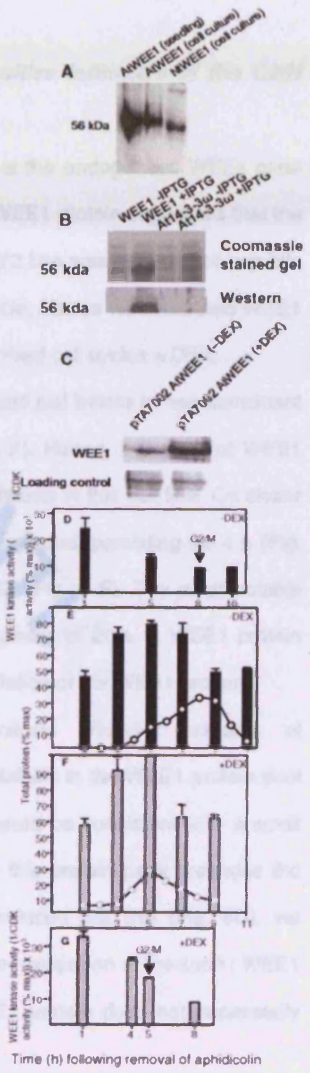

Figure 9. WEE1 antibody raised to Nicta;WEE1 also detects Arath;WEE1 on a Western blot of Arabidopsis and tobacco proteins (A) and identifies a specific band when *Nicta;WEE1* is expressed in *E.coli*, following induction of the recombinant protein with IPTG (B). *In vitro*-expressed At14-3-3omega protein is the negative control. There is a clear increase in the levels of WEE1 shown by Western blotting following induction with DEX in cultures expressing *Arath*;WEE1 under the DEX-inducible promoter (C).

Means (±SE) of total WEE1 protein (% max) -DEX and +DEX (E-F). Line plots of mitotic indices are indicated on the same y-axis. Above (D) and below (G) are mean (± S.E.) WEE1 kinase activities as the reciprocal of the CDK activity on histone H1 following the addition of pulled down WEE1 (where error bars are absent, variation about the mean was <1%) The G2/M transition is extrapolated from the peak of the mitotic index in both cases. n = 2

compared to levels prior to induction (Fig 9C), and there is a clear increase in Wee1 protein (approximately four fold) in the induced culture. Thus, expression of the *Arath;WEE1* gene does contribute to increased levels of WEE1 protein.

WEE1 protein and kinase levels are sensitive indicators of the G2/M transition

The changes in transcriptional timing of the endogenous WEE1 gene coupled with an overall increase in levels of WEE1 protein suggested that the unexpected phenotype of the *Arath;WEE1* BY2 line was because of a subtle regulation of WEE1 levels through the cell cycle. Hence we measured WEE1 protein and kinase activity during the synchronised cell cycles ± DEX.

Plus or minus DEX, WEE1 protein peaked just before or was coincident with the peak of the mitotic index (Fig. 9 E-F). Hence, the peak of WEE1 protein is a sensitive marker of the onset of mitosis in this cell line. On closer inspection, note that the protein peak –DEX is broad, persisting for 4 h (Fig. 9E) whereas it lasts only for about 2 h +DEX (Fig. 9 F). The most notable differences to the –DEX treatment were increases of 20% in WEE1 protein levels at 3h and 5h, and an anticipated degradation of the WEE1 protein.

One explanation for precocious mitosis following induction of *Arath*;WEE1 might be that this triggers an instability in the WEE1 protein pool resulting in its premature destruction. This would be consistent with a small cell size and shortened G2. Moreover, since this protein peak precedes the major peak of *Nicta;WEE1* mRNA in the induced cell line (Fig. 8C), we conclude that the protein peak is mainly due to expression of the*Arath* ; WEE1 in this treatment. However presence of WEE1 protein does not necessarily

352 equate to WEE1 activity since most cell cycle proteins are post-translationally
353 regulated. We therefore assayed WEE1 kinase activity by measuring CDK
354 activity in $psuc^{13}$- precipitated CDK, challenged with antibody-precipitated
355 WEE1. We calculated mean WEE1 kinase activity as the reciprocal of CDK
356 activity following the protocol of McGowan and Russell (1995). Sampling
357 times were chosen to coincide with early S-phase and G2/M ±DEX.
358 Minus DEX, WEE1 kinase activity was maximal in early S-phase (1 h)
359 falling by about a half at 5 h (S/G2) and was minimal at 8 h (G2/M) and 10 h
360 (M) (Fig. 9D). Thus in the absence of transgene expression there is a logical
361 and temporal order to a fall in WEE1 protein level, a fall in WEE1 kinase
362 activity, an increase in CDKB activity and the entry of cells into mitosis. Note
363 however that the fall in kinase activity precedes the fall in WEE1 protein levels
364 suggesting an inactivation of the enzyme prior to its degradation.
365 Plus DEX, WEE1 kinase activity decreased as the cell cycle
366 progressed from early S-phase (1 h) to late G2 (4 h), to G2/M (5 h) through to
367 G1 (8 h) (Fig. 9G). Hence again entry into mitosis was accompanied by a fall
368 in both WEE1 protein and WEE1 kinase levels.
369

Discussion

CDK and WEE1 activity

We report the unusual occurrence of a small cell size phenotype resulting from the induction of *Arath;WEE1* in tobacco BY-2 cells. In so doing we provide compelling evidence that WEE1 is a plant cell cycle regulatory gene. Furthermore WEE1 kinase activity falls at 5 h (late S) as CDKB activity rises. Hence it is inversely proportional to CDKB but not CDKA activity as proliferative cells traverse a synchronised cell cycle in a remarkably similar fashion to human WEE1 and human CDK1 (McGowan and Russell, 1995; see Fig. 10). In the –DEX treatment, the CDKA and CDKB profiles are also remarkably similar to those reported in wild type (Sorrell et al., 2001). In other words, we confirm a cell cycle dependent regulation of CDKB in G2 whilst CDKA activity is relatively constant for the whole of G2 although highest in early S-phase and G2/M (Fig. 10). Nevertheless, our data show that CDKA is active during

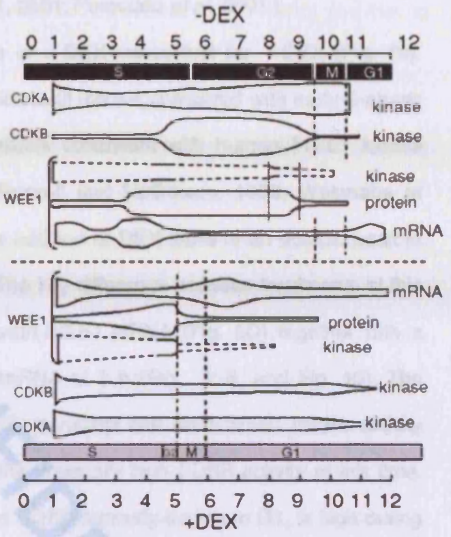

Figure 10. Profile of CDK A, CDKB and WEE1 kinase activity during the cell cycle together with *Nicta;WEE1* mRNA and protein levels in the *Arath;WEE1* inducible cell line ± DEX. Note that in the – DEX treatment, onset of mitosis was an hour earlier in the WEE1 kinase and protein experiment compared with the CDK measurements (see Figs. 3, 5 and 8). WEE1 kinase profiles are projected activities between intermittent sampling times used to coincide with G2/M in each treatment (see Fig. 8)

394 cell cycle progression from G2 to mitosis in agreement with earlier findings in
395 BY-2 wild type cells (Sorrell *et al.*, 2001; Porceddu *et al*, 2001).
396 The WEE1 kinase profile in + DEX mirrorsthat for –DEX (Fig. 10).
397 Hence, WEE1 kinase activity is lower at mitosis compared with early S-phase
398 and WEE1 protein drops at mitosis consistent with human WEE1 kinase
399 activity during the cell cycle (Russell and McGowan, 1996; Watanabe et
400 al.1995). One hour following the addition of DEX there is an ectopic peak in
401 CDKB activity (Fig. 6; Fig. 10). The key difference between treatments at this
402 time is a substantial level of *Arath;WEE1* mRNA (Fig. 5D) together with a
403 substantial level of *Nicta;WEE1*mRNA at 1 h (Fig. 8 B, and Fig. 10). The
404 additional presence of Arath;WEE1 transcript and Arath;WEE1 kinase activity
405 (see Fig. 9 A-C) coincides with the unusually high CDKB activity at this time.
406 Note that transcription of tobacco CDKB normally begins in G1, is high during
407 S-phase and maximal in G2 whilst CDKB activity peaks in G2 (Fig. 10; Sorrell
408 *et al.*, 2001). These transcriptional and translational patterns fit well with our
409 recorded CDKB activity –DEX treatment. Hence, when DEX is added, rapid
410 *Arath;WEE1* expression could perturb the system that normally ensures
411 CDKB activity does not begin until S/G2. The mechanism of this CDKB
412 release in early S-phase must be complex perhaps involving Arath;WEE1
413 kinase competing with Nicta;WEE1 for the CDKB substrate and perhaps
414 involving perturbation of a network of regulatory proteins that normally
415 negatively regulates CDKB at this time. Proteins known to be both negative
416 regulators of the G1/S transition and expressed strongly at this time include:
417 Rb, KRP 6 and 7 (Menges *et al.*, 2005). Rb is a suppressor of the S-phase
418 E2F transcription factors and KRPs negatively regulate CDK activity in G1

419 (reviewed by Francis, 2007) including CDKB (Nakai *et al.*, 2006). Full
420 knowledge of the proteins involved in such complexes clearly requires a
421 proteomic analysis.
422 In Arabidopsis, WEE1 kinase can phosphorylate CDKA;1 at tyr15, *in vitro*
423 (Shimotohno *et al.*, 2001), and most recently, it binds CDKB in a 2-hybrid
424 assay (our lab, unpublished data) and can also phosphorylate CDKB types
425 (Umeda pers comm.) suggesting a phoshoregulatory role of WEE1 kinase in
426 the cell cycle. However, our data are at odds with the finding that Arabidopsis
427 WEE1 KOs develop without an obvious phenotype making WEE1 redundant
428 in a normal cell cycle (de Schutter et al., 2007). Clearly, the differences may
429 be because we are comparing cell cycle results from cultured tobacco cells
430 with *Arabidopsis* seedlings. However, we have observed subtle phenotypic
431 effects in *Arabidopsis* WEE1 T-DNA insertion lines (Lentz et al., unpublished
432 data) suggesting much more needs to be understood about the G2/M
433 transition.

Cell size

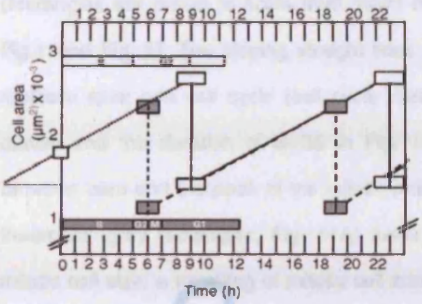

Figure 11A. Premature cell division in i-*Arath;WEE1* +DEX, but constant cell growth rates ± DEX.
White and grey rectangles represent mitotic cell size (plotted to scale from Fig. 1) with an equal partition at the beginning of the next cell cycle, in i-*Arath;WEE1* (-DEX) and i-*Arath;WEE1* (+DEX) , respectively. The dotted line extrapolates to the birth of two new -DEX cells of the previous cell cycle. The sloping lines connecting newly born and mitotic cells, span one cell cycle (plotted to scale data from Fig.2). Cell cycle phases (from Fig. 2) are given as horizontal bars, black on white, i-*Arath;WEE1* (- DEX) white on grey, *i-Arath;WEE1* (+ DEX).

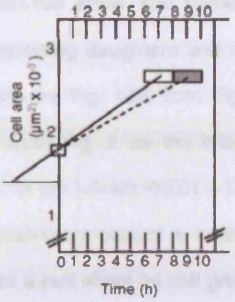

Figure 11B Over expression of *NictaWEE1* slows cell growth rate

Cell growth rates in BY-2 cells in a Nicta:WEE1 DEX-inducible line -DEX (white boxes and solid line, or +DEX (grey box, dotted line) based on the timing of mitosis and measurements of mitotic cell size. (data from Fig. 9)

Typically, *Arath;WEE1*^{OE} both in Arabidopsis and in fission yeast induces an over-expressing WEE1 phenotype of long cell length (Sorrell *et al.*, 2002). Either constitutive or inducible expression of *Arath;WEE1* in tobacco resulted in a small cell size but cell cycle length remained remarkably constant compared with wild type and empty vector. Notably, tomato plants expressing *WEE1* in anti-sense orientation also exhibited a short G2 and a reduced cell size (Gonzalez *et al.*, 2007) which is consistent with a role for WEE1 in determining cell size at division.

Figure 11 depicts models of cell growth rate based on cell size and mitotic cycle times ± DEX treatment. The white rectangles connected by

445 vertical lines portray mitotic cells that generate two identical daughters
446 (rectangles are drawn to scale from mean mitotic cell areas, first shown in
447 Fig.1 and Fig. 5). The sloping straight lines connecting daughters and new
448 mothers span one cell cycle (cell cycle durations for Fig. 11A from Fig. 2
449 curves and the duration of S+G2 in Fig. 11B from Fig. 5 as the interval
450 between zero and the peak of the mitotic index). In the i-*Arath;WEE1* + DEX
451 treatment (grey rectangles, Fig. 11A) these parameters predict a smaller
452 mitotic cell size, a resetting of mitotic cell size but a null effect on cell growth
453 rate (Fig. 11A) In the Nicta;WEE1^{oe} line, the data are more consistent with a
454 slower growth rate of these cells from S-phase to G2/M (Fig. 10B). In fission
455 yeast, a size control operates where large cells at birth required less growth to
456 achieve critical size (Fantes, 1977; Fantes and Nurse, 1977). Our model
457 predicts a "sizer" mechanism that operates independently of cell growth rates
458 rather like fission yeast (Fantes and Nurse, 1977).

459 Interestingly, the lengthening of G2 when *Nicta;WEE1* was over
460 expressed matches a similar lag when tomato *Solly;WEE1* was expressed
461 constitutively in BY-2 cells (Gonzalez *et al.*, 2007). They reported an increase
462 in cell size but this was for both mitotic and interphase cells non-sycnhronised
463 cultures but the error bars overlapped in their data. In our view, their cell size
464 data are more consistent with a null effect of *Solly;WEE1* on cell size in BY-2
465 cells. Interestingly, tomato WEE1 is more closely related to tobacco WEE1
466 than Arabidopsis WEE1 (see Fig. 3)

467 In conclusion, we present data consistent with a role for WEE1 in the
468 normal plant cell cycle in tobacco BY2 cells. We also discovered an inverse
469 relationship between WEE1 and CDKB activities strongly suggesting that in

the normal BY-2 cell cycle, CDKB kinase is negatively regulated by WEE1 kinase. Furthermore a major feature of the *Arath;WEE1*-induced response, is an anticipation in the activity of CDKB that precedes the onset of mitosis approximately 4 hours later. This suggests that the timing of CDKB activity is a key regulator of entry into mitosis in plant cells. The unusual induction of a small mitotic cell size observed only when *Arath;WEE1* was expressed in BY-2 cells provides evidence that perturbations in WEE1 affect both cell cycle progression and cell size. A better understanding of its role in protein complexes in G2 and G2/M will help to unlock the sensitive mechanisms that regulate the timing of mitosis in relation to cell size and other cellular factors.

Experimental procedures

Cloning Nicta;WEE1

Degenerate primers were designed on a comparison of the maize *ZmWEE1* (accession number: AAD52983) and *Arath;WEE1* (accession number: CAD28679) sequences: WEE1F TCKTGGTTYGARAAYGARCA and WEE1R AGAGAAGATRTCNACYTTRTC and used to amplify a 339 bp fragment of *Nicta;WEE1* from *Nicotiana tabacum* var. Samsung genomic DNA, thermocycle conditions: 35 cycles of 95 °C (1 min), 60 °C (1 min), 72 °C (1min). The PCR product was cloned in pGEM T-Easy (Promega, Southampton, UK) and sequenced. The whole open reading frame was obtained with one cycle of 3' RACE and two cycles of 5' RACE (using the BD SMART™ RACE cDNA amplification Kit, Clontech).These sequences were deposited in the EMBL data bank with accession nos.: AJ866274, AJ866275, AJ866276, AJ866277. The entire ORF was amplified using PCR primers:

Ntwee1XhoI: CGAGATGAAGAGGAAAACCCTAGGCCT and Ntwee1 Spe1B:GCACACTAGTTTACTTGTTAGCATTTC, from BY-2 cDNA and cloned into pTA7002 by digestion with Xho1/Spe1. The ORF was fully sequenced (EMBL data base accession no.AM408785). Clustal W within DNAstar (Lasergene), BIOEDIT version 7.0.1 (Hall 1999) and MEGA software version 3.1 (Kumar *et al.* 2004) were used to compare the tobacco ORF to other WEE1 sequences.

Constructs and transformation into BY-2 cells and Arabidopsis

The *Arath;WEE1* open reading frame was PCR amplified using primers P35SX (5'-AGGCCCCGGCTCGAGATGTTCGAGAAGAACGG-3') and P36SS (5'GCACACTAGTCGACTCAACCTCGAATCCTAT-3') and cloned into the Bin Hyg TX vector (Gatz *et al.*, 1992) using *Sma* I/*Sal* I restriction sites. The same PCR product was also cloned into the inducible vector pTA7002 (Aoyama and Chua, 1997) using *Xho* I/*Spe* I. Individual clones were sequenced and a clone for each construct in which the amino acid sequence was intact was chosen for further work. Stable transformation of BY-2 cells was achieved using a modified version of the method described by An (1985) with the addition of 20 µM Acetosyringon (Sigma-Aldrich) during co-cultivation of the *Agrobacterium* (LBA4404) with the BY-2 cells. Transformants were selected on solidified BY2 medium (0.8% agar) supplemented with 250 µg/ml Timentin and 80 µg/ml hygromycin. Calli were cultured in 50 ml BY-2 medium, 250 µg/ml Timentin and 80 µg/ml hygromycin until stationary phase (1 – 3 weeks). Cells were sub-cultured at least four times before being used in synchrony experiments.

519 The same Bin Hyg TX construct was transformed into Arabidopsis using
520 *Agrobacterium* (GV3101 Vir G^{++}) mediated floral dip method (Bent and
521 Clough, 1998). Two independent lines expressing *Arath;WEE1* (checked by
522 RT-PCR, data not shown), were selected for the cell length measurements.
523 Epidermal root meristem cells were visualised by Feulgen staining (Francis *et*
524 *al.*, 1995), and images captured digitally from an Olympus BH2 microscope.
525 Cell lengths were determined from images using Sigmascan software.
526 *Semi-quantitative RT-PCR*
527 Total RNA was extracted from BY-2 cells using TRI reagent (Sigma Aldrich,
528 Gillingham, UK) and residual genomic DNA removed by DNase treatment
529 (Ambion, Austin, Tex., USA). RNA (5 µg) was reacted with Superscript II
530 reverse transcriptase (GIBCO, Paisley, UK). To measure *Arath;WEE1*
531 expression, primers were designed which do not amplify the endogenous
532 tobacco WEE1 gene (*Nicta;*WEE1): *Arath*WEE1F:
533 AGCTTGTCAGCTTTGCCT and *Arath*WEE1R:
534 GTGCATCTCCTTCTTCTACT. Thermocycle conditions were: 35 cycles of 95
535 °C (1 min), 55 °C (1 min), 72 °C (1 min). Two sets of specific primers for
536 *Nicta;WEE1:* (*Nicta;*WEE1F: 5'-CCAAATGGAGCTCTGTGACC and
537 *Nicta;*WEE1R: 5'-CTCTTCGATCGGCTGGCTCTTA; NtWEE1F3: 5'-
538 AGGGGTAGCTCATTTAGA and NtWEE1TOTR: 5'-
539 TGGCAAAAGTAGCACCATCA) were used to analyse expression of the
540 endogenous tobacco WEE1 gene, *Nicta;WEE1* (Tm = 60 °C and 55 °C
541 respectively). The first set was used for the quantification of *Nicta;WEE1*
542 expression in synchronised cells while the second set were used to quantify
543 expression in exponential phase cultures. For detection of *Nicta;WEE1*

544 transgene expression only, a primer was designed to bind to the vector
545 sequence: (35STRS 5'-ACGCTGAAGCTAGTCGACTC) and used in
546 conjunction with NtWEE15R 5'-TTATCCCCATCGGCAGCATCAG.
547
548 Histone H4 primers (H4F: 5'-GGCACAGGAAGGTTCTGAGGGATAACA and
549 H4R: 5'-TAACCGCCGAAACCGTAGAGAGTCC) were used to verify cell cycle
550 stage, and primers to 18S rRNA: PUV2 5'-TTCCATGCTTAATGTATTCAGA
551 and PUV4, 5'-ATGGTGGTGACGGGTGAC were used as a control (Orchard
552 *et al.*, 2005) (Tm = 60°C). Thermocycle conditions were as above.
553 For all semi quantitative RT-PCRs, cycle number was reduced and optimised
554 so that product amount was proportional to input amount of total RNA. This
555 was verified with a dilution series of cDNA in each PCR experiment. Three
556 replicate PCRs were performed for each primer set and products quantified
557 from ethidium bromide stained agarose gels using GeneGenius (Syngene,
558 Cambridge, UK).
559 *Cell cycle and cell size measurements*
560 Cultures were synchronised using aphidicolin as described previously (Francis
561 et al, 1995). After release from aphidicolin, 100 µl samples were taken at
562 hourly intervals for 24 h and mixed immediately with 5 µl of Hoechst stain
563 (Bisbenzimide, Sigma, 100 µg/ml in 2% (v/v) Triton X-100). The mitotic index
564 was derived from scoring at least 300 cells per slide in a random transect
565 visualised using a fluorescence microscope (Olympus BH2, UV, λ = 420 nm).
566 Digital images were analysed using Sigmascan®. Mitotic cell area was
567 measured for approximately 300 cells per sample from both exponential
568 phase and throughout synchronised cell cycles.

569 *Histone kinase assays*

570 Proteins were extracted from 5 ml of synchronised cultures and assayed
571 (Cockcroft *et al.* 2000). Immunoprecipitations were carried out using antisera
572 raised to Nicta;CDKA;1 and Nicta;CDKB1 as described in Sorrell *et al.* (2001).
573 H1 protein kinase assays were as described in *Cockcroft et al.* (2000) using
574 2μl of antiserum. Incorporation was assayed by quantitation of
575 autoradiographs using GeneGenius (Syngene, Cambridge, UK).

576 *WEE1 protein and kinase assays*

577 Using the *Arath;WEE1*- inducible line 1, following synchronisation with
578 aphidicolin (see above), 5 ml of cells were sampled at times coinciding with
579 early S-phase, G2/M and mitosis (± DEX) and assayed essentially as
580 described in Cockcroft et al. (2000); new mitotic index plots were made for this
581 experiment. For Western blotting, NtWEE1 antibody was used at 1:1000
582 dilution. For the WEE1 kinase assays, 5 μL of Nicta;WEE1 antibody was used
583 for immunoprecipitating WEE1 from protein extracts in samples obtained from
584 the synchronies. The immunoprecipitate was mixed with CDKs purified from
585 protein extracts from wild type BY2 cells using $p13^{SUC1}$ beads (Upstate, New
586 York) in a kinase assay buffer. As with the CDKA and CDKB assays,
587 incorporation of ^{32}P was assayed by quantitation of autoradiographs using
588 GeneGenius (Syngene, Cambridge, UK).

589 *Expression and purification of recombinant proteins*
590
591 The *Nicta;WEE1* and *Arath;14-3-3ω* ORFs were PCR amplified using
592 *WEE1*FW (5'- ATGGAAGCTTCATATGATGAAGAGGAAAAC CC-3'),
593 *WEE1*RV (5'- ATGGATCCTTACTTGTTAGCATTTCTTTGACAT-3'), *14ω*FW
594 (5'- ATGGAAGCTTCATATGATGGCGTCTGGGCGTG-3') and *14ω*RV(5'-

595 ATGGATCCTCACTGCTGTTCCTCGGTCG-3') cloned into the pET15B vector
596 (Novagen) using *Nde*I/*Bam*HI resulting in an in-frame N-terminal fusion of
597 *Nicta;WEE1* and *Arath;14-3-3ω* ORFs, respectively, to the HIS_6-tag of the
598 pET15B vector. Correct insertions of the ORFs were confirmed by sequencing
599 plasmids transformed into *E. coli* DE3 Rosetta pLysS cells (Invitrogen).
600 Overnight cultures were diluted 1:20 into LB medium containing 50 µg/mL
601 ampicillin and grown to OD_{600} of 0.4 at 37°C. Adding isopropyl-1-thio-β-D-
602 galactopyranoside (IPTG) to a final concentration of 0.5 mM IPTG induced
603 protein expression. Cultures were incubated overnight at 22°C. Harvested
604 cells were resuspended in 2 mL lysis buffer (50 mM NaH_2PO_4, 300 mM NaCl,
605 10 mM imidazole pH 8.0). The His_6-tagged recombinant proteins were purified
606 using Novagen His -Bind® Kit manual (Novagen). Cells were adjusted to 1
607 mg/mL lysozyme and incubated on ice for 1 h, lysed by sonication (3 x 30 s
608 bursts) and the soluble protein fraction recovered by centrifugation at 4°C for
609 30 min at 15000g. His-beads (100 µL) were added to the supernatant and
610 incubated for 30 min at 4°C with rotation followed by centrifugation at 4°C (3
611 min at 3000g). The beads were washed (x 3) with 1 mL wash buffer (0.25 M
612 NaCl, 30 mM Imidazole, 10 mM Tris-HCl pH 7.9) and after the final wash
613 resuspended in 50 µL elution buffer (0.25 M NaCl, 0.5 M Imidazole, 10 mM
614 Tris-HCl pH 7.9) and incubated for 20 min at 4°C with rotation followed by
615 centrifugation at 4°C for 3 min at 3000g. Recombinant proteins were analyzed
616 by SDS-PAGE and Western blotting.
617 *Dexamethasone inductive conditions*
618 Induction of transgenes was achieved by addition of DEX (Sigma, UK) to a
619 final concentration of between 1 µM and 30 µM. Induction of *Arath*;WEE1 was

620 achieved using 1 μM DEX, while for the *Nicta*;WEE1 lines 30 μM were used.
621 DEX was added immediately following release from the aphidicolin block for
622 synchronised cells, and three days after subculture for assays on
623 exponentially growing cultures.

624 **Acknowledgements**

625 IS and NS thank the University of Calabria for an international research award
626 (borsa di specializzazione all'estero per giovani ricercatori), IS, AL and NS
627 thank Cardiff University and University College Worcester for seed corn
628 funding and research studentships. We also thank Dr. M. Menges and Prof.
629 J.A.H. Murray (Cambridge University) for CDK antibodies, and G. Lewis, S.
630 Hope and S. Turner for sequencing.

631 **References**

632 **An, G.H.** (1985) High-efficiency transformation of cultured tobacco cells. *Plant*
633 *Physiol.* **79**,568 -570.
634 **Aoyama, T. and Chua, N.H.** (1997) A glucocorticoid-mediated transcriptional
635 induction system in transgenic plants. *Plant J* **11**, 605-612
636 **Clough, S.J. and Bent, A.F.** (1998) Floral dip: a simplified method for
637 Agrobacterium-mediated transformation of *Arabidopsis thaliana*. *Plant*
638 *J.* **16**, 735-743.
639 **Cockcroft, C.E., den Boer, B.G., Healy, J.M.S. and Murray, J.A.H.** (2000)
640 Cyclin D control of growth rate in plants. *Nature*, **405**, 575-579.
641 **De Schutter, K., Joubes, J., Cools, T., Verkest, A., Corellou, F.,**
642 **Babiychuk E., Can Der Scheren, E., Beeckman, T., Kushnir, S.,**
643 **Inze, D. and De Veylder, L.** (2007) Arabidopsis WEE1 kinase controls

644 cell cycle arrest in response to activation of the DNA integrity
645 checkpoint. *Plant Cell* 19: 211-225.
646 **DeWitte W., and Murray, J.A.H.** (2003) The plant cell cycle. *Ann. Rev. Plant*
647 *Biol.* **54**, 235-264.
648 **Fantes, P.A.** (1977). Control of cell size and cycle time in
649 Schizosaccharomyces pombe. *J. Cell Sci.* **24**, 51-67.
650 **Fantes, P.A. and Nurse, P.** (1977). Control of the timing of cell division in
651 fission yeast. Cell size mutants reveal a second control pathway. *Exp.*
652 *Cell Res.* **115**, 317-329 .
653 **Francis, D. (2007)** The plant cell cycle, 15 yr on. *New Phytol.* **174**, 261-278.
654 **Francis, D., Davies, M.S., Braybrook A., James NC., and Herbert, R.J.**
655 (1995). An effect of zinc on M-phase and G1 of the plant cell cycle in
656 the synchronous TBY-2 tobacco cell suspension. *J. Exp. Bot.* **46**, 1887-
657 1894.
658 **Gatz, C., Frohberg, C. and Wendenberg, R.** (1992) Stringent repression and
659 homogenous derepression by tetracycline of a modified CaMV 35S
660 promoter in intact transgenic tobacco plants. *Plant J.* **2**, 397-404.
661 **Gonzalez, N., Hernould, M., Delmas, F., Gevaudant, F., Duffe, P., Causse,**
662 **M., Mouras, A. and Chevalier, C.** (2004). Molecular characterization
663 of a WEE1 gene homologue in tomato (Lycopersicon esculentum Mill.).
664 *Plant Mol Biol* **56**, 849–861
665 **Gonzalez N., Ge´ vaudant F, Hernould, M., Christian Chevalier C. and**
666 **Armand Moura, A.** (2007). The cell cycle-associated protein kinase
667 WEE1 regulates cell size in relation to endoreduplication in developing
668 tomato fruit. *Plant Journal* **51**, 642–655

669 **Gould, K.L. and Nurse, P.** (1989) Tyrosine phosphorylation of the fission
670 yeast cdc2 protein kinase regulates entry into mitosis. *Nature*, **342**, 39-
671 45.
672 **Hall, T.A.**, (1999) BioEdit: a user-friendly biological sequence alignment editor and
673 analysis program for Windows 95/98/NT. *Nucleic Acids Symp Series* **41**,
674 95-98.
675 **Joubes, J., Chevalier C., Dudits, D., Heberle Bors, E., Inze, D., Umdea, M.**
676 **and Renaudin, J.P.** (2000) CDK-related protein kinases in the plant
677 cell cycle. *Plant Mol. Biol.* **43**, 607-620.
678 **Krek, W. and Nigg, E.A.** (1991). Differential phosphorylation of vertebrate $p34^{cdc2}$ at
679 the G1/S and G2/M transitions of the cell cycle: identification of major
680 phosphorylation sites. *EMBO J.* **10**, 305-316.
681 **Kumar, S., Tamura, K., and Nei, M.**, (2004). MEGA3: Integrated software for
682 Molecular Evolutionary Genetics Analysis and sequence alignment. *Briefings in*
683 *Bioinformatics* **5**, 150-163.
684 **Lee, J., Kumagai A., and Dunphy, W.G.** (2001). Positive regulation of Wee1
685 by Chk1 and 14-3-3 proteins. *Mol. Biol. Cell* **12**, 551-563.
686 **Menges, M., de Jager, S.M., Gruissem, W, Murray, J.A.H. (2005).** Global
687 analysis of the core cell cycle regulators of Arabidopsis identifies novel
688 genes, reveals multiple and highly specific profiles of expression and
689 provides a coherent model for plant cell cycle control. *Plant Journal* **41**,
690 546–566.
691 **McGowan, C.H. and Russell, P.** (1995). Cell cycle regulation of human
692 WEE1. *EMBO J.* **14**, 2166 2175.

693 **Nachtwey, D.S. and Cameron, J.L.** (1968) Cell cycle analysis. In: Methods
694 in Cell Physiology, vol.3, Prescott, D.M. ed.). Academic Press:New
695 York. Pp 213-259.
696 **Nakai T. Kato, K., Shinmyo A. and Sekine, M.** (2006) Arabidopsis KRPs
697 have distinct inhibitory activity toward cyclin D2-associated kinases,
698 including plant-specific B-type cyclin-dependent kinase *FEBS Letters*
699 **580, 336-340.**
700 **Nurse, P.** (1990) Universal control mechanism regulating onset of M-phase.
701 *Nature*, **256**, 547-551.
702 **Nurse, P. and Bisset, Y.** (1981). Gene required in G1 for the commitment to
703 the cell cycle in G2 for control in mitosis in fission yeast. *Nature* **292**,
704 558-560.
705 **Orchard, C.B., Siciliano, I., Sorrel, D.A., Marchbank, A., Rogers, H.J.,**
706 **Francis, D., Herbert, R.J., Suchomelova, P., Lipavska, H., Azmi, A.,**
707 **and Van Onckelen, H.** (2005). Tobacco BY-2 cells expressing fission
708 yeast cdc25 bypass a G2/M block on the cell cycle. *Plant J.* **44**,290 -
709 299.
710 **Parfitt, D., Herbert, R.J., Rogers, H.J., and Francis D.** (2004). Differential
711 expression of putative floral genes in Pharbitis nil shoot apices on
712 glucose compared with sucrose. *J. Exp Bot.* **55**, 2169-2177.
713 **Porceddu A., Stals H., Reichheld J.P., Segers G., De Veylder L., Barroco**
714 **R.P., Casteels, P., Van Montagu, M., Inze, D., Mironov, V.** (2001) A
715 plant-specific cyclin-dependent kinase is involved in the control of G2/M
716 progression in plants. *J.I Biol.I Chem.* **276**, 36354-36360

717 **Rothblum-Oviatt, C.J., Ryan, C.E., and Piwcnica-Worms, H. (2001).** 14-3-
718 binding regulates catalytic activity of human Wee1 kinase. *Cell Growth*
719 *and Differentiation* **12**, 581-589.
720 **Russell, P. and Nurse, P.** (1987) Negative regulation of mitosis by *wee1*$^{+}$, a
721 gene encoding a protein kinase homologue. *Cell*, **49**, 559-567.
722 **Shimotohno, A., Umeda-Hara, C , Bisova, K , Uchimiya, H , Umeda, M.**
723 (2004) The plant-specific kinase CDKF;1 is involved in activating
724 phosphorylation of cyclin-dependent kinase-activating kinases in
725 Arabidopsis. *Plant Cell* **16**, 2954-2966.
726 **Sorrell D.A., Menges M., Healy J.M.S., Deveaux Y., Amano C., Su Y.,**
727 **Nakagami H., Shinmyo A., Doonan J.H., Sekine M., and Murray**
728 **J.A.H.** (2001) Cell cycle regulation of cyclin-dependent kinases in
729 tobacco cultivar bright yellow-2 cells. *Plant Physiol.* **126**, 1214-1223.
730 **Sorrell D.A., Marchbank A., McMahon, K., Dickinson, J.R., Rogers, H.J.**
731 **and Francis, D.** (2002) A WEE1 homologue from *Arabidopsis thaliana*.
732 *Planta*, **215**, 518-522 .
733 **Sun, Y., Dilkes, B.P., Zhang, C., Dante, R.A., Carneiro, N.P., Lowe, K.S.,**
734 **Jug, R., Gordon-Kamm. W.J. and Larkins, B.A.** (1999)
735 Characterization of maize (*Zea mays* L.) Wee1 and its activity in
736 developing endosperm. *Proc. Nat. Acad. Sci. U.S.A.* **96**, 4180 4185.
737 **Tominaga, Y., Tominaga, Y., Cuiling L., Rui-Hong C.,Wang, R-H. and**
738 **Chu-Xia Deng C-X.** (2006) Murine Wee1 Plays a Critical Role in Cell
739 Cycle Regulation and Pre-Implantation Stages of Embryonic
740 Development. *Int. J. Biol. Sci.* **2**,161-170.

741 **Wagstaff, C., Leverentz, M. K., Griffiths, G., Thomas, B., Chanasut, U.,**
742 **Stead, A. D. and. Rogers, H. J.** (2002) Protein degradation during
743 senescence of *Alstroemeria* petals *J. Exp. Bot.* **53**,233 -240.
744 **Wagstaff, C., Malcolm P., Rafiq, A., Leverentz, M., Griffiths, G., Thomas,**
745 **B., Stead, A., and Rogers, H.J.** (2003) Programmed Cell Death (PCD)
746 processes begin extremely early in *Alstroemeria* petal senescence.
747 *New Phytol.* **160**, 49-59.
748 **Watanabe, N., Broome M. and Hunter, T.** (1995) Regulation of the human
749 WEE1Hu CDK tyrosine 15-kinase during the cell cycle. *EMBO J.* **14**, :
750 1878–1891.

751 **Figure Legends**

752 **Figure 1.** Constitutive or induced expression of *Arath;WEE1* in BY-2 cells
753 results in a small mitotic cell size. **(B)** *Arath;WEE1* expression in line 1
754 induced by Dexamethasone (DEX), first detected after 15 min of DEX
755 **(C)** Mean mitotic cell area (µm2 ±SE) in wild type (WT), constitutively (c)
756 expressing WEE1 lines: 2, 6 and 10, empty vector (EV), inducible (i) lines 1
757 and 6 ±DEX and corresponding empty vector line EV-i-1 (n=300) . Below is a
758 matrix that compares all treatments by t-tests. Shaded boxes mark the strictly
759 valid statistical comparisons. *p <05, **P <0.01, ***<0.001, ns not significant.
760 There were no significant differences in mitotic cell size within treatments
761 **Figure 2.** Constitutive or inducible Arath;WEE1 expressing BY-2 cells have a
762 short G2.
763 Mitotic indices following synchronisation with and removal of aphidicolin **(A)** :
764 constitutive (c) - *Arath; WEE1* line 10 (-----) and its corresponding Empty
765 Vector (EV-c-10) (♦ solid lines). ⇩↓ mark cell cycle durations for
766 constitutively expressing *Arath;WEE1* and EV line 10, respectively;
767 representative data from replicate experiments. **(B)** in the inducible (i)- *Arath;*
768 *WEE1* line 1 +DEX (grey dashed lines) or -DEX (black lines) at time 0. arrows
769 mark the cell cycle times; representative data from replicate experiments.
770 BY2 cells blocked in late G1 and S-phase by aphidicolin and then released
771 show an initial rise in the curve when cells trapped at the end of S-phase
772 during the aphidicolin block, are the first to traverse G2 and enter mitosis
773 following removal of the block. The first peak is when the bulk of
774 synchronised cells enter mitosis; this point in time minus S-phase is an
775 alternative measure of G2. Either way, G2 is less than 1 hour in the +DEX

776 treatment, and 4 h -DEX. Above and below cell cycle plots for the inducible
777 lines, are mean histone H4 expression profiles from semi quantitative RT-
778 PCR as percentages of maximum expression ± DEX, used to calculate S-
779 phase (4.5 h +DEX, 5.5 h –DEX). SEM was <3 %. throughout (n=3). M-phase
780 duration was calculated from the average mitotic index for each treatment (M)
781 using formulae of Nachtwey and Cameron (1968) which account for
782 exponential growth: dM= C/ln2 x ln (M+1). G1 is calculated by difference. All
783 phase durations are in hours rounded up or down to the nearest 0.5 h

i-Arath;WEE1	S-phase	G2	M	G1	C
+ DEX	4.5	0.5	1	7	13
- DEX	5.5	4.0	1	1.5	12

784
785
786 **Figure 3.** Phylogenetic tree showing relationship between the six available
787 higher plant and two algal WEE1 sequences.

788
789 The tree was constructed using the Neighbour-joining algorithm, boot strap
790 values are indicated above branches. Nicta;WEE1, *Nicotiana tabacum* ,
791 Zeama;WEE1, *Zea mays* (AAD52983); Arath;WEE1, *Arabidopsis thaliana*
792 (CAD28679), Glyma;WEE1, *Glycine max* (AAS 13373), Orysa;WEE1, *Orysa*
793 *sativa* (XP_464040); Lyces;WEE1, *Lycopersicon esculentum* (AM180939);
794 Cyame;WEE1, *Cyanidioschyzon merolae;* (CMT590C); Ostta;WEE1,
795 *Ostreococcys tauri* (AY675101)
796

797 **Figure 4.** Alignment of Nicta;WEE1 and Arath;WEE1 predicted amino acid
798 sequences showing conserved (black) and similar (grey) residues. Roman
799 numerals indicate kinase sub domains in catalytic domain. Inverted closed
800 triangles, 'EGD' Motif conserved in most WEE1 sequences. The line above
801 the Nicta;WEE1 sequence Indicates the peptide used to raise an antibody.
802 **Figure 5.** *Nicta;WEE1* over expression does not induce a small mitotic size
803 phenotype but G2 lengthens.
804 (A). Mean (±SE) expression levels of *Nicta;WEE1* by semi-quantitative RT
805 PCR, ±DEX (μM) as a percentage of max. in two transgenic lines: (L6 and
806 L7). n = 3.
807 **Figure 6.** Nicta;CDKB1 kinase activity is premature when *Arath;WEE1* is
808 expressed in BY-2 cells
809 (B). Mitotic indices in the *Nicta;WEE1* inducible line 6 ± 30 μM DEX (μM)
810 following synchronisation with aphidicolin. DEX was added at time 0, and 500
811 cells were scored per sampling time. Mean (±SE), mitotic cell areas (mca) are
812 added. (n= 48) Mean histone H1 kinase activities (±SE) of (A) CDKA ±DEX
813 and (B) CDKB ± DEX. Immunoprecipitates in triplicate experiments were
814 quantified as a percentage of maximum. Protein extracts for these assays
815 were sampled from the same experiment used for generate mitotic index
816 curves in Fig. 2 and phase durations are carried over. Between-treatment
817 differences were assessed using the Student's t test: * $P < 0.05$, ** $P = 0.02$-
818 0.05 Where error bars are absent, variation about the mean was <5%. (n=3).
819 Above and below are gel images from one of the three replicates.

820 **Figure 7.** Mean expression (±SE) of *Nicta;WEE1* (percentage of max) by
821 semi-quantitative RT-PCR in three day old cultures in BY-2 cells in which
822 *Arath;WEE1* (+DEX) was induced for 12 h compared with wild type of
823 comparable age. n = 3
824
825 **Figre 8.** Expression of *Arath;WEE1* disrupts *Nicta;WEE1* expression
826 profile during synchronised cell cycles.
827 (A) WT (representative data and mitotic index), and mean expression level
828 (±SE) (%max) of (B) *Nicta;WEE1* –DEX;(C) *Nicta;WEE1* +DEX; (D)
829 *Arath;WEE1* induced in BY-2 cells. Excluding 4 (A), n = > 3 and < 6. Plots of
830 mitotic index in (B) and (C), are from Fig. 2.
831
832 **Figure 9.** WEE1 antibody raised to Nicta;WEE1 also detects Arath;WEE1 on
833 a Western blot of Arabidopsis and tobacco proteins (A) and identifies a
834 specific band when *Nicta;WEE1* is expressed in *E.coli*, following induction of
835 the recombinant protein with IPTG (B). *In vitro*-expressed At14-3-3omega
836 protein is the negative control. There is a clear increase in the levels of WEE1
837 shown by Western blotting following induction with DEX in cultures expressing
838 *Arath;*WEE1 under the DEX-inducible promoter (C).
839 Means (±SE) of total WEE1 protein (% max) -DEX and +DEX (E-F). Line plots
840 of mitotic indices are indicated on the same y-axis. Above (D) and below (G)
841 are mean (± S.E.) Mean (±SE) WEE1 kinase activities as the reciprocal of the
842 CDK activity on histone H1 following the addition of pulled down WEE1
843 (where error bars are absent, variation about the mean was <1%) The G2/M

844 transition is extrapolated from the peak of the mitotic index in both cases. n =
845 2
846
847 **Figure 10**. Profile of CDK A, CDKB and WEE1 kinase activity during the cell
848 cycle together with *Nicta;WEE1* mRNA and protein levels in the *Arath;WEE1*
849 inducible cell line ± DEX. Note that in the –DEX treatment, onset of mitosis
850 was an hour earlier in the WEE1 kinase and protein experiment compared
851 with the CDK measurements (see Figs. 3, 5 and 8). WEE1 kinase profiles are
852 projected activities between intermittent sampling times used to coincide with
853 G2/M in each treatment (see Fig. 8).
854
855 **Figure 11A**. Premature cell division in i-*Arath;WEE1* +DEX, but constant cell
856 growth rates ± DEX.
857 White and grey rectangles represent mitotic cell size (plotted to scale from
858 Fig. 1) with an equal partition at the beginning of the next cell cycle, in i-
859 *Arath;WEE1* (-DEX) and i-*Arath;WEE1* (+DEX) , respectively. The dotted line
860 extrapolates to the birth of two new -DEX cells of the previous cell cycle.
861 The sloping lines connecting newly born and mitotic cells, span one cell cycle
862 (plotted to scale data from Fig.2). Cell cycle phases (from Fig. 2) are given
863 as horizontal bars, black on white, i-*Arath;WEE1* (- DEX) white on grey, *i-*
864 *Arath;WEE1* (+ DEX). **Figure 11B** Over expression of *NictaWEE1* slows cell
865 growth rate. Cell growth rates in BY-2 cells in a Nicta;WEE1 DEX-inducible
866 line -DEX (white boxes and solid line, or +DEX (grey box, dotted line) based
867 on the timing of mitosis and measurements of mitotic cell size. (data from Fig.
868 9)